Developing vaccines to prevent mycobacterial infections

Kirstie Maree Mangas

BSc (Hons)

ORCID: 0000-0001-9803-2294

Doctor of Philosophy

February 2020

Department of Microbiology & Immunology,
The University of Melbourne at The Peter Doherty Institute for Infection & Immunity

Submitted in total fulfilment of the requirements of the degree of Doctor of Philosophy

Abstract

Tuberculosis (TB) is a leading cause of disease by an infectious agent. It is the most common mycobacterial disease of humans, followed by leprosy and Buruli ulcer. TB is caused by infection with *Mycobacterium tuberculosis* (MTB). TB affects people in every part of the world, predominantly throughout Asia (especially India and China) and Africa. Roughly one-quarter of the world's population is latently infected with MTB. Asymptomatically infected people carry an approximate 10% risk of developing active disease. In 2018, there were an estimated 10 million new cases of TB and 1.45 million associated deaths. TB is treatable however it requires six months of combination antibiotic therapy. Buruli ulcer (BU), is a neglected tropical disease and has been reported in more than 30 countries world-wide but the dominant endemic foci of this disease occur in rural regions of West Africa. In the past five years BU cases have increased dramatically in South-East Australia, near Melbourne. BU is caused by infection of subcutaneous tissue with *Mycobacterium ulcerans*, typically presenting as deep and extensively ulcerated skin lesions. MTB and *M. ulcerans* are closely related mycobacterial species, therefore a vaccine against one of these bacteria might induce cross-protection against the other. The *Mycobacterium bovis* 'bacille Calmette-Guérin' (BCG) vaccine, a live-attenuated whole cell vaccine against MTB, is widely used. It is most effective in children below two years of age and against disseminated TB but efficacy wanes after about 10-15 years. In adults, BCG is between 0-80% effective. There is no effective vaccine against any mycobacterial disease and immune correlates of protection for mycobacterial vaccines are not well defined.

This thesis sought to address these knowledge gaps and explored the development of different vaccines to protect against TB and BU. The vaccines were tested in murine infection models and the types of immune responses induced by each vaccine were measured. Where a vaccine was able to elicit robust immune responses, the animals were then challenged with the mycobacterial pathogen to assess protective efficacy.

The first chapter is an introduction to this thesis and includes a literature review of TB and BU, their respective causative agents, immune responses to infection, and recent vaccine developments. This chapter introduces the key concepts and motivations for this thesis.

The second chapter describes the development of a protein-based vaccine against TB. The vaccines utilised MTB-specific proteins ESAT-6 and Ag85B in conjunction with lipopeptide adjuvant R_4Pam_2Cys in C57BL/6 mice. The vaccines were not capable of generating measurable interferon (IFN)-γ responses from $CD4^+$ T cells recovered from the spleen or from the lungs, which have been shown to be crucial to the control of TB. The vaccines were however able to induce high protein-

specific antibody titres against Ag85B. These vaccines were then modified with *M. ulcerans*-specific proteins to try and develop a vaccine against *M. ulcerans*.

The third chapter focusses on the development of two protein-based vaccines against two highly expressed *M. ulcerans* cell wall-associated proteins, MUL_3720 and Hsp18. These proteins were bound to lipopeptide adjuvant R_4Pam_2Cys and their ability to generate a strong antibody response was measured in BALB/c and C57BL/6 mice. *M. ulcerans* is predominantly an extracellular pathogen and a strong antibody response against *M. ulcerans* could play a role in prevention of infection. Both MUL_3720 and Hsp18 in conjunction with R_4Pam_2Cys were capable of generating strong protein-specific antibody responses in both mouse strains. These antibody responses remained augmented after subcutaneous challenge with *M. ulcerans* on the mouse tail, however strong antibody responses did not correlate to protection. All vaccinated mice succumbed to infection 40 days after *M. ulcerans* infection. This suggests that these proteins were not suitable vaccine candidates. There was also no difference in protection between vaccinated mice and mice vaccinated with BCG. The BCG vaccine is not wholly protective against *M. ulcerans* but previous studies have shown that the vaccine delays the onset of disease. The lack of difference in this study may be due to the high bacterial challenge dose and suggested the need for a different animal model of infection.

The fourth chapter describes the development of a vaccine targeting the mycolactone biosynthesis pathway. Mycolactone is a polyketide toxin and is the main virulence factor of *M. ulcerans*. Mycolactone affects the host immune response, causing immune cells to display modulated or decreased cell function which enables bacteria to evade immune responses. Prior to the creation of a new vaccine formulation, a new murine model of infection was established to reflect a more realistic, lower pathogen challenge dose. In this new murine model, mouse tails were coated in engineered bioluminescent *M. ulcerans* and the contaminated skin was subcutaneously pierced with a sterile needle to replicate trauma-induced introduction of bacteria into the subcutaneous tissue. The bioluminescent bacteria enabled the visualisation and quantification of bacterial load over time using an *in vivo* imaging system (IVIS). Once a new murine challenge model was established, this chapter assessed the efficacy of a new vaccine formulation comprising a protein domain, enoyl reductase (ER). The ER functional domain is required for the biosynthesis of mycolactone. Recombinant ER protein was coupled to R_4Pam_2Cys and BALB/c mice were vaccinated and boosted. This vaccine provided comparable protection against BU compared to the BCG vaccine. Additionally, this vaccine was statistically more protective than no vaccination. Analysis of systemic cytokine responses suggest that control of disease correlates to the level of inflammatory cytokines found in the spleen compared to the draining lymph node (site of infection). The immune responses correlating to protection from a BCG vaccine differed to the responses generated by ER+R_4Pam_2Cys. This study indicates that protection against BU may be achievable by different immune responses. This study also suggests that the highly conserved

mycolactone biosynthesis pathway may be an effective target for a vaccine. However, understanding the immune correlates of protection requires much further study.

In conclusion, this thesis demonstrated that MTB proteins in conjunction with the chosen adjuvant (R_4Pam_2Cys) do not elicit immune responses, in particular IFN-γ responses, that are typically required to protect against TB in a murine model. *M. ulcerans* proteins, Hsp18 and MUL_3720 also using the R_4Pam_2Cys adjuvant, did not induce protection against BU in a murine challenge model. However, vaccine-induced protection was observed by incorporating the *M. ulcerans* mycolactone ER functional domain with R_4Pam_2Cys and a murine model more reflective of a natural *M. ulcerans* infectious dose. These experiments highlighted the potential for an effective vaccine that targets the mycolactone biosynthesis pathway. This work also demonstrated that protection against *M. ulcerans* might be achieved via different combinations of immune responses. An effective vaccine against *M. ulcerans* will likely have useful lessons for developing vaccines protective against MTB (and vice-versa), whether through cross protection or by using vaccines as tools to probe and measure the host immune responses required for control or protection against infection.

Declaration

This is to certify that:

I. This thesis, entitled "Developing vaccines to prevent mycobacterial infections", comprises only my original work towards this PhD except where otherwise indicated;

II. Due acknowledgement has been made in the text to all other material used;

III. The thesis is fewer than 100,000 words in length, exclusive of tables, figures, figure legends, bibliography, and appendices.

.....

Kirstie Maree Mangas BSc (Hons)

Department of Microbiology & Immunology

The University of Melbourne at The Peter Doherty Institute for Infection & Immunity

Preface

This preface provides a summary of the contents of each chapter in this thesis. The chapters that include publications are indicated. The nature and extent of the contributions to each chapter made by the author of this thesis are listed.

Funding: Kirstie Maree Mangas was supported in part by a Millis-Jackson Research Scholarship, provided by the University of Melbourne to continue research collaborations in respective to vaccine development. Funding awarded to co-authors of the publications presented in this thesis are indicated below.

Chapter 1: Introduction and Literature Review is an original overview of the background, key concepts and motivations for this thesis, with the original works cited.

The content of Chapter 1 includes some sections from a manuscript that was prepared and accepted during this PhD. Some portions of the following manuscript are included.

Kirstie M. Mangas, Andrew H. Buultjens, Jessica L. Porter, Sarah L. Baines, Estelle Marion, Laurent Marsollier, Nicholas J. Tobias, Sacha J. Pidot, Kylie M. Quinn, David Price, Katherine Kedzierska, Weiguang Zeng, David C. Jackson, Brendon Y. Chua and Timothy P. Stinear. **Vaccine-specific immune responses against *Mycobacterium ulcerans* infection in a low-dose murine challenge model.** *Infection and Immunity*; doi: 10.1128/IAI.00753-19. Accepted 7th December, 2019. Published 20th February, 2020.

Chapter 2: Murine immune responses to subunit vaccination with *Mycobacterium tuberculosis* protein antigens linked to a TLR-2 agonist, is an original work that resulted in the following *in-progress* publication:

"Murine immune responses to subunit vaccination with *Mycobacterium tuberculosis* protein antigens linked to a TLR-2 agonist".

Kirstie M. Mangas, Chinn Yi Wong, Acep R. Wijayadikusumah, Weiguang Zeng, Toshiki Sekiya, Jessica L. Porter, Sacha J. Pidot, Kylie M. Quinn, Katherine Kedzierska, Timothy P. Stinear, David C. Jackson and Brendon Y. Chua.

The author of this thesis was the first author and main contributor of the work presented in this publication. The nature and extent of my contributions to this chapter are described below.

- I contributed to the design of the study, generation of data (exceptions listed below), interpretation of results, and development of the concepts described in the chapter with TPS and BYC.
- I performed all animal and laboratory experiments. All animal studies were performed in accordance with the Animal Research Ethics Committee at The University of Melbourne (Ethics Application #1513513 and 1613870).
- The bacterial ESAT-6 protein expression vector was created by TS.
- The production of the adjuvant used in this study was performed by ARW and WZ.
- I was responsible for the planning, drafting, and editing of the manuscript with TPS and BYC.
- All co-authors reviewed and edited the manuscript included in this thesis.

Funding associated with this publication include National Health and Medical Research Council, Australia: GNT1071916. Fellowships awarded to TPS (APP1008549) and BYC (CR Roper).

Chapter 3: High antibody titres induced by protein subunit vaccines against Buruli ulcer using *Mycobacterium ulcerans* antigens Hsp18 and MUL_3720, is an original work that resulted in the following *in-progress* publication:

"High antibody titres induced by protein subunit vaccines against Buruli ulcer using *Mycobacterium ulcerans* antigens Hsp18 and MUL_3720".

Kirstie M. Mangas, Nicholas J. Tobias, Estelle Marion, Jérémie Babonneau, Laurent Marsollier, Jessica L. Porter, Sacha J. Pidot, Chinn Yi Wong, David C. Jackson, Brendon Y. Chua and Timothy P. Stinear.

The author of this thesis was the first author and main contributor of the work presented in this publication. The nature and extent of my contributions to this chapter are described below.

- I contributed to the design of the study, generation of data (exceptions listed below), interpretation of results, and development of the concepts described in the chapter with TPS and BYC.
- I created the Hsp18 bacterial expression system but the MUL_3720 bacterial expression system was created by NJT.
- I designed the animal experiments and the vaccination-challenge in mice was performed by EM, JB and LM. All animal studies were performed in accordance with the Ethics Committee of region Pays de la Loire (France) (Ethics protocol # CEEA 2009.14 and CEEA 2012.145).
- I prepared the vaccine and performed the laboratory experiments (excluding sera collection and enumeration of bacterial dose – performed by EM, JB and LM) and data analyses.
- The production of the adjuvant used in this study was performed by BYC.
- I was responsible for the planning, drafting, and editing of the manuscript with TPS and BYC.
- All co-authors reviewed and edited the manuscript included in this thesis.

Funding associated with this publication include National Health and Medical Research Council, Australia: GNT1008549. Fellowships awarded to TPS (APP1008549) and BYC (CR Roper).

Chapter 4: Vaccine-specific immune responses against *Mycobacterium ulcerans* infection in a low-dose murine challenge model, is an original work that resulted in the following publication:

"Vaccine-specific immune responses against *Mycobacterium ulcerans* infection in a low-dose murine challenge model".

Kirstie M. Mangas, Andrew H. Buultjens, Jessica L. Porter, Sarah L. Baines, Estelle Marion, Laurent Marsollier, Nicholas J. Tobias, Sacha J. Pidot, Kylie M. Quinn, David Price, Katherine Kedzierska, Weiguang Zeng, David C. Jackson, Brendon Y. Chua and Timothy P. Stinear. *Infection and Immunity;* doi: 10.1128/IAI.00753-19. Accepted for publication, 7th December 2019. Published, 20th February 2020.

The author of this thesis was the first author and main contributor of the work presented in this publication. The nature and extent of my contributions to this chapter are described below.

- I contributed to the design of the study, generation of data (exceptions listed below), interpretation of results, and development of the concepts described in the chapter with TPS and BYC.
- I performed all animal and laboratory experiments. The statistical analyses of data was performed by me however the initial bioinformatics analyses were performed by SLB and final machine learning analyses of immune parameters were performed by AHB, DP and TPS. All animal studies were performed in accordance with the Animal Research Ethics Committee at The University of Melbourne (Ethics Application #1613870).
- The interpretation of the machine learning analyses of immune parameters was guided by AHB and TPS.
- Assistance was provided by AHB and TPS in the interpretation of machine learning analyses of immune parameters.
- The production of the adjuvant used in this study was performed by WZ.
- I was responsible for the planning, drafting, and editing of the manuscript with TPS and BYC.
- All co-authors reviewed and edited the manuscript.

Funding associated with this publication include National Health and Medical Research Council, Australia: Fellowships awarded to TPS (APP1008549) and BYC (CR Roper).

Chapter 5: Conclusions is an original summary of the significance, implications and limitations of the work presented in this thesis.

Additional publications arising during candidature

Gherardin NA, Souter MN, Koay H, **Mangas KM,** Seemann T, Stinear TP, Eckle SB, Berzins SP, d'Udekem Y, Konstantinov IE, Fairlie DP, Ritchie DS, Neeson PJ, Pellicci DG, Uldrich AP, McCluskey J. and Godfrey D. I. 2018. Human blood MAIT cell subsets defined using MR1 tetramers. Immunol Cell Biol 96: 507-525; doi: 10.1111/imcb.12021.

Wallace JR, **Mangas KM**, Porter JL, Marcsisin R, Pidot SJ, Howden B, Omansen TF, Zeng W, Axford JK, Johnson PDR, Stinear TP. 2017. *Mycobacterium ulcerans* low infectious dose and mechanical transmission support insect bites and puncturing injuries in the spread of Buruli ulcer. PLoS Negl Trop Dis 11:e0005553; doi: 10.1371/journal.pntd.0005553.

Vandelannoote K, Meehan CJ, Eddyani M, Affolabi D, Phanzu DM, Eyangoh S, Jordaens K, Portaels F, **Mangas K**, Seemann T, Marsollier L, Marion E, Chauty A, Landier J, Fontanet A, Leirs H, Stinear TP, de Jong BC. 2017. Multiple Introductions and Recent Spread of the Emerging Human Pathogen *Mycobacterium ulcerans* across Africa. Genome Biol Evo. 9:414-426; doi: 10.1093/gbe/evx003.

Ablordey AS, Vandelannoote K, Frimpong IA, Ahortor EK, Amissah NA, Eddyani M, Durnez L, Portaels F, de Jong BC, Leirs H, Porter JL, **Mangas KM**, Lam MM, Buultjens A, Seemann T, Tobias NJ, Stinear TP. 2015. Whole Genome Comparisons Suggest Random Distribution of *Mycobacterium ulcerans* Genotypes in a Buruli Ulcer Endemic Region of Ghana. PLoS Negl Trop Dis 9:e0003798; doi: 10.1371/journal.pntd.0003681.

Conference communications

Kirstie Mangas, Sacha Pidot, Jessica Porter, Brendon Chua, David C. Jackson and Timothy P. Stinear Development of a subunit vaccine targeting the mycolactone production pathway in *Mycobacterium ulcerans. BacPath Conference 2017*, Adelaide, Australia (oral presentation).

Kirstie Mangas, Sacha Pidot, Jessica Porter, Brendon Chua, David C. Jackson and Timothy P. Stinear Development of a subunit vaccine targeting the mycolactone production pathway in *Mycobacterium ulcerans. BacPath Conference 2017*, Adelaide, Australia (poster presentation).

Kirstie Mangas, Estelle Marion, Laurent Marsollier, Brendon Chua, Nicholas J. Tobias, David C. Jackson and Timothy P. Stinear. Development of a subunit vaccine against *Mycobacterium ulcerans. Australian Society for Microbiology Annual Scientific Meeting 2016*, Perth, Australia (oral presentation).

Kirstie Mangas, Estelle Marion, Laurent Marsollier, Brendon Chua, Nicholas J. Tobias, David C. Jackson and Timothy P. Stinear. Development of a subunit vaccine against *Mycobacterium ulcerans. Australian Society for Microbiology Annual Scientific Meeting 2016*, Perth, Australia (poster presentation).

Kirstie Mangas, Estelle Marion, Laurent Marsollier, Brendon Chua, Nicholas J. Tobias, Renee Marcsissins, David C. Jackson and Timothy P. Stinear. The development of a subunit vaccine against *Mycobacterium ulcerans. European Congress of Immunology Scientific Meeting 2015*, Vienna, Austria (poster presentation).

Acknowledgements

The work presented in this thesis was made possible through the assistance, support and guidance from many individuals.

First and foremost, I would like to thank Tim Stinear, Brendon Chua and Dave Jackson for their continual support and guidance, both in research and in life. I greatly appreciate the time, knowledge and resources they have shared with me. This has enabled me to develop as a scientist and as an individual, making this PhD an invaluable experience. Tim enthusiastically encouraged me to pursue my interests, reminded me that no idea is too ambitious, and was always available for advice. I am truly grateful for his mentorship.

I would also like to thank the other members of my PhD committee, Kylie Quinn, Katherine Kedzierska and Jaclyn Pearson for their guidance, creative suggestions and different perspectives. They helped me develop my research skills and provided insightful career advice and friendship.

I owe a great deal of gratitude to the fellow members of the Stinear, Howden and Jackson labs, past and present, who have all provided me with assistance during my PhD. Acep Wijayadikusumah, Toshiki Sekiya and Chinn Yi Wong – for teaching me every cell-based assay I know and always offering to help me before I needed to ask. Thank you to the original BU team: Jess Porter – for all the assistance with animal work and ability to trouble shoot any problem; Sacha Pidot – for the continual advice, support, protein skills and humour; and Nick Tobias– for inspiring my initial love of research. Thank you Ian Monk and Wei Gao for all the novel ideas; Jean Lee, Sarah Baines and Andrew Buultjens, my fellow PhD candidates, for the moral support and always being available to bounce ideas; Jean Lee – for being a wonderful desk buddy; Sarah Baines – for the hilarious marathon chats; Andrew Buultjens – for inspiring me to try new things; and Andre Mu, Claire Gorrie and Danielle Ingle – for always being available for some sage advice.

I would like to thank our collaborators in Angers, France – Estelle Marion, Laurent Marsollier and Jérémie Babonneau – for all their assistance with our animal modelling.

I must thank many of the labs throughout the Department of Microbiology and Immunology, including the Godfrey, Kedzierska and Mackay lab, for sharing reagents, knowledge and equipment; and the teaching staff, particularly Helen Cain, Louise Adams and Karena Waller – for the constant opportunities to grow my love of teaching throughout my PhD.

I would like to pay special regards to the School of Biomedical Sciences, particularly Effie Keramidaris and Gillian Waters and for providing me with opportunities to complement my research training and expand my University experience. I also owe a great deal of gratitude to Rebecca Whitsed, who has gone above and beyond to support me throughout my PhD, for remembering important dates and regularly checking in with me.

I would like to express my gratitude to the friends who supported me through my PhD and were understanding of my time commitments. Particularly, my fellow scientists: Simone Park, Susan Christo and Nick Gherardin – for the measured advice and witty banter; and my JFK co-members, Jess Chadderton and Fern Koay – for endless events and absolute understanding; and the friends outside the lab: the 'Munchkins' for providing me with an outlet outside of science; Jess Dowling – for the honest counsel, and sympathetic ear; Alex Muirhead – for the unwavering support, and celebrating every win; and finally, Mike Gell – for all the reassurance, understanding my late nights, and riding through every high and low by my side.

Lastly, I would like to thank my family. Mum and Dad – for supporting everything that I do, inspiring me to follow my passions and for providing me a break from research when I needed it; and Brad – my favourite (only) brother, for reminding me to keep things in perspective and being my number one cheerleader.

Table of Contents

List of Tables and Figures

Chapter 1

Tables

Figures

Chapter 2

Tables

Figures

Chapter 3

Tables

Figures

Chapter 4

Tables

Figures

List of Abbreviations

°C	Degrees Celcius
Ab	Antibody
Ag	Antigen
APC	Antigen presenting cell
BCG	Bacille Calmette-Guérin
BU	Buruli ulcer
CDS	**(**Protein) Coding DNA sequence
CFU	Colony forming units
Da	Daltons
DC	Dendritic cell
DLN	Draining lymph node
DNA	Deoxyribonucleic acid
ELISA	Enzyme linked immunosorbent assay
ER	Enoyl reductase
GBUI	Global Buruli Ulcer Initiative
HIV	Human immunodeficiency virus
ID_{50}	Infectious dose 50
IFN	Interferon
Ig	Immunoglobulin
IGRA	Interferon gamma release assay
IL	Interleukin
IS	Insertion sequence
Kb	Kilobase(s)
kDa	KiloDalton(s)
LAMP	Loop-mediated isothermal amplification
LN	Lymph node
LTBI	Latent tuberculosis infection
Mb	Megabase
MDa	Mega Daltons
MDR	Multi-drug resistant
MHC	Major histocompatibility complex
mRNA	Messenger ribonucleic acid
MTB	*Mycobacterium tuberculosis*
MU	*Mycobacterium ulcerans*
NK	Natural killer
OD	Optical density

PCR	Polymerase chain reaction
PKS	Polyketide synthase
PPD	Purified protein derivative
RD	Region of difference
RIF	Rifampin
RR	Rifampin resistance
RNA	Ribonucleic acid
RT	Room temperature
TB	Tuberculosis
T_h	T-helper
TLR	Toll-like receptor
TNF	Tumour necrosis factor
TST	Tuberculin skin test
WHO	World Health Organization
XMDR	Extensive multi-drug resistant

Chapter 1

Introduction and Literature Review

Mycobacterium tuberculosis* and *Mycobacterium ulcerans

1.1 The genus *Mycobacterium*

The genus *Mycobacterium* belongs to the class of bacteria called *Actinobacteria* (1). There has been a recent suggestion to divide the genus into five separate genera, but this idea has not met widespread acceptance (2, 3). Some *Actinobacteria* are capable of producing bioactive metabolites used as medicine for humans, while others can be pathogenic in humans (1, 4-7). Members of the genus *Streptomyces*, the largest genus of *Actinobacteria,* produces over two-thirds of clinically used antibiotics. These antibiotics include neomycin, chloramphenicol, streptomycin, daptomycin, tetracycline and kanamycin (8, 9). Pathogenic *Actinobacteria* include *Corynebacterium diphtheria*, the causative agent of diphtheria and some members of the *Streptomyces* genus are capable of causing abscesses and pneumonia (4).

There are greater than 180 named mycobacterial species, however relatively few cause disease (around 20 species) (2). Some examples of causative agents of mammalian disease include *Mycobacterium tuberculosis,* the causative agent of human tuberculosis, and *Mycobacterium ulcerans,* which causes Buruli ulcer (9, 10).

1.2 *M. tuberculosis* and *M. ulcerans* are important human pathogens

The genus *Mycobacterium* is the sole genus in the family *Mycobacteriacae.* The greater than 180 different species of *Mycobacteria* can be found in many diverse environments including soil, bodies of water, and animals. Whole genome comparisons of species have shown that mycobacteria can be separated into "slow growers" and "rapid growers" with an accompanying "intermediate" group (2, 3, 11). Rapid growers were found to be more ancestral than slow growers (11). In the study by Gupta et al., 150 mycobacterial species were compared to create a maximum-likelihood tree based on 1941 core proteins found in greater than 80% of the species. This study showed that *Mycobacterium* could be separated into five distinct clades (2). Three of these clades contain slow-growing species of mycobacteria (greater than seven days to form colonies), while the remaining two clades encompass fast-growing bacteria (less than seven days to form colonies). As shown in Figure 1.1, this tree could be used to separate the species into five clades, with clade 'Tuberculosis-Simiae' comprising most of the clinically relevant mycobacterial species (2). These species include members of the *M. tuberculosis*-species complex, e.g. *M. tuberculosis*, *M. bovis* and *M. africanum* (hereafter abbreviated as MTB complex) alongside nontuberculous mycobacteria such as *M. ulcerans* and *M. leprae.* Figure 1.1 shows that *M. ulcerans* and *M. marinum* are extremely closely related (2), with both species having previously been identified as possessing greater than 97% DNA homology (12). This figure also shows that *M. marinum* and *M. ulcerans* are amongst the closest relatives to the MTB complex, though there are a few species more closely related to the MTB complex (13, 14). *M. marinum* and *M. tuberculosis* share greater than 85% nucleotide identity (3, 15, 16).

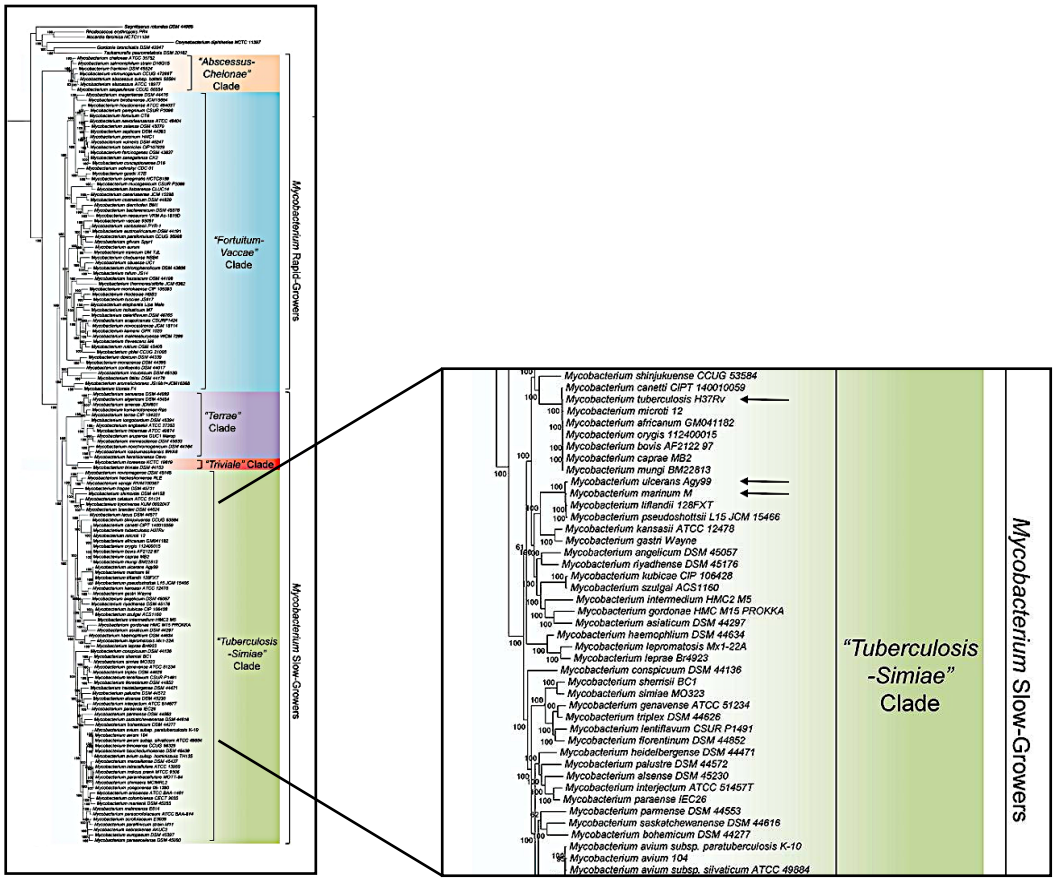

Figure 1.1. Maximum-likelihood phylogenetic tree for 150 *Mycobacterium* species based on the concatenated sequence of 1941 core proteins from the genus *Mycobacterium*.

This phylogenetic tree (adapted from Gupta et al. (2)) depicts the demarcation of five clades of *Mycobacterium.* The clade "*Abscessus-Chelonae*" is in orange, "*Fortuitum-Vaccae*" is in blue, "*Terrae*" is in purple, "*Triviale*" is in red and clade "*Tuberculosis-Simiae*" is in green. The positions of *M. marinum, M. ulcerans* and *M. tuberculosis* within clade "*Tuberculosis-Simiae*" are indicated by the black arrows.

Tuberculosis (TB) is the greatest cause of mycobacterial morbidity in the world and the second greatest cause of mortality due to a single infectious agent. In 2006, the World Health Organization (WHO) launched the Stop TB Strategy to halve the prevalence and deaths due to TB by 2015 compared to the baseline numbers reported in 1990 (17, 18); and the End TB Strategy to eliminate TB as a public health problem by the year 2050 (19, 20). In 1882, Robert Koch first identified *Mycobacterium tuberculosis* as the causative agent of human tuberculosis (21). *M. tuberculosis* (MTB*)* is a member of the MTB complex, which includes *M. bovis*, *M. microti* and *M. africanum* (22, 23). As well as causing disease in humans they also infect cattle, badgers, deer, domestic cats, possums and voles (24-32). The complete genome was first sequenced in 1998 (33). *Mycobacterium marinum and Mycobacterium ulcerans* are closely related to the MTB complex (12, 34). As an intracellular human pathogen, MTB optimally

replicates at 37°C whereas *M. marinum* and the extracellular pathogen, *M. ulcerans*, replicate optimally around 30°C (35).

M. marinum and *M. ulcerans* share over 97% DNA homology (12) but are phenotypically distinct. *M. marinum* is an intracellular pathogen mainly affecting fish and other ectotherms, but in humans causes granulomatous lesions at the extremities (12). *M. ulcerans* is an extracellular pathogen with a significantly slower growth rate (doubling time >48 hours) than *M. marinum* (doubling time of four hours) and MTB (doubling time 18-24 hours) (36). *M. marinum* and *M. ulcerans* share a recent common progenitor (37). Stinear et al. proposed *M. ulcerans* diverged from *M. marinum* during adaptation to a specific (but undiscovered) environmental niche (12). One key difference in *M. ulcerans* is the acquisition of the pMUM plasmid, pMUM001, which is absent in *M. marinum* (38, 39). pMUM001 is required to produce the main virulence factor, mycolactone (40). *M. ulcerans* has also acquired the insertion sequence (IS) IS*2404*. High copy numbers (>200) of IS*2404* across the *M. ulcerans* genome have facilitated the rearrangement of the genome and many gene inactivations and deletions (37). Facilitated by the presence of several hundred copies of IS*2404*, *M. ulcerans* has undergone genomic arrangements and deletions, resulting in a smaller genome compared to *M. marinum* and many pseudogenes (41-43). This suggests that *M. ulcerans* has deleted genes that are not required for survival in a niche environment (37). The nature of this hypothetical niche is unknown.

M. ulcerans is the causative agent of Buruli ulcer (BU), the third most prevalent mycobacterial disease after tuberculosis and leprosy. The first published description of *M. ulcerans* occurred in 1948, in Bairnsdale, Victoria (44). It was identified as a new mycobacterial species and the disease was subsequently named Bairnsdale ulcer (45). However, the disease was likely described by missionaries working in Uganda during the 1890s (46). Since an outbreak in the Buruli county of Uganda during the 1960s (47, 48), the disease has been known as Buruli ulcer. In 1998, the WHO launched the Global Buruli Ulcer Initiative (GBUI) to coordinate control and research efforts. In 2004, at the WHO 57th World Health Assembly, a resolution was passed to increase surveillance and control, and to advocate for research towards developing diagnostics tools, treatments and preventions for BU (49).

1.3 Clinical features of disease

Though MTB and *M. ulcerans* are closely related they present very different clinical manifestations. TB is an infection of the lungs (50) whereas BU is primarily an infection of subcutaneous tissue (51). In cases where the diseases are left untreated, the bacteria can disseminate to infect bones and other organs (50, 52). TB can be a fatal infection, whereas little mortality is associated with BU.

1.3.1 Clinical features of tuberculosis

There are many different symptoms associated with TB. These include a cough with sputum and blood at times, chest pains, weakness, weight loss, fever and night sweats. In cases of active disease, individuals will develop granulomas in the lung due to the inflammation surrounding replicating bacteria (53). Long-term inflammation leads to 'caseation', a form of necrosis. The diseased tissue forms a firm, dry mass – described as cheese-like in appearance (54). Bacteria may escape the lungs and replicate in the bones or other organs, e.g. the brain, causing significant morbidity and mortality. The mechanism of bacterial escape from the lungs is describe further in section 1.6.1. Disseminated TB infection rather than pulmonary TB mostly affects infants and children under the age of two (55, 56). An infection with MTB that cease to replicate is termed 'latent TB infection' (57). Often these individuals are not diagnosed, as they are asymptomatic. Roughly one-quarter of the world's population is latently infected, and these individuals carry a 10% lifetime risk of progressing to active disease (57, 58).

1.3.2 Clinical features of Buruli ulcer

M. ulcerans infection involves predominantly subcutaneous tissue but can affect all skin layers. Buruli ulcer is characterised by two key stages of disease: pre-ulcerative and ulcerative. Infection often begins as a small painless nodule, papule, plaque or oedema (Figure 1.2A), which if untreated can become ulcerative (Figure 1.2B and 1.2C) (51, 59). The progression to ulceration is often slow, painless and lacking systemic inflammation, commonly causing affected individuals to delay seeking treatment (52). Ulcerative disease, as shown in Figure 1.2B and 1.2C, is characterized by a necrotic slough of subcutaneous tissue and mycobacteria, with deeply undermined edges of skin (60). If untreated, necrosis will continue, which can eventually affect bones or even disseminate systemically (52, 60). There are increasing reports linking BU and osteomyelitis, often in patients who delay treatment or have lesions adjacent to joints (61-63). Lesions can impose significant cosmetic and functional deformities. A study of 579 patients in Australia found that 5.5% had multiple ulcers and that ulcers were mainly found on the lower (70%) and upper (27.1%) limbs (64). The ulcers were predominantly focused around ankles, elbows and calves.

Human immunodeficiency virus (HIV) is not considered a risk factor for BU but co-infection can occur in co-endemic regions (65). Co-infection with HIV weakens the immune system, leading to a more aggressive clinical progression of BU and poor treatment outcomes (65-68).

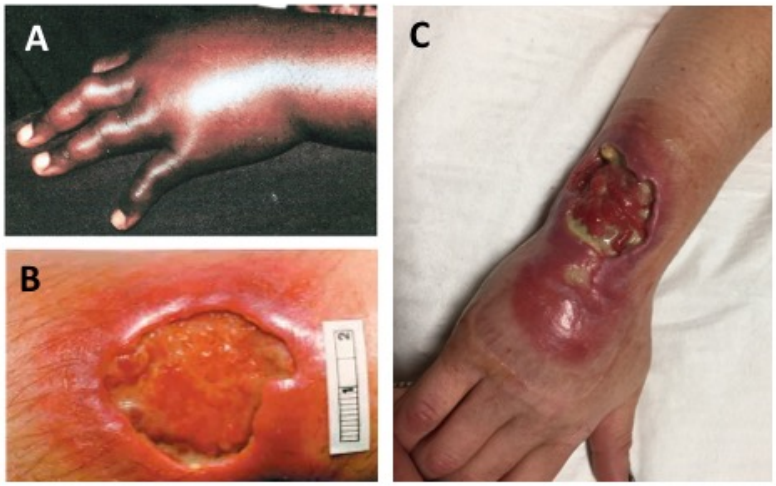

Figure 1.2. Infection caused by *Mycobacterium ulcerans.*

(A) Oedema in the left hand caused by *M. ulcerans* infection**.** There is no visible skin lesion, however the patient is also afflicted with osteomyelitis due to the progression of the disease (61). **(B)** Ulcerative lesion caused by *M. ulcerans* infection of the lower leg of an 11-year-old boy, Coastal Victoria, Australia (69). **(C)** Right forearm of young woman with Buruli ulcer acquired on the Mornington Peninsula, Australia (64).

1.4 Epidemiology

There are many more cases of TB compared to BU each year (70, 71). TB appears to be globally distributed whereas BU mostly appears in specific regions such as West and sub-Saharan Africa and South Eastern Australia (70, 71).

1.4.1 Epidemiology of tuberculosis

TB is globally distributed, as depicted in Figure 1.3, but has been described as a disease of poverty (72) and is most prevalent in developing areas such as Africa, China, India, Russia, South-East Asia and the Western Pacific regions (58). There is a strong correlation between areas that are endemic for HIV and areas with high incidence of TB infection (73). In 2018, the highest incidence of cases occurred in South East Asia, Africa and the Western Pacific (44%, 24% and 18% of cases, respectively) (58). In that same year around 87% of reported cases occurred in 30 high burden countries and two-thirds of the total TB cases occurred in only eight countries. India, China, Indonesia, Philippines, Pakistan, Nigeria, Bangladesh and South Africa reported the greatest incidence (58). Some countries are reporting a decline in cases, including China, Indonesia and the Philippines. These countries carry a heavy disease burden yet have a sustained decline in TB cases over the past decade (58).

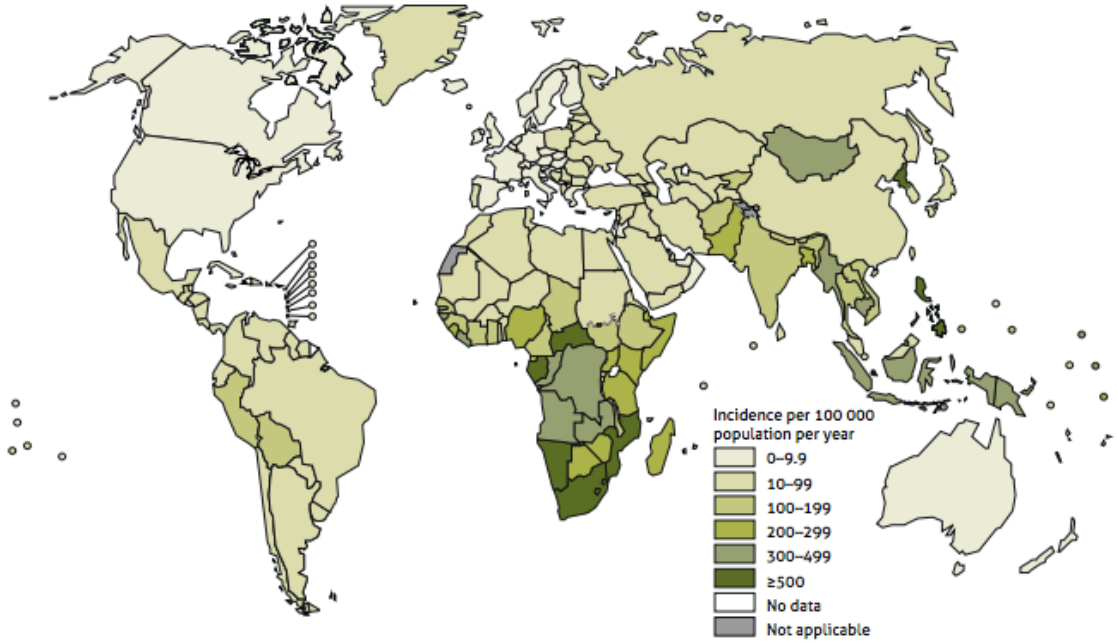

Figure 1.3. The estimated incidence rates and global distribution of tuberculosis, in 2018.
High endemic areas include India, Indonesia, China, Philippines, Pakistan, Nigeria, and South Africa. Image sourced from the WHO (58).

There are a multitude of risk factors for infection and active disease, some of which include genetic factors, immunosuppression, smoking, indoor air pollution and alcohol consumption (57, 74). The greatest risk occurs from immunodeficiency or immunosuppression through malnutrition or illnesses e.g. diabetes or HIV infection (75-77). In 2018, TB was estimated to account for 251,000 HIV-related deaths and is the greatest cause of mortality in HIV positive individuals (58). There is higher risk for tobacco smokers compared to non-smokers (76, 77). Those most at risk are individuals from low socioeconomic backgrounds, in densely populated areas (76, 77). Often in these circumstances, disease is poorly contained, and treatment is expensive and difficult to access.

1.4.2 Epidemiology of Buruli ulcer

Buruli ulcer was first identified in humans but *M. ulcerans* is now known to infect other mammalian species, including cats, dogs, possums and horses (78-82). Fish and frogs are affected by other mycolactone-producing mycobacteria (83, 84). Cases of human BU infection have appeared globally, as shown in Figure 1.4. Most cases appear in tropical and sub-tropical regions but are also occasionally reported in colder climates (Australia, Japan and China). Thirty-three countries have previously reported BU infections and 14 countries currently report cases (85). Between 2002 and 2010 there were approximately 5000 suspected cases annually and the number of cases between 2010 and 2016 decreased, reaching the minimum of 1961 cases reported in 2016 (86). Since 2016, the number have

cases have risen, reaching 2713 cases in 2018 (86). The number of reported cases between 2002 and 2018 was around 63,000 (86). The reason for the decline and recent incline in cases is not known. In 2018, 2206 cases of BU were reported and 1676 of them occurred in Africa (86). BU is most prevalent in sub-Saharan Africa in areas such as Benin, Côte d'Ivoire, Democratic Republic of Congo, Nigeria, Ghana, Cameroon and Gabon (71). The disease has also previously appeared in Japan, Papua New Guinea, French Guiana and Liberia (which reported an increase in cases in 2018). Outside of West and sub-Saharan Africa the greatest number of cases occur in Australia. Australia has recorded many cases of BU, mainly in coastal regions of Victoria and sporadic cases in rainforest areas of Queensland (87). There were 296 cases of BU in 2019, almost triple the amount of reported cases (107) from 2015 (88).

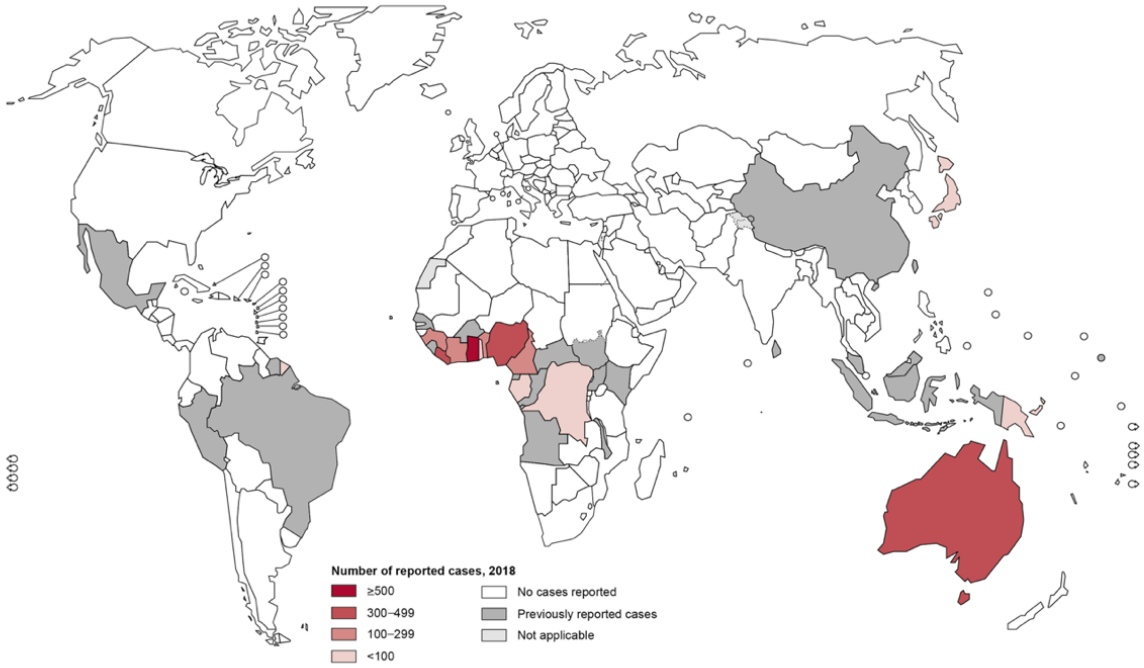

Figure 1.4. The estimated incidence rates and global distribution of Buruli ulcer, in 2018.
High endemic areas include west and sub-Saharan Africa and Australia. Image sourced from the WHO (71).

Cases of BU have been reported in both children and adults though the infection is most prevalent in children less than 15 years of age. In Africa 48% of BU infections occurred in children under the age of 15 years (85). In Australia the percentage of cases in children aged less than 15 years is 10% (85).

1.5 Transmission

The transmission of MTB occurs from host to host (89), however transmission of *M. ulcerans* between hosts is extremely rare and infection occurs from environmental contact (90, 91).

1.5.1. Transmission of tuberculosis

MTB is transmitted person to person by aerosol transmission from carriers of active disease (89). The life cycle of MTB is depicted in Figure 1.5. Individuals with active disease have replicating bacteria in their lungs and can spread the bacteria within saliva by coughing, sneezing or spitting in close proximity to another person (57). Individuals with active disease can infect between 5-15 people per year through close contact (75). Although it is unclear what is considered a biologically relevant dose of bacteria, the infectious dose for an individual is reported to be between 1 and 200 bacteria. A single aerosol droplet can contain anywhere between 1 and 400 bacilli (92, 93).

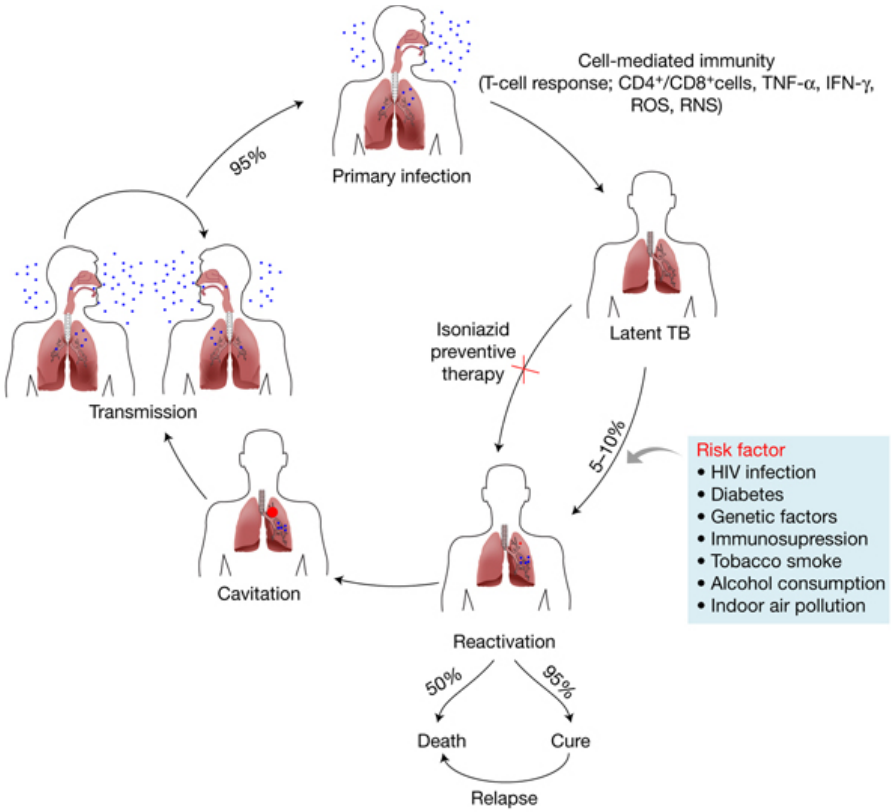

Figure 1.5. Virulence life cycle of *Mycobacterium tuberculosis* and progression of TB.
In summary, inhalation of MTB can lead to primary infection in 95% of cases and progression to latent tuberculosis infection (LTBI) (57). In 5-10% of LTBI cases the disease becomes active (57). Once the bacteria are actively replicating in the lung they can appear in droplets of saliva from the infected person. These droplets can be inhaled, and the cycle of infection can begin again in another individual (57). Image adapted from Kumar et al. (57).

1.5.2 Transmission of Buruli ulcer

Cases of BU suggest that humans are infected with *M. ulcerans* from the environment, as human-to-human contact is extremely rare (91, 94). Studies have examined the possible modes of transmission

from environment to human. A polymerase chain reaction (PCR) assay specific for the *M. ulcerans* insertion sequences, IS*2404* and IS*2606,* has identified the presence of *M. ulcerans* in the environment (95). This assay identified *M. ulcerans* DNA in aquatic insects, fish, snails, plants, biofilms, mosquitoes and possum faeces (82, 96-98). Marsollier et al*.,* demonstrated the ability of water insects to transfer *M. ulcerans* infection to laboratory mice during biting, stimulating a hypothesis whereby transmission can occur from insect to human (99). A survey of fish from BU endemic areas, discovered *M. ulcerans* PCR positive samples in a high percentage of insectivorous fish and none in carnivorous or omnivorous fish (100). A study from South Eastern Australia identified high levels of *M. ulcerans* positive mosquitoes through real time quantitative PCR, implicating a role for these insects in transmission (98). A recent laboratory study by Wallace et al. showed mosquitoes can facilitate transmission of *M. ulcerans* infection (101). This study also calculated the minimum infectious dose-50 (ID_{50}) and showed it to be very low; approximately three colony forming units (CFU) of bacteria (101). This is similar to the low infectious dose reported for TB infection (92, 93). Human cases of disease have coincided with some form of skin trauma such as gunshot wounds, vaccination or land mine accidents (90). These data suggest that infection occurs via skin trauma that allows environmental or skin-contaminating *M. ulcerans* to penetrate the epidermal layers.

1.6 Immune responses

MTB and *M. ulcerans* are closely related, however the clinical manifestations of both diseases differ greatly (102-104). Although they are both capable of infecting the same areas (e.g. subcutaneous tissue (51, 105)), MTB tends to primarily infect the lungs and typically *M. ulcerans* primarily infects the subcutaneous skin. Both bacteria differ in their mechanisms of infection, as will be discussed further in section 1.6.1 and 1.6.2. As such, the immune responses generated towards each infection can vary slightly and there are notable differences in clinical outcomes.

1.6.1 Human immune responses against *M. tuberculosis*

In some cases of MTB exposure, MTB is inhaled into the lungs and the host immune response – led by alveolar macrophages and neutrophils – effectively clears all bacteria prior to the development of an adaptive immune response (57, 106). From numerous exposure studies, the proportion of exposed individuals who remain tuberculin skin test (TST) or interferon-gamma release assay (IGRA) negative typically ranges between 4-10% but has been observed to higher (e.g. 47%) (106-111). Individuals unable to clear the MTB develop a primary infection, which can lead to active disease if the bacteria continue to multiply or the disease can become latent if the bacteria cease replicating (53). It is estimated that a quarter of the world's population is latently infected (58). Individuals with latent TB infection have an approximate 10% lifetime risk of disease re-activation (58, 112, 113).

During a primary MTB infection there is an influx of phagocytic cells into the lungs (57), particularly macrophages activated in response to TNF-α and IFN-γ signalling (114, 115). However, these cells are not always capable of controlling infection (57). MTB dissemination from the lungs is shown in Figure 1.6. MTB produces virulence proteins (including early secreted antigenic target 6kDa (ESAT-6), culture filtrate protein 10 kDa (CFP-10) and PknG) and alter host responses (e.g. coronin 1 production) to prevent the maturation and acidification of the phagolysosome (116-119). Around 10 days after primary infection the bacteria disseminate into draining lymph nodes (DLNs) and activate dendritic cells (DCs) to induce a T cell mediated response. Activated T cells migrate towards the primary site of infection at around 15-18 days post infection. Immune cells then surround the bacteria, forming granulomas. If replication ceases, the disease enters latent tuberculosis infection (LTBI) (53).

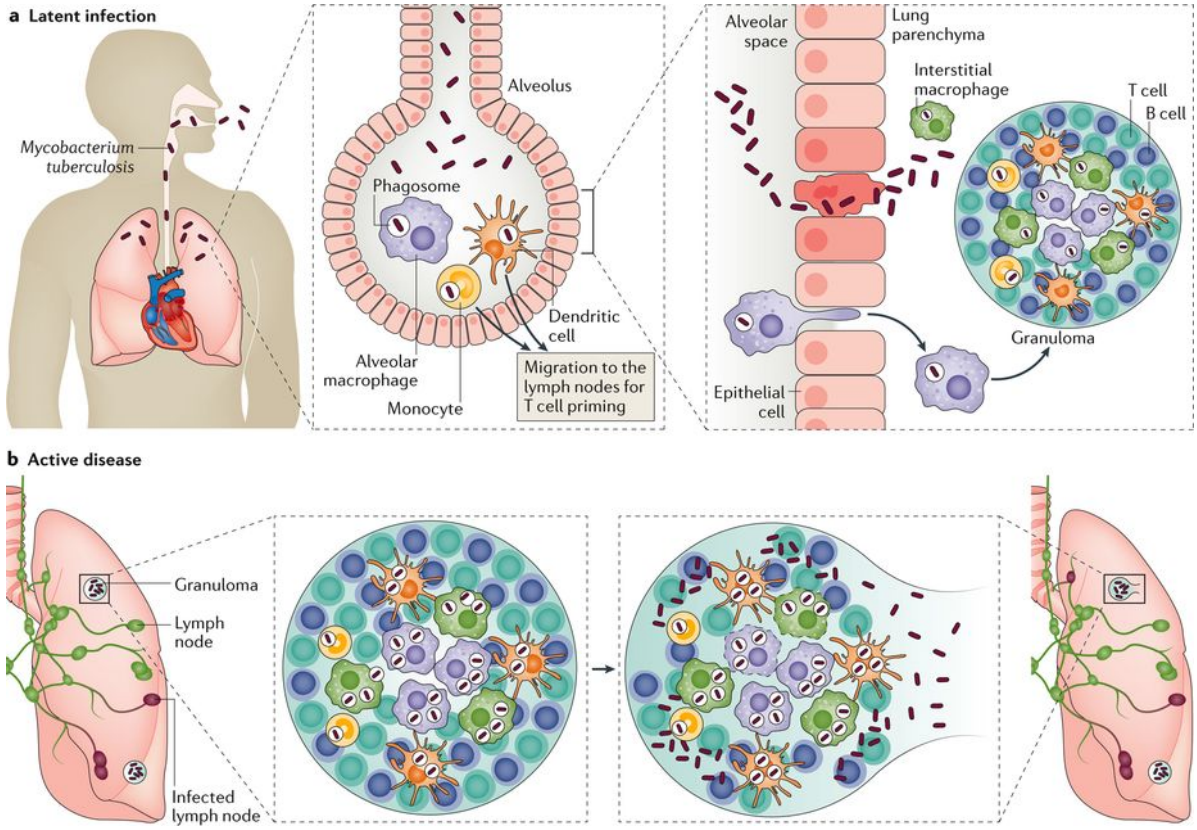

Figure 1.6. *Mycobacterium tuberculosis* infection.

(A) Infection begins when MTB is inhaled into the lungs and encounters resident alveolar macrophages in the alveolar space. If the bacteria are not eliminated, MTB invades the lung interstitial tissue and either DCs or inflammatory monocytes transport the bacteria to pulmonary DLNs for T cell activation. This leads to the recruitment of immune cells, e.g. T and B cells into the lungs to form a granuloma (120). **(B)** The bacteria replicate within the growing granuloma and if the bacterial load becomes too great the bacteria will escape the granuloma. At this stage, MTB can enter the bloodstream to disseminate to other organs or re-enter the respiratory tract for release. The host is now infectious, symptomatic and is described to have active TB disease (120). Image sourced from Pai et al. (120).

A granuloma contains a central mass of macrophages infected with bacteria, stimulated macrophages that have differentiated into multinucleated giant cells, epithelioid cells, and neutrophils. The granuloma is encased by a peripheral fibrotic capsule formed by lymphocytes, predominantly $CD4^+$ T cells, but also contains $CD8^+$ T cells, B cells and fibroblasts (121). A depiction of the tuberculous granuloma can be seen in Figure 1.7. In the granuloma T cells have a decreased capacity to present antigens (Ags). In cases of disease reactivation or in the failure of isoniazid prevention therapy, active bacterial replication and insufficient clearance maintains inflammation and increases cellular influx, leading to granuloma growth (57, 120). Inability to clear dead cells within the granuloma causes the necrotic caseous core (103).

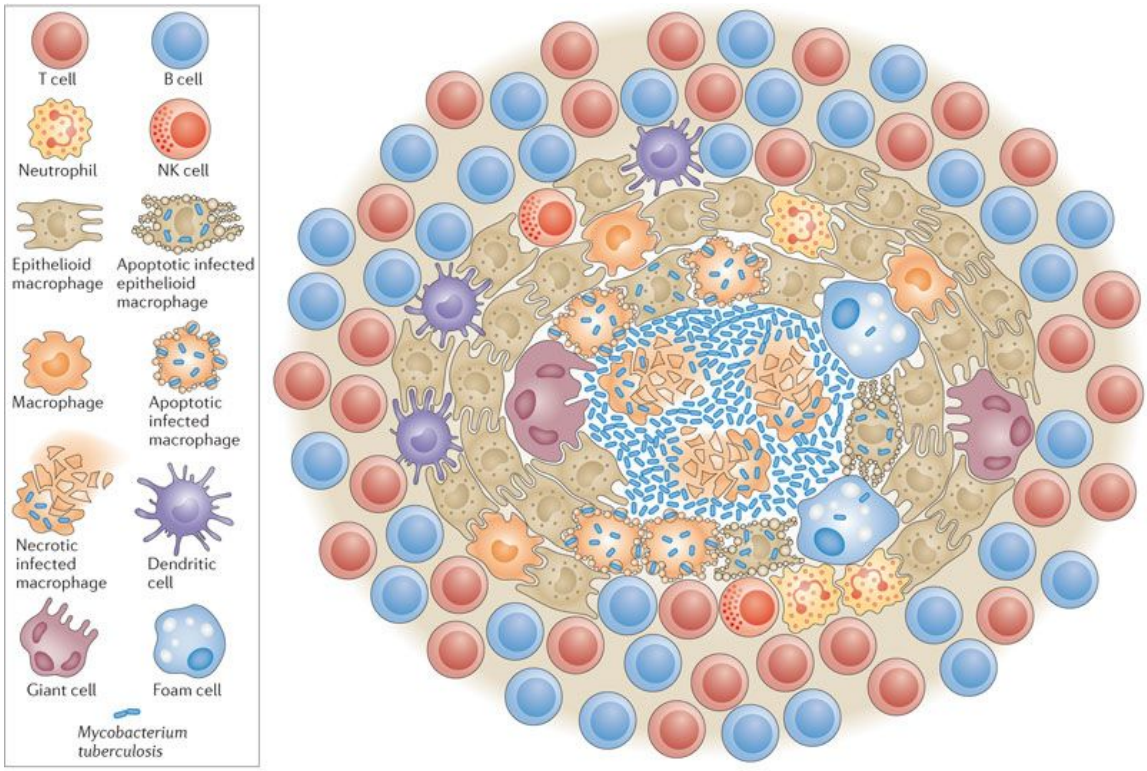

Figure 1.7. Representation of a tuberculous granuloma formed by *M. tuberculosis* bacteria and cells of the immune response.

The bacteria are situated in the core of the granuloma amongst necrotic infected macrophages. The macrophages are surrounded by apoptotic infected epithelioid macrophages, granuloma macrophages which have fused into multinucleated giant cells, or differentiated into foam cells. Foam cells which are characterized by lipid accumulation are most frequently located at the rim of the necrotic centre of a mature tuberculous granuloma. Surrounding the infected core are uninfected epithelioid macrophages, macrophages, neutrophils. Lining the edges of the granuloma are T cells, B cells, DCs, natural killer cells, fibroblasts (not shown) and cells excreting extracellular matrix components (not shown). Image sourced from Ramakrishnan et al. (121).

1.6.2 Human immune responses against Buruli ulcer

The human immune responses to infection with *M. ulcerans* are not as well investigated as MTB. Observations to date show that during *M. ulcerans* infection of humans, untreated lesions display an increased expression of TNF-α, IFN-γ and IL-10 cytokine mRNA (122). TNF-α and IFN-γ are both cytokines of the T-helper (T_h)-1 immune response (114, 115), indicative of an acute local inflammatory response. IFN-γ is highly expressed in BU patients with both developed ulcers and early lesions, in comparison to healthy controls (122). This implies an early onset of a T_h1 immune response. IL-10 is an immuno-regulatory cytokine produced by B-cells and T-helper T_h2 cells, which down-regulates T_h1, T_h2 and T_h17 responses (123). Disease progression may be enhanced by the presence of IL-10 (124). Ulcerative lesions without granulomas have increased expression of IL-10 and higher bacterial loads (124, 125). Once granulomas form, there is a higher expression of IFN-γ and other proinflammatory cytokines, however IL-10 is not present (122). IFN-γ is also highly expressed in healed ulcers alongside low IL-10 levels (126). This suggests that the suppression of the immune response enables bacterial proliferation and healing may be linked to the onset of a T_h1 immune responses. In a mouse model of *M. ulcerans* infection, *M. ulcerans*-specific $CD4^+$ T cells are generated in the draining lymph nodes early in infection (127). These cells migrated to the site of infection, however persisting infection led to the local depletion of recruited cells. This depletion of immune cells did not increase mice susceptibility to systemic co-infection with *Listeria monocytogenes* (127), showing that this immune cell depletion was localised to the site of *M. ulcerans* infection.

Gooding et al. demonstrated that patients with a current or past BU possessed T cell anergy towards *M. ulcerans* (128). These patients lacked the normal proliferative response of lymphocytes and IFN-γ production. Eighty-one percent of patients showed antibody recognition to *M. ulcerans,* indicative of ineffective phagocytosis, bacterial escape prior to T cell presentation or affected T cell responsiveness (128). A follow up study by Gooding et al. showed that individuals with a history of BU produced a T_h2 cytokine profile rather than the T_h1 response seen in unaffected controls (129). The household exposed control group produced few T_h2 cytokines, coinciding with a higher T_h1 response (129). Gooding et al. observed the cytokine expression from a patient among the unaffected yet exposed group, who later developed BU (130). Initially, the patient's T_h1 response mirrored those of the unaffected group. After the ulcer was excised the patient's cytokine profile shifted from a T_h1 to a T_h2 response, similar to individuals who currently or previously had BU, suggesting the T cell anergy is an acquired response (130). Studies have shown that T cell responsiveness during infection can be affected by the presence of *M. ulcerans* exotoxin mycolactone (131-133) and that this T cell anergy towards *M. ulcerans* can remain after infection has cleared. Mycolactone and its effects will be discussed further in section 1.6.2.1.

1.6.2.1 *M. ulcerans* lipid toxin, mycolactone

In the early 1960s, pathologists suggested that *M. ulcerans* may produce a toxin, as tissue destruction was observed distal to the dominant burden of bacteria within patient lesions (134). This hypothesis was confirmed when a cytotoxin was found in *M. ulcerans* culture filtrates (135, 136). Initially believed to be a phospholipoprotein-polysaccharide complex (137), it was subsequently shown to be a cytotoxic polyketide lipid (138). The name mycolactone was derived from its mycobacterial origin and its characteristic 12-membered lactone ring (138). The molecule has a mass of approximately 740 Da and is characterised by an invariant upper chain and variable lower acyl side-chain (see discussion below) (40, 83, 138-141). Mycolactone was the first polyketide known to act as a virulence factor for a human pathogen (142).

The pMUM001 plasmid

The ability of *M. ulcerans* to produce mycolactone is attributed to the acquisition of a plasmid, pMUM001 (Figure 1.8). The pMUM001 plasmid (174,155 bp in size) comprises 81 coding DNA sequences (CDS), six of which are involved in mycolactone biosynthesis. These six genes *(mlsA1, mlsA2, mlsB, mup038, mup045* and *mup053*) comprise 60% of the plasmid (40). The remainder of the plasmid contains insertion sequence elements, plasmid replication genes and CDS for hypothetical proteins (39, 40).

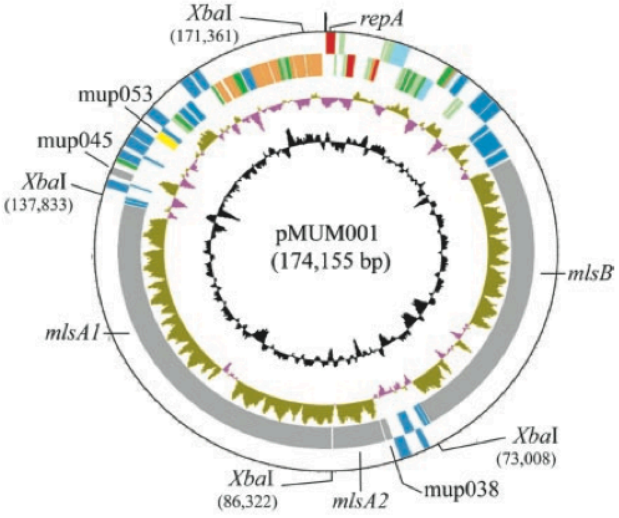

Figure 1.8. Circular representation of pMUM001.

Sourced from Stinear et al. (40), this image depicts an outer black circle representing size in base pairs. The next two circles depict forward and reverse strand protein-coding DNA sequences respectively. Functional classification by colour are red: replication; light blue: regulation; light green: hypothetical protein; dark green: cell wall and cell process; orange: conserved hypothetical protein; cyan: insertion sequence elements; yellow: intermediate metabolism; grey: lipid metabolism. The following inner circle represents the GC skew. The final circle signifies G + C content. Mycolactone biosynthesis clusters and *Xba*I sites are shown.

Polyketide synthases

The genes *mlsA1, mlsA2* and *mlsB* encode three type I polyketide synthases (PKS) (40). Type I PKS are multienzyme complexes that synthesize polyketides (143). MLSA1 (1.8 MDa) and MLSA2 (0.26 MDa) jointly contain nine discrete enzymatic modules (40). The MLSB PKS (1.2 MDa) comprises seven distinct modules (40). The domains present within each module are highlighted in Figure 1.9.

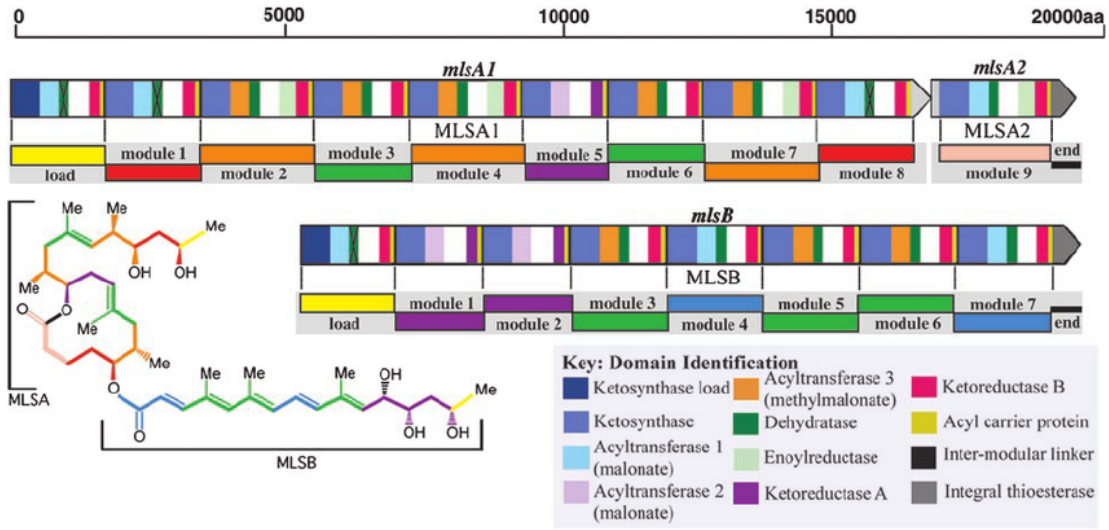

Figure 1.9. Domain and module organization of the three PKS genes and the structure of their polyketide product: mycolactone.

Each domain is represented by a different colour and labelled in the key. Modules are labelled below each gene. White blocks indicate interdomain regions of 100% identity. Modules are colour-coded to represent >98% identity both in function and sequence. *mlsA1* and *mlsA2* produce the PKS which forms the mycolactone core and *mlsB* produces the PKS which creates the side chain. Each module is responsible for the synthesis of the respective colour co-ordinated mycolactone structure (40). Image sourced from Stinear et al. (40).

Mycolactone biosynthesis

As previously mentioned, *M. ulcerans* produces a macrolide lipid toxin called mycolactone (138). Macrolides are characterized by the presence of large lactone rings and belong to the class of organic compounds called polyketides. The polyketide synthases, MLSA1 and MLSA2, co-synthesize the mycolactone core and upper side chain by progressive decarboxylative condensation reactions (40). Each module is responsible for a condensation reaction that incorporates either an acetate or propionate subunit (40). Chemical variation at each condensation step is introduced by different combinations of functional domains within a module, as illustrated in Figure 1.9, MLSB produces the acyl side chain by seven progressive decarboxylative condensation reactions (40). An accessory type III ketosynthase encoded by another plasmid gene (*mup045*) putatively catalyses the ester bond formation linking the

core and upper side chain to the acyl side chain (39). The gene, *mup053*, encodes a P450 hydroxylase, with a potential role in the hydroxyl group addition at C-12' of the acyl side chain (144). *Mup038* encodes a type II thioesterase, with a predicted proof-reading function during mycolactone synthesis (39).

At least seven mycolactone structural variants (A to G) have been reported, distinguished by side chain group modifications (83, 138-141). Mycolactone A/B, present in African *M. ulcerans* strains, is notably the most cytotoxic (138). Mycolactone C differs by a lack of hydroxylation at C-12' of the side chain and is predominantly produced by Australian strains of *M. ulcerans* (139). Mycolactone E and F are created by mycolactone-producing mycobacteria from frogs and fish, respectively (145). Mycolactone G is a biosynthetic engineered form of mycolactone expressed by a plasmid cloned into *M. marinum* (141). Side chain variants have differing biological potencies (138, 141, 146, 147).

Effects of mycolactone

Mycolactone is present in the supernatant of *M. ulcerans* cultures, indicative of cellular export or cell wall-interaction leading to dispersal from the cell (138). Mycolactone has proven to be the major virulence determinant during *M. ulcerans* infection and some key modes of action and the cellular target(s) of mycolactone have recently been described (131, 132). Guinea pigs injected with purified mycolactone develop pathology reminiscent of BU (138). Higher mycolactone concentrations induce cellular apoptosis and necrosis in different cell types (148), such as J774 mouse macrophages (149), human adipocytes (150) and human keratinocytes (151). Mycolactone causes cell cycle arrest in the G_1 phase and cell cytopathicity due to cytoskeletal rearrangement (152). The toxin disrupts DC function, suggesting the obstruction of primary immune response induction and recruitment of inflammatory cells (153). Mycolactone also plays a role in the persistence of *M. ulcerans* infection via the inhibition of phagocytosis and induction of apoptosis in recruited antigen-presenting cells (APC) (153, 154). Studies have identified that mycolactone mediates this cytotoxic effect by inhibiting the Sec61 translocon; an endoplasmic reticulum membrane protein translocator (131, 132). Mycolactone directly targets the alpha subunit of the Sec61 translocon to block the production of secreted and integral membrane proteins. A downstream effect of the inhibition of the Sec61 translocon is the activation of an integrated stress response within cells that is independent from endoplasmic reticulum stress sensor activation (131). Chronic stress activation without remediation enhances autophagy and cell apoptosis (131). The inhibition of the Sec61 translocon affects T cell activation, particularly a selective subset of secretory proteins including key signal-transmitting receptors and adhesion molecules (132). The toxin has been attributed to the distortion of normal T cell function and cytokine production. Guenin-Macé et al. previously identified that mycolactone affects T cell homing by silencing the mRNA *let-7b* and disrupting the regulation of homing ligands CD62L and CCR7 (155). The depletion of T cell homing

to peripheral lymph nodes affects B cell activation and migration from the lymphatics (155). Distorted cytokine profiles have been observed during *M. ulcerans* infection, due to impaired T cell responsiveness (133). In particular, inhibition of IFN-γ production by T cells and macrophages and inhibition of TNF production by monocytes in humans have been identified (156, 157).

1.7 Correlates of protection

As mentioned previously, there is some cross-over in immune responses to these two diseases, likely due to their genetic similarity. Some immune responses have been linked to protection in both MTB and *M. ulcerans*, however MTB is predominantly an intracellular pathogen and *M. ulcerans* – though it has a short intracellular phase – is predominantly an extracellular pathogen. This difference, as well as the production of mycolactone by *M. ulcerans*, suggests that there may be slight variances in the immune responses required for protection against these two diseases.

1.7.1 Correlates of protection against *M. tuberculosis*

The immune correlates of protection against MTB are not clearly defined. T_h1 responses are implicated in the control of disease and T_h2 responses in susceptibility (158). The presence of $CD4^+$ T cells and IFN-γ appear to play a role in infection control, as their absence strongly decreases the host's ability to manage bacterial replication (159-161). $CD8^+$ cells appear to also play a role in control of MTB infection, as the removal of $CD8^+$ T cells by antibody depletion in knock-out mouse strains have shown an increased susceptibility to infection. In humans however, $CD8^+$ T cells can destroy intracellular mycobacteria via the release of the antimicrobial peptide granulysin but this molecule is not present in mice (162). Therefore, in mouse models of TB $CD8^+$ T cells do not play as important a role in control of infection. MTB-specific $CD8^+$ T cells are involved in cytokine production, particularly IFN-γ and TNF which suggests they play a supportive role to $CD4^+$ T cells in maintaining the cytokine environment during infection (115, 163). $CD8^+$ T cells may also be capable of recognising infected cells that are not recognised by $CD4^+$ T cells. Studies have shown that macrophages downregulate Major Histocompatibility Complex (MHC) class II expression through TLR-2-dependent inhibition with exposure to MTB lipoproteins (including LpqH, LprA, LprG (164-166)) and glycoproteins, causing them to be unrecognisable by $CD4^+$ T cells (167, 168). In latently infected individuals, MHC class I $tetramer^+$ $CD8^+$ T cells specific for MTB have been identified, which suggests that $CD8^+$ cells play a role during latency. Since the addition of T_h17 cells to the T_h1/T_h2 paradigm, many studies have alluded to the potential role for IL-17 in protection (169). Studies in mice lacking the IL-17A receptors are unable to control MTB infection (170). Few studies have explored the role of B cells and humoral responses to TB, however mice lacking functional B cells appear to have reduced control of MTB infection (171-173). A recent study showed that MTB-specific antibodies can decrease bacterial load during latent MTB infection (174).

1.7.2 Correlates of protection against *M. ulcerans*

There are no definitive correlates of BU protection however some studies suggest that healing is linked to a T_h1- type response (129, 175, 176). In addition, disease is exacerbated in the downregulation or absence of a T_h1 responses in BU affected humans and in animal studies (122, 124, 125, 177, 178). A recent study has shown that IFN-γ is critical in the activation of early host immune responses against *M. ulcerans* in mice (177). IFN-γ knock out mice succumb to BU significantly faster than mice with functioning IFN-γ production, suggesting that IFN-γ is required for control of *M. ulcerans* infection (177). A study in Ghana of human *iNOS* and *ifn-γ* gene polymorphisms showed a link between genotype and susceptibility to *M. ulcerans* (179). Antibody responses to *M. ulcerans* can be detected in serum of BU patients and household contacts but it is not known if these antibodies are protective (128, 180).

Healing of Buruli ulcer

Healing of BU ulcers have been studied in some mice, guinea pig and pig models of infection. During infection the BU site contains oedematous and focally necrotic dermis with diffuse infiltration of neutrophils and histiocytes (181, 182). Bacteria are mainly present in clumps within the necrotic foci but also identified co-localised with phagocytic cells (182, 183). Necrotic areas expand progressively in the beginning of infection leading to an increase in cells showing apoptotic morphology and epidermal destruction (183).

Active tissue healing is indicated by sloughing of the mycobacteria-rich necrotic tissue, accumulation of fibroblasts in the subcutaneous tissue, extensive neovascularisation and granulation tissue that slowly replace the initial acute cellular infiltrate (184).

As healing progresses, there is ongoing skin re-epithelialisation shown by the formation of an eschar comprising degeneration epidermis and collagen over the ulcerated wound accompanied by thickening of the adjacent epidermal layer (184). Few bacilli remain scattered throughout the granulation tissue, found mainly by the wound surface (181). In the guinea pig model of infection, by the end of the experimental infectious period, re-epithelialisation was complete but increased presence of collagen fibres and epidermal hyperplasia (elongation of rete ridges) remains (184).

1.8 Diagnosis

As will be described further in this section, the WHO has guidelines for the diagnosis of both TB and BU.

1.8.1 Diagnosis of tuberculosis

The two widely used diagnostic methods are i) tuberculin skin test (TST), utilizing purified protein derivatives (PPD) injected under the skin to elicit an immune reaction; and ii) interferon gamma release assay (IGRA), which mixes patient blood with synthetic antigenic peptides (ESAT-6, CFP-10, TB7.7) to identify an IFN-γ response. Chest X-rays and sputum smears are utilized to confirm active disease in the lungs (185). Sputum samples can be analysed via microscopy or loop-mediated isothermal amplification (TB-LAMP) (186). In 2010, the WHO supported the use of the Xpert MTB/RIF assay to as the primary assay to diagnose TB and rifampin resistance in individuals with signs and symptoms of TB (187). Since 2019, the WHO has endorsed the use of the lateral flow lipoarabinomannan assay (Alere Determine TB-LAM) to detect TB infection in HIV infected individuals, particularly those with low $CD4^+$ T cell counts (58, 188).

1.8.2 Diagnosis of Buruli ulcer

The WHO has proposed global guidelines for the diagnosis and treatment of BU. For laboratory diagnosis, the WHO requires two positive results from the following four tests (189): microscopic examination of a smear for acid-fast bacilli, a positive culture of *M. ulcerans*, histopathological study of excised diseased tissue or positive PCR to detect the high copy insertion sequence, IS*2404* or IS*2606*, present in *M. ulcerans* (95). A TaqMan real time PCR assay was later developed to detect IS*2404* and IS*2606* from a wider range of clinical specimens (190). This newer method improved the specificity and sensitivity for *M. ulcerans* diagnosis (190).

Generally, health professionals in highly endemic areas can readily diagnose BU infections. Due to international travel, some cases of BU have been misdiagnosed and mismanaged. Early nodular lesions can be misdiagnosed as other subcutaneous infections such as fungal infections, boils, lipomas or insect bites (189, 191).

1.9 Treatment

Both infections respond to antibiotic treatments (192, 193). While the antibiotic regimens are different, in both cases treatment of infections is prolonged and can be difficult to manage, particularly in isolated and rural areas (194-197).

1.9.1 Treatment of tuberculosis

Treatment involves the six-month administration of three to four “first-line” antibiotics: rifampin, isoniazid, pyrazinamide, streptomycin or ethambutol (193). In some cases, the first-line antibiotics may fail, and second line antibiotics are required. These include aminoglycosides (eg. amikacin, kanamycin), polypeptide antibiotics, fluoroquinolones, macrolides and linezolid (198). TB infections resistant to two

or more first line antibiotics, termed multi-drug resistant TB (MDR-TB), are increasing world-wide. The greatest incidence occurs in India, China and Russia, as depicted in Figure 1.10. Extensive MDR-TB (XMDR-TB) due to resistance to second-line antibiotics has increased in the last decade (199).

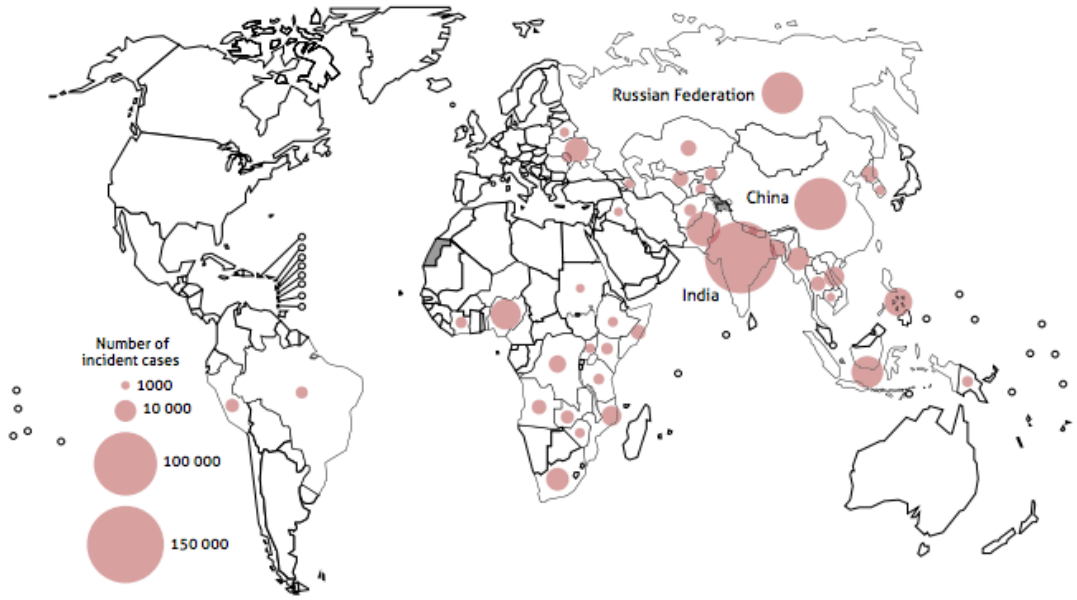

Figure 1.10. The global distribution of multidrug-resistance (MDR)/rifampicin-resistance (RR) in countries with at least 1000 incident cases, in 2018.

High incidence of MDR/RR cases occur in India, China and Russia. Image sourced from the WHO (58).

1.9.2 Treatment of Buruli ulcer

The WHO recommended treatment for BU is eight weeks of chemotherapy with oral rifampicin (daily) and clarithromycin (twice daily) (200). In some cases, the excision of pre-ulcerative lesions without drug treatment has prevented the development of disease (201). Antibiotic treatment is sometimes augmented with surgery for progressed BU. Combination antibiotics alone is an effective treatment if disease is detected early (192, 202, 203). At present there are no clinical cases of antibiotic resistance, however three rifampicin-resistant *M. ulcerans* mutants were isolated after rifampicin monotherapy in mice (204). There are no preventative treatments for *M. ulcerans* but studies exploring vaccine development will be discussed in section 1.13.2.

1.9.3 Alternative treatments of Buruli ulcer

The use of intramuscular streptomycin has been previously recommended, however treatment was difficult to administer and caused ototoxicity (205). While there are no clinical cases of *M. ulcerans* antibiotic resistance yet, some studies have explored the use of alternative therapeutic drugs to treat BU

infection. Some studies have shown avermectins have bactericidal capabilities (206, 207). Omansen et al. have shown that the use of avermectins, typically used for the treatment of helminths and parasites in humans and animals, can work synergistically with oral rifampicin to reduce *M. ulcerans* viability over eight weeks (206). Avermectins are inexpensive, widely available and well tolerated. Another study has generated neutralising antibodies against the mycolactone toxin and shown that these antibodies are capable of rescuing mammalian cells from apoptosis in *in vitro* culture (208). Antibodies against mycolactone are not typically found in humans or animals during BU infection (209). Neutralising antibodies against mycolactone could be utilised as another alternative or addition to antibiotic treatment (208).

1.10 Prevention of disease caused by *M. ulcerans* and *M. tuberculosis*

The prevention of these mycobacterial diseases can be accomplished through physical barrier prevention. As discussed later (section 1.12.1), prevention of disease by prophylaxis is only applicable to TB.

1.10.1 Physical prevention of *M. tuberculosis* transmission and infection

As MTB is spread via aerosolised bacteria, wearing masks or other filtered breathing apparatus may prevent the inhalation of saliva containing MTB (210, 211). This measure may be quite costly and difficult to enforce, as infected individuals are not easily identified and wearing a mask can hinder common daily activities.

1.10.2 Physical prevention of *M. ulcerans* transmission and infection

Transmission of *M. ulcerans* is incompletely understood, however case reports indicate infection occurs via introduction of the bacteria into the subcutaneous tissue, possibly following micro-trauma that breaches the skin (90, 99, 101). Several studies have shown an association between the proximity of the home or farm site to bodies of water and increased risk of BU (212-216). As *M. ulcerans* can be found close to bodies of water (in the soil, water and aquatic insects) (100, 217, 218), BU may be prevented by staying away from open areas of water, especially stagnant water in endemic areas. Protective clothing has been shown to be associated with decreased risk of *M. ulcerans* infection (212-215). Fully covering the extremities, such as arms and legs, with long-sleeved clothing may prevent *M. ulcerans* from entering through any nicks or cuts on the skin. In South East Australia, mosquitoes are likely mechanical vectors of *M. ulcerans* (101). The use of insect repellents and mosquito netting in combination with protective clothing may protect from *M. ulcerans* infection.

1.11 Vaccines to prevent tuberculosis and Buruli ulcer

1.11.1 Role of vaccination

The purpose of vaccination is to increase immune responses against a pathogen(s). The vaccine is used to prime or train the immune response, in particular the adaptive immune response, to respond to a particular pathogen (219-222). In instances of subsequent pathogen infection, successful vaccination enables the immune system to mount a more rapid, augmented, and targeted response to prevent the onset of disease and/or decrease the duration of infection (219-222).

1.11.2 Innate immune response

The innate immune system is comprised of defenses against infection that can immediately activate upon pathogen invasion (220). The innate immune system acts as a barrier to prevent the invasion of micro-organisms into your body or limit their spread throughout the body. Components of the innate immune system include physical barriers, such as skin and body hair; defense mechanisms such as secretions including mucous, gastric acid, saliva, tears; and general immune responses such as complement, inflammation and non-specific cellular responses (220).

Cells of the innate immune response include phagocytes, macrophages, neutrophils, mast cells, eosinophils, natural killer (NK) cells and DCs (220). These cells typically patrol the entire body and depending on cell type are capable of engulfing foreign pathogens, killing infected cells, producing cytokines to signal to and recruit other cells, and producing chemokines to mediate inflammation during infection (220, 223). DCs act as a link between the innate and adaptive immune system, by presenting antigen (Ag) to cells of the adaptive immune response (224, 225). The activation of the adaptive immune response is described further in section 1.11.3. The innate immune system is non-specific and targets any pathogen, specifically pathogen-associated molecular patterns from a pathogen it identifies as foreign or “non-self” (220). Unlike the adaptive immune response, the innate immune response cannot easily be primed to respond specifically to pathogens (226).

1.11.3 Adaptive immune response

In contrast to the innate immune system, which acts on the identification of general pathogen associated molecular patterns, the adaptive immune response is activated by contact with a specific Ags, such as a protein or peptide, found on a pathogen (220). The adaptive immune response is capable of remembering these Ags and therefore remembering the pathogen to enhance the immune response upon repeated exposure. This phenomenon is known as “immunological memory” (227). Compared to the innate response, the adaptive immune response is much slower to respond to infection however the adaptive response is much more targeted and specific to the invading pathogen (220).

The adaptive immune response primarily relies on two main cell types, B cells and T cells (227). Naïve B cells upon exposure to Ag can differentiate into memory B cells and effector B cells, known as plasma cells (228). Plasma cells secrete antibodies that can bind directly to Ags to neutralise and/or identify free pathogens in circulation (220). B cells also express a receptor, called the B cell receptor, to assist with Ag binding, as well as internalisation and processing of the Ag (220). B cell receptors also play a role in initiating signalling pathways, leading to cytokine release to communicate with other cells of the immune system (227, 228).

T cells can be further divided into $CD4^+$ or $CD8^+$ T cells based on whether they express the CD4 or CD8 T cell receptor (227). T cells that express both receptors are removed during thymic development. T cell receptors can only recognize Ags that are presented on certain molecules called Major Histocompatibility Complex (MHC) class I and class II (229). These MHC molecules are membrane-bound surface receptors on APCs like DCs (229). $CD4^+$ T cells recognise MHC class II and $CD8^+$ T cells recognise MHC class I (230). Mature T cells recognise only foreign antigens combined with self-MHC molecules in order to mount an appropriate immune response (229). The majority of $CD4^+$ cells are helper cells that aid in the activation of cytotoxic T cells and B cells as well as other immune cells (227, 231). Some $CD4^+$ cells also expressed CD25 and are known as regulatory T cells, which help distinguish between self and non-self molecules to reduce the risk of autoimmune disease (232). Cytotoxic T cells express CD8 and are responsible for removing pathogens and infected host cells (233).

The adaptive immune response can also be described as humoral or cell-mediated (234). This is dependent on the functions of B and T cells, as described above. Humoral immunity is immunity from serum antibodies produced by effector B cells (234). Cell-mediated immunity refers to the immune response being directed by T helper and cytotoxic T cells (234).

1.11.4 Vaccine components

Vaccinations often incorporate an Ag or immunogenic portion of the pathogen (e.g. protein, carbohydrate or whole cell) to direct an immune reaction to target the pathogen (219-222). These immunogenic moieties may or may not be used in conjunction with adjuvants, which help to boost the immune response (235, 236).

There are many different forms of vaccines approved for use. These include live-attenuated, inactivated, toxoid, subunit and conjugate (221, 237). Some examples of these are the tetanus toxoid conjugate vaccine (238), live-attenuated vaccinia vaccine (239), live-attenuated measles, mumps and rubella vaccine (240), inactivated hepatitis A vaccine (241, 242), and hepatitis B (243, 244) and human papilloma virus conjugate/subunit vaccines (245, 246). Some studies are examining the potential of

DNA-based vaccines against human diseases. Presently, there are no approved DNA-based vaccines for humans, but some DNA-based vaccines have recently been licensed for veterinary use (247-249).

1.12 Approved vaccines against mycobacterial pathogens

1.12.1 *M. bovis* 'bacille Calmette Guérin' (BCG) vaccination

The most widely used mycobacterial vaccine is the live-attenuated vaccine, *M. bovis* 'bacille Calmette-Guérin' (BCG) (250-252). BCG induces cross-protective immune responses against MTB. *M. bovis* is closely related to MTB. A key distinguishing feature between MTB and BCG is that BCG strains are missing a critical virulence region present in MTB, a region of difference (RD) termed RD1 (253-256). RD1 spans the ESX-1 Type VII secretion system, and protein effectors secreted by this system are critical for MTB pathogenesis (257-259), including the well-described T cell antigens ESAT-6 and CFP-10 (260-266). As a vaccine, BCG protects children from severe disseminated forms of TB, such as meningitis (267), yet protection begins to wane after 10-15 years (268). When given later in life, the efficacy of BCG varies in different regions of the world (250). The vaccine is between 0-80% effective at preventing pulmonary TB in adults (269). This variation is incredibly problematic as the lowest levels of protection are generally in regions with the highest incidence of TB (250). A recent study has shown a promising improvement to the efficacy of BCG in non-human primates when BCG is administered intravenously rather than intradermally (270). BCG does not cause disease in healthy individuals, however as it is live-attenuated it can potentially replicate and cause disease in immuno-compromised individuals (271). As a result, the WHO has adjusted the vaccination guidelines to prevent HIV infected children from being administered the BCG vaccine (272).

Using BCG to protect against BU was first tested in humans in 1969 (273), and since then several reports have cited the potential for BCG as a cross-reactive vaccine against BU (274-276). To date, studies on the effectiveness of BCG denote little or no protection against BU (277, 278) even with a BCG boost (279), yet BCG based vaccines continue to be pursued.

1.13 Vaccine developments

As previously mentioned, there is currently no effective vaccine against pulmonary TB, especially in adults, and no vaccine against BU. There are many TB vaccine candidates at the pre-clinical stage but very few have entered clinical trials (280, 281). Recent vaccines in clinical trials will be described further in this section. BCG still remains the most effective vaccine. Only a few attempts have been made to create a vaccine against BU and they will be described further in this section. No BU vaccine candidates have entered clinical trials.

1.13.1 Vaccination developments against *M. tuberculosis*

The increase of XMDR-TB suggests that antibiotic therapy is not sustainable. An alternative way to reduce TB incidence would be to vaccinate individuals to either prevent infection or prevent the onset of active disease. This is supported by a mathematical model devised by Lietman and Blower to predict the effect of vaccination on TB incidence (282). They calculated that if a post-exposure vaccine (inducing life-long immunity) is administered to 88% of LTBI patients and it prevents 50% progressing to active disease, after about 30 years TB incidence would halve from 200 cases per 100,000 individuals to 100 cases per 100,000. Further modelling predicted that post-exposure vaccination would produce the greatest short-term effect (282). However, pre-exposure vaccination in 88% of newborns with a vaccine that blocks 50% of cases from progressing to active disease may eventually be more effective in the long-term (>50 years after first vaccination).

There are currently three main vaccine strategies: i) booster for BCG vaccination; ii) replacement for BCG vaccination; and iii) therapeutic vaccination (280, 281, 283-285). Pre-clinical testing of putative vaccines utilise murine, guinea pig lung and primate lung challenge models. There are many putative vaccines at pre-clinical stages but few vaccines have progressed to human clinical trials (280, 281, 283-285). The types of vaccines recently in clinical trials include adjuvanted subunit, viral vectored, whole cell recombinant, whole cell fragmented and recombinant, as described in Table 1.1.

Table 1.1. Summary of *M. tuberculosis* vaccines recently involved in clinical trials.

Description of vaccine components and stage of clinical trial.

Vaccine type	Name	Description of components	Stage of clinical trial[a]
		Booster	
Viral vectored	MVA85A	Live viral vector that cannot replicate in humans. An intradermal vaccine comprised of a recombinant strain of modified vaccinia virus Ankara expressing the *M. tuberculosis* antigen, Ag85A (286).	Phase II
Viral vectored	Ad35 (Aeras 402)	Non-replicating adenovirus vector expressing a fusion protein which combines MTB Ag85A, Ag85B and TB10.4 antigens (287).	Phase II (terminated)
Viral vectored	Ad5Ag85A	Recombinant adenovirus (serotype 5) that expresses MTB antigen, Ag85A (288, 289).	Phase I
Viral Vectored	TB-FLU-04L	A replication-deficient H1N1 strain A/Puerto Rico/8/34 influenza virus expressing Ag85A and ESAT-6 (290).	Phase IIa
Whole cell	DAR-901	Based on the SL172 vaccine, which was derived from an inactivated non-tuberculous mycobacterium, *Mycobacterium obuense* (291).	Phase IIb
Cell Fragmented	AEC/BC02	Freeze-dried recombinant vaccine expressing Ag85B and fusion protein ESAT-6 and CFP-10 in addition to CpG (from BCG) and an alum salt-based adjuvant (292).	Phase I
Subunit	M72/AS01E	Formed from a fusion of two MTB antigens, Mtb32A and Mtb39A (M72), and an adjuvant combining immunostimulants with liposomes (AS01E) (293, 294).	Phase IIb
Subunit	H1/IC31	Comprised of a hybrid containing ESAT-6 and Ag85B MTB proteins, plus IC31 adjuvant. IC31 is formed by cationic protein polyaminoacid KLK and oligodeoxynucleotide ODN1a (295).	Phase IIa (terminated)
Subunit	HyVac4	Comprised of a hybrid containing TB10.4 and Ag85B MTB proteins, plus IC31 adjuvant (296).	Phase IIa (terminated)
Subunit	H56/IC31 (Aeras 404)	Comprised of a fusion protein formed by Ag85B, ESAT-6 and MTB latency-associated protein Rv2660c, plus IC31 adjuvant (297).	Phase IIb

[a]Status as of August, 2019 (58).

Table 1.1. Summary of *M. tuberculosis* vaccines recently involved in clinical trials (continued).

Description of vaccine components and stage of clinical trial.

Vaccine type	Name	Description of components	Stage of clinical trial[a]
Booster and Priming			
Viral Vectored	ChAdOx185A	Simian adenovirus expressing Ag85A. Has been used in a prime-booster regime with MVA85A vaccine (298).	Phase I
Subunit	ID93/GLA-SE	Comprised of ID93, a fusion of four MTB antigens (Rv2608 Rv3619, Rv3620 and Rv1813) in combination with glucopyranosyl lipid adjuvant-stable emulsion GLA-SE) (299).	Phase IIa
Therapeutic			
Whole cell	Vaccae™	Utilising the whole *Mycobacterium vaccae* cell that has been heat-inactivated (300, 301).	Phase III
Whole cell	MIP/Immuvac	An inactivated non-tuberculosis mycobacterium, *Mycobacterium indicus pranii* (302).	Phase IIa
Cell Fragmented	RUTI®	Composed of detoxified liposomal fragments from MTB (303).	Phase IIa
Priming			
Whole cell recombinant	VMP1002	Recombinant BCG strain expressing listeriolysin, a membrane-perforating enzyme from *Listeria monocytogenes* (304).	Phase III
Whole cell Live-attenuated	MTBVAC	*M. tuberculosis* strain with mutations in *phoP* and *fadD26* genes (305).	Phase IIa

[a]Status as of August, 2019 (58).

1.13.1.1 Booster vaccines

The infant protection afforded by BCG vaccination begins to wane after 10-15 years (268). Booster vaccines are designed to boost immune responses against MTB in healthy adults who have been immunized with BCG. The appeal for designing booster vaccines is that they can supplement BCG, which is still being administered in endemic TB regions and known to be effective against the disease in infants. As these vaccines may be given to pre-exposed individuals with infection at a dormant stage, these formulations typically include proteins expressed during active replication and also latency.

Viral-vectored booster vaccines

MVA85A

It is the first new TB vaccine to enter clinical trials and be tested in infants since BCG (286). MVA85A induces a polyfunctional $CD4^+$ T cell population capable of inducing IFN-γ, IL-2 and TNF-α, plus low $CD8^+$ T cell responses (306). Despite increasing immune responses against TB in healthy previously BCG vaccinated individuals, recent clinical trials confirmed that the vaccine was poorly protective against TB infection (286).

Ad35

The vaccine produced strong $CD4^+$ and $CD8^+$ T cells responses in mice vaccinated intranasally and also when administered as a BCG booster in adult humans (287). However, in an ongoing Phase IIa study, Ad35 induced predominantly $CD8^+$ T cell responses in HIV-negative people with active or newly infected TB (307).

Ad5Ag85A

This vaccine reached Phase I clinical trials, however failed to progress to Phase II (308). Another bivalent version of this adenovirus-vectored vaccine expressing recombinant Ag85A and TB10.4 antigens showed improved protection against pulmonary TB infection in mice (288, 289).

TB-FLU-04L

Utilising the Ag85A and ESAT-6 protein in conjunction with the replication deficient influenza H1N1 virus, this vaccine has completed Phase I trials and is planned for Phase IIa (290). The vaccine was well tolerated and produced local nasal cytokines IL-1ß, TNF-α and IL-2 as early responses to vaccination (310). T cell responses to Ag85A and ESAT-6 peaked at day 21 and no antibodies to influenza were induced (310).

ChAdOx185A

A Phase I trial of ChAdOx185A in BCG-vaccinated adults was completed in the United Kingdom. This trial administered the vaccine intramuscularly, both alone and in conjunction with the MVA85A vaccine in a prime boost vaccine strategy (58, 200, 309). It was found to be tolerable in humans. In mice it has improved the immunogenicity of BCG when given with a follow up MVA85A vaccination (298). A Phase I trial of aerosol administration of ChAdOx185A in BCG vaccinated adults is currently ongoing in Switzerland (58). A Phase IIa study of ChadOx185A and MVA85A given intramuscularly to adults and adolescents was started in Uganda in 2019 (58).

Protein and adjuvant subunit booster vaccines

M72/AS01E

The subunit vaccine, M72 + AS01E is one of the TB vaccines furthest along the clinical trial pipeline. Phase IIa clinical trials indicated that M72 + AS01E was well tolerated, induced high frequencies of multifunctional T cells and boosted distinct T cell responses primed by natural MTB infection (293, 294, 311).

H1/IC31, HyVac4 and H56/IC31

These three subunit vaccines utilize the same adjuvant, IC31. H1/IC31 provided long lasting T_h1 type responses in mycobacterial-naïve and BCG vaccinated individuals (295). These responses can be increased with booster vaccinations. HyVac4/Aeras404 used as a booster vaccine for BCG in a mouse model induces expression of IFN-γ, TNF-α and IL-12 triple positive $CD4^+$ T cells (296). These cells appear to correlate with protection against TB. In a non-human primate model H56/IC31 was safe and tolerated, showing control of latent TB infection (297). An ongoing phase I/IIa trial on safety and immunogenicity of H56/IC31 is being undertaken in HIV-negative, BCG-vaccinated individuals with and without latent TB.

ID93/GLA-SE

This protein-adjuvant vaccine induced strong T_h1 immune responses in naïve mice and guinea pigs and animals previously vaccinated with BCG (299). It was well tolerated and induced T_h1 and T_h2 type responses in BCG vaccinated non-human primates (312). One study showed that ID93/GLA-SE protected against MDR-TB in mice (313). This vaccine is currently in two human trials to evaluate the safety, tolerability and efficacy as a booster and priming vaccine against TB (314).

Whole cell booster vaccines

DAR-901

This vaccine is based on the SL172 vaccine, which was derived from a non-tuberculous mycobacterium, *Mycobacterium obuense* (291). SL172 has been well documented in a phase III trial among HIV-infected adults in Tanzania (291). DAR-901 induced cellular and humoral immune responses to mycobacterial antigens (315), but unlike SL172, did not result in the conversion of the IGRA for TB (316).

Cell fragmented booster vaccines

AEC/BC02

A Phase I study assessing the safety and immunogenicity of the vaccine is ongoing in China (58). In a guinea pig model of TB, it controlled the reactivation of MTB and lowered bacterial load in the lung and spleen (292).

1.13.1.2 Therapeutic vaccines

As BCG is only effective in uninfected individuals, it provides little protection for those infected with latent TB (317). Therapeutic vaccines are designed to prevent the onset of active disease in individuals with a latent TB infection.

Whole cell recombinant therapeutic vaccines

Vaccae™

This therapeutic vaccine is one of the furthest along in clinical trials. Comprising heat-inactivated whole cell *Mycobacterium vaccae*, this vaccine has shown a 72.5% protection rate in Chinese LTBI children, adolescents and adults from progressing to active disease (300, 301). It induces variable IFN-γ and humoral responses. The vaccine has been found to have a significant effect on MDR-TB (318). Phase III trials have shown that oral *M. vaccae* is tolerable and can reduce hepatoxicity of TB drugs, improve sputum conversion by three-fold and reduce treatment length by six-fold (319).

MIP/Immuvac

Mycobacterium indicus pranii shares antigens with *M. leprae* and MTB (302). It has also been tested as a vaccine against leprosy (320). While there was no significant difference in conversion between vaccinated and unvaccinated groups, there was significantly decreased sputum culture conversion at the fourth week compared to the placebo group (302). This may aid in the control of disease transmission.

Cell fragmented therapeutic vaccines

RUTI®

Its purpose is to complete latent TB treatment after a short course of antibiotic therapy. It is capable of inducing T_h1, T_h2, and T_h3 responses, and a shift in monocyte phenotype in mice (303, 321). A Phase I trial administering RUTI subcutaneously was well tolerated and induced MTB-specific cellular and humoral responses (322).

1.13.1.3 Priming vaccines

Priming vaccines are designed to replace the BCG vaccine. Since priming or pre-exposure vaccines are likely to be confronted with actively replicating MTB, Ags for this type of vaccine typically include those expressed during periods of active replication and metabolism.

Whole cell recombinant priming vaccines

VMP1002

This vaccine is currently in Phase II trials measuring the safety and efficacy compared to the BCG vaccine in infants (323). In mice, VMP1002 has shown better protection against TB than the BCG vaccine by stimulating T_h1 and T_h17 T cells (324). VPM1002 was found as safe and stimulated IFN-γ -producing and multifunctional T cells and antibody-producing B cells in BCG-naïve and BCG-immune individuals (304). This vaccine is currently being pursued as a preventative post-exposure vaccine as it is well-tolerated in BCG immunized individuals and protected against TB in post-exposure mouse model studies (324).

MTBVAC

In 2013, MTBVAC became the first live-attenuated MTB vaccine to enter clinical trials (305, 325). This strain of MTB contains mutations in *phoP* and *fadD26* genes (305). PhoP is a transcriptional regulator which controls the expression of many genes, including virulence genes such as ESAT-6 (305). The product of FadD26 is required for the synthesis of cell envelope component, phthiocerol dimycocerosates, which aids in protection of MTB from host defences. MTBVAC is immunogenic and induces lasting $CD4^+$ T responses in neonates (326).

1.13.2 Vaccination against *M. ulcerans*

There is currently no effective vaccine against BU. Some attempts have been made at designing vaccines to elicit immunological protection against *M. ulcerans*, as shown in Table 1.2. Many animal models have been utilised to study disease progression, including guinea pig, primate, pig, armadillo and mouse models, via tail, ear, hock and footpad challenge (101, 125, 181, 279, 327-330), but most studies measuring vaccine efficacy have been performed with mice.

Table 1.2. Summary of putative *M. ulcerans* vaccines tested in murine model of BU infection.

Description of vaccine components and, if applicable, *M. ulcerans* challenge dose and protective efficacy compared to BCG vaccination. Table modified from accepted manuscript (331).

Vaccine type	Description of components	*M. ulcerans* challenge dose	Test for mycolactone production[a]	Challenge model	Efficacy compared to BCG
DNA-based	pCDNA3 vector encoding Hsp65 (332).	10^4 AFB (strain 1615 ATCC35840)	Not mentioned	Tail	Less protective
DNA-based	V1Jns.tPA vector encoding Ag85A (333, 334).	3 x 10^4 AFB (strain 5150) or 10^5 AFB (strain 04-855)	Not mentioned	Footpad	Less protective
DNA-based	Primary vaccination with V1Jns.tPA plasmid encoding mycolactone polyketide domains and boosted with recombinant domain proteins emulsified in Gerbu adjuvant (335).	10^5 AFB (strain 1615)	Not mentioned	Footpad	Less protective
Viral	Vesicular stomatitis virus (VSV) replicon particles expressing *M. ulcerans* codon optimised antigens MUL_2232 and MUL_3720 (336).	30ul of 2.8 x 10^5 CFU/ml stock (8.4 x 10^3 CFU/dose) (strain S1013)	Not mentioned	Footpad	Less protective
Subunit	MUL2232 and MUL3720 adjuvanted with GLA-SE (EM408) (337).	1.5 x 10^6 or 1.5 x 10^5 CFU (strain S1013)	Not mentioned	Footpad	Less protective
Whole Cell	*M. ulcerans* (338).	$10^{6.3}$ or $10^{4.3}$ viable bacteria	Not mentioned	Footpad	Less protective
Whole Cell	*M. marinum* (339).	10^5 bacteria (strain 1615)	Not mentioned	Footpad	More protective[b]
Whole Cell recombinant	*M. marinum* expressing Ag85A (on vector) (339).	10^5 bacteria (strain 1615)	Not mentioned	Footpad	More protective[b]

[a] Identifying whether the bacterial culture used for challenge was assessed for mycolactone production before infection.

[b] Vaccine was more protective than the BCG vaccine, however all mice eventually developed footpad swelling.

Table 1.2. Summary of putative *M. ulcerans* vaccines tested in murine model of BU infection (continued).

Description of vaccine components and, if applicable, *M. ulcerans* challenge dose and protective efficacy compared to BCG vaccination. Table modified from accepted manuscript (331).

Vaccine type	Description of components	*M. ulcerans* challenge dose	Test for mycolactone production[a]	Challenge model	Efficacy compared to BCG
Whole Cell recombinant	*M. bovis* BCG expressing Ag85A (on vector pMV261) (340).	10^5 bacteria (strain 1615)	Not mentioned	Footpad	More protective
Whole Cell recombinant	*M. bovis* BCG expressing Ag85B-EsxH fusion protein Ag85A (on vector pMV261) (341).	10^5 bacteria (strain 1615)	Not mentioned	Footpad	More protective
Inactivated whole cell	Mycolactone-negative *M. ulcerans* (strain 5114) (275).	4 $\log_{10}$ or 3 $\log_{10}$ CFU (strain 98-912)	Not mentioned	Footpad	Less protective
Inactivated whole cell	Mycolactone-deficient attenuated *M. ulcerans* (strain ATCC19423) (342).	10^6 bacteria (strain TMC1615)	Not mentioned	Footpad	Not compared
Inactivated whole cell	Formalin-treated *M. ulcerans* (strain TMC1615) (342).	10^6 bacteria (strain TMC1615)	Not mentioned	Footpad	Not compared
Inactivated whole cell	Dewaxed *M. ulcerans* (strain TMC1615) (342).	10^6 bacteria (strain TMC1615)	Not mentioned	Footpad	Not compared
Phage	Mycobacteriophage D29 (therapeutic vaccine) (343).	5.5 $\log_{10}$ AFB (strain 1615)	Not mentioned	Footpad	Not comparable

[a] Identifying whether the bacterial culture used for challenge was assessed for mycolactone production before infection.

[b] Vaccine was more protective than the BCG vaccine, however all mice eventually developed footpad swelling.

1.13.2.1 Priming vaccines

DNA based vaccines

Researchers have examined the potential for DNA based vaccines targeting conserved *M. ulcerans* proteins. DNA based vaccines incorporating the mycobacterial Ag, Ag85A (333, 334), or the heat shock protein, Hsp65 (332), proved no more effective than the BCG vaccine. Hsp65, is also believed to increase the risk of autoimmune disease in humans due to its strong homology to the human Hsp60 protein. A study by Roupie et al. analysed the potential of vaccination with plasmid DNA encoding *M. ulcerans* mycolactone polyketide domains (335). In this study, mice were vaccinated with plasmid DNA encoding one of nine mycolactone polyketide domains followed by a protein-boost of the corresponding domain mixed with Gerbu adjuvant. The enoyl reductase domain (ER) significantly reduced bacterial load in a footpad challenge model. The acyltransferase with proprionate specificity (ATp) was the only domain that showed significant although modest protection measured as delay to onset of footpad swelling (335). These vaccinations were less protective than the BCG vaccine and did not prevent the eventual onset of disease.

Virus based vaccines

Recombinant virus replicon particles encoding MUL_2232 and MUL_3720 have been examined as a novel vaccine (336). This study also utilised a prime-boost regimen – priming with recombinant replicon particles expressing MUL_2232 or MUL_3720 and boosting with recombinant MUL_2232 or MUL_3720 protein. This vaccine strategy induced strong immune responses but only slightly reduced bacterial load in mouse footpad challenge.

Subunit vaccines

Subunit vaccines comprising recombinant *M. ulcerans* proteins MUL_2232 and MUL_3720 in combination with GLA-SE adjuvant were also tested for vaccine efficacy (337). These recombinant protein vaccines induced strong immune responses, in particular high protein-specific antibody titres. These responses however did not correlate to protection as mice succumbed to *M. ulcerans* infection in a footpad challenge model.

Whole-cell vaccines

Immunisation with mycolactone-negative *M. ulcerans* was not any more protective than BCG vaccination (275). It delayed the onset of BU symptoms in a footpad challenge model but mice were not able to control infection and eventually succumbed to disease. The potential of inactivated whole-cell *M. ulcerans* as a vaccine has been tested in a mouse footpad challenge model (342). Formalin-

treated *M. ulcerans* did not elicit any protection compared to unvaccinated mice (342). This study also created a dewaxed whole-cell *M. ulcerans* vaccine and found that it was protective compared to naïve mice in a footpad challenge model (342). The vaccination induced T_h2 dependent immune responses. The protection correlated with serum immunoglobulin (Ig)G levels however onset of disease was only measured until four weeks post-challenge and was not compared to BCG vaccination. *M. marinum*, the closest relative to *M. ulcerans* has also been tested as a putative vaccine against BU (339). *M. marinum* vaccination was not as protective as BCG vaccination in a mouse footpad model however the addition of a vector expressing the *M. ulcerans* Ag85A protein increased the immunogenicity of the *M. marinum* vaccine.

Whole-cell recombinant vaccines

The BCG vaccine, whilst not protective against BU can delay the onset of disease (274, 275, 279). Studies have attempted to improve the BCG vaccine by incorporating *M. ulcerans*-specific proteins. Hart et al. showed enhanced protection against BU using a recombinant BCG vaccine that expresses *M. ulcerans* Ag85A in a mouse footpad challenge model (340). This protective effect is enhanced by replacing Ag85A to create a recombinant BCG vaccine that expresses the Ag85B-EsxH fusion protein (341). Mice vaccinated with BCG expressing Ag85B-EsxH had a significantly decreased bacterial burden by weeks six and 12 post-infection and significantly longer survival times compared to vaccination with BCG alone.

1.13.2.2 Therapeutic vaccines

Mycobacteriophage treatment

Treatment with mycobacteriophage D29 has been shown to reduce pathology and prevent ulceration when administered to a mouse footpad, 33 days after bacterial challenge (343). This protection resulted in a significant reduction of *M. ulcerans* CFU in addition to increased cellular infiltrate of lymphocytes and macrophages. This study demonstrates the potential for the development of a phage-related therapeutic approach.

1.14 Designing a novel vaccine against *M. tuberculosis* and *M. ulcerans*

Since the late 1800s when MTB was first identified as the causative agent of TB, many putative vaccines were developed, which eventually proved to be less effective than BCG at preventing active disease. There remains a need for a vaccine that provides long-lasting protection, has low toxicity and is more effective than BCG at preventing TB. There is currently no vaccine against *M. ulcerans*, however in animal models BCG has proven to be the most effective at delaying the onset of BU disease.

One key reason for the difficulty in vaccine development against mycobacteria, particularly TB and BU, may be that the exact immune responses required to elicit protection against disease are unclear. The close-relatedness of BCG offers some cross-protection however there appears to be a missing feature in the vaccine to correctly shape the immune response for full protection. This phenomenon can be seen in the tetanus vaccine, whereby the vaccine elicits a different immune response to tetanus than a natural infection with *C. tetani* (344-346). Natural infection with tetanus does not induce lasting antibodies in those who recover from disease, however toxoid vaccination induces lasting antibodies (347).

The lack of well-defined correlates of mycobacterial protection prevents researchers from designing vaccines with a clear target. Therefore, current mycobacterial vaccine developments have many varied modes and targets. If a vaccine is successful at inducing protection it could then be used as a tool to identify correlates of protection. The alternative is to identify correlates of protection first. This is often performed with the use of knock-out animal models, which are infected with the bacteria or given vaccines with very specific modes of action to identify the roles of specific immune responses in their contribution to protection (348-351). This has limitations also, as weakening one portion of the immune response often has unintended effects on other parts of the immune response (352). Therefore, is not always a true reflection of the importance of particular immune responses.

The efficacy of BCG as a whole-cell vaccine suggests that utilising immunogenic portions of either MTB or *M. ulcerans* could aid in the development of a protective immune response. However, whole-cell vaccines are not able to be given to immunocompromised individuals (271, 272), which may be a large limitation as co-infection with MTB greatly increases chances of mortality in HIV infected individuals (76, 77). Using immunogenic proteins, rather than the whole-cell would eliminate the side-effects caused by whole-cell vaccination. One major limitation of this vaccination strategy is the choice of Ag and adjuvant. Without the whole cell, the choice of Ag(s) is an important element for the recognition of the bacteria and the generation of the immune response. Different Ags will induce varied immune responses; therefore, the correct Ag or group of Ags is an important factor. Additionally, the choice of adjuvant can help shape the immune response to the Ag and the right Ag-adjuvant combination is required to mount a strong and effective immune response.

1.14.1 Subunit vaccine

Subunit vaccines are less likely to induce adverse reactions as they utilise only the immune stimulant, such as a protein, rather than the whole pathogen. Soluble proteins alone can be poorly immunogenic, or not induce protective responses so are often formulated with an adjuvant to increase immune responses (235, 236).

1.14.1.1 Protein antigens

Vaccines are constructed in various ways and one common form is a subunit vaccine (353). Subunit vaccines require part of the pathogen, such as a protein, to act as an immune stimulant or Ag. Ags are ideally immunodominant or immunogenic on their own and accessible for recognition by immune cells during infection. Some immunogenic MTB proteins identified in literature include ESAT-6, TB10.4, Ag85A and Ag85B (264, 354, 355). They are recognised by the human immune system and capable of eliciting cell-mediated immune responses, suggesting that they would be promising vaccine Ags. A study attempting to develop serodiagnostic tests for *M. ulcerans* infections identified the immunogenic proteins, Hsp18 (356, 357), MUL_3720 (358) and enoyl reductase (ER) (356, 357).

ESAT-6

A well-studied protein, early secreted antigenic target – 6 kiloDaltons (kDa) or ESAT-6, was first identified from MTB culture filtrate (264). It forms a complex with culture filtrate protein-10 or CFP-10 (359) and is implicated in controlling macrophage cell death. CFP-10 may play a chaperone role for ESAT-6 as strains which express ESAT-6 but not CFP-10 do not secrete ESAT-6 (263). ESAT-6 also plays a role in preventing the phagolysosome formation within macrophages, avoiding the destruction of viable MTB (360). It is extremely immunomodulatory and is a noted virulence factor in MTB as ESAT-6 is absent in attenuated *M. bovis* BCG (264). ESAT-6 is a suitable vaccine antigen due to its immunogenicity in humans (361) and subunit vaccination with ESAT-6 in mice can control TB infection to the same level as BCG vaccination (362). ESAT-6 vaccination can induce T cell responses and IFN-γ production (363).

TB10.4

As the name suggests, TB10.4 is 10.4 kDa in size. It is a secreted culture filtrate protein belonging to the same family as ESAT-6 (354, 364). Thus, it has been used as a substitute antigen for ESAT-6 in vaccine formulations (365). Studies have identified TB10.4-specific $CD8^+$ T cells that are capable of producing high levels of T_h1 cytokines in mice (366, 367). Adjuvanted TB10.4 is capable of inducing $CD4^+$ T cell responses (368) and would be a favourable vaccine antigen.

Ag85A and Ag85B

Ag85A and Ag85B are 30 kDa and 33 kDa sized proteins, respectively. They form part of a three-protein complex with Ag85C and act as mycolytransferases involved in the final stages of cell wall assembly (369). They are suitable vaccine antigens as they form the largest products found in culture filtrate and are highly immunodominant in humans (355, 370). Vaccination with Ag85A and Ag85B can induce protective cell-mediated responses in mice (371, 372). The expression of Ag85A in a modified vaccinia Ankara vaccine induces robust polyfunctional $CD4^+$ T cell responses in humans (373). Ag85B has shown to induce strong T_h1 responses in vaccinated mice (374). A vaccine

incorporating the fusion of Ag85B and ESAT-6 produced levels of protection comparable to BCG in mice, as well as stable immunological memory (375). This suggests that multiple Ags may augment immune responses to MTB subunit vaccines.

Hsp18

Hsp18 is an *M. ulcerans* constitutively expressed small heat shock protein, 18 kDa in size. It is present among the cell membrane and secreted fractions (356). Pidot et al. identified the ability of Hsp18 to promote biofilm formation (357). The contribution of Hsp18 to BU is not well understood, though its extracellular presence makes it a suitable candidate as an Ag.

MUL_3720

MUL_3720 is a 22 kDa-sized protein found in *M. ulcerans* (376). BLAST analysis of MUL_3720 amino acid sequence reveals a LysM and mannose binding lectin domains (376). LysM domains enable peptidoglycan binding in bacterial cell walls. Lectin domains are capable of binding specific carbohydrate substrates. MUL_3720 localises on the cell surface and interacts with cell wall associated molecules (376). MUL_3720 may have a role in the cell attachment and cell-to-cell interactions.

ER

The polyketide synthases used by *M. ulcerans* to synthesize mycolactones are highly conserved and appear to be immunogenic (180, 335, 377, 378). One domain in particular, the enoyl reductase (ER) protein domain, elicits serum antibodies in BU patients and healthy controls in BU endemic regions (180). ER used as Ag in a DNA-protein prime-boost vaccine can reduce bacterial burden in an *M. ulcerans* mouse footpad challenge model (335).

1.14.1.2 Vaccination adjuvant

Protein based vaccines are often accompanied by an adjuvant to enhance immunogenicity (221). Adjuvants can enhance immune recognition and responses (235, 236).

Pam_2Cys lipopeptide adjuvant

Chua et al. have produced a lipopeptide adjuvant, which can bind to protein Ags and also stimulate DCs to make the Ag more immunogenic (379).

Previous studies have found that the correct engagement of Toll-like receptors (TLRs) expressed on APS (such as DCs and macrophages) can elicit significant cytokine, antibody and cell-mediated responses (380-382). The TLR family recognises structurally conserved molecules derived from micro-organisms, such as lipopeptides, glycolipids, lipopolysaccharide, flagellin, RNA and DNA (380-382). A study by Chua et al. developed a lipopeptide adjuvant utilising a TLR-2 agonist derived from

Mycoplasma fermentans (379). This agonist is a diacylated lipopeptide known as dipalmitoyl-S-glyceryl cysteine (Pam_2Cys). It engages with TLR-2 to form a heterodimeric complex with TLR-6 (383, 384). This Pam_2Cys moiety is capable of binding to protein Ags through electrostatic linkage rather than covalent conjugation and stimulating (DCs) to make the Ag more immunogenic. To enable strong association of Pam_2Cys with protein Ag, Pam_2Cys was constructed with branched cationic arginine residues, denoted R_4Pam_2Cys, or branched anionic glutamic acid residues, denoted E_8Pam_2Cys, as illustrated in Figure 1.11. The branched residues create a tentacle-like structure, enhancing the ability to bind electrostatically to negatively or positively charged Ags, respectively. This increased capacity for binding reduces the need for chemical intervention or modification for attachment to Ags.

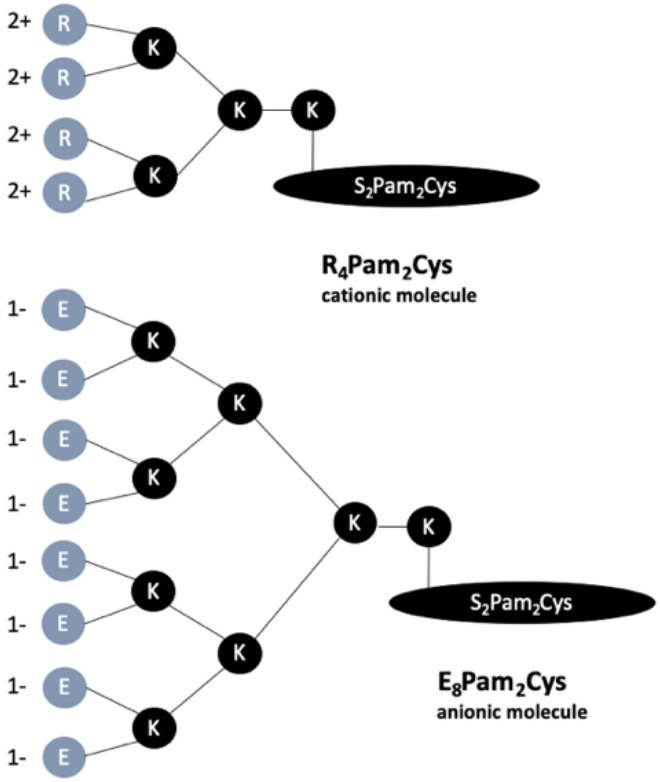

Figure 1.11. Schematic representation of the branched cationic lipopeptide R_4Pam_2Cys and branched anionic lipopeptide E_8Pam_2Cys.

R_4Pam_2Cys consists a two-tier branched lysine (K) structure which attach to four arginine (R) amino acid residues and E_8Pam_2Cys consists of a three-tier lysine structure attaching to eight glutamic acid (E) residues. Each lipopeptide is then attached to Pam_2Cys via the C-terminal lysine residue. In the case of R_4Pam_2Cys, the positively charged R amino groups give the lipopeptide an overall charge of +8. For E_8Pam_2Cys, the negatively charged E residues imparted an overall negative charge of 8 (379). This image was adapted from Chua et al. (379).

Pam_2Cys adjuvant mode of action

DCs have the ability to direct immunity towards T_h1 or T_h2 adaptive immune response depending on signals received upon activation. Stimulation via TLR-2 leads to the activation of transcription factors such as NF-κβ for DC maturation (380). DCs play a role in stimulating the secretion of proinflammatory cytokines and the eventual activation of Ag-specific naïve T-cells (385). Chua et al. demonstrated that electrostatically associated Pam_2Cys and protein Ag elicited higher $CD8^+$ T-cell responses, in comparison to similarly charged lipopeptide and protein Ag (379, 386). The addition of Pam_2Cys also increased Ag-specific antibody responses compared to vaccination with the protein alone and comparable to the adjuvant, alum (387). These increased responses may occur due to simultaneous delivery of Ag and DC stimulation. Chua et al. found that only small doses are necessary to elicit strong immune responses (379). This may prevent the toxicity often associated with adjuvant use. Recent studies have shown Pam_2Cys when administered intranasally provides protection against the development of disease caused by influenza virus in the respiratory system (388, 389) and can protect against viral hepatitis C (390, 391). Studies have also shown that a pegylated Pam_2Cys reduces the impact of influenza-associated secondary *Streptococcus pneumoniae* infection (392). While this adjuvant demonstrates promising protection against influenza and secondary bacterial infections, the effect of this Pam_2Cys adjuvant directly against primary bacterial infections has not been well studied.

1.15 Research Objectives

At the commencement of this PhD, BCG was the most widely used vaccine against TB and the most effective vaccine against BU, even though BCG does not fully protect against either disease. As MTB co-infection significantly increases mortality in HIV-infected individuals, there exists a need for more tolerable therapeutics in immunocompromised individuals. There are also reports that constant exposure to environmental mycobacteria may reduce the efficacy of BCG in BU endemic areas (250). This supports the development of alternative vaccine formulations to whole cell vaccination. Therefore, this thesis addressed the absence of a protective mycobacterial vaccine against TB and BU. One key challenge of vaccine development is the incomplete understanding of correlates of protection against these diseases. Although T_h1 responses and particularly IFN-γ responses have been strongly implicated in the control of these diseases, particularly TB, these responses alone do not fully protect against TB or BU. Therefore, this thesis aimed to assess vaccine-derived responses and to explore immune correlates of protection (and markers of disease) against TB and BU and contribute to the understanding of protective responses.

This thesis focussed on the development of a sub-unit vaccine against two of the most clinically significant mycobacteria, *M. tuberculosis* and *M. ulcerans*. The vaccines comprised known immunogenic proteins from *M. tuberculosis* or *M. ulcerans* in association with the Pam_2Cys adjuvant. The specific aims listed below are addressed in three results chapters:

1. *To develop a subunit vaccine against Mycobacterium tuberculosis*
2. *To develop a subunit vaccine against Mycobacterium ulcerans utilising cell wall-associated proteins*
3. *To create a subunit vaccine targeting the mycolactone toxin biosynthesis pathway of Mycobacterium ulcerans*

Chapter 2

Murine immune responses to subunit vaccination with *Mycobacterium tuberculosis* protein antigens linked to a TLR-2 agonist

2.1 Introduction

This chapter focusses on the development of a vaccine against tuberculosis (TB). To address this task two experimental *M. tuberculosis* (MTB) protein subunit vaccines were formulated. These vaccines included two well-studied immunogenic MTB proteins, ESAT-6 and Ag85B in association with the TLR-2 agonist, Pam_2Cys.

TB is the leading cause of disease by a single infectious agent. TB affects every part of the world, predominantly throughout parts of Asia (especially India and China) and Africa. In 2018, there were an estimated 10 million new cases of TB and 1.45 million deaths (58). The treatment of TB requires a six-month administration of three to four "first-line" antibiotics (rifampin, isoniazid, pyrazinamide, streptomycin or ethambutol) (193). Failure of this treatment requires second-line antibiotics with increased side effects. Resistance to first-line antibiotics, termed multi-drug resistant TB (MDR-TB), and rifampin in particular has increased in the last decade (58). This highlights a need for more effective prevention against disease.

There is presently an approved vaccine against TB. It is a live-attenuated vaccine, *Mycobacterium bovis* 'bacille Calmette-Guérin' (BCG), which provides cross-protective immune responses against MTB infection. The BCG vaccine protects children (between six-months to two-years old) from severe disseminated forms of TB, such as meningitis, but protection begins to wane after 10-15 years (268). When given later in life, the efficacy of BCG varies between 0-80% efficacy in preventing pulmonary TB in adults. Since the late 1800s, many TB vaccines have been developed however none have been found to be more protective than BCG (285). The BCG vaccine is a live-attenuated vaccine and therefore cannot be given to immunocompromised individuals (393). This is an issue for HIV infected individuals, particularly because TB co-infection significantly increases mortality (77, 394, 395). There remains a need for a vaccine that provides long-lasting protection, has low toxicity and is more effective than BCG at preventing TB.

This chapter describes the creation of low-toxicity subunit vaccines. Subunit vaccines utilise an immune stimulant or Ags specific to the pathogen and are therefore less-likely to induce side effects compared to whole-cell and live-attenuated vaccines (220, 222). The immunogenic MTB proteins Ag85A, Ag85B, Early Secreted Antigenic Target – 6kDa (ESAT-6), and TB10.4 are recognised by the human immune system and capable of eliciting cell-mediated immune responses (264, 354, 355, 365, 396-399), and therefore chosen for this study. The adjuvant used in this chapter, is a charged lipopeptide which can bind to protein Ags via electrostatic binding rather than covalent linkage (379). This

lipopeptide adjuvant utilises the TLR-2 agonist Pam_2Cys. It increases antigen uptake by DCs, promotes trafficking to lymph nodes (LNs), and induces strong $CD8^+$ T cell and antibody responses (379, 386).

The repertoire of immune responses required for protection against TB have not been fully identified however, T_h1 responses have been widely accepted as the major mediators for controlling infection (158, 400). The presence of $CD4^+$ T cells and IFN-γ are recognised as important in controlling infection (161, 401, 402), but the role of $CD8^+$ T cells has not been as extensively studied. $CD8^+$ T cells (both IFN-γ -producing and cytotoxic T cells) have been shown to play a non-redundant role in the control of TB infection, during acute infection and prevention of reactivation (367, 401, 403, 404). Human $CD8^+$ T cell responses can be modelled in transgenic mice containing the human MHC class I presentation molecule, HLA-A2 (405, 406). HLA-A2 is present in a large proportion of the human population – including Asians (>50%), Caucasians, American Indians and South Americans (407, 408). $CD8^+$ T-cell responses have not been as widely studied as $CD4^+$ T cell responses for TB. Identifying $CD8^+$ epitopes that can be recognised by HLA-A2 transgenic mice would enhance the re-stimulation of MTB-specific $CD8^+$ T cells in further vaccination experiments using whole protein.

2.2 Research Objectives

The main aim of this study was to evaluate immune responses to protein-based vaccines against *M. tuberculosis*, utilising MTB-specific proteins in a mouse model.

- To formulate two vaccines with ESAT-6 and Ag85B in conjunction with lipopeptide adjuvant Pam_2Cys for examination in mice. The protein-specific $CD4^+$ and $CD8^+$ T cell responses, particularly IFN-γ production, will be measured.
- To screen peptides derived from MTB antigens ESAT-6, Ag85B, Ag85A and TB10.4 for human $CD8^+$ T cell responses to these peptides in HLA-A2 restricted mice.

2.3 Results and Discussion

The methods and results for this study have been reported in a manuscript in-progress, soon to be submitted.

Manuscript "Murine immune responses to subunit vaccination with *Mycobacterium tuberculosis* protein antigens linked to a TLR-2 agonist"

Kirstie M. Mangas, Chinn Yi Wong, Acep R. Wijayadikusumah, Weiguang Zeng, Toshiki Sekiya, Jessica L. Porter, Sacha J. Pidot, Kylie M. Quinn, Katherine Kedzierska, Timothy P. Stinear, David C. Jackson and Brendon Y. Chua.

The following is the author-accepted version of the manuscript, formatted to include the figures within the text.

Murine immune responses to subunit vaccination with *Mycobacterium tuberculosis* protein antigens linked to a TLR-2 agonist.

Kirstie M. Mangas[1], Chinn Yi Wong[1], Acep R. Wijayadikusumah[1,2], Weiguang Zeng[1], Toshiki Sekiya[1], Jessica L. Porter[1], Sacha J. Pidot[1], Kylie M. Quinn[3], Katherine Kedzierska[1], Timothy P. Stinear[1], David C. Jackson[1,*] and Brendon Y. Chua[1,*].

1. Department of Microbiology and Immunology, Doherty Institute, University of Melbourne, Melbourne, Victoria, 3000, Australia
2. Research and Development Division, PT. BioFarma (Persero), Bandung, West Java 40161, Indonesia
3. School of Health and Biomedical Sciences; RMIT University, Bundoora 3083, Australia.

* Joint senior authors

Corresponding Author:
Brendon Chua, University of Melbourne, 792 Elizabeth St, Melbourne, Victoria, 3000, Australia
Email address: bychua@unimelb.edu.au

Abstract

Background. Tuberculosis (TB) is the leading cause of disease by a single infectious agent (*Mycobacterium tuberculosis* (MTB)). In 2018, there were an estimated 10 million new cases of TB and 1.45 million deaths. *Mycobacterium bovis* 'BCG', is a widely used vaccine against MTB and somewhat effective in children (< 2 years old). However, efficacy wanes after 10-15 years of life and BCG boosting does not increase protection.

Methods. We assessed the ability of MTB protein subunit vaccine formulations to generate immune responses. The MTB proteins ESAT-6 and Ag85B were adjuvanted with a TLR-2 agonist to stimulate MTB-specific immune responses in mice.

Results. The vaccines induced high protein-specific antibody titres against Ag85B protein suggesting potential efficacy against the extracellular presence of MTB. However, neither of these vaccine formulations generated measurable interferon-gamma (IFN-γ) responses from $CD4^+$ T cells in the spleen or lungs and only minor $CD8^+$ T cell responses.

Conclusions. T_h1 responses, particularly $CD4^+$ T cells and IFN-γ, are known to play key roles in the control of TB. Although the vaccines in this study generated strong antibody responses, they induced poor $CD4^+$ IFN-γ^+ T cell responses. Therefore, alternative antigen and vaccination routes should be considered to enhance MTB-specific T_h1 responses of future vaccination formulations.

Introduction

Tuberculosis (TB) is the leading cause of disease by a single infectious agent and the most common mycobacterial disease. It is caused by the bacteria, *Mycobacterium tuberculosis* (MTB) a slow growing, acid-fast bacilli and contains high sequence homology to other human pathogens *M. marinum* and *M. ulcerans* (1, 2). TB affects every part of the world, predominantly throughout parts of Asia (especially India and China), Africa and the Western Pacific (3). Moreover, there is a strong correlation between areas that are endemic for HIV and those with a high incidence of TB infection. In 2018, there was an estimated 10 million new cases of TB and 1.45 million deaths (0.25 million among HIV infected individuals) (3).

MTB is transmitted by inhaling bacteria contained within airborne droplets emitted from lungs of those with active disease (4). The bacteria can be cleared immediately by host immune responses, reside inactive in the lungs (latent TB infection (LTBI)) or actively replicate to cause disease (5). TB can present in many different clinical manifestations, including a cough presenting sputum and blood at times, chest pains, weakness, weight loss, fever and night sweats (5). Inflammation surrounding replicating bacteria leads to granuloma development in the lung and long-term inflammation leads to lung necrosis, termed caseation (5). Bacteria can also escape the lungs and replicate in the bones or other organs (6). It is believed that up to one-third of the world's population is infected with MTB (7) and these individuals carry a 10% lifetime risk of presenting with active disease (8).

Treatment of TB requires a six-month administration of three to four "first line" antibiotics (rifampin, isoniazid, pyrazinamide, streptomycin or ethambutol) with failure requiring the use of second line antibiotics albeit with increased side effects. Resistance to all treatments however, termed extensive multidrug resistant TB (XMDR-TB), has increased in the last decade (9). As approximately 90% of cases occur in middle-low income countries, the monitoring and distribution of antibiotics can be difficult, costly and place great burden on already struggling health-care systems (3).

The only approved vaccine against TB is the live-attenuated vaccine, *M. bovis*-derived bacille Calmette-Guérin (BCG) which induces cross-protective immune responses against MTB. Both strains are closely related except all BCG strains are missing the virulence region present in MTB, termed RD1 (10). BCG vaccine protects children (between six months to two-years-old) from severe disseminated forms of TB, such as meningitis, but protection begins to wane after 10-15 years (11). When given later in life, the efficacy of BCG varies between 0-80% (12). This is problematic as regions with lower levels of protection often coincide with highest TB incidences. BCG does not cause disease in healthy individuals, however as it is live-attenuated it may cause disease in immuno-compromised individuals

(13). As a result, the World Health Organisation (WHO) has adjusted the vaccination guidelines to prevent HIV infected children from being administered the BCG vaccine (14).

We also know from correlative studies that T_h1 responses are implicated in the control of TB and T_h2 responses with susceptibility (15, 16). The presence of $CD4^+$ T cells and IFN-γ for example has been postulated to play a role in infection control, as their absence is associated with the inability to manage bacterial replication (17, 18). Though not as widely explored as $CD4^+$ T cells, $CD8^+$ T cells (both IFN-γ -producing and cytotoxic T cells) have also been shown to play a non-redundant role in the control of TB infection, during acute infection and prevention of reactivation (17, 19-21). The relevance of humoral responses for protection remains unclear (22, 23), however some studies support a role for antibodies in the control of bacterial load during TB infection and limiting dissemination (24-26). In regard to BCG vaccination, BCG-specific antibodies have been considered to be of little importance for vaccine efficacy. However, long-lived BCG-induced memory B cells have been identified in individuals 13-45 years after vaccination (27). BCG-induced antibodies have been shown to improve phagocytic cell activity against MTB and enhance proliferation and IFN-γ production in mycobacterium-specific $CD4^+$ and $CD8^+$ T cells (28, 29).

Experimental TB vaccines furthest along in clinical trials include the therapeutic vaccine, heat-inactivated whole cell *Mycobacterium vaccae* (Phase III) (30), and the AS01E-adjuvanted subunit-based vaccine, M72*,* a fusion of two MTB antigens, Mtb32A and Mtb39A (Phase IIa) (31). These candidates have so far been shown to prevent progression to active disease in LTBI children, adolescents and adults, and induce high frequencies of multifunctional T cells, and boost T cell responses primed by natural MTB infection (32). Although these are undoubtedly promising results, there remains a need to develop options in the TB vaccine pipeline should these candidates not meet expectations.

Several MTB-derived antigens in particular show promise as they are recognised by the human immune system and capable of eliciting cell-mediated immune responses. First identified from culture filtrate (33), early secreted antigenic target – 6 kiloDaltons (kDa) (ESAT-6) forms a complex with culture filtrate protein-10 (CFP-10) (34) and plays a role in preventing the phagolysosome formation within macrophages, avoiding the destruction of viable MTB (35). ESAT-6 is a virulence factor in MTB and is absent in attenuated *M. bovis* (33) and has been proposed as a vaccine antigen in humans (36). ESAT-6 vaccination of mice induces IFN-γ-production by T cells (37) and controls MTB infection to the same extent as BCG vaccination in the murine model of TB (38). Another potential antigen is Ag85B, a 33 kDa mycolytransferase involved in the final stages of mycobacterial cell wall assembly (39). In mice, vaccination with Ag85B induces T_h1 responses (40) and protective cell-mediated responses (41, 42).

Ag85A is a 30kDa protein that forms part of the three-protein mycolytransferase complex, with Ag85B and Ag85C (39). This complex is among the largest protein product found in culture filtrate and is highly immunodominant in mice (41, 42) and humans (43, 44). The expression of Ag85A in a modified vaccinia Ankara vaccine induces robust polyfunctional $CD4^+$ T cell responses in humans (45) and is a promising vaccine antigen. Of particular interest is the observation that a fusion complex of both Ag85B and ESAT-6 can elicit protection as well as stable immunological memory (46), suggesting that the incorporation of multiple antigens in a vaccine candidate is beneficial against TB. TB10.4 is also a well-described immunogenic MTB protein. As the name suggests, TB10.4 is 10.4 kDa in size and is a culture filtrate protein belonging to the same family as ESAT-6 (47, 48). Thus, it has been used as a substitute antigen for ESAT-6 in vaccine formulations (49). TB10.4 has the advantage over ESAT-6 of not cross-reacting with the Quantiferon Gold test for TB infection, and so we also explored TB10.4 in this study. Studies have identified TB10.4-specific $CD8^+$ T cells capable of producing high levels of T_h1 cytokines in mice (21, 50). Adjuvanted TB10.4 can also induce $CD4^+$ T cell responses (51), suggesting it has application as a vaccine antigen.

Many protein antigens, however, often lack inherent features that are attractive to the immune system and adjuvants are often utilised to enhance their immunogenicity. Adjuvants, in particular those that can target antigens to Toll-like receptors (TLRs) are ideal for this and one such approach is based on the cationic and anionic TLR-2 agonist Pam_2Cys-based systems developed by Chua et al (52). These lipopeptides are capable of electrostatically binding to protein antigens to facilitate their delivery to dendritic cells (DCs) and concurrently induce their activation, leading to the induction of protective $CD8^+$ T cell and antibody responses (52, 53).

The aims of this study were to therefore evaluate the ability of protein-based vaccines against *M. tuberculosis*, utilising *M. tuberculosis*-specific proteins ESAT-6 and Ag85B to induce immune responses when formulated with Pam_2Cys. As $CD8^+$ T cell responses have been implicated in preventing TB but are not as widely studied as $CD4^+$ T cells, we also investigate the potential of these vaccine candidates to induce these responses in transgenic mice that express the human MHC Class I presentation molecule, HLA-A2 (54, 55). This haplotype is present in a large proportion of the human population – including Asians (>50%), Caucasians, American Indians and South Americans (56, 57) and the use of these transgenic mice provides information on the potential of these formulations to induce cell-mediated responses in humans.

Materials & Methods

Strains and culture conditions

Escherichia coli BL21 (DE3) containing plasmid pET30a-ESAT-6 (strain pDJ001) was grown at 37°C in Terrific broth (24 g/L yeast extract (Difco USA), 20 g/L tryptone (Difco USA), 4 ml/L glycerol, and phosphate buffer containing 0.017M KH_2PO_4 and 0.072M K_2HPO_4) supplemented with 100 µg/ml ampicillin (Sigma-Aldrich, USA) to express 6xHIS-tagged early secretory antigenic target 6kDa (ESAT-6) protein.

Recombinant protein expression

Overnight culture of pDJ001 was diluted to OD_{600} = 0.05 in Terrific broth. The culture was incubated at 37°C with shaking at 200 rpm until OD_{600} = 0.6-0.7, then 1 mM IPTG (Isopropyl b-D-1-thiogalactopyr-anoside) was added to induce protein expression. The cells were incubated for a further four hours, resuspended in wash buffer (8 M urea, 150 mM sodium chloride, 10% glycerol) and sonicated at amplitude 60 (QSonica Ultrasonic Liquid Processor S-4000, Misonix) until the solution turned clear. The lysate was filtered with a 0.22 µM filter (Millipore) and expressed protein was column-purified using anti-histidine resin (ClonTech). The resin was washed ten times with 10x column volumes of wash buffer mixed with an increasing proportion of tris buffer (20 mM Tris-HCl, 150 mM sodium chloride, 10% glycerol) until the column was washed with only tris buffer. The resin was washed a further two times with tris buffer containing 20 mM imidazole. Protein was eluted in tris buffer containing 200 mM imidazole and dialysed in phosphate buffered saline (PBS) before concentration using a 3K MWCO PES concentration column (Pierce, Thermo Scientific, USA). Ag85B was purchased from the company MyBiosource. This protein was produced by an *E. coli* expression vector, purified via SUMO-tag which was cleaved after purification. Relative protein size was confirmed using sodium dodecyl sulphate polyacrylamide gel electrophoresis.

Sodium dodecyl sulphate polyacrylamide gel electrophoresis (SDS-PAGE)

Samples were denatured in an equal volume of 2 x sample loading buffer (40% (v/v) 0.5M Tris-HCL pH6.8, 10% glycerol, 1.7% (w/v) SDS, 10% 2-B-mercaptoethanol, 0.13% (w/v) bromophenol blue in distilled water) at 100°C for five minutes. Fifty microlitres of the ESAT-6 purification flow through and wash, ten microliters of each purified sample and SeeBlue® Plus2 pre-stained protein standard (Invitrogen) were loaded into a 0.5mm 12% polyacrylamide gel under reducing conditions, as previously described (58). The gel was run in running buffer (0.3% (w/v) Tris, 1.44% (w/v) glycine and 0.1% (w/v) SDS in distilled water) for 1 hour at 150 volts (Mini-protean vertical electrophoresis cell, Bio-Rad, Australia). The gels were stained in Coomassie stain (45% methanol, 10% acetic acid 0.25% (w/v) Coomassie brilliant blue in distilled water) for 1 hour and destained in Coomassie destain solution (33% methanol, 10% acetic acid, 60% distilled water) until the protein bands could be identified.

Western Blotting

Protein was separated on a 12% polyacrylamide gel as per the method for SDS-PAGE. After separation the protein was transferred to a nitrocellulose membrane in a tris-glycine transfer buffer (1.5 mM Tris, 12mM glycine, 15 % methanol (v/v) in distilled water) for 1 hour at 100 volts (Mini Trans-Blot Cell, Bio-Rad, Australia). The nitrocellulose membrane was blocked in blocking buffer (5% (w/v) skim milk powder and 0.1% Tween-20 in PBS) overnight at 4°C. The membrane was incubated in blocking buffer containing anti6xHIS-HRP antibody (Roche Applied Science, USA) at 1:500 dilution. The membrane was washed in PBS containing 0.1% Tween-20 and then exposed to developing solution (Western Lighting Chemiluminescence kit, Perkin Elmer, USA) according to manufacturer's guidelines. Chemiluminescence was detected using an MF ChemiBIS gel imaging system (DNR Bio-Imaging Systems, Israel).

Particle size analysis of protein antigen and lipopeptide formulations by dynamic light scattering (DLS)

Protein and lipopeptide interactions were analysed by dynamic light scattering (DLS). Ten micrograms of protein were added to increasing moles of lipopeptide (R_4Pam_2Cys or E_8Pam_2Cys) in 50 µl PBS and the dynamic light scattering of the particles were measured using a DynaPro NanoStar (Wyatt Technology, CA, USA) equipped with 658nm laser with a scattering angle of 90°. The level of light scattering by the particles in solution determined the hydrodynamic radius of the particles in solution. Data was analysed using Dynamics software (v7.1.7.16). The changes in particle size over time were graphed using Prism v8 (GraphPad, CA, USA).

Formulation of antigens with lipopeptide

Each vaccine dose contained 25 µg protein added to R_4Pam_2Cys at a ratio of 1:5 mole of protein to lipopeptide. PBS was added to a final volume of 100 µl for subcutaneous vaccination, or final volume of 50 µl for intranasal vaccination, and the combination sonicated in a water bath for 30 seconds. Control vaccine preparations were made containing 25 µg protein alone or R_4Pam_2Cys lipopeptide alone and also sonicated prior to administration.

Formulation of antigens with complete Freund's adjuvant (CFA) or incomplete Freund's adjuvant (IFA)

For protein antigen studies, each vaccine dose contained 25 µg protein emulsified in 10X volume of CFA. For peptide antigen studies, each vaccine dose contained 10 µg peptide emulsified in 10X volume of complete Freund's adjuvant in a total volume of 100 µl. For booster vaccinations, each dose was formulated with IFA instead of CFA.

Peptide synthesis

Peptides for TB antigens ESAT-6, Ag85A, Ag85B and TB10.4 were synthesized using methods previously described (59). The peptides to be made were identified from previous studies using HLA-A2 patient samples and also by using SYFPEITHI, an online epitope predictor (http://www.syfpeithi.de/) (60) (see Table 1). Peptides were purified using HPLC (Agilent) with a C18 Prep column (Agilent). Purified peptides were analysed via mass spectrometry (Ion Trap series 1100, Agilent) to identify their size in kiloDaltons (kDa).

Table 1. Epitopes for TB protein antigens Ag85A, Ag85B, TB10.4 (HLA-A2) and ESAT-6 (C57BL/6).

Protein	Epitope amino acids	Epitope sequence[a]	Molec. weight (Daltons)[b]
Ag85A	242-250	KLIANNTRV (HLA-A2)	1028
	48-56	GLPVEYLQV (HLA-A2)	
Ag85B	199-207	KLVANNTRL (HLA-A2)	1028
	37-45	YLLDGLRAQ (HLA-A2)	1048
	158-166	GMGPSLIGL (HLA-A2)	
TB10.4	4-12	IMYNYPAML (HLA-A2)	
	83-89	MMARDTAEA (HLA-A2)	995
ESAT-6	1-20	MTEQQWNFAGIEAAASAIQG[c] (C57BL/6)	2123

Notes: [a] HLA-A2 epitopes were identified from previous studies (15, 63, 64) and also by online epitope predictor SYFPEITHI.

[b]Predicted by Genscript molecular weight calculator: *https://www.genscript.com/tools/peptide-molecular-weight-calculator*

[c]ESAT-6 peptide was synthesized and used in C57BL/6 mice vaccination experiments.

Epitopes highlighted in grey were synthesized and utilized in this study for HHD mice vaccination experiments

Vaccination of animals

Six-week old, male C57BL/6 mice and eight-week old, female HLA-A2.1 transgenic mice (termed HHD mice) were housed at the Peter Doherty Institute Bioresource Facility and housed in individual ventilated cages. HHD mice express a chimeric monochain of the α1-α2 domains of HLA-A2.1 and α3 and cytoplasmic and transmembrane domains of H-2D^{b} on a double-knockout H-2D$^{b-/-}$ β2m$^{-/-}$ mouse background. Food and water were given *ad libertum*. Experiments were approved by The University of

Melbourne Animal Ethics Committee (Animal Ethics approval identification numbers 1513513 and 1613870).

For intranasal (i.n.) inoculation, mice were anaesthetised by isoflurane inhalation and protein alone or protein + Pam_2Cys then administered by intranasal instillation. For subcutaneous (s.c.) vaccination, mice were vaccinated subcutaneously at the base of tail (50 µl per flank) with protein alone, protein + Pam_2Cys, or protein + CFA.

To measure responses induced by ESAT-6 protein vaccination, C57BL/6 mice were subcutaneously vaccinated with ESAT alone, ESAT-6 + CFA or ESAT-6 with either R_4Pam_2Cys or E_8Pam_2Cys. Chicken ovalbumin with CFA was included as a positive control. Mice were sacrificed after seven days and spleens were obtained for immune analysis. To measure responses to ESAT-6_{1-20} peptide, C57BL/6 mice were vaccinated with ESAT-6_{1-20} peptide alone or ESAT-6_{1-20} peptide with CFA. Mice were sacrificed seven days post-vaccination, and spleens were obtained for immune analysis. To measure responses induced by Ag85B protein vaccination, C57BL/6 mice were subcutaneously or intranasally vaccinated with Ag85B alone, or Ag85B with either R_4Pam_2Cys or E_8Pam_2Cys. Chicken ovalbumin (OVA) + R_4Pam_2Cys was included as a positive control. Mice were sacrificed after seven days and spleens were obtained for immune analysis. To measure sera responses to Ag85B, C57BL/6 mice were vaccinated with Ag85B alone, or Ag85B with either R_4Pam_2Cys or E_8Pam_2Cys and boosted 21 days later. Mice were sacrificed after a following seven days and sera was obtained for immune analysis.

To determine the kinetics of the TB peptide + CFA cellular response, HHD mice were vaccinated subcutaneously with GILGFVFTL (GIL) peptide (HLA-A2-restricted epitope from influenza Matrix 1_{58-66} protein) plus CFA. Some mice were sacrificed seven and ten days later and their spleens were obtained for analysis of immune responses. The remainder of the mice were given a booster vaccination containing GIL peptide + IFA. Mice were sacrificed five, seven and ten days later (days 26, 28 and 31 post-primary vaccination) and their spleens were obtained for immune analysis.

To measure TB peptides, HHD mice were vaccinated with each TB peptide (KLIANNTRV, KLVANNTRL, YLLDGLRAQ or MMARDTAEA) emulsified with CFA. Mice were boosted with TB peptide + IFA after 21 days and sacrificed seven days later (28 days after primary vaccination). Spleens were obtained for immune analysis. GIL peptide + CFA/IFA and TYQRTRALV (TYQ) peptide (H-$2K^d$ restricted epitope from influenza Nucleoprotein$_{147-155}$ protein) with CFA/IFA were included as controls.

Intracellular cytokine staining (ICS)

For each mouse 5 ml single cell suspensions were made from the spleen and draining lymph nodes in RP10 (RPMI 1640 (Sigma) supplemented with 10% foetal bovine serum (Gibco), 2mM L-glutamine, 1mM sodium pyruvate, 55 µM 2-mercaptoethanol, 12 µg gentamycin, 100 U/ml penicillin and 100 µg/ml streptomycin). Cells from the spleen and draining lymph nodes were separately cultured in 96-well plates (CoStar, Corning, USA) containing 1 $x10^7$ cells/per well and 1 $x10^5$ cells/well, respectively. The cells were cultured in 200 µl RP10 containing 10 U/ml IL-2 (Roche, Mannheim, Germany), 1µg/ml plate-bound anti-CD28 (BD Pharmigen, Becton Dickinson, Clone 37.51) and either 20 µg/ml protein or 2 µg/ml peptide for 12 hours at 37°C in 5% CO_2. Golgiplug (1µg/ml) (Becton Dickinson) was added for the last 4 hours of incubation. Cells were harvested and stained with the appropriate dilution of PE-antiCD3 (Biolegend, Clone R17A2), PerCP-Cy5.5-antiCD4 (BD, Clone GK1.5), APC-anti-CD8 (BD Pharmigen, Clone 53-6.7) anti-mouse monoclonal antibodies at 4°C in the dark. To perform the ICS assay the surface stained cells were permeabilized using Cytofix/Cytoperm (Becton Dickinson, USA) and incubated with the appropriate dilution of FITC-IFN-γ (BD Horizon, Clone XM G1.2) anti-mouse monoclonal antibodies for 30 minutes at 4°C. Finally, cells were washed twice in Perm Wash buffer (Becton Dickinson, USA) followed by FACS buffer (PBS containing 5mM EDTA and 1% fetal bovine serum). The stained cells (1 $x10^6$/sample of splenocytes and 1 $x10^5$/sample of lymph node cells) were acquired in an LSR Fortessa flow cytometer system by the use of BD FACS Diva software (BD Biosciences). Data analyses were performed using FlowJo v10.0 (Tree Star, OR, USA).

Cytometric Bead Array

For each mouse 1 $x10^7$ splenocytes and 1 $x10^5$ cells from the draining lymph nodes were separately incubated in 500 µl RP10 supplemented with 25 µg/ml protein for 72 hours at 37°C in 5% CO_2. Supernatant was collected and a cytokine bead array was performed using a mouse flex set (BD Biosciences, USA) detecting cytokines IL-2, IL-4, IL-6, IL-10, IL-12/IL-23p40, IL-17, IFN-g, MCP-1 and TNF as per manufacturer's instructions. The samples were acquired in a FACSCanto II (BD Biosciences). Cytokine quantities were calculated using FCAP Array™ Software v3.0.

Serum antibody titre measurements

Serum was prepared from blood obtained from mice at day 20, day 35 and at time of sacrifice. Antibody titres were measured using enzyme linked immunosorbent assay (ELISA) as per methods described in (52). Briefly, ELISA plates (Nunc, Thermo Scientific) were coated overnight with 5 µg protein diluted in $PBSN_3$ and blocked with $BSA_{10}PBS$ for 2 hours at room temperature. Plates were washed with PBS containing 0.05% Tween-20 (PBST). Neat sera were sequentially diluted in BSA_5PBST and incubated at room temperature for 6 hours. Bound antibody was detected by adding horse radish peroxidase conjugated rabbit anti-mouse IgG (Dako, Glostrup, Denmark) at a concentration of 1:400 in BSA_5PBST for 2 hours. Plates were developed with developing solution (hydrogen peroxide, citric acid and ABTS)

and incubated for 10-15 with gentle agitation to observe a colour change. The reaction was stopped with 50mM sodium fluoride. Plates were read at dual wavelengths of 505 and 595 nm on plate reader (LabSystems Multiskan Multisoft microplate reader).

Statistical Analyses

Intracellular cytokine and antibody data were analysed by one-way analysis of variance (ANOVA) with Tukey's correction for multiple comparisons. Cytokine bead array data was analysed by Mann-Whitney U-test (Prism v8, Graphpad, CA, USA). For all tests *$p < 0.05$, **$p < 0.01$ and ***$p < 0.001$ and **** $p < 0.0001$ were considered statistically significant.

Results

Formulation of the TB antigen + lipopeptide subunit vaccine

To produce our vaccine candidates, recombinant ESAT-6 protein was expressed and purified whilst Ag85B was procured commercially. When analysed by SDS-PAGE, recombinant ESAT-6 corresponded with a band migrating around 6kDa (Fig. 1A), whilst Ag85B appeared as a band ~33 kDa (Fig. 1B), each in line with their reported molecular weights.

We formulated both antigens with either cationic R_4Pam_2Cys, which contains N-terminal arginine residues (allowing it to electrostatically associate with negatively charged regions on a protein antigen) or anionic E_8Pam_2Cys, which contains N-terminal glutamic acid residues (allowing association with positively charged regions).

The association of antigen and lipopeptide was analysed by measuring the size of particles formed in solution by dynamic light scattering (DLS). As the putative charge of ESAT-6 is -5, it appeared to preferentially bind to R_4Pam_2Cys when mixed at a 1:1 ratio, depicted by the increase in peak intensity and particle size (peak 6; Fig 1C) compared to 1:3 and 1:5 ratio. In contrast, very little increase in particle size was observed when ESAT-6 was mixed with increasing E_8Pam_2Cys ratios (Fig. 1D, Table 2). Whilst the putative charge of Ag85B is -3, mixing with R_4Pam_2Cys (Fig. 1E) or E_8Pam_2Cys (Fig. 1F) did not appear to result in notable increases in particle sizes (Table 3). However, mixing with R_4Pam_2Cys did result in more monodispersed peaks (peaks 3 and 4; Fig 1E) compared to the polydispersed profile exhibited by the antigen alone in solution (Peak 1; Fig 1E). Moreover, there also appeared to be a slight peak shift (peak 4; Fig 1F) when Ag85B is mixed with E_8Pam_2Cys at a 1:5 ratio. It therefore appears that both R_4Pam_2Cys and E_8Pam_2Cys can associate with Ag85B although these interactions are not as distinct as observed for ESAT-6.

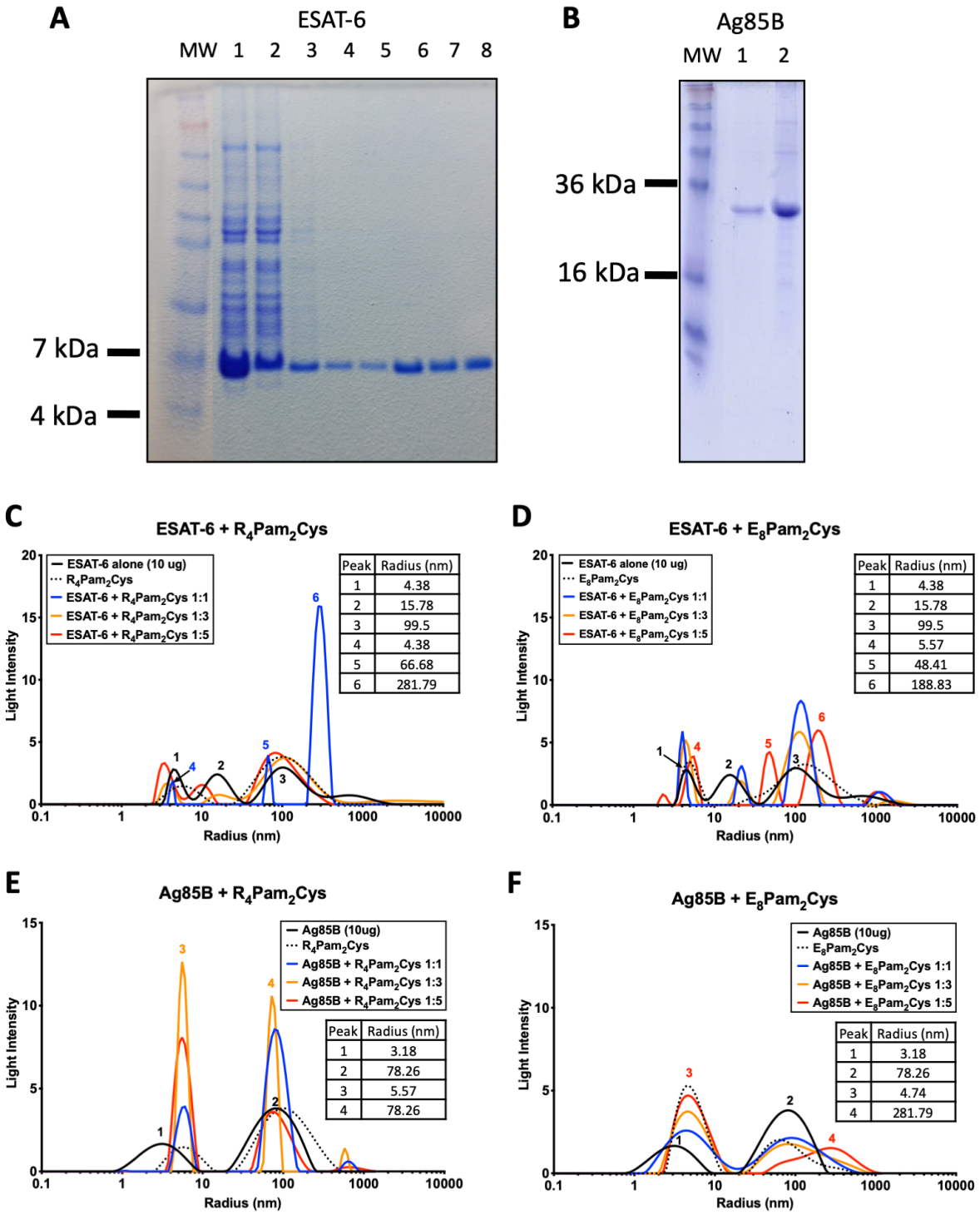

Figure 1. Analysis of purified recombinant ESAT-6 and Ag85B protein antigen characteristics (continued next page).

(A) ESAT-6 recombinant protein obtained during purification, separated by SDS-PAGE. Lanes: 1 – whole cell lysate (WCL), 2 – column flow through, 3-7 – washes 1-5, and 8 – ESAT-6 protein elution (10 µg). The identified band is approximately 7 kDa in size. **(B)** Ag85B protein, separated by SDS-PAGE. Lanes: 1 – Ag85B (5 µg) after dialysis (24 hour), and 2 – Ag85B (50 µg) before dialysis. The identified band is approximately 30 kDa.

Figure 1. Analysis of purified recombinant ESAT-6 and Ag85B protein antigen characteristics (continued).

The hydrodynamic radius (nm) of complexes formed by ESAT-6 protein (10 µg) and differing molecular ratios of (**C**) R_4Pam_2Cys, and **(D**) E_8Pam_2Cys, in 50 µl PBS, were measured by Dynamic Light Scattering (DLS). Shown here is the particles size dispersion for formulations containing ESAT-6 alone (solid black line in **C** and **D**), R_4Pam_2Cys alone (black dotted line in **C**), E_8Pam_2Cys alone (black dotted line in **F**) and increasing ESAT-6 + adjuvant ratio of 1:1 (blue), 1:3 (orange) and 1:5 (red) for adjuvant R_4Pam_2Cys in **C**, and adjuvant E_8Pam_2Cys in **D.** The hydrodynamic radius (nm) of complexes formed by Ag85B protein (10 µg) and differing molecular ratios of **(E)** R_4Pam_2Cys, and **(F)** E_8Pam_2Cys, in 50 µl PBS, were measured by Dynamic Light Scattering (DLS). Shown here is the particle size dispersion for formulations containing ESAT-6 alone (solid black line in **E** and **F**), R_4Pam_2Cys alone (black dotted line in **E**), E_8Pam_2Cys alone (black dotted line in **F**) and increasing ESAT-6 + adjuvant ratio of 1:1 (blue), 1:3 (orange) and 1:5 (red) for adjuvant R_4Pam_2Cys in **E**, and adjuvant E_8Pam_2Cys in **F.** Highlighted in **C**, **D**, **E**, **F** are peaks corresponding to a shift in particle size between protein alone and protein + adjuvant. The radius size (nm) correlating to the peaks for each formulation shown in **D** and **E** are listed on Table 2, and in **E** and **F** are listed on Table 3.

Table 2. Particle size for ESAT-6, R_4Pam_2Cys, and E_8Pam_2Cys formulations measured by dynamic light scattering.

	Particle size (nm) corresponding to peak number[b]		
Component[a]	**Peak 1**	**Peak 2**	**Peak 3**
ESAT-6 alone (10 µg)	4.38	15.78	99.5
R_4Pam_2Cys alone (3 moles)	5.57	99.5	NA
ESAT-6 + R_4Pam_2Cys 1:1	4.38	66.68	281.79
ESAT-6 + R_4Pam_2Cys 1:3	3.73	15.78	107.81
ESAT-6 + R_4Pam_2Cys 1:5	3.44	10.57	84.79
E_8Pam_2Cys alone (3 moles)	4.74	126.53	NA
ESAT-6 + E_8Pam_2Cys 1:1	4.04	21.73	116.8
ESAT-6 + E_8Pam_2Cys 1:3	4.38	21.73	116.8
ESAT-6 + E_8Pam_2Cys 1:5	5.57	48.41	188.83

Notes: [a]All components were diluted in 50 µl PBS and measured at 21 degrees Celcius.

[b]Peak numbers are numbered from left to right, correlate with increase in particle size.

Table 3. Particle size for Ag85B, R_4Pam_2Cys and E_8Pam_2Cys formulations measured by dynamic light scattering.

	Particle size (nm) corresponding to peak number[b]		
Component[a]	**Peak 1**	**Peak 2**	**Peak 3**
AG85B alone (10 µg)	3.18	78.26	NA
R_4Pam_2Cys alone (3 moles)	5.57	99.5	NA
AG85B + R_4Pam_2Cys 1:1	6.03	78.26	627.5
AG85B + R_4Pam_2Cys 1:3	5.57	72.24	579.35
AG85B + R_4Pam_2Cys 1:5	5.57	72.24	679.25
E_8Pam_2Cys alone (3 moles)	4.74	91.86	NA
AG85B + E_8Pam_2Cys 1:1	4.38	91.86	NA
AG85B + E_8Pam_2Cys 1:3	4.74	91.86	NA
AG85B + E_8Pam_2Cys 1:5	4.74	281.79	NA

Notes: [a]All components were diluted in 50 µl PBS and measured at 21 degrees Celcius.

[b]Peak numbers are numbered from left to right, correlate with increase in particle size.

ESAT-6$_{1-20}$ peptide could restimulate CD4$^+$ T cells but not CD8$^+$ T cells

ESAT-6 is known to be able to generate strong T lymphocyte responses, and it has been reported that murine responses are directed to the epitope ESAT-6_{1-20} (61). To therefore confirm that our recombinant ESAT-6 could indeed induce these responses, C57BL/6 mice were vaccinated and seven days later, splenocytes harvested and restimulated *ex vivo* with ESAT-6_{1-20} to measure IFN-γ production by $CD4^+$ or $CD8^+$ T cells in. While vaccination with ESAT-6 antigen alone induced detectable $CD4^+$ IFN-γ^+ T cells, vaccination with ESAT-6 + CFA induced significantly stronger responses (p = 0.0268; Fig. 2A). These responses were similar to those induced by vaccination with ESAT-6_{1-20} peptide alone or with CFA. However, very little ESAT-6_{1-20}-specific IFN-γ^- production was observed by $CD8^+$ T cells in mice vaccination with all formulations (Fig. 2B). In comparison, mice vaccinated with the model antigen ovalbumin (OVA) with CFA resulted in the induction of OVA-specific $CD8^+$ T cell responses indicating that the ability of these mice to induce these responses was not impaired.

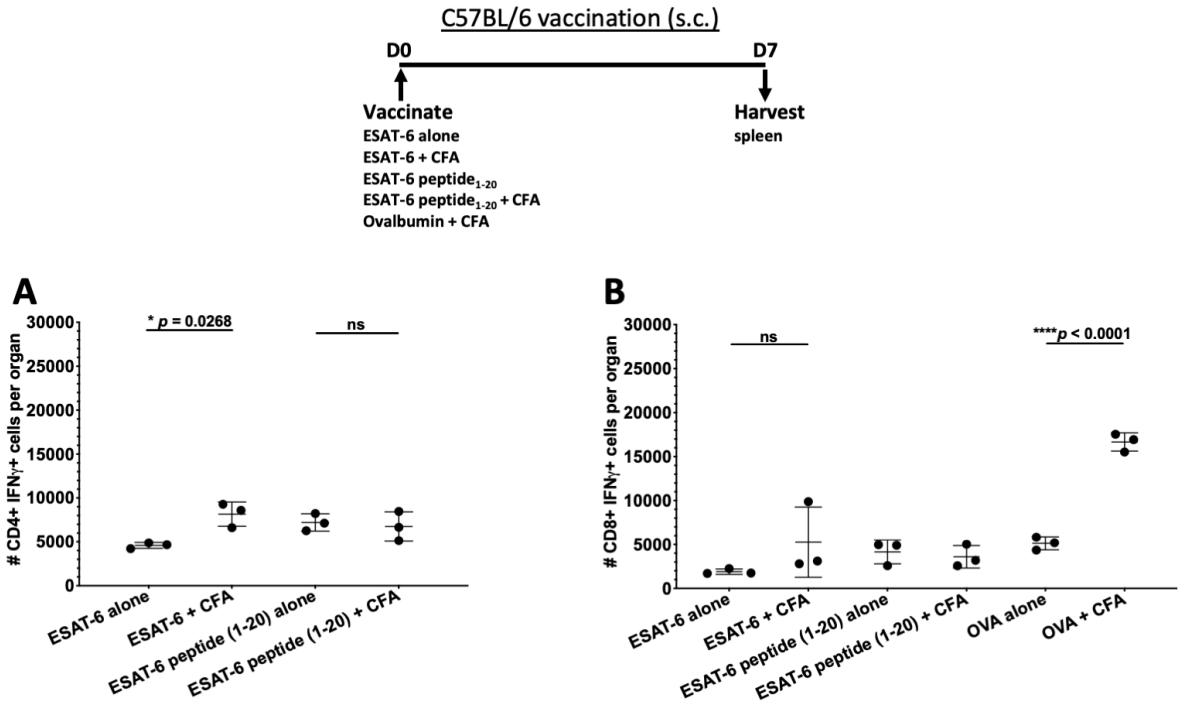

Figure 2. Enumeration of CD4$^+$ and CD8$^+$ T cells producing interferon-gamma (IFN-γ) after vaccination with ESAT-6 and ESAT-6 peptide$_{1-20}$.

(A) CD4$^+$ IFN-γ$^+$ T cells, and **(B)** CD8$^+$ IFN-γ$^+$ T cells enumerated from splenoctyes of C57BL/6 mice sacrificed seven days after subcutaneous vaccination with ESAT-6 protein or ESAT-6 peptide$_{1-20}$ (with or without complete Freund's adjuvant (CFA)) were stimulated with ESAT-6 peptide$_{1-20}$. CD8$^+$ IFN-γ$^+$ T cell responses after vaccination with chicken ovalbumin (OVA) protein with or without CFA in response to SIINFEKL peptide (epitope from OVA$_{257-264}$ – H-2K^b-restricted) were graphed as a control. Data were analysed by one-way ANOVA with Tukey post-test. The null hypothesis (no difference in mean cell numbers between treatment groups) was rejected if *$p < 0.05$, **$p < 0.01$, ***$p < 0.001$ or ****$p < 0.0001$. The error bars represent standard deviation (n=4).

Vaccination with ESAT-6 + R$_4$Pam$_2$Cys induced greater numbers of IFN-γ$^+$ T cells in the spleen of both intranasally and subcutaneously vaccinated mice

To evaluate the ability of Pam$_2$Cys to adjuvant ESAT-6-specific T cell responses, mice were vaccinated with ESAT-6 formulated with R$_4$Pam$_2$Cys or E$_8$Pam$_2$Cys. Mice were vaccinated intranasally as the typical site of MTB infection is via the lungs, but also subcutaneously as most vaccines are administered in this manner. We then harvested and restimulated cells from lungs or spleens with ESAT-6 protein and measured IFN-γ production by T cells. Irrespective of route, mice vaccinated with ESAT-6 + R$_4$Pam$_2$Cys appeared to have higher T cell responses overall (Fig. 3B, 3C) than those vaccinated with ESAT-6 + E$_8$Pam$_2$Cys (Fig. 3D, 3E). However, there were no significant differences in IFN-γ$^+$ CD4$^+$ T cells induced by any ratio of ESAT+ R$_4$Pam$_2$Cys mixtures compared to vaccination with ESAT-6 alone

in either lungs or spleens or by any route (Fig. 3B). While this was also true for IFN-γ^+ $CD8^+$ T cell responses, we did observe much stronger responses between 4- and 10-fold compared to IFN-γ^+ $CD4^+$ T cell responses. There was additionally, more IFN-γ^+ $CD8^+$ T cells in subcutaneously vaccinated mice compared to intranasally vaccinated mice, especially when they received the 1:1 formulation (p = 0.0336; Fig 3C). This suggests that vaccination with ESAT-6 + R_4Pam_2Cys induced not only better $CD8^+$ than $CD4^+$ T cell responses, but vaccination via the subcutaneous route was more effective than the intranasal route.

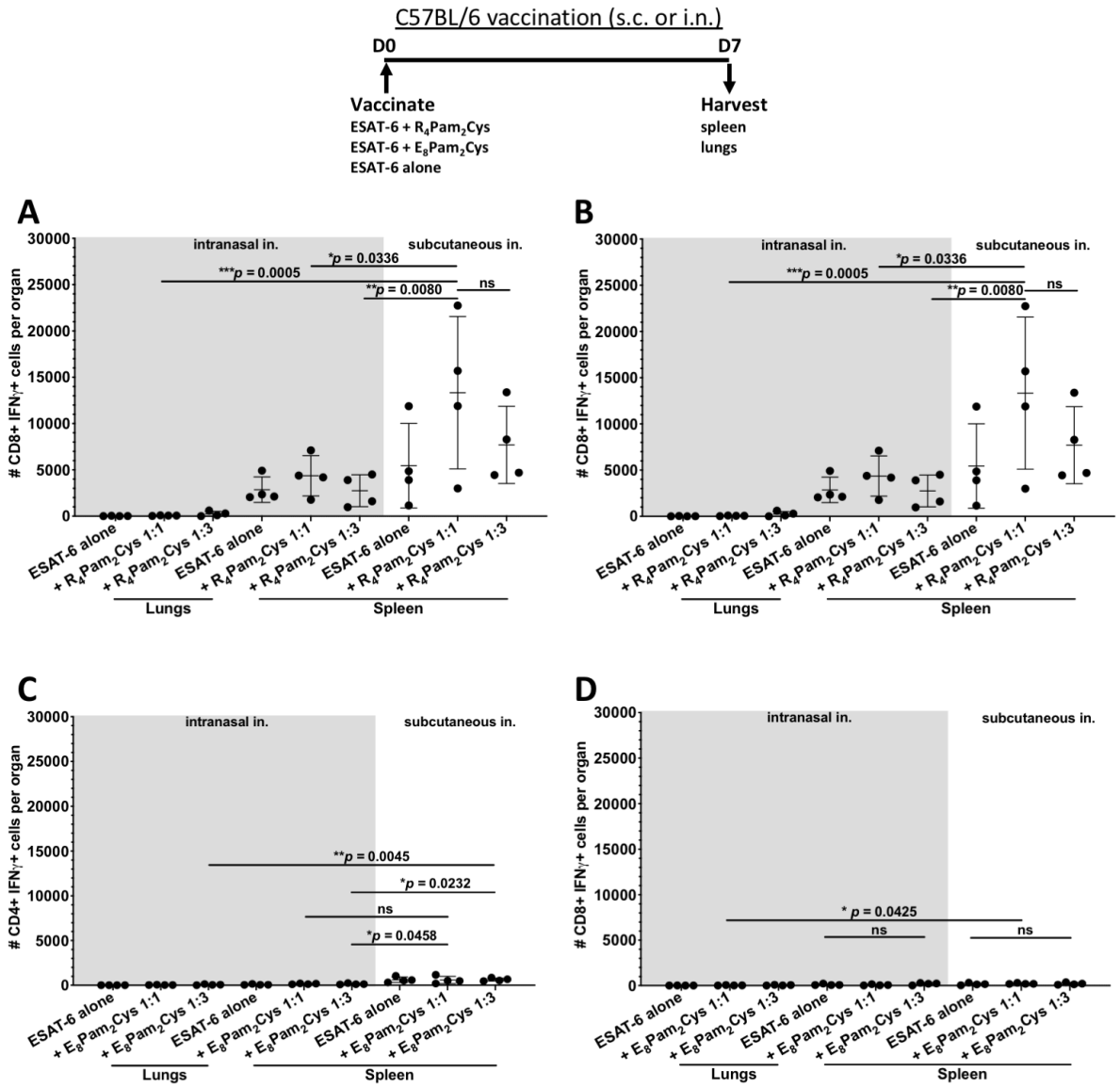

Figure 3. Enumeration of $CD4^+$ and $CD8^+$ T cells producing interferon-gamma (IFN-γ) after vaccination with ESAT-6 and lipopeptide (continued next page).

(A) $CD4^+$ IFN-γ^+ T cells, and **(B)** $CD8^+$ IFN-γ^+ T cells enumerated from the lungs and spleens of mice vaccinated with ESAT-6 protein + R_4Pam_2Cys after restimulation with ESAT-6 protein.

Figure 3. Enumeration of $CD4^+$ and $CD8^+$ T cells producing interferon-gamma (IFN-γ) after vaccination with ESAT-6 and lipopeptide (continued).

(C) $CD4^+$ IFN-γ^+ T cells and **(D)** $CD8^+$ IFN-γ^+ T cells enumerated from the lungs and spleens of mice vaccinated with ESAT-6 protein + E_8Pam_2Cys after restimulation with ESAT-6 protein. Intranasally vaccinated mice are demarcated by a grey box, the groups outside this box were vaccinated subcutaneously (**A, B, C, D**). The null hypothesis (no difference in mean cell numbers between treatment groups) was rejected if $*p < 0.05$, $**p < 0.01$, $***p < 0.001$ or $****p < 0.0001$. The error bars represent standard deviation (n=4).

Vaccination with ESAT-6 + R_4Pam_2Cys produced IL-17A, IL-2 and IL-10 cytokines in the lungs but not IFN-γ or TNF.

As above, cells from the lungs and spleens of ESAT-6 + R_4Pam_2Cys vaccinated mice were restimulated with ESAT-6 protein to examine recall immune responses via the production of specific cytokines. Intranasal ESAT-6 + R_4Pam_2Cys 1:3 induced IL-17A responses, which were greater than both ESAT-6 alone and ESAT-6 + R_4Pam_2Cys 1:3 in the spleen ($p = 0.0286$; Fig. 4A). Intranasal ESAT-6 + R_4Pam_2Cys 1:3 produced more IL-2 and IL-10 in the lungs than in the spleen ($p = 0.0481$; Fig. 4B and $p = 0.0230$; Fig. 4C, respectively). ESAT-6 + R_4Pam_2Cys 1:3 when given intranasally appeared to be the most effective at inducing ESAT-6-specific cytokines (Fig. 4A-C). Both vaccine formulations induced poor IFN-γ responses by both vaccination routes (Fig. 4D) and induced only minor TNF responses in the lung (Fig. 4E), which were not significant. ESAT-6 did not induce IL-4, IL-6 or MCP-1 responses (Supp. Fig. S2). Overall, subcutaneous vaccination was the least effective at inducing these cytokine responses. Intranasal vaccination induced higher cytokine responses to ESAT-6, particularly in the lungs (Fig. 4A-F), although IL-12 was the only cytokine that was significantly induced in the spleen without also being generated in the lungs (Fig. 4F). This suggests that the ESAT-6 vaccines are capable of generating ESAT-6-specific responses in the lungs via intranasal administration but are less proficient at inducing protein-specific systemic cytokines responses (either by intranasal or subcutaneous vaccination).

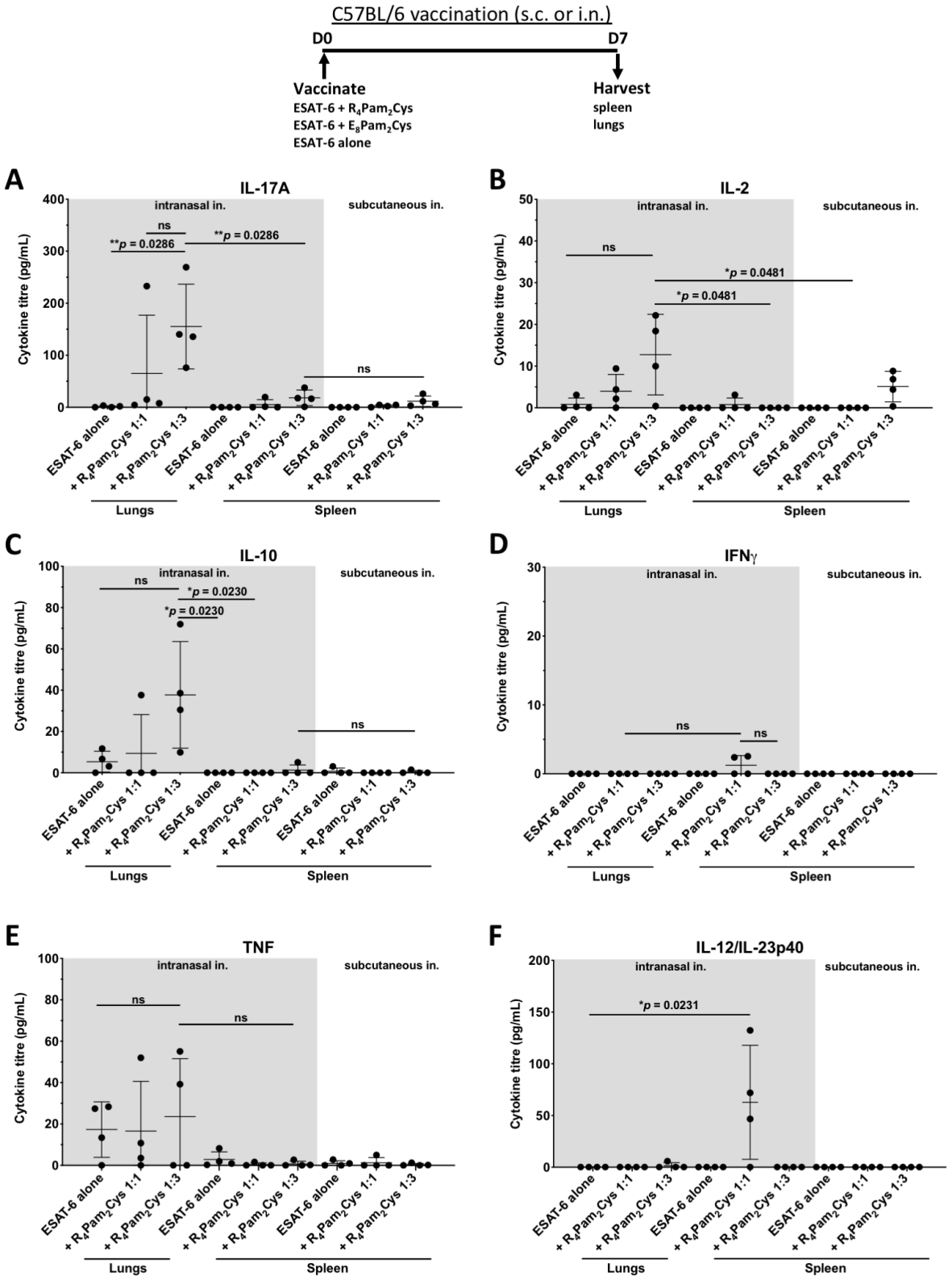

Figure 4. Cytokine responses after ESAT-6 + R_4Pam_2Cys vaccination (continued next page).
C57BL/6 mice were vaccinated intranasally and subcutaneously with ESAT-6 alone or ESAT-6 + R_4Pam_2Cys and sacrificed after seven days. Lung and spleen cells from these mice were restimulated with ESAT-6 protein to measure cytokine responses.

Figure 4. Cytokine responses after ESAT-6 + R_4Pam_2Cys vaccination (continued).
Shown here are plots for cytokines **(A)** IL-17A, **(B)** IL-2, **(C)** IL-10, **(D)** Interferon-gamma (IFN-γ), **(E)** Tumour necrosis factor (TNF), and **(F)** IL-12/IL-23p40 produced. The null hypothesis (no difference in mean titres between treatment groups) was rejected if *$p < 0.05$, **$p < 0.01$, ***$p < 0.001$ or ****$p < 0.0001$. The error bars represent standard deviation (n=4).

Vaccination with Ag85B + R_4Pam_2Cys or Ag85B + E_8Pam_2Cys did not induce IFN-γ$^+$ T cells in mouse spleens.

In examining the immunogenicity of Ag85B containing formulations, C57BL/6 mice were vaccinated and IFN-γ^+ production by T cells measured upon stimulation with protein in culture. Mice vaccinated with Ag85B + R_4Pam_2Cys did not induce $CD4^+$ or $CD8^+$ T cells compared to vaccination with Ag85B alone (Fig. 5A, B). Similarly, mice vaccinated with Ag85B + E_8Pam_2Cys also showed no significant differences in $CD4^+$ IFN-γ^+ or $CD8^+$ IFN-γ^+ T cell responses compared to mice vaccinated with protein alone (Fig. 5C, D).

Vaccination with Ag85B + Pam_2Cys induced IL-17A and IL-4 cytokines but not IFN-γ or TNF responses.

Cells from the spleens of mice vaccinated with Ag85B + R_4Pam_2Cys or Ag85B + E_8Pam_2Cys were also restimulated with Ag85B protein to assess recall immune responses as measured by cytokine expression. Ag85B + R_4Pam_2Cys 1:1 induced IL-17A responses greater than both Ag85B alone and Ag85B + E_8Pam_2Cys 1:1 ($p = 0.0286$; Fig. 6A). Ag85B + R_4Pam_2Cys 1:1 produced more IL-4 than Ag85B alone vaccination ($p = 0.0286$; Fig. 6B). Similar to ESAT-6 + Pam_2Cys vaccination, Ag85B + Pam_2Cys vaccine formulations did not induce more IFN-γ or TNF than protein alone (Fig. 6C, D). Ag85B + lipopeptide induced minor IL-2 (Fig. 6E) but strong IL-10 responses (Fig. 6F), although none of these cytokine titres was significantly greater than that observed using Ag85B alone. Ag85B + R_4Pam_2Cys or E_8Pam_2Cys did not induce IL-12/IL-23p40, IL-6 and MCP-1 responses greater than protein alone (Supp. Fig. S3A-C). Ag85B + R_4Pam_2Cys 1:1 was the only Ag85B + Pam_2Cys formulation to induce cytokine (IL-17A and IL-4) responses greater than Ag85B alone vaccination (Fig. 6A, B). However, high cytokine responses were induced by Ag85B + R_4Pam_2Cys or E_8Pam_2Cys vaccinations (Fig. 6A-F, Supp. Fig. S3A-C). These data suggest that there is no dose dependent response to increasing lipopeptide concentrations, but the addition of R_4Pam_2Cys 1:1 can enhance IL-17A and IL-4 responses to Ag85B vaccination.

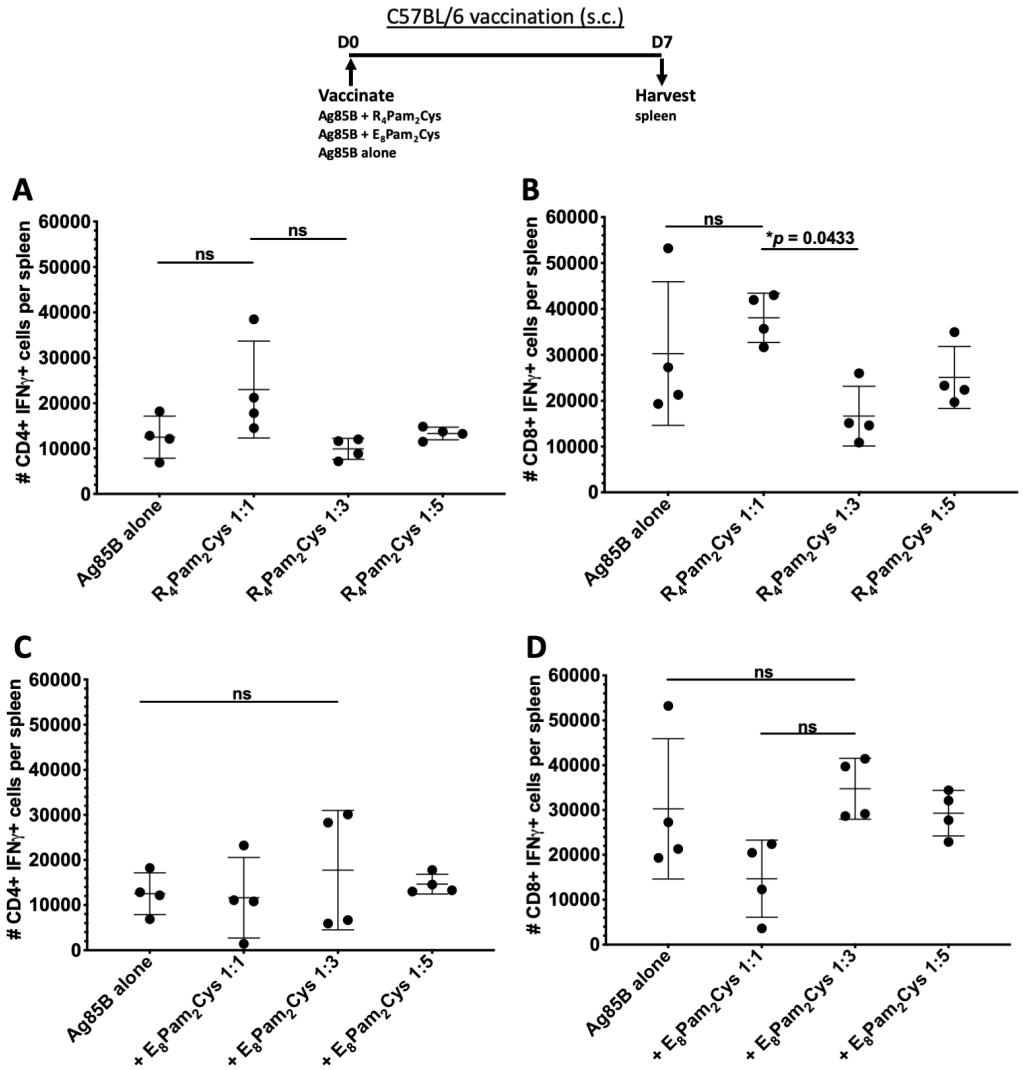

Figure 5. Enumeration of CD4$^+$ and CD8$^+$ T cells producing interferon-gamma (IFN-γ) and Ag85B-specific antibody titres after vaccination with Ag85B.

C57BL/6 mice were vaccinated subcutaneously with Ag85B alone, Ag85B protein + R_4Pam_2Cys or Ag85B protein + E_8Pam_2Cys and sacrificed after seven days. **(A)** CD4$^+$ IFN-γ$^+$ T cells, and **(B)** CD8$^+$ IFN-γ$^+$ T cells enumerated from the spleens of Ag85B protein + R_4Pam_2Cys after restimulation with Ag85B protein. **(C)** CD4$^+$ IFN-γ$^+$ T cells, and **(D)** CD8$^+$ IFN-γ$^+$ T cells enumerated from the spleens of Ag85B protein + E_8Pam_2Cys after restimulation with Ag85B protein. The null hypothesis (no difference in mean cell numbers between treatment groups) was rejected if $*p < 0.05$, $**p < 0.01$, $***p < 0.001$ or $****p < 0.0001$. The error bars represent standard deviation (n=4).

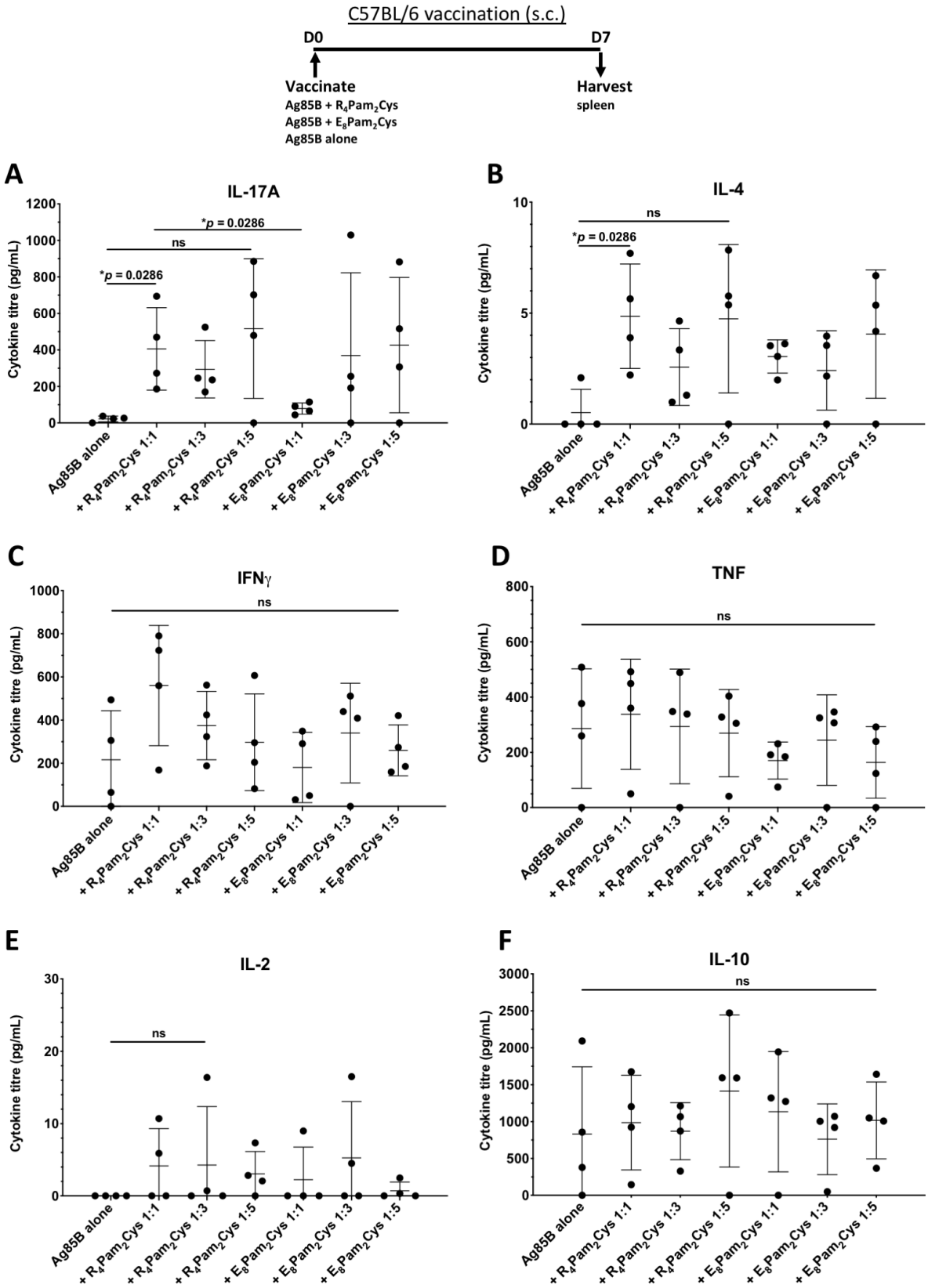

Figure 6. Cytokine responses after Ag85B + R_4Pam_2Cys vaccination (continued next page).

C57BL/6 mice were vaccinated subcutaneously with Ag85B, Ag85B + R_4Pam_2Cys or Ag85B + E_8Pam_2Cys and sacrificed after seven days. Splenocytes from these mice were restimulated with Ag85B protein to measure cytokine responses.

Figure 6. Cytokine responses after Ag85B + R_4Pam_2Cys vaccination (continued).

Shown here are plots for cytokines **(A)** IL-17A, **(B)** IL-4, **(C)** Interferon-gamma (IFN-γ), **(D)** Tumour necrosis factor (TNF), **(E)** IL-10, and **(F)** IL-2 produced from immune cells in the spleen. The null hypothesis (no difference in mean titres between treatment groups) was rejected if $*p < 0.05$, $**p < 0.01$, $***p < 0.001$ or $****p < 0.0001$. The error bars represent standard deviation (n=4).

Higher Ag85B-specific antibody responses in mice vaccinated with Ag85B + R_4Pam_2Cys and Ag85B + E_8Pam_2Cys compared to Ag85B protein alone.

To evaluate the ability of the vaccine to induce Ag85B-specific antibody responses and identify whether the addition of Pam_2Cys had an adjuvanting effect, mice were vaccinated with Ag85B + R_4Pam_2Cys, Ag85B + E_8Pam_2Cys and Ag85B alone. Following two doses of vaccine, sera were obtained from vaccinated animals and Ag85B-specific titres measured. Vaccination with Ag85B + R_4Pam_2Cys or Ag85B + E_8Pam_2Cys induced significantly more IgG_1 Ag85B-antibodies compared to Ag85B alone (p <0.0001; Fig. 7). However, there was no significant differences in antibodies induced by antigens formulated with either lipopeptide.

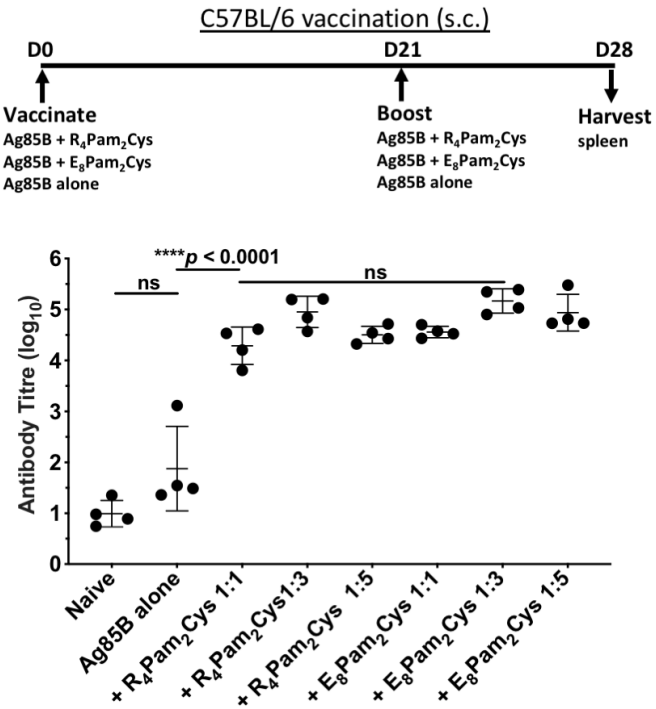

Figure 7. Antibody responses to Ag85B vaccination.

Ag85B-specific (IgG_1) antibody titres from sera obtained from mice vaccinated and boosted with Ag85B alone, Ag85B + R_4Pam_2Cys and Ag85B + E_8Pam_2Cys, at day 28. Naïve mice are included as as a control. The null hypothesis (no difference in mean antibody titres between treatment groups) was rejected if $*p < 0.05$, $**p < 0.01$, $***p < 0.001$ or $****p < 0.0001$. The error bars represent standard deviation (n=4).

Suitability of HHD mice to induce HLA-A2-specific CD8$^+$ T cell responses to TB-derived antigens

To measure the ability of the two vaccines to induce CD8$^+$ T cell responses in a human HLA-A2-restrictive manner, HHD transgenic mice which possess the HLA-A2*01 allele (54, 55), were used. To determine the suitability of these mice to induce CD8$^+$ T cell responses against HLA-A2-restricted epitopes, mice were vaccinated with a known human HLA-A2-specific epitope, GILGFVFTL (GIL), derived from influenza Matrix-1 (M1) protein (62), formulated with CFA. GIL-specific CD8$^+$ IFN-γ^+ T cell responses were detected from seven days following a single vaccination and subsequently increased to peak between 28-31 days (Fig. 8A). Similar responses to challenge with whole influenza virus strain X-31 were also observed 10 days post-infection (Fig. 8B). HLA-A2 specific CD8$^+$ T cell responses against TB-derived antigens were subsequently examined utilising an array of four epitopes derived from Ag85A, Ag85B and TB10.4 (Table 1). MTB antigenic HLA-A2 peptides were predicted using SYFPEITHI. Identified peptides that were also referenced in literature (15, 63, 64) were chosen as putative antigens to test in the HHD mouse model. After vaccination and boost, no significant increases in the CD8$^+$ IFN-γ^+ T cell responses were observed against each of these peptides compared to vaccinations using an epitope that is only recognisable by the murine MHC Class I molecule, H2-K^d (TYQRTRALV) (65) (Fig. 8C). In contrast, GIL-specific CD8$^+$ T cell responses were induced when this epitope was used for vaccination (Fig. 8C). These results therefore indicate that these TB peptides are not capable of inducing CD8$^+$ IFN-γ^+ immune responses in HHD mice and were therefore unsuitable for analysing HLA-A2 specific responses induced by our vaccine candidates.

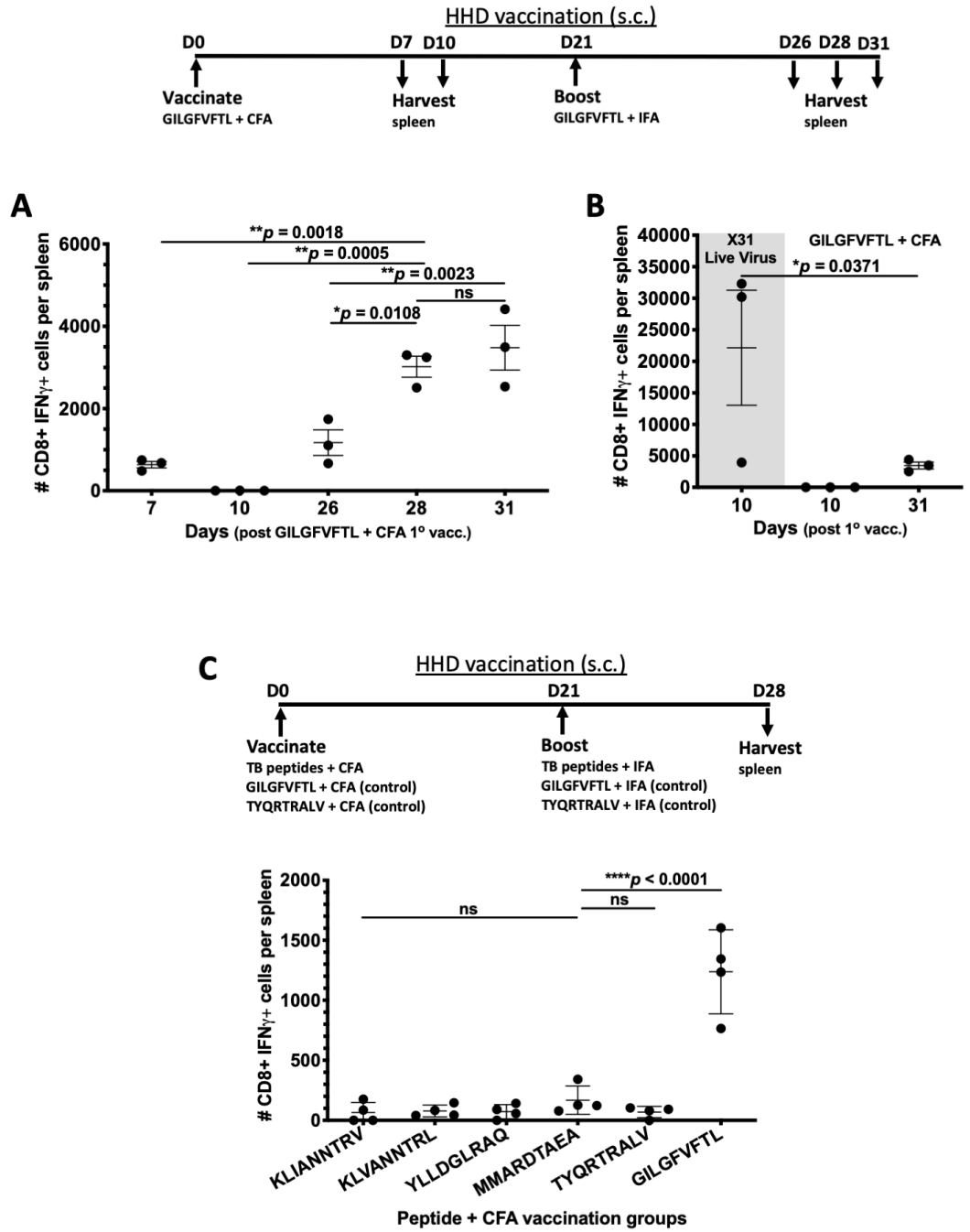

Figure 8. Enumeration of CD8$^+$ T cells producing interferon-gamma (IFN-γ) against putative TB peptide epitopes in HLA-A2-restricted (HHD) mice (continued next page).

(A) The kinetics of CD8$^+$ IFN-γ$^+$ T cell responses from HLA-A2 restricted (HHD) mice splenocytes were measured at days 7, 10, 26, 28 and 31 after vaccination with GILGFVFTL (GIL) peptide (from influenza Matrix $1_{58\text{-}66}$ protein – HLA-A2-restricted epitope) + CFA and booster vaccination with GIL + incomplete Freund's adjuvant (IFA) at day 21. CD8$^+$ IFN-γ$^+$ T cell responses to GIL peptide vaccination was measured from the splenocytes of mice sacrificed at each timepoint and restimulated with the GIL peptide. The error bars represent standard error of the mean (n=3).

Figure 8. Enumeration of $CD8^+$ T cells producing interferon-gamma (IFN-γ) against putative TB peptide epitopes in HLA-A2-restricted (HHD) mice (continued).

(B) HHD CD8+ IFN-γ+ T cell responses to influenza virus X-31 infection after 10 days, from splenocytes restimulated with GIL peptide. Responses from splenocytes of HHD mice infected with X-31 influenza virus are demarcated with a grey box. CD8+ IFN-γ+ T cell responses from HHD mice vaccinated with GIL + CFA at days 10 and 31 (boosted with GIL + IFA at day 21) are also plotted for comparison (white background). The error bars represent standard error of the mean (n=3). **(C)** HHD CD8+ IFN-γ+ T cells from peptide-restimulated splenocytes at day 28, after vaccination with TB peptide (KLIANNTRV, KLVANNTRL, YLLDGLRAQ or MMARDTAEA) + CFA at day 0 and booster at day 21 with TB peptides + IFA. Mice vaccinated with GIL peptide and TYQRTRALV (TYQ) peptide (from influenza Nucleoprotein147-155 – H-2Kd-restricted epitope) have been included as experimental controls. The error bars represent standard deviation (n=4). The null hypothesis (no difference in mean cell numbers between treatment groups) was rejected if $*p < 0.05$, $**p < 0.01$, $***p < 0.001$ or $****p < 0.0001$.

Discussion

In this study, we utilised known immunogenic TB proteins, ESAT-6 and Ag85B, to explore whether the addition of a TLR-2 agonist can increase protein-specific immune responses, in particular $CD8^+$ and $CD4^+$ T cells and antibody responses. Though $CD4^+$ IFN-γ^+ T cells are typically associated with TB protection (17, 18, 66-69), previous studies have shown that $CD8^+$ T cells play a non-redundant role in TB protection (17, 19-21). For this we utilised HLA-A2 restricted (HHD) mice to identify whether human HLA-A2 epitopes from known and predicted immunogenic TB antigens could induce a measurable $CD8^+$ IFN-γ^+ T cell responses.

ESAT-6 and Ag85B have been widely described as having immunodominant immune responses in patients infected with TB. These proteins are easily recognisable by the human immune system and able to elicit cellular mediated immune responses, suggesting that they would be promising vaccine antigens but may require an adjuvant to help shape and stimulate the immune responses required to prevent infection. Previous mouse studies have shown that ESAT-6 and Ag85B are capable of inducing T_h1 type immune responses, in particular strong T cell and IFN-γ responses.

The ESAT-$6_{1\text{-}20}$ epitope alone was immunogenic and did not require adjuvant to induce detectable responses, supporting previous findings of its immunogenicity (37, 61). We also found that it could only restimulate $CD4^+$ T cells, presumably as it is 20 amino acids long and more suited to an open MHC class II molecule peptide binding groove, rather than MHC class I (70).

When comparing intranasal or base-of-tail subcutaneous vaccination routes, subcutaneous vaccination was better at priming ESAT-6 specific responses in the spleen compared to intranasal vaccination. Intranasal vaccination also appeared to induce higher numbers of lymphocytes in the spleen compared to the lungs with highest responses obtained using ESAT-6 + R_4Pam_2Cys at a 1:1 ratio. This increase in protein-specific $CD8^+$ T cell responses induced by R_4Pam_2Cys has previously been shown using chicken ovalbumin protein (52). This formulation, however, does not appear to be as effective at generating higher $CD4^+$ T cell responses than ESAT-6 alone vaccination even though vaccinations using ovalbumin were capable of inducing $CD4^+$ IFN-γ^+ T cells (Supp. Fig. S1A).

Ag85B is well described as immunogenic (40, 44, 63, 71, 72), therefore detectable cellular responses to Ag85B alone were expected. While it appeared that the binding of Ag85B (with a putative charge of -3) with R_4Pam_2Cys resulted in more dramatic changes to the homogeneity of the complexes formed, there were no significant increases in overall T cell responses compared to Ag85B vaccination alone. This might be due to the properties of the complexes formed which are in contrast to the more significant changes in particle size observed using ESAT-6. In fact, previous studies have highlighted that a strong

association between protein and adjuvant is required to increase DC uptake and induce T cell responses (52, 53).

Vaccination with either ESAT-6 or Ag85B and R_4Pam_2Cys induced significantly more IL-17A production than protein alone. The role of IL-17 in TB remains unclear. IL-17 is produced by T_h17 cells and T_h17 cells have been implicated in TB pathology via inflammation and tissue damage, but also as mediators of antimicrobial and pro-inflammatory responses (73, 74). IL-17A driven responses can be induced in the lungs by intranasal vaccination with BCG (75) and have been shown to play an essential role in granuloma formation in the lungs (76). Mice deficient in IL-17A are unable to control MTB infection (76-78) and humans with chronic TB have decreased levels of IL-17A (79).

In this study, increased IL-2 and IL-10 were induced by ESAT-6 + R_4Pam_2Cys vaccination and increased IL-4 was induced by Ag85B + R_4Pam_2Cys vaccination. T_h2 cytokines such as IL-4 and IL-10 have been linked to TB infection and TB reactivation (80, 81). In mice, IL-4 in lung lesions coincide with pneumonia and necrosis, and increased mortality (82). Mice with defective IL-10 exhibit an increase in antimycobacterial immunity (83). Humans with advanced TB disease produce higher levels of IL-4 and IL-10 (84, 85), suggesting that these responses may not lead to protection by ESAT-6 and Ag85B + R_4Pam_2Cys vaccination.

IL-2 is a T_h1 cytokine and plays a role in regulating T cell differentiation and expansion (86). IL-2 can reduce mycobacterial replication in murine studies (87, 88), and humans with active TB often have decreased IL-2-induced cell proliferation, IL-2 receptor production and serum IL-2 (89, 90). Yet in this study, the production of IL-2 by intranasal ESAT-6 + R_4Pam_2Cys vaccination does not coincide with a strong T cell response in the lungs. The IL-10 response may possibly be suppressing T cell activation and expansion (91). T_h1 responses, such as IFN-γ and TNF production, have been largely implicated in protection against TB (66-69, 92), though neither ESAT-6 or Ag85B vaccines generated strong IFN-γ or TNF responses. However, T_h1 responses are not fully protective against TB (93, 94) and therefore other immune correlates need to be explored.

The low T cell responses and cytokine induction observed using our two vaccines suggest that these formulations are unlikely to be protective against TB. We did, however, identify that intranasal vaccination was capable of inducing improved splenic T cell responses and protein-specific cytokine production. Increased protective responses against TB from mice intranasally vaccinated with the BCG vaccine compared to subcutaneous vaccination has previously been identified (95, 96). The findings from our study suggest the intranasal route of administration may still be an effective method of vaccination against TB, though it may require a change in antigen or adjuvant selection to enhance IFN-

γ responses. Other delivery methods could be assessed, as a recent study has shown that high-dose BCG administered intravenously could protect nine out of ten macaques from virulent TB (97). The efficacy of intravenous BCG contrasts the widely varied protection afforded by intradermal vaccination with BCG (11, 12, 98). This implicates the importance of vaccine delivery and its effect on immune responses.

Nevertheless, as these vaccine formulations are capable of inducing strong antibody responses, the protein and lipopeptide vaccine formulations may be more suited to target the extracellular phase of MTB infectious cycle.

This study also explored the use of transgenic mice expressing human HLA-A2 molecules as a model for testing TB-vaccine efficacy in humans. We chose peptides from Ag85B, Ag85B, and TB10.4. As TB10.4 is from the same *M. tuberculosis* ESX-family as ESAT-6, we chose to test epitopes from this protein as ESAT-6 is used in the Quantiferon Gold test for TB infection and its presence could affect the validity of any positive T cell responses observed. However, the previously reported epitopes and SYPETHI-predicted epitopes did not induce detectable $CD8^+$ IFN-γ^+ responses in HHD mice. As we did not examine other cytokines, we cannot exclude that non-IFN-γ responses were induced instead. We also did not test whether whole MTB proteins could be used to induce responses in these mice and there may have been HLA-A2 immune responses that were not detected.

Given the lacklustre T cell responses observed using these antigens in their peptide or protein formulations, we did not proceed with mouse MTB challenge studies. We did see the induction of strong antibody responses, however the role of humoral responses during active and latent TB remains contentious. Nevertheless, recent studies have identified a functional role for TB antibodies in latent infection by increasing macrophage killing of intracellular MTB (24, 69) providing an impetus to evaluate the protective efficacies of the vaccine formulations used in this study in the future.

Conclusions

T_h1 responses, particularly $CD4^+$ T cells and IFN-γ, are known to play key roles in the control of TB. The vaccines in this study generated strong protein- specific antibody responses, however they induced poor vaccine-specific $CD4^+$ IFN-γ^+ T cell responses. Although these vaccines could potentially be used to examine antibody responses against TB during infection, it is likely that they will be unable to control infection against MTB without accompanying T_h1 immune responses. Therefore, alternative antigen and vaccination routes should be further investigated to enhance MTB-specific T_h1 responses of future vaccination formulations.

Acknowledgements

We would like to thank Kylie Horracks for assistance with murine intranasal challenge experiments.

References

1. Tønjum T, Welty DB, Jantzen E, Small PL. 1998. Differentiation of *Mycobacterium ulcerans*, *M. marinum*, and *M. haemophilum*: Mapping of Their Relationships to *M. tuberculosis* by Fatty Acid Profile Analysis, DNA-DNA Hybridization, and 16S rRNA Gene Sequence Analysis. J Clin Micro 36: 918-925.
2. Stinear TP, Jenkin GA, Johnson PD, Davies JK. 2000. Comparative genetic analysis of *Mycobacterium ulcerans* and *Mycobacterium marinum* reveals evidence of recent divergence. J Bacteriol 182: 6322-6330.
3. World Health Organization. 2019. Global tuberculosis report 2019. World Health Organization, Geneva. Licence: CCBY-NC-S3.0IGO. Accessed 20 December 2019.
4. Ottenhoff TH, Kaufmann SH. 2012. Vaccines against tuberculosis: where are we and where do we need to go? PLoS Pathog 8: e1002607.
5. O'Garra A, Redford PS, McNab FW, Bloom CI, Wilkinson RJ, Berry MP. 2013. The immune response in tuberculosis. Annu Rev Immunol 31: 475-527.
6. Harisinghani MG, McLoud TC, Shepard JA, Ko JP, Shroff MM, Mueller PR. 2000. Tuberculosis from head to toe. Radiographics 20: 449-470.
7. Houben RMGJ, Dodd PJ. 2016. The Global Burden of Latent Tuberculosis Infection: A Re-estimation Using Mathematical Modelling. PLoS Med 13: e1002152-e1002152.
8. Lin, P. L., and J. L. Flynn. 2010. Understanding Latent Tuberculosis: A Moving Target. J Immunol 185: 15.
9. World Health Organization. 2010. *Treatment of tuberculosis: guidelines (fourth edition)*. Accessed 20 December 2019.
10. Lewis KN, Liao R, Guinn KM, Hickey MJ, Smith S, Behr MA, Sherman DR. 2003. Deletion of RD1 from *Mycobacterium tuberculosis* mimics bacille Calmette-Guérin attenuation. J Infect Dis 187: 117-123.
11. Sterne JA, Rodrigues LC, Guedes IN. 1998. Does the efficacy of BCG decline with time since vaccination? Int J Tuberc Lung Dis 2: 200-207.
12. Andersen P, Doherty TM. 2005. The success and failure of BCG - implications for a novel tuberculosis vaccine. Nat Rev Microbiol 3: 656-662.
13. Hesseling AC, Marais BJ, Gie RP, Schaaf HS, Fine PE, Godfrey-Faussett P, Beyers N. 2007. The risk of disseminated Bacille Calmette-Guérin (BCG) disease in HIV-infected children. Vaccine 25: 14-18.

14. World Health Organization. 2007. Meeting of the Global Advisory Committee on Vaccine Safety, 29-30 November 2006. In *Weekly Epidemiological Record*, Geneva. 82: 18-24. Accessed 20 December 2019.
15. Smith SM, Brookes R, Klein MR, Malin AS, Lukey PT, King AS, Ogg GS, Hill AV, Dockrell HM. 2000. Human $CD8^+$ CTL specific for the mycobacterial major secreted antigen 85A. J Immunol 165: 7088-7095.
16. Rook GA. 2007. Th2 cytokines in susceptibility to tuberculosis. *Curr Mol Med* 7: 327-337.
17. Rueda CM, Marin ND, Garcia LF, Rojas M. 2010. Characterization of CD4 and CD8 T cells producing IFN-gamma in human latent and active tuberculosis. Tuberculosis 90: 346-353.
18. Yao S, Huang D, Chen CY, Halliday L, Wang RC, Chen ZW. 2014. $CD4^+$ T cells contain early extrapulmonary tuberculosis (TB) dissemination and rapid TB progression and sustain multieffector functions of $CD8^+$ T and CD3- lymphocytes: mechanisms of $CD4^+$ T cell immunity. J Immunol 192: 2120-2132.
19. Cho S, Mehra V, Thoma-Uszynski S, Stenger S, Serbina N, Mazzaccaro RJ, Flynn JL, Barnes PF, Southwood S, Celis E, Bloom BR, Modlin RL, Sette A. 2000. Antimicrobial activity of MHC class I-restricted $CD8^+$ T cells in human tuberculosis. Proc Natl Acad Sci USA 97: 12210-12215.
20. Silva BD, Trentini MM, da Costa AC, Kipnis A, Junqueira-Kipnis AP. Junqueira-Kipnis. 2014. Different phenotypes of $CD8^+$ T cells associated with bacterial load in active tuberculosis. Immunol Lett 160: 23-32.
21. Kamath A, Woodworth JS, Behar SM. 2006. Antigen-specific $CD8^+$ T cells and the development of central memory during *Mycobacterium tuberculosis* infection. J Immunol 177: 6361-6369.
22. Jacobs AJ, Mongkolsapaya J, Screaton GR, McShane H, Wilkinson RJ. 2016. Antibodies and tuberculosis. Tuberculosis 101: 102-113.
23. Achkar JM, Casadevall A. 2013. Antibody-mediated immunity against tuberculosis: implications for vaccine development. Cell Host Microbe 13: 250-262.
24. Lu LL, Chung AW, Rosebrock TR, Ghebremichael M, Yu WH, Grace PS, Schoen MK, Tafesse F, Martin C, Leung V, Mahan AE, Sips M, Kumar MP, Tedesco J, Robinson H, Tkachenko E, Draghi M, Freedberg KJ, Streeck H, Suscovich TJ, Lauffenburger DA, Restrepo BI, Day C, Fortune SM, Alter G. 2016. A Functional Role for Antibodies in Tuberculosis. Cell Host Microbe 167: 433-443.e414.
25. Li H, Wang X-X, Wang B, Fu L, Liu G, Lu Y, Cao M, Huang H, Javid B. 2017. Latently and uninfected healthcare workers exposed to TB make protective antibodies against *Mycobacterium tuberculosis*. Proc Natl Acad Sci USA 114: 5023-5028.
26. de L. Costello AM, Kumar A, Narayan V, Akbar MS, Ahmed S, Abou-Zeid C, Rook GAW, Stanford J, Moreno C. 1992. Does antibody to mycobacterial antigens, including

lipoarabinomannan, limit dissemination in childhood tuberculosis? Trans R Soc Trop Med Hyg 86: 686-692.

27. Sebina I, Cliff JM, Smith SG, Nogaro S, Webb EL, Riley EM, Dockrell HM, Elliott AM, Hafalla JCR, Cose S. 2012. Long-lived memory B-cell responses following BCG vaccination. PloS One 7: e51381-e51381.
28. de Vallière S, Abate G, Blazevic A, Heuertz RM, Hoft DF. 2005. Enhancement of Innate and Cell-Mediated Immunity by Antimycobacterial Antibodies. Infect Immun 73: 6711.
29. Chen T, Blanc C, Eder AZ, Prados-Rosales R, Souza ACO, Kim RS, Glatman-Freedman A, Joe M, Bai Y, Lowary TL, Tanner R, Brennan MJ, Fletcher HA, McShane H, Casadevall A, Achkar JM. 2016. Association of Human Antibodies to Arabinomannan With Enhanced Mycobacterial Opsonophagocytosis and Intracellular Growth Reduction. J Infect Dis 214: 300-310.
30. Bourinbaiar AS, Batbold U, Efremenko Y, Sanjagdorj M, Butov D, Damdinpurev N, Grinishina E, Mijiddorj O, Kovolev M, Baasanjav K, Butova T, Prihoda N, Batbold O, Yurchenko L, Tseveendorj A, Arzhanova O, Chunt E, Stepanenko H, Sokolenko N, Makeeva N, Tarakanovskaya M, Borisova V, Reid A, Kalashnikov V, Nyasulu P, Prabowo SA, Jirathitikal V, Bain AI, Stanford C, Stanford J. 2019. Phase III, placebo-controlled, randomized, double-blind trial of tableted, therapeutic TB vaccine (V7) containing heat-killed *M. vaccae* administered daily for one month. J Clin Tuberc Other Mycobact Dis 18: 100141-100141.
31. da Costa C, Walker B, Bonavia A. 2015. Tuberculosis Vaccines - state of the art, and novel approaches to vaccine development. Int J Inf Dis 32: 5-12.
32. Day CL, Tameris M, Mansoor N, van Rooyen M, de Kock M, Geldenhuys H, Erasmus M, Makhethe L, Hughes EJ, Gelderbloem S, Bollaerts A, Bourguignon P, Cohen J, Demoitie MA, Mettens P, Moris P, Sadoff JC, Hawkridge A, Hussey GD, Mahomed H, Ofori-Anyinam O, Hanekom WA. 2013. Induction and regulation of T-cell immunity by the novel tuberculosis vaccine M72/AS01 in South African adults. Am J Resp Crit Care Med 188: 492-502.
33. Harboe M, Oettinger T, Wiker HG, Rosenkrands I, Andersen P. 1996. Evidence for occurrence of the ESAT-6 protein in *Mycobacterium tuberculosis* and virulent *Mycobacterium bovis* and for its absence in *Mycobacterium bovis* BCG. Infect Immun 64: 16-22.
34. Guo S, Xue R, Li Y, Wang SM, Ren L, Xu JJ. 2012. The CFP10/ESAT6 complex of *Mycobacterium tuberculosis* may function as a regulator of macrophage cell death at different stages of tuberculosis infection. Med Hypotheses 78: 389-392.
35. Tan T, Lee WL, Alexander DC, Grinstein S, Liu J. 2006. The ESAT-6/CFP-10 secretion system of *Mycobacterium marinum* modulates phagosome maturation. Cell Microbiol 8: 1417-1429.
36. Mustafa AS, Oftung F, Amoudy HA, Madi NM, Abal AT, Shaban F, Rosen Krands I, Andersen P. 2000. Multiple epitopes from the *Mycobacterium tuberculosis* ESAT-6 antigen are recognized by antigen-specific human T cell lines. Clin Inf Dis 30 Suppl 3: S201-205.

37. Reiley WW, Calayag MD, Wittmer ST, Huntington JL, Pearl JE, Fountain JJ, Martino CA, Roberts AD, Cooper AM, Winslow GM, Woodland DL. 2008. ESAT-6-specific CD4 T cell responses to aerosol *Mycobacterium tuberculosis* infection are initiated in the mediastinal lymph nodes. Proc Natl Aca Sci USA 105: 10961-10966.
38. Brandt L, Elhay M, Rosenkrands I, Lindblad EB, Andersen P. 2000. ESAT-6 subunit vaccination against *Mycobacterium tuberculosis*. Infect Immun 68: 791-795.
39. Belisle JT, Vissa VD, Sievert T, Takayama K, Brennan PJ, Besra GS. 1997. Role of the major antigen of *Mycobacterium tuberculosis* in cell wall biogenesis. Science 276: 1420-1422.
40. Takamura S, Matsuo K, Takebe Y, Yasutomi Y. 2005. Ag85B of mycobacteria elicits effective CTL responses through activation of robust Th1 immunity as a novel adjuvant in DNA vaccine. J Immunol 175: 2541-2547.
41. Horwitz MA, Lee BW, Dillon BJ, Harth G. 1995. Protective immunity against tuberculosis induced by vaccination with major extracellular proteins of *Mycobacterium tuberculosis*. Proc Natl Acad Sci USA 92: 1530-1534.
42. Tanghe A, Denis O, Lambrecht B, Motte V, van den Berg T, Huygen K. 2000. Tuberculosis DNA vaccine encoding Ag85A is immunogenic and protective when administered by intramuscular needle injection but not by epidermal gene gun bombardment. Infect Immun 68: 3854-3860.
43. Andersen P, Askgaard D, Ljungqvist L, Bennedsen J, Heron I. 1991. Proteins released from *Mycobacterium tuberculosis* during growth. Infect Immun 59: 1905-1910.
44. Huygen K. 2014. The Immunodominant T-Cell Epitopes of the Mycolyl-Transferases of the Antigen 85 Complex of *M. tuberculosis*. Front Immun 5: 321.
45. Scriba TJ, Tameris M, Mansoor N, Smit E, van der Merwe L, Isaacs F, Keyser A, Moyo S, Brittain N, Lawrie A, Gelderbloem S, Veldsman A, Hatherill M, Hawkridge A, Hill AV, Hussey GD, Mahomed H, McShane H, Hanekom WA. 2010. Modified vaccinia Ankara-expressing Ag85A, a novel tuberculosis vaccine, is safe in adolescents and children, and induces polyfunctional $CD4^+$ T cells. Eur J Immunol 40: 279-290.
46. Weinrich Olsen A, van Pinxteren LA, Meng Okkels L, Birk Rasmussen P, Andersen P. 2001. Protection of mice with a tuberculosis subunit vaccine based on a fusion protein of antigen 85b and esat-6. Infect Immun 69: 2773-2778.
47. Skjot RL, Brock I, Arend SM, Munk ME, Theisen M, Ottenhoff TH, Andersen P. 2002. Epitope mapping of the immunodominant antigen TB10.4 and the two homologous proteins TB10.3 and TB12.9, which constitute a subfamily of the esat-6 gene family. Infect Immun 70: 5446-5453.
48. Skjot RL, Oettinger T, Rosenkrands I, Ravn P, Brock I, Jacobsen S, Andersen P. 2000. Comparative evaluation of low-molecular-mass proteins from *Mycobacterium tuberculosis*

identifies members of the ESAT-6 family as immunodominant T-cell antigens. Infect Immun 68: 214-220.

49. Dietrich J, Aagaard C, Leah R, Olsen AW, Stryhn A, Doherty TM, Andersen P. 2005. Exchanging ESAT6 with TB10.4 in an Ag85B fusion molecule-based tuberculosis subunit vaccine: efficient protection and ESAT6-based sensitive monitoring of vaccine efficacy. J Immunol 174: 6332-6339.
50. Billeskov R, Vingsbo-Lundberg C, Andersen P, Dietrich J. 2007. Induction of CD8 T cells against a novel epitope in TB10.4: correlation with mycobacterial virulence and the presence of a functional region of difference-1. J Immunol 179: 3973-3981.
51. Hervas-Stubbs S, Majlessi L, Simsova M, Morova J, Rojas MJ, Nouze C, Brodin P, Sebo P, Leclerc C. 2006. High frequency of $CD4^+$ T cells specific for the TB10.4 protein correlates with protection against *Mycobacterium tuberculosis* infection. Infect Immun 74: 3396-3407.
52. Chua BY, Pejoski D, Turner SJ, Zeng W, Jackson DC. 2011. Soluble proteins induce strong $CD8^+$ T cell and antibody responses through electrostatic association with simple cationic or anionic lipopeptides that target TLR2. J Immunol 187: 1692-1701.
53. Chua BY, Olson MR, Bedoui S, Sekiya T, Wong CY, Turner SJ, Jackson DC. 2014. The use of a TLR2 agonist-based adjuvant for enhancing effector and memory CD8 T-cell responses. Immunol Cell Biol 92: 377-383.
54. Pascolo S, Bervas N, Ure JM, Smith AG, Lemonnier FA, Pérarnau B. 1997. HLA-A2.1–restricted Education and Cytolytic Activity of $CD8^+$ T Lymphocytes from β2 Microglobulin (β2m) HLA-A2.1 Monochain Transgenic H-2Db β2m Double Knockout Mice. J Exp Med 185: 2043-2051.
55. Firat H, Garcia-Pons F, Tourdot S, Pascolo S, Scardino A, Garcia Z, Michel M-L, Jack RW, Jung G, Kosmatopoulos K, Mateo L, Suhrbier A, Lemonnier FA, Langlade-Demoyen P. 1999. H-2 class I knockout, HLA-A2.1-transgenic mice: a versatile animal model for preclinical evaluation of antitumor immunotherapeutic strategies. Eur J Immunol 29: 3112-3121.
56. Ellis JM, Henson V, Slack R, Ng J, Hartzman RJ, Katovich Hurley C. 2000. Frequencies of HLA-A2 alleles in five U.S. population groups. Predominance Of A*02011 and identification of HLA-A*0231. Human Immunol 61: 334-340.
57. Fernandez-Viña MA, Falco M, Sun Y, Stastny P. 1992. DNA typing for HLA class I alleles: I. Subsets of HLA-A2 and of -A28. Human Immunol 33: 163-173.
58. Laemmli UK. 1970. Cleavage of structural proteins during the assembly of the head of bacteriophage T4. Nature 227: 680-685.
59. Jackson DC, Fitzmaurice CJ, Brown LE, Zeng W. 1999. Preparation and properties of totally synthetic immunogens. Vaccine 18: 355-361.
60. Rammensee H, Bachmann J, Emmerich NP, Bachor OA, Stevanovic S. 1999. SYFPEITHI: database for MHC ligands and peptide motifs. Immunogenetics 50: 213-219.

61. Brandt L, Oettinger T, Holm A, Andersen AB, Andersen P. 1996. Key epitopes on the ESAT-6 antigen recognized in mice during the recall of protective immunity to *Mycobacterium tuberculosis*. J Immunol 157: 3527-3533.
62. Tan AC, La Gruta NL, Zeng W, Jackson DC. 2011. Precursor frequency and competition dictate the HLA-A2-restricted $CD8^+$ T cell responses to influenza A infection and vaccination in HLA-A2.1 transgenic mice. J Immunol 187: 1895-1902.
63. Geluk A, van Meijgaarden KE, Franken KL, Drijfhout JW, D'Souza S, Necker A, Huygen K, Ottenhoff TH. Ottenhoff. 2000. Identification of major epitopes of *Mycobacterium tuberculosis* AG85B that are recognized by HLA-A*0201-restricted $CD8^+$ T cells in HLA-transgenic mice and humans. J Immunol 165: 6463-6471.
64. Axelsson-Robertson R, Weichold F, Sizemore D, Wulf M, Skeiky YA, Sadoff J, Maeurer MJ. 2010. Extensive major histocompatibility complex class I binding promiscuity for *Mycobacterium tuberculosis* TB10.4 peptides and immune dominance of human leucocyte antigen (HLA)-B*0702 and HLA-B*0801 alleles in TB10.4 CD8 T-cell responses. Immunology 129: 496-505.
65. Lambe T, Carey JB, Li Y, Spencer AJ, van Laarhoven A, Mullarkey CE, Vrdoljak A, Moore AC, Gilbert SC. 2013. Immunity against heterosubtypic influenza virus induced by adenovirus and MVA expressing nucleoprotein and matrix protein-1. Sci Rep 3: 1443-1443.
66. Cavalcanti YV, Brelaz MC, Neves JK, Ferraz JC, Pereira VR. 2012. Role of TNF-Alpha, IFN-Gamma, and IL-10 in the Development of Pulmonary Tuberculosis. Pulm Med 2012: 745483.
67. de Martino M, Lodi L, Galli L, Chiappini E. 2019. Immune Response to *Mycobacterium tuberculosis*: A Narrative Review. Front Pediatr 7: 350.
68. Almeida AS, Lago PM, Boechat N, Huard RC, Lazzarini LC, Santos AR, Nociari M, Zhu H, Perez-Sweeney BM, Bang H, Ni Q, Huang J, Gibson AL, Flores VC, Pecanha LR, Kritski AL, Lapa e Silva JR, Ho JL. 2009. Tuberculosis is associated with a down-modulatory lung immune response that impairs Th1-type immunity. J Immunol 183: 718-731.
69. Zeng G, Zhang G, Chen X. Chen. 2018. Th1 cytokines, true functional signatures for protective immunity against TB? Cell Mol Immunol 15: 206-215.
70. Wieczorek M, Abualrous ET, Sticht J, Álvaro-Benito M, Stolzenberg S, Noé F, Freund C. 2017. Major Histocompatibility Complex (MHC) Class I and MHC Class II Proteins: Conformational Plasticity in Antigen Presentation. Front Immunol 8: 292-292.
71. Aagaard C, Hoang T, Dietrich J, Cardona P-J, Izzo A, Dolganov G, Schoolnik GK, Cassidy JP, Billeskov R, Andersen P. 2011. A multistage tuberculosis vaccine that confers efficient protection before and after exposure. Nature Med 17: 189-194.
72. Lindenstrøm T, Agger EM, Korsholm KS, Darrah PA, Aagaard C, Seder RA, Rosenkrands I, Andersen P. Andersen. 2009. Tuberculosis Subunit Vaccination Provides Long-Term

Protective Immunity Characterized by Multifunctional CD4 Memory T Cells. J Immunol 182: 8047.

73. Lyadova IV, Panteleev AV. 2015. Th1 and Th17 Cells in Tuberculosis: Protection, Pathology, and Biomarkers. Mediators Inflamm 2015: 854507.
74. Umemura M, Yahagi A, Hamada S, Begum MD, Watanabe H, Kawakami K, Suda T, Sudo K, Nakae S, Iwakura Y, Matsuzaki G. 2007. IL-17-mediated regulation of innate and acquired immune response against pulmonary *Mycobacterium bovis* bacille Calmette-Guérin infection. J Immunol 178: 3786-3796.
75. Aguilo N, Alvarez-Arguedas S, Uranga S, Marinova D, Monzón M, Badiola J, Martin C. 2015. Pulmonary but Not Subcutaneous Delivery of BCG Vaccine Confers Protection to Tuberculosis-Susceptible Mice by an Interleukin 17–Dependent Mechanism. J Infect Dis 213: 831-839.
76. Okamoto Yoshida Y, Umemura M, Yahagi A, O'Brien RL, Ikuta K, Kishihara K, Hara H, Nakae S, Iwakura Y, Matsuzaki G. 2010. Essential role of IL-17A in the formation of a mycobacterial infection-induced granuloma in the lung. J Immunol 184: 4414-4422.
77. Freches D, Korf H, Denis O, Havaux X, Huygen K, Romano M. 2013. Mice genetically inactivated in interleukin-17A receptor are defective in long-term control of *Mycobacterium tuberculosis* infection. Immunology 140: 220-231.
78. Segueni N, Tritto E, Bourigault M-L, Rose S, Erard F, Le Bert M, Jacobs M, Di Padova F, Stiehl DP, Moulin P, Brees D, Chibout S-D, Ryffel B, Kammüller M, Quesniaux VF. 2016. Controlled *Mycobacterium tuberculosis* infection in mice under treatment with anti-IL-17A or IL-17F antibodies, in contrast to TNFα neutralization. Sci Rep 6: 36923-36923.
79. Shen H, Chen ZW. 2018. The crucial roles of Th17-related cytokines/signal pathways in *M. tuberculosis* infection. Cell Mol Immunol 15: 216-225.
80. Seah GT, Scott GM, Rook GAW. 2000. Type 2 Cytokine Gene Activation and Its Relationship to Extent of Disease in Patients with Tuberculosis. J Infect Dis 181: 385-389.
81. Gong JH, Zhang M, Modlin RL, Linsley PS, Iyer D, Lin Y, Barnes PF. 1996. Interleukin-10 downregulates *Mycobacterium tuberculosis*-induced Th1 responses and CTLA-4 expression. Infect Immun 64: 913-918.
82. Hernández-Pando R, Orozcoe H, Sampieri A, Pavón L, Velasquillo C, Larriva-Sahd J, Alcocer JM, Madrid MV. Madrid. 1996. Correlation between the kinetics of Th1, Th2 cells and pathology in a murine model of experimental pulmonary tuberculosis. Immunology 89: 26-33.
83. Murray PJ, Young RA. 1999. Increased antimycobacterial immunity in interleukin-10-deficient mice. Infect Immun 67: 3087-3095.
84. Dlugovitzky D, Torres-Morales A, Rateni L, Farroni MA, Largacha C, Molteni O, Bottasso O. 1997. Circulating profile of Th1 and Th2 cytokines in tuberculosis patients with different degrees of pulmonary involvement. FEMS Immunol Med Microbiol 18: 203-207.

85. Boussiotis VA, Tsai EY, Yunis EJ, Thim S, Delgado JC, Dascher CC, Berezovskaya A, Rousset D, Reynes JM, Goldfeld AE. Goldfeld. 2000. IL-10-producing T cells suppress immune responses in anergic tuberculosis patients. J Clin Invest 105: 1317-1325.
86. Ross SH, Cantrell DA. 2018. Signaling and Function of Interleukin-2 in T Lymphocytes. Annu Rev Immunol 36: 411-433.
87. Bermudez LE, Young LS. 1988. Tumor necrosis factor, alone or in combination with IL-2, but not IFN-gamma, is associated with macrophage killing of *Mycobacterium avium* complex. J Immunol 140: 3006.
88. Jeevan A, Asherson GL. Asherson. 1988. Recombinant interleukin-2 limits the replication of *Mycobacterium lepraemurium* and *Mycobacterium bovis* BCG in mice. Lymphokine Res 7: 129-140.
89. Toossi Z, Kleinhenz ME, Ellner JJ. 1986. Defective interleukin 2 production and responsiveness in human pulmonary tuberculosis. J Exp Med 163: 1162-1172.
90. Biselli R, Mariotti S, Sargentini V, Sauzullo I, Lastilla M, Mengoni F, Vanini V, Girardi E, Goletti D, D' Amelio R, Nisini R. 2010. Detection of interleukin-2 in addition to interferon-γ discriminates active tuberculosis patients, latently infected individuals, and controls. Clin Microbiol Infect 16: 1282-1284.
91. Flynn JL, Chan J. 2001. Immunology of tuberculosis. Annu Rev Immunol 19: 93-129.
92. Vesosky B, Flaherty DK, Turner J. 2006. Th1 cytokines facilitate CD8-T-cell-mediated early resistance to infection with *Mycobacterium tuberculosis* in old mice. Infect Immun 74: 3314-3324.
93. Zuñiga J, Torres-García D, Santos-Mendoza T, Rodriguez-Reyna TS, Granados J, Yunis EJ. 2012. Cellular and humoral mechanisms involved in the control of tuberculosis. Clin Dev Immunol 2012: 193923-193923.
94. Majlessi L, Simsova M, Jarvis Z, Brodin P, Rojas MJ, Bauche C, Nouze C, Ladant D, Cole ST, Sebo P, Leclerc C. 2006. An increase in antimycobacterial Th1-cell responses by prime-boost protocols of immunization does not enhance protection against tuberculosis. Infect Immun 74: 2128-2137.
95. Chen L, Wang J, Zganiacz A, Xing Z. Single Intranasal Mucosal *Mycobacterium bovis* BCG Vaccination Confers Improved Protection Compared to Subcutaneous Vaccination against Pulmonary Tuberculosis. Infect Immun 72: 238.
96. Giri PK, Verma I, Khuller GK. 2006. Protective efficacy of intranasal vaccination with *Mycobacterium bovis* BCG against airway *Mycobacterium tuberculosis* challenge in mice. J Infection 53: 350-356.
97. Darrah PA, Zeppa JJ, Maiello P, Hackney JA, Wadsworth MH, Hughes TK, Pokkali S, Swanson PA, Grant NL, Rodgers MA, Kamath M, Causgrove CM, Laddy DJ, Bonavia A, Casimiro D, Lin PL, Klein E, White AG, Scanga CA, Shalek AK, Roederer M, Flynn JL, Seder

RA. 2020. Prevention of tuberculosis in macaques after intravenous BCG immunization. Nature 577: 95-102.

98. Orme IM. 2010. The Achilles heel of BCG. Tuberculosis 90: 329-332.

2.4 Supplementary Material

2.4.1 Supplementary Figures

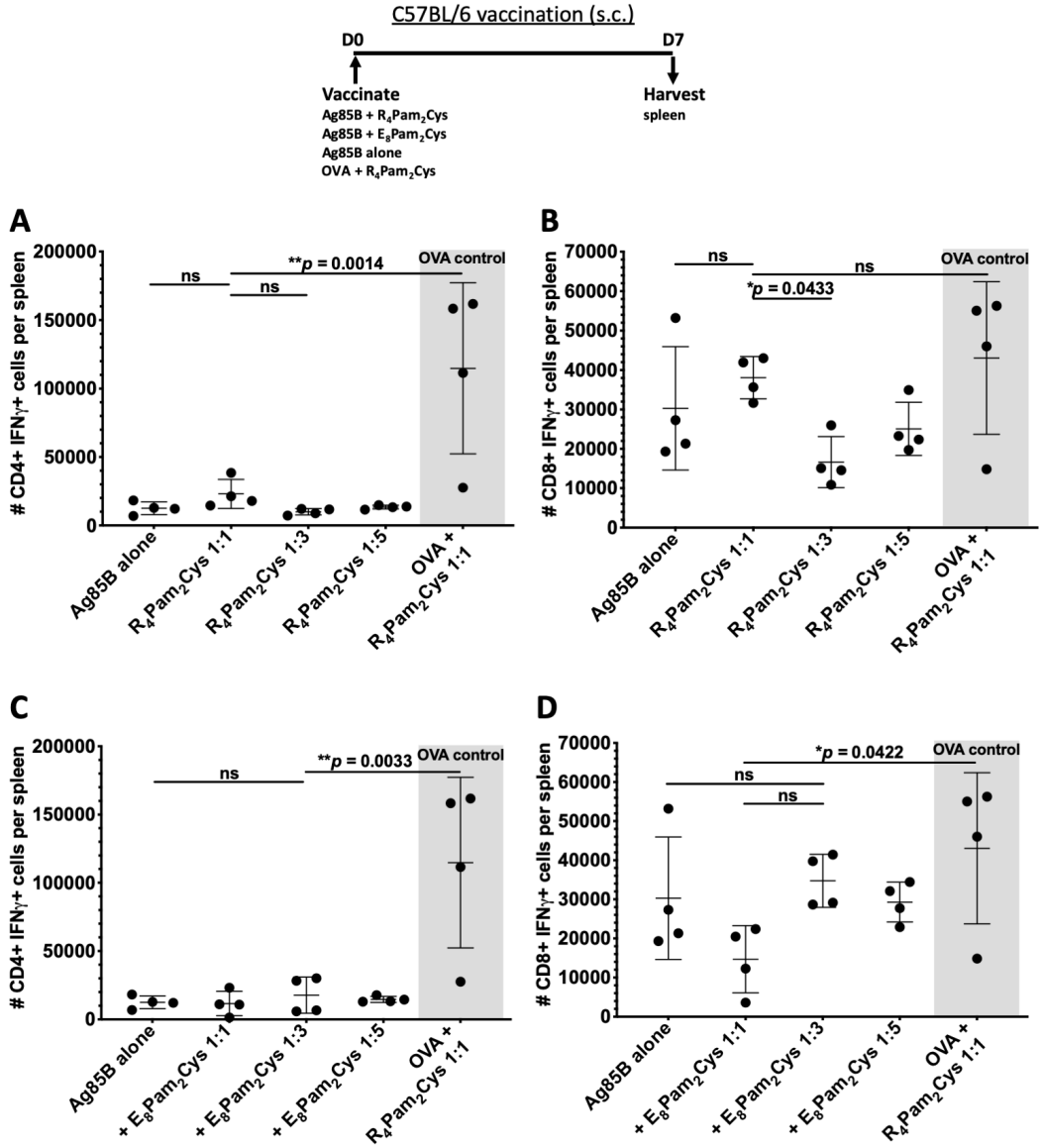

Figure S1. Enumeration of CD4$^+$ and CD8$^+$ T cells producing interferon-gamma (IFN-γ) after vaccination with chicken ovalbumin (OVA) + R_4Pam_2Cys.

(A) CD4$^+$ IFN-γ$^+$ T cell, and **(B)** CD8$^+$ IFN-γ$^+$ T cell numbers from spleens of mice sacrificed seven days after vaccination with Ag85B + R_4Pam_2Cys graphed alongside CD4$^+$ or CD8$^+$ IFN-γ$^+$ T cell numbers (day seven) from mice vaccinated with OVA + R_4Pam_2Cys at 1:1 ratio (highlighted in grey). The error bars represent standard error of the mean. **C.** CD4$^+$ IFN-γ$^+$ T cells, and **D.** CD8$^+$ IFN-γ$^+$ T cell numbers from mice sacrificed seven days after vaccination with Ag85B + E_8Pam_2Cys graphed alongside CD4$^+$ or CD8$^+$ IFN-γ$^+$ T cell numbers (day seven) from mice vaccinated with OVA + R_4Pam_2Cys at 1:1 ratio (highlighted in grey). The null hypothesis (no difference in mean cell numbers between treatment groups) was rejected if *p < 0.05, **p < 0.01, ***p < 0.001 or ****p < 0.0001. The error bars represent standard deviation (n=4).

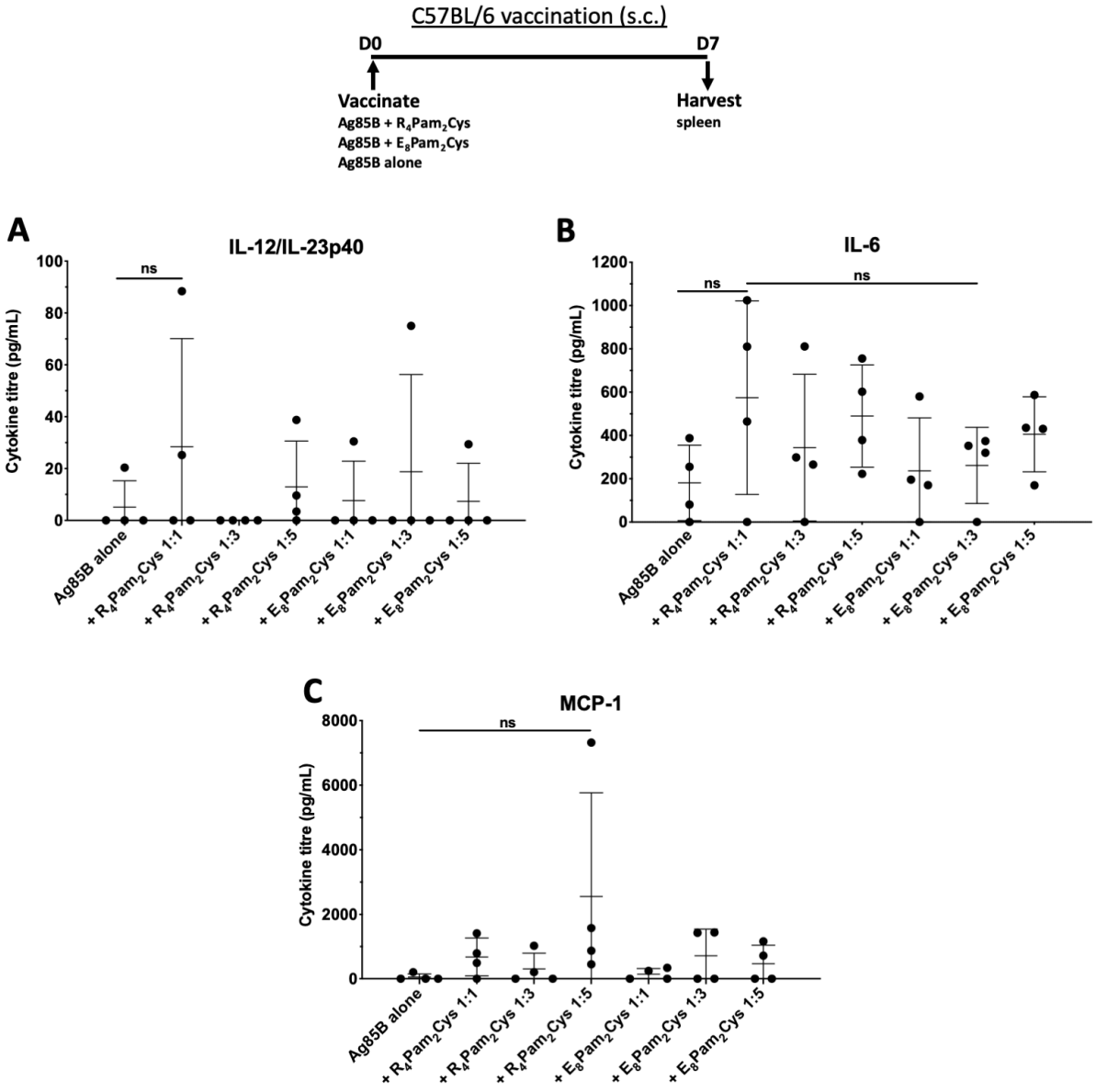

Figure S2. Cytokine responses after ESAT-6 + R_4Pam_2Cys vaccination.

C57BL/6 mice were vaccinated intranasally and subcutaneously with ESAT-6 alone or ESAT-6 + R_4Pam_2Cys and sacrificed after seven days. Lung and spleen cells from these mice were restimulated with ESAT-6 protein to measure cytokine responses. Shown here are plots for cytokines **(A)** IL-4, **(B)** IL-6, and **(C)** monocyte chemoattractant protein (MCP)-1 produced. The null hypothesis (no difference in mean cell numbers between treatment groups) was rejected if *$p < 0.05$, **$p < 0.01$, ***$p < 0.001$ or ****$p < 0.0001$. The error bars represent standard deviation (n=4).

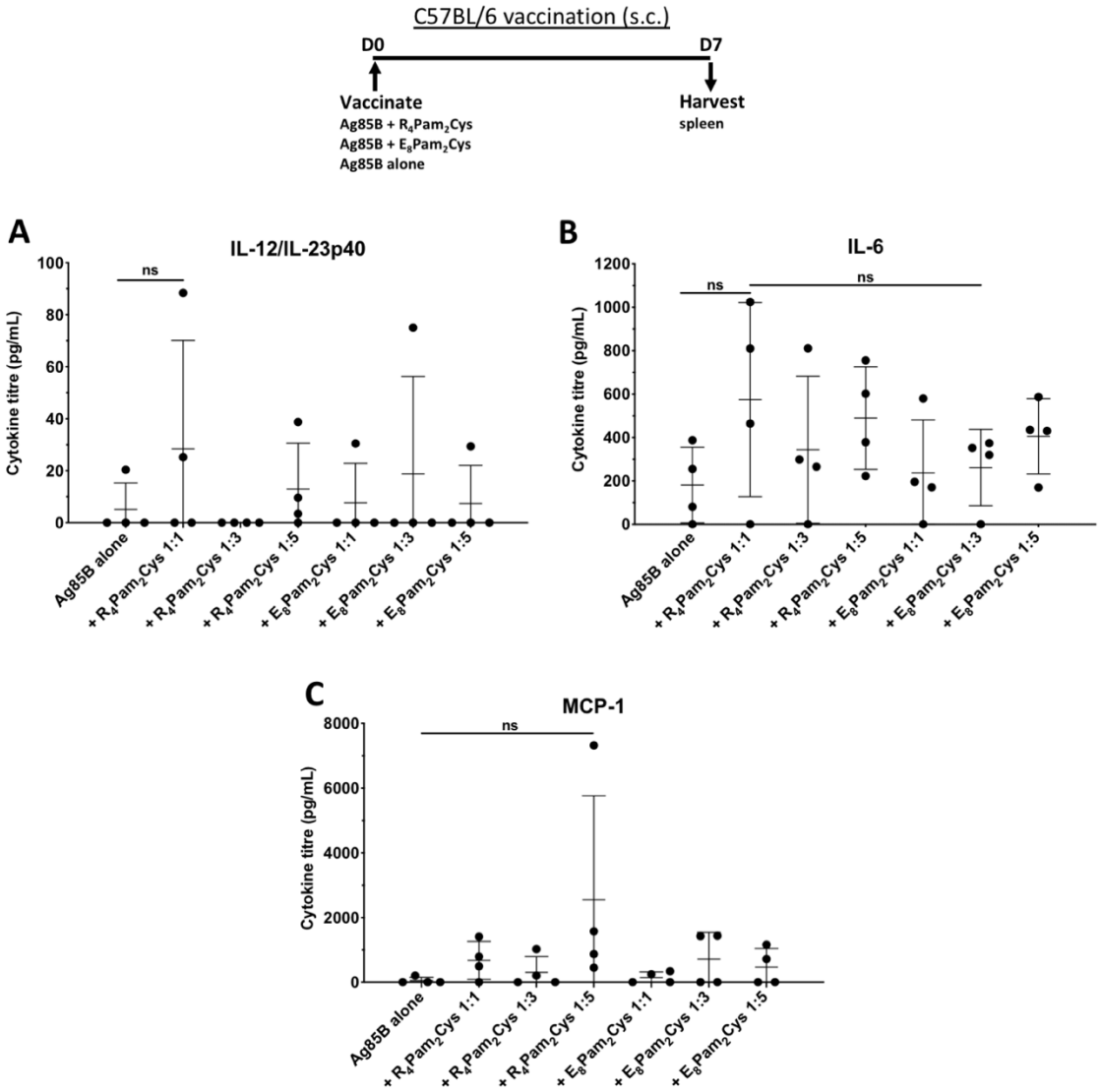

Figure S3. Cytokine responses after Ag85B + R_4Pam_2Cys vaccination.

C57BL/6 mice were vaccinated subcutaneously with Ag85B, Ag85B + R_4Pam_2Cys or Ag85B + E_8Pam_2Cys and sacrificed after seven days. Splenocytes from these mice were restimulated with Ag85B protein to measure cytokine responses. Shown here are plots for cytokines **(A)** IL-12/IL-23p40, **(B)** IL-6, and **(C)** Macrophage chemoattractant protein (MCP)-1 produced from immune cells in the spleen. The null hypothesis (no difference in mean cell numbers between treatment groups) was rejected if *p < 0.05, **p < 0.01, ***p < 0.001 or ****p < 0.0001. The error bars represent standard deviation (n=4).

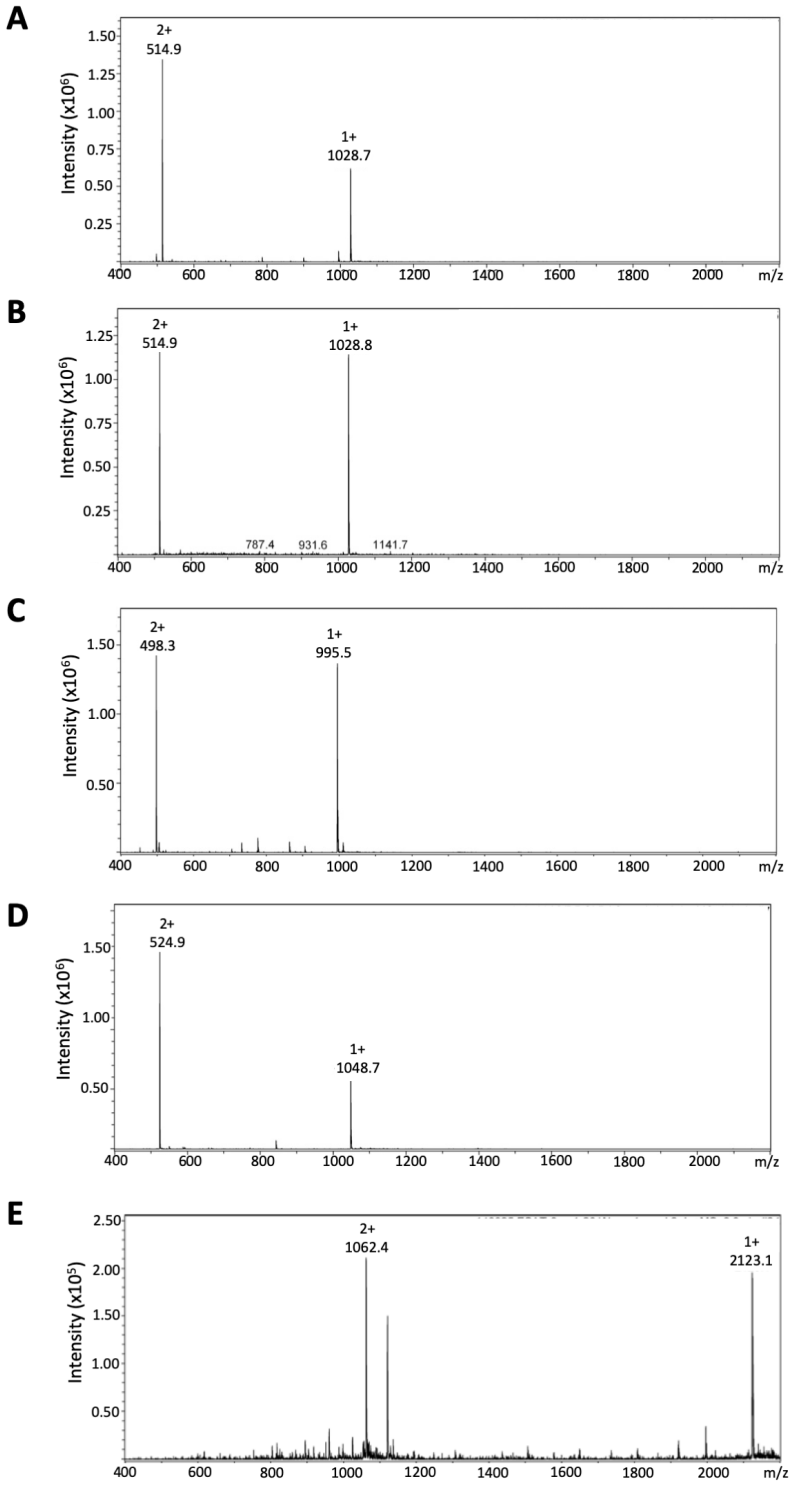

Figure S4. Mass spectrometry analysis of TB peptides and their size in Daltons (Da).

Synthesized, cleaved and purified TB peptides **(A)** KLIANNTRV (from Ag85A), **(B)** KLVANNTRL (from Ag85B), **(C)** YLLDGLRAQ (from Ag85B) **(D)** MMARDTAEA (from TB10.4), and **(E)** MTEQQWNFAGIEAAASAIQG (from ESAT-6) were analysed via mass spectrometry to determine their size. Their sizes were identified to be 1028.2 Da for KLIANNTRV, 1028.8 Da for KLVANNTRL, 995.5 Da for YLLDGLRAQ, 1048.7 Da for MMARDTAEA and 2123.1 for MTEQQWNFAGIEAAASAIQG.

2.5 Summary

ESAT-6 and Ag85B have been previously shown to be highly immunogenic in humans and mice. In this chapter the vaccine formulations were not able to increase T cell responses specific to ESAT-6 and Ag85B in a murine model. This failure to increase protein immunogenicity suggests that the protein and adjuvant formulations tested are unlikely to protect against TB infection. This study identified that pulmonary vaccination could induce splenic T cells and protein-specific cytokines (but not IFN-γ responses), indicating that vaccination to the site of infection with the right protein-adjuvant combination could be an effective method of TB vaccination. Although Ag85B + Pam_2Cys vaccination could not increase T cell responses compared to protein alone vaccination, it was capable of significantly enhancing Ag85B-specific antibody responses. This suggests that the vaccine formulation is generating a protein-specific humoral immune response and therefore the vaccine may be suited to target extracellular bacterial pathogens and could be targeted to the extracellular presence of TB.

ESAT-6, Ag85B, Ag85A and TB10.4 proteins have been studied extensively and their immunodominant properties are well described (264, 354, 355, 365, 396-399). In this chapter, the predicted epitopes that were screened did not generate a high number of $CD8^+$ T cells or a strong $CD8^+$ IFN-γ^+ response. As the cytokine production of the peptide vaccines was not tested, it cannot be deduced whether non-IFN-γ responses were produced.

From the results of this chapter it's likely that immunodominant proteins without the correct adjuvant do not induce an appropriate immune response for the host to clear the bacteria and may not prove to be useful in future vaccine developments. The vaccines in this study did not generate immune responses indicative of protection (161, 401, 402, 409), e.g. produced weak $CD4^+$, $CD8^+$ and IFN-γ immune responses against the TB antigens. Therefore, the study did not continue with TB challenge, though the vaccines may have induced immune responses in murine immune cells that were not explored e.g. CD1-restricted T cells, γδ T cells and natural killer cells (103, 410).

Future vaccination attempts could focus on generating immune responses to less immunodominant proteins or utilising novel adjuvants to change the host immune response to immunodominant antigens. Though this study has failed to induce strong $CD8^+$ or $CD4^+$ T cells, these vaccine formulations did induce strong protein-specific antibody responses and could be used to target extracellular pathogens.

Chapter 3

High antibody titres induced by protein subunit vaccines against Buruli ulcer using *Mycobacterium ulcerans* antigens Hsp18 and MUL_3720

3.1 Introduction

Chapter 3 focusses on the development of a vaccine against Buruli ulcer. As was previously shown in Chapter 2, the protein-adjuvant formulation using *M. tuberculosis* proteins generated strong protein-specific antibody titres. Therefore, in this chapter, two putative *M. ulcerans* subunit vaccines were formulated. These vaccines comprised two cell wall-associated *M. ulcerans* proteins, MUL_3720 and Hsp18, in association with the TLR-2 agonist, Pam_2Cys, utilised in Chapter 2.

Buruli ulcer (BU) is a disease caused by *Mycobacterium ulcerans*. The bacterium infects subcutaneous tissue and in humans ulcers typically present with deep undermined edges and have a necrotic core comprised of a slough of bacteria, dead skin and immune cells (60, 183). Untreated ulcers can destroy fat tissue, muscles and bones (50, 52). Ulcers are predominately found on extremities, especially upper (27%) and lower limbs (70%) (64). *M. ulcerans* is a slow-growing bacterium, with a doubling time of greater than 48 hours, so symptoms of BU can take months to appear after primary infection. If diagnosed early, BU can be treated effectively by combination antibiotic therapy (200). Though unlikely to be fatal, BU has a high morbidity rate. In many cases the disease can initially be misdiagnosed as other more common skin infections (189, 191). Delayed treatment may require surgical removal of affected tissue and can lead to disfigurement and permanent disability (201). A retrospective study in Australia showed that most diagnoses (87%) occurred once ulceration had been reached (411) and in Ghana 66% cases were diagnosed with active lesions (412). There is currently no protective treatment for BU and no clearly defined mechanism of transmission. This highlights the need for an effective vaccine to protect those particularly in highly endemic areas of West and sub-Saharan Africa where treatment may be delayed, misdiagnosed, or difficult to access.

The most widely used mycobacterial vaccine is *Mycobacterium bovis* 'BCG', a vaccine against tuberculosis. The BCG vaccine is somewhat cross-protective against *M. ulcerans*, and in a murine challenge model has been shown to delay the onset of BU symptoms and decrease bacterial load (279, 333). Therefore, the BCG vaccine is the field benchmark for assessing potential BU vaccines.

This chapter focusses on the development of a subunit vaccine. To enhance immune recognition, the *M. ulcerans* antigens chosen for the vaccine formulation were bacterial surface-associated proteins. Two proteins, MUL_3720 and Hsp18, were identified as potential candidates for vaccine antigens. Hsp18 is a protein associated with bacterial biofilm formation and *M. ulcerans*-infected individuals produce antibodies against Hsp18 (180, 357). MUL_3720 is a highly expressed cell wall-associated protein with a putative role in cell wall biosynthesis (376, 413). The lipopeptide adjuvant R_4Pam_2Cys, used in Chapter 2, was again utilised as the adjuvant for the subunit formulations in this study.

3.2 Research Objectives

The main aim of this study was to develop a preventative subunit vaccine against Buruli ulcer, comprising highly expressed cell wall-associated proteins bound to a Pam_2Cys-based lipopeptide adjuvant.

- To develop two vaccine formulations comprising MUL_3720 or Hsp18 alongside the lipopeptide adjuvant Pam_2Cys.
- To measure the protein-specific antibody response to these proteins in a murine model.
- To assess the efficacy of these vaccines at preventing the onset of Buruli ulcer in a murine model.

3.3 Results and Discussion

The methods and results for this study have been reported in a manuscript in-progress, soon to be submitted.

Manuscript "High antibody titres induced by protein subunit vaccines against Buruli ulcer using *Mycobacterium ulcerans* antigens Hsp18 and MUL_3720"

Kirstie M. Mangas, Nicholas Tobias, Estelle Marion, Jérémie Babonneau, Laurent Marsollier, Jessica L. Porter, Sacha J. Pidot, Chinn Yi Wong, David C. Jackson, Brendon Y. Chua and Timothy P. Stinear.

The following is the author-accepted version of the manuscript, formatted to include the figures within the text.

High antibody titres induced by protein subunit vaccines against Buruli ulcer using *Mycobacterium ulcerans* antigens Hsp18 and MUL_3720

Kirstie M. Mangas[1], Nicholas Tobias[2,3], Estelle Marion[3], Jérémie Babonneau[3], Laurent Marsollier[3], Jessica L. Porter[1], Sacha J. Pidot[1], Chinn Yi Wong[1], David C. Jackson[1], Brendon Y. Chua[1,*] and Timothy P. Stinear[1,*].

[1] Department of Microbiology and Immunology, Doherty Institute, University of Melbourne, Melbourne, Victoria, Australia
[2] Molekulare Biotechnologie, Fachbereich Biowissenschaften, Goethe-Universität Frankfurt, Frankfurt am Main, Germany
[3] LOEWE Centre for Translational Biodiversity in Genomics (TBG), Germany
[4] CRCINA, INSERM, Université de Nantes, Université d'Angers, Angers, France

Corresponding Authors:
Timothy Stinear, University of Melbourne, 792 Elizabeth St, Melbourne, Victoria, 3000, Australia
Brendon Chua, University of Melbourne, 792 Elizabeth St, Melbourne, Victoria, 3000, Australia
Email addresses: tstinear@unimelb.edu.au, bychua@unimelb.edu.au

Abstract

Background. *Mycobacterium ulcerans* is the causative agent of a debilitating skin and soft tissue infection known as Buruli ulcer (BU). There is no vaccine against BU. The purpose of this study was to investigate the vaccine potential of two previously described immunogenic *M. ulcerans* proteins, MUL_3720 and Hsp18, using a mouse tail infection model of BU.

Methods. Recombinant versions of the two proteins were each electrostatically coupled with a previously described lipopeptide adjuvant. Seven C57BL/6 and seven BALB/c mice were vaccinated and boosted with each of the formulations. Vaccinated mice were then challenged with *M. ulcerans* via subcutaneous tail inoculation. Vaccine performance was assessed by time-to-ulceration compared to unvaccinated mice.

Results. The MUL_3720 and Hsp18 vaccines induced high titres of antigen-specific antibodies that were predominately subtype IgG_1. However, all mice developed ulcers by day-40 post-*M. ulcerans* challenge. No significant difference was observed in the time-to-onset of ulceration between the experimental vaccine groups and unvaccinated animals.

Conclusions. These data align with previous vaccine experiments using Hsp18 and MUL_3720 that indicated these proteins may not be appropriate vaccine antigens. This work highlights the need to explore alternative vaccine targets and different approaches to understand the role antibodies might play in controlling BU.

Introduction

Buruli ulcer (BU) is a disease caused by *Mycobacterium ulcerans*. *M. ulcerans* infects subcutaneous tissue and commonly presents as a skin nodule (in Africa) or papule (in Australia), sometimes accompanied by redness; however, oedema is another common initial presentation. As the disease progresses, the skin around the infected area breaks down and an ulcer develops (1, 2). Ulcers typically present with deep undermined edges and have a necrotic core comprised of slough of bacteria, dead skin and immune cells (3, 4). Infections are rarely fatal but untreated ulcers can destroy fat tissue, blood vessels, muscles and bone (5, 6).

The transmission of BU is likely caused by the introduction of *M. ulcerans* beneath the skin. This could be achieved through the puncture of *M. ulcerans*-contaminated skin (with examples in the literature of infections following human bite, bullet and land mine wounds, or vaccination) or by the introduction of *M. ulcerans* contaminated objects into the subcutaneous tissue, such as following insect bites (7-9). BU endemic areas are focused in certain rural regions across west, sub-Saharan and central Africa, including Nigeria, Ghana, Togo, Cameroon, Benin, Democratic Republic of Congo and Côte d'Ivoire. The disease also occurs in Australia, primarily on the Bellarine and Mornington Peninsulas near the major metropolitan centre of Melbourne (10-12). The disease can affect all age groups and ethnicities (13). In Australia, ulcers are predominately reported on upper (27%) and lower limbs (70%) (14).

M. ulcerans is a slow-growing bacterium, with a doubling time of greater than 48 hours. As such, symptoms of BU can take months to appear after primary infection. If diagnosed early, BU can be treated effectively by combination antibiotic therapy (15). Unfortunately, in many cases the disease can initially be misdiagnosed as other more common skin infections (16, 17). Delayed diagnosis and treatment can lead to extensive lesions that leave victims with life-long disfigurement and disability. Reparative surgery is often required for severe cases (18). A retrospective study in Australia showed that most diagnoses (87%) occurred once ulceration has been reached (19) and in Ghana 66% cases were diagnosed with active lesions (20). There is currently no protective vaccine for BU and no distinct mechanism of transmission. Furthermore, treatment can be difficult to access for those in rural areas. Thus, there is a need to develop an effective vaccine to protect those particularly in highly endemic areas.

The *M. bovis* 'BCG' vaccine has been shown to delay the onset of BU symptoms and decrease bacterial load in both experimental animal BU infection models and in studies of human populations (21-25). Therefore, the BCG vaccine is the benchmark for assessing potential *M. ulcerans* vaccines. Some studies have assessed the efficacy of putative BU vaccines although none have reached clinical trials

(21, 22, 26-37). All these vaccines were tested in murine challenge models in this study and were not capable of preventing the eventual onset of disease.

One approach to vaccination is to use antigens from a specific pathogen, e.g. certain proteins(s), that are recognized by the immune system and can induce neutralizing antibodies (38, 39). For rapid immune recognition these proteins would ideally be cell surface associated. Two *M. ulcerans* proteins MUL_3720 and Hsp18 have been identified as potential candidates for vaccine antigens. Hsp18 is a protein associated with biofilm formation and *M. ulcerans*-infected individuals have been shown to produce antibodies against Hsp18 (40, 41). MUL_3720 is a highly expressed cell wall-associated protein with a putative role in cell wall biosynthesis (42, 43).

As protein antigens may be poorly immunogenic on their own, adjuvants are used to enhance antigenic potency. A lipopeptide adjuvant known as Pam_2Cys has been found to increase antigen uptake, increase dendritic cell trafficking to lymph nodes, and enhance antibody production against antigens derived from pathogens including influenza and hepatitis C in murine models (44-47).

The aim of this study was to try to develop a preventative vaccine against Buruli ulcer, comprising two highly expressed cell wall-associated proteins, MUL_3720 or Hsp18, bound to an R_4Pam_2Cys-based lipopeptide adjuvant.

Materials & Methods

Strains and culture conditions

Escherichia coli Rosetta2 containing plasmid pET30b-Hsp18 (strain TPS681) or pDest17-MUL_3720 (strain TPS682) was grown at 37°C in Luria-Bertani (LB) broth (Difco, Becton Dickinson, MD, USA) supplemented with 100 µg/ml ampicillin (Sigma-Aldrich, USA) or 50 µg/ml kanamycin to express 6xHIS-tagged Hsp18 or MUL_3720 recombinant protein. *Mycobacterium ulcerans* (strain Mu_1G897) was grown at 30°C in 7H9 broth or 7H10 agar (Middlebrook, Becton Dickinson, MD, USA) supplemented with oleic acid, albumin, dextrose and catalase growth supplement (OADC) (Middlebrook, Becton Dickinson, MD, USA), and 0.5% glycerol (v/v). *M. bovis* BCG (strain Sanofi Pasteur) used for vaccinations was grown at 37°C in 7H9 broth or 7H10 agar supplemented with OADC. Mycobacterial colony counts from cultures or tissue specimens were performed using spot plating as previously described (48).

Recombinant protein expression

Overnight cultures of strains TPS681and TPS682 were diluted to OD_{600} = 0.05 in LB broth. Each culture was incubated at 37°C with shaking at 200 rpm until OD_{600} = 0.6-0.7, then 1 mM IPTG (Isopropyl b-D-1-thiogalactopyr-anoside) was added to induce protein expression. The cells were incubated for a further four hours to express the protein. To harvest the protein, cells were resuspended in wash buffer (8 M urea, 150 mM sodium chloride, 10% glycerol) and sonicated at amplitude 60 (QSonica Ultrasonic Liquid Processor S-4000, Misonix) until the solution turned clear. The lysate was filtered with a 0.22 µM filter (Millipore) to remove cellular debris and the protein was column-purified using anti-histidine resin (ClonTech). The resin was washed ten times with 10x column volumes of wash buffer mixed with an increasing proportion of tris buffer (20 mM Tris-HCl, 150 mM sodium chloride, 10% glycerol) until the column was washed with only tris buffer. The resin was washed a further two times with tris buffer containing 20 mM imidazole. Protein was eluted in tris buffer containing 200 mM imidazole and dialysed in phosphate buffered saline (PBS) before concentration using a 3K MWCO PES concentration column (Pierce). Protein was endotoxin purified using Triton X-114 phase separation until less than 0.1 endotoxin unit/ml (detectable limit), measured by PierceTM LAL choromogenic endotoxin quantitation kit (ThermoFisher) as per manufacturer's instructions.

Sodium dodecyl sulphate polyacrylamide gel electrophoresis (SDS-PAGE)

Samples were denatured in an equal volume of 2 x sample loading buffer (40% (v/v) 0.5M Tris-HCL pH 6.8, 10% glycerol, 1.7% (w/v) SDS, 10% 2-β-mercaptoethanol, 0.13% (w/v) bromophenol blue in distilled water) at 100°C for 5 minutes. Ten microlitres of each sample and SeeBlue® Plus2 pre-stained protein standard (Invitrogen) were loaded into a 0.5mm 12% polyacrylamide gel under reducing conditions, as previously described (49). The gel was run in running buffer (0.3% (w/v) Tris, 1.44%

(w/v) glycine and 0.1% (w/v) SDS in distilled water) for 1 hour at 150 volts (Mini-protean vertical electrophoresis cell, Bio-Rad). The gels were stained in Coomassie stain (45% methanol, 10% acetic acid 0.25% (w/v) Coomassie brilliant blue in distilled water) for 1 hour and destained in Coomassie destain (33% Methanol, 10% acetic acid, 60% distilled water) until the protein bands could be identified.

Western Blotting

Proteins were separated on a 12% polyacrylamide gel as per the method for SDS-PAGE. After separation proteins were transferred to a nitrocellulose membrane in tris-glycine transfer buffer (1.5 mM Tris, 12mM glycine, 15 % methanol (v/v) in distilled water) for 1 hour at 100 volts (Mini Trans-Blot Cell, Bio-Rad). The nitrocellulose membrane was blocked in blocking buffer (5% (w/v) skim milk powder and 0.1% Tween-20 in PBS) overnight at 4°C. The membrane was incubated in blocking buffer containing anti-6xHIS-HRP antibody (Roche Applied Science) at 1:500 dilution. The membrane was washed in PBS containing 0.1% Tween-20 and then exposed to developing solution (Western Lighting Chemiluminescence kit, Perkin Elmer) according to manufacturer's guidelines. Chemiluminescence was detected using an MF ChemiBIS gel imaging system (DNR Bio-Imaging Systems).

Analysis of electrostatic interaction between protein antigen and lipopeptide formulations

The association between each protein and R_4Pam_2Cys was measured by mixing 25 µg of protein with increasing amounts of lipopeptide in 50 µl PBS in a 96-well plate (Nunc, Thermo Scientific). The formation of protein-lipopeptide complexes through electrostatic interaction was measured by an increase in light absorbance. Plates were read at dual wavelengths of 505 and 595 nm on plate reader (LabSystems Multiskan Multisoft microplate reader).

Lipopeptide vaccine preparation

Each vaccine dose contained 25 µg protein added to R_4Pam_2Cys at a ratio of 1:5 mole of protein to lipopeptide. PBS was added to a final volume of 100 µl and the combination sonicated in a water bath for 30 seconds. Control vaccine preparations were made containing 25 µg protein alone or R_4Pam_2Cys lipopeptide alone and sonicated before administration.

Ethics statement for animal experiments

All animal experiments were performed in full compliance with national guidelines (articles R214-87 to R214-90 from French "rural code") and European guidelines (directive 2010/63/EU of the European Parliament and of the council of September 22, 2010 on the protection of animals used for scientific purposes). All protocols were approved by the Ethics Committee of region Pays de la Loire under protocol nos. CEEA 2009.14 and CEEA 2012.145. Animals were maintained under specific pathogen-free conditions in the animal house facility of the Centre Hospitalier Universitaire, Angers, France

(agreement A 49 007 002). Six-week old female C57BL/6 and BALB/c mice were obtained from Charles River Laboratories (Saint-Germain-Nuelles, France) and housed at CHU Angers. Food and water were given *ad libitum*.

Vaccination of animals

The synthesis and purification of the branched cationic lipopeptide, R_4Pam_2Cys, was performed as previously described (45, 50, 51). Each vaccine dose contained 25 µg protein formulated in PBS with R_4Pam_2Cys at a 1:5 molar ratio of protein to lipopeptide in a final volume of 100 µl. The protein alone control formulation contained 25 µg protein per dose diluted in PBS. The R_4Pam_2Cys alone formulations contained the same amount of lipopeptide used in each of the protein + adjuvant formulations, calculated by the 1:5 molecular ratio (with the omission of the protein from the solution). The R_4Pam_2Cys alone formulations were diluted to the correct concentration in PBS. Live-attenuated *M. bovis* BCG strain 'Sanofi Pasteur' was grown to log phase and stored at -80°C in 20% glycerol until use. Bacteria were washed with PBS and resuspended in 200ul, before administration at 4.7 x 10^5 bacteria per dose. All vaccines and control formulations were sonicated for 5 minutes in a waterbath sonicator before being administered.

For vaccination using R_4Pam_2Cys, animals were inoculated subcutaneously at the base of tail (100µl per dose at 50 µl per flank) and boosted 21 days later with the same formulations. Mice vaccinated with approximately 1 x 10^3 CFU *M. bovis* BCG resuspended in PBS at the base of tail (100 µl per dose at 50µl per flank).

M. ulcerans challenge

Mice were challenged on day 35 by subcutaneous injection on the tail with 1 x 10^4 CFU *M. ulcerans* (Mu_1G897) resuspended in 50 µl PBS. Mice were allowed to recover, monitored for up to 40 days after infection and euthanised when tail ulceration was observed wherein sera were obtained for immunological analysis.

Serum antibody titre measurements

Serum was prepared from blood obtained from mice at day 0, day 18, day 33 and day 63. Antibody titres were measured using enzyme linked immunosorbent assay (ELISA) as per methods described in (45). Briefly, ELISA plates (Nunc, Thermo Scientific) were coated overnight with 5 µg/ml protein diluted in $PBSN_3$ and blocked with $BSA_{10}PBS$ for 2 hours at room temperature. Plates were washed with PBS containing 0.05% Tween-20 (PBST). Neat sera were sequentially diluted in BSA_5PBST and incubated at room temperature for 6 hours. Bound antibody was detected by adding horse radish peroxidase conjugated rabbit anti-mouse IgG (Dako, Glostrup, Denmark) or rat anti-mouse IgM, IgG1, IgG2a, IgG2b or IgG3 antibodies (Southern Biotech, USA) at a concentration of 1:400 in BSA_5PBST

for 2 hours. Plates were developed with developing solution (hydrogen peroxide, citric acid and ABTS) and incubated for 10-15 min with gentle agitation to observe a colour change. The reaction was stopped with 50 mM sodium fluoride. Plates were read at dual wavelengths of 505 and 595 nm on plate reader (LabSystems Multiskan Multisoft microplate reader). The titers of antibody are expressed as the reciprocal of the highest dilution of serum required to achieve an optical density of 0.2.

Statistical analysis

Graphpad Prism software (GraphPad Software v7, CA, USA) was used to perform statistical analyses on the antibody titre. Antibody titres were analysed using two-way ANOVA with Tukey's correction for multiple comparisons. The time to ulceration data were displayed as a Kaplan-Meier plot and statistical significance was determined using a Log-Rank (Mantel-Cox) test. For all tests $*p < 0.05$, $**p < 0.01$ and $***p < 0.001$ and $**** p < 0.0001$ were considered statistically significant.

Results

MUL_3720 and Hsp18 have previously been shown to be immunogenic and cell wall-associated (40, 43). The adjuvant Pam_2Cys has been shown to induce strong antibody responses to proteins from infectious agents such as influenza and hepatitis C (46, 47, 52-54). Therefore, this study measures the ability of MUL_3720 and Hsp18 based vaccines, incorporating the charged Pam_2Cys adjuvant, to generate protein-specific antibodies and to protect against BU.

Recombinant MUL_3720 and Hsp18 both bound to R_4Pam_2Cys

Recombinant MUL_3720 and Hsp18, expressed from inducible *E. coli* expression vectors, were prepared for use as antigens in the vaccine formulations (Supp. Table S1). Purification of the recombinant proteins was confirmed by SDS-PAGE and Western blot analyses of the eluate (Fig. 1). DLS analysis was then performed to identify whether recombinant MUL_3720 or Hsp18 would electrostatically bind to either the positively charged lipopeptide adjuvant R_4Pam_2Cys, or its negatively charged counterpart, E_8Pam_2Cys. The optical density of solutions containing these constituents at a wavelength of 450nm (OD_{450}) is related to the particle size of molecules in solution, reflecting the strength of the ionic interaction between protein and lipopeptide (45). MUL_3720 preferentially bound to R_4Pam_2Cys compared to E_8Pam_2Cys (Fig. 2A). This is shown as a gradual increase in optical density following the addition of increasing amounts of R_4Pam_2Cys to a constant amount of MUL_3720. At a 5-fold molar excess of protein to lipopeptide the OD_{450} plateaued, suggesting MUL_3720 bound most strongly to R_4Pam_2Cys at a 1:5 protein to lipopeptide ratio. Conversely, when E_8Pam_2Cys was added to MUL_3720 the optical density remained static and did not increase with increasing lipopeptide concentrations, indicating a lack of binding. Hsp18 also appeared to bind preferentially to R_4Pam_2Cys and also at a 1:5 ratio of Hsp18 to R_4Pam_2Cys (Fig. 2B). Therefore, two protein-adjuvant formulations were prepared using MUL_3720 with R_4Pam_2Cys and Hsp18 with R_4Pam_2Cys, both at a 1:5 protein to lipopeptide molar ratio.

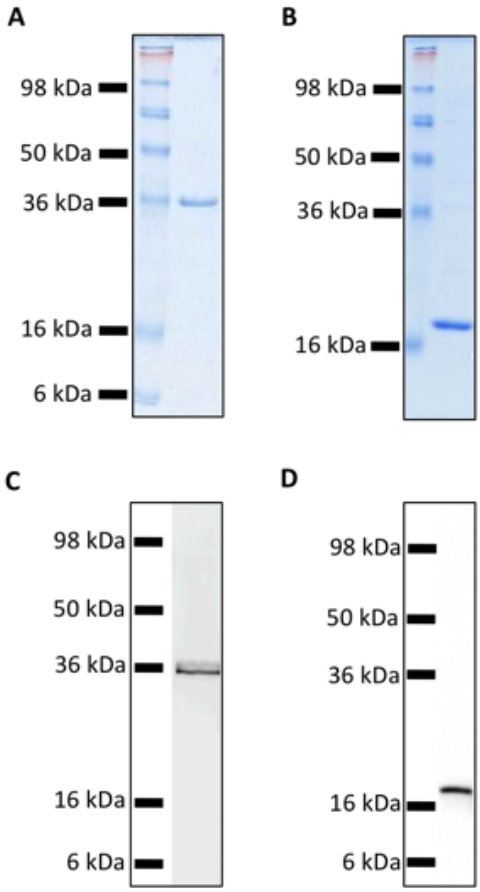

Figure 1. SDS-PAGE and Western Blot Analysis of purified recombinant MUL_3720 and Hsp18 proteins.

(A) SDS-PAGE of MUL_3720 protein elution (containing 10 µg protein) shows a band ~36 kDa. (**B)** SDS-PAGE of Hsp18 protein elution (containing 10 µg protein) shows a band ~18 kDa. **(C)** Protein in the final MUL_3720 elute was analysed by Western Blot using an anti-6xHIS-tag antibody to detect the presence of a single band corresponding to the band as the SDS- PAGE analysis. (**D)** Protein in the final Hsp18 elute was analysed by Western Blot using an anti-6xHIS-tag antibody to detect the presence of a single band corresponding to the 18 kDa band as the SDS-PAGE analysis.

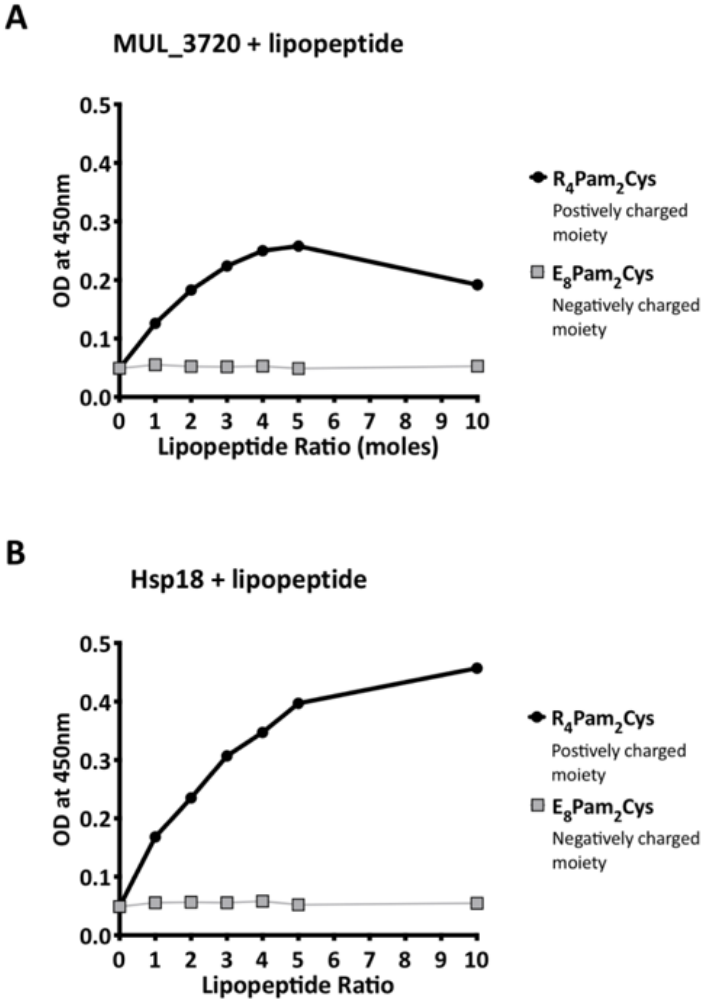

Figure 2. Recombinant MUL_3720 and Hsp18 protein formulation linked with Pam_2Cys.
To analyse the formation of antigen-lipopeptide complexes, a constant amount of antigen **(A)** MUL_3720 (25µg) and **(B)** Hsp18 (25µg) was mixed with lipopeptide at different protein:lipopeptide molar ratios in 50 µl of PBS. These graphs depict the absorbance values of these solutions at an optical density of 450nm (OD_{450}). In these assays either R_4Pam_2Cys or E_8Pam_2Cys lipopeptides were added to the proteins at increasing amounts. The addition of R_4Pam_2Cys is depicted with black circles and the addition of E_8Pam_2Cys is depicted with grey squares. An increase in absorbance in correlation to an increase in lipopeptide was indicative of protein binding to lipopeptide.

Vaccination induced strong protein-specific antibody responses

Prior to challenge with *M. ulcerans*, the ability of the vaccine candidates to generate murine immune responses was assessed. ELISAs were utilized to measure the antibody (IgG) titres in sera obtained from two strains of mice (BALB/c and C57BL/6) immunized with either MUL_3720 + R_4Pam_2Cys or Hsp18 + R_4Pam_2Cys after the primary vaccination dose (day 18) and a secondary dose (day 33).

Vaccination with MUL_3720 recombinant protein alone or MUL_3720 + R_4Pam_2Cys were capable of inducing MUL_3720-specific antibody titres in both BALB/c and C57BL/6 strains of mice (Fig. 3A, B). Primary vaccination with MUL_3720 protein alone induced MUL_3720-specific antibody responses that significantly increased following a vaccine boost ($p < 0.0001$ in BALB/c, and $p = 0.0234$ in C57BL/6) (Fig. 3A, B). Additionally, MUL_3720 + R_4Pam_2Cys generated MUL_3720 specific antibody responses after primary vaccination ($p < 0.0001$ in BALB/c and C57BL/6) (Fig. 3A, B), which were increased after the secondary boost ($p < 0.0001$ in BALB/c, and not statistically significant in C57BL/6). The titres after the boost in particular were greater than MUL_3720 alone vaccination ($p = 0.0031$ in BABL/c, and $p = 0.006$ in C57BL/6). Mice that were not vaccinated with recombinant MUL_3720 (R_4Pam_2Cys alone and BCG) did not have an increase in MUL_3720-specific antibodies compared to naïve mice (Fig. 3A, B).

Vaccination with Hsp18 recombinant protein alone or Hsp18 + R_4Pam_2Cys induced Hsp18-specific antibody titres in both strains of mice (Fig. 3C, D). Vaccine boost with Hsp18 recombinant protein alone induced significantly higher Hsp18-specific antibody responses in BALB/c mice compared to a single vaccination with Hsp18 protein ($p < 0.0001$; Fig. 3C). Boosting with protein alone in C57BL/6 mice did not significantly increase antibody titres (Fig. 3D). Hsp18 + R_4Pam_2Cys induced Hsp18-specific antibody responses in both mouse strains after primary vaccination ($p < 0.0001$ in BALB/c and $p = 0.0165$ in C57BL/6) and the Hsp18-specific antibody titre significantly increased after booster vaccination ($p < 0.0001$ in BALB/c and $p = 0.0016$ in C57BL/6). In all strains, the antibody titres induced by Hsp18 + R_4Pam_2Cys were significantly higher than vaccination with Hsp18 protein alone ($p = 0.0004$ in BALB/c and $p < 0.0001$ in C57BL/6) (Fig. 3C, D) with negligible levels of antibodies seen in mice vaccinated with only R_4Pam_2Cys, or BCG.

Measurement of IgG antibody subtypes following MUL_3720 + R_4Pam_2Cys and Hsp18 + R_4Pam_2Cys vaccination

Quantifying levels of IgG antibody shows that the predominant isotypes produced by MUL_3720 were IgG_1 and $IgG2_b$ (Fig. 3E) with no significant difference between these isotype titres. Vaccination with MUL_3720 + R_4Pam_2Cys produces significantly more IgG_1 and $IgG2_b$ antibodies ($p = 0.0076$). The antibody titres for both isotypes were highest prior to infection with *M. ulcerans* (day 33) and decreased after infection by day 63. This vaccine was capable of inducing IgG2a antibodies, which was detected also on day 33, however in smaller amounts than IgG_1 and $IgG2_b$ ($p = 0.0399$ for MUL_3720 + R_4Pam_2Cys) (Fig. 3E).

Similar to vaccination with MUL_3720, Hsp18 was also capable of inducing strong IgG antibody titres. The predominant isotype was IgG_1 which Hsp18 + R_4Pam_2Cys elicited more than any other isotype (Fig. 3F) including $IgG2_a$ and $IgG2_b$, Again, these titres were highest at day 33 and decreased

significantly after infection on day 63. This trend was also observed after vaccination with Hsp18 alone ($p = 0.0018$ vs $IgG2_a$ and $p = 0.0076$ vs $IgG2_b$, respectively at day 33).

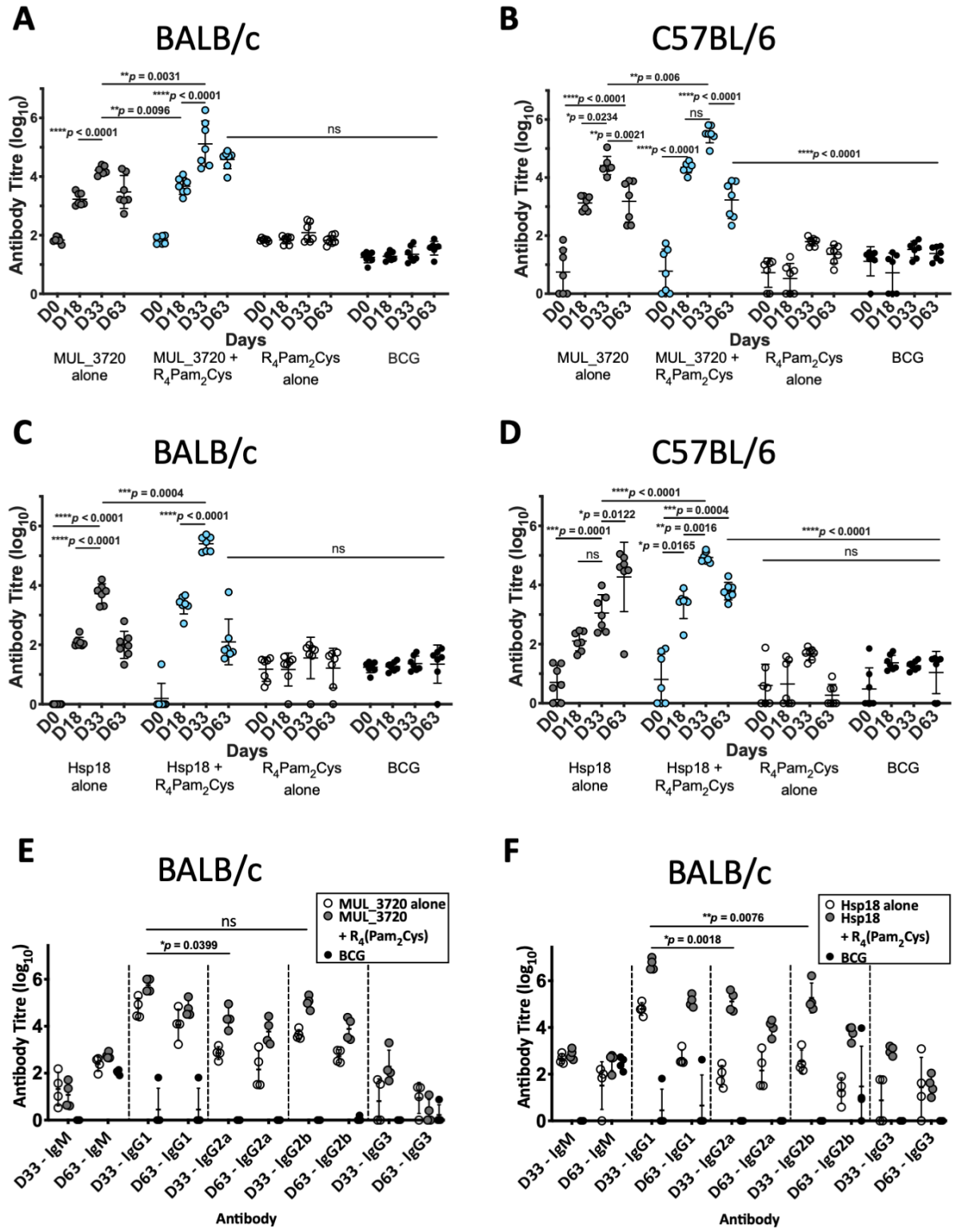

Figure 3. Antibody titres from BALB/c and C57BL/6 mice immunized with recombinant MUL_3720 or Hsp18 linked to R_4Pam_2Cys lipopeptide adjuvant (continued next page).

Figure 3. Antibody titres from BALB/c and C57BL/6 mice immunized with recombinant MUL_3720 or Hsp18 linked to R_4Pam_2Cys lipopeptide adjuvant (continued).

MUL_3720-specific antibody titres from **(A)** BALB/c and **(B)** C57BL/6 mice. Mice were vaccinated with protein alone (MUL_3720) (grey circles), recombinant protein + R_4Pam_2Cys (blue circles), R_4Pam_2Cys alone (clear circles) and *M. bovis* BCG (black circles). A separate ELISA was performed to measure Hsp18-specific antibody titres in **(C)** BALB/c and **(D)** C57BL/6 mice. Mice were vaccinated with protein alone (Hsp18) (grey circles), recombinant protein + R_4Pam_2Cys (blue circles), R_4Pam_2Cys alone (clear circles) and *M. bovis* BCG (black circles). IgG isotypes (IgG1, $IgG2_a$, $IgG2_b$ and IgG3) were quantified from BALB/c mice immunized with **(E)** MUL_3720 + R_4Pam_2Cys and **(F)** Hsp18 + R_4Pam_2Cys. Mice were vaccinated with protein antigen alone (either MUL_3720 or Hsp18) (clear circles), protein + R_4Pam_2Cys (grey circles) and BCG (black circles). Results are shown as zero if below detectable limits. The null hypothesis (no difference in mean antibody responses between treatment groups) was rejected if $*p < 0.05$, $**p < 0.01$, $***p < 0.001$ or $****p < 0.0001$. The error bars represent standard deviation (n=7).

MUL_3720 + R_4Pam_2Cys and Hsp18 + R_4Pam_2Cys do not protect against the onset of BU

As both vaccines were capable of inducing protein-specific antibody responses, they were tested in a murine challenge model to measure their protective efficacy. Efficacy was measured by time delay to the onset of ulceration in a mouse tail infection model. There is a progression of clinical symptoms for Buruli ulcer in this model (Fig. 4). Once ulceration has been reached the disease would likely continue until the tail became necrotic. Therefore, the experimental endpoint was deemed to be the point of ulceration.

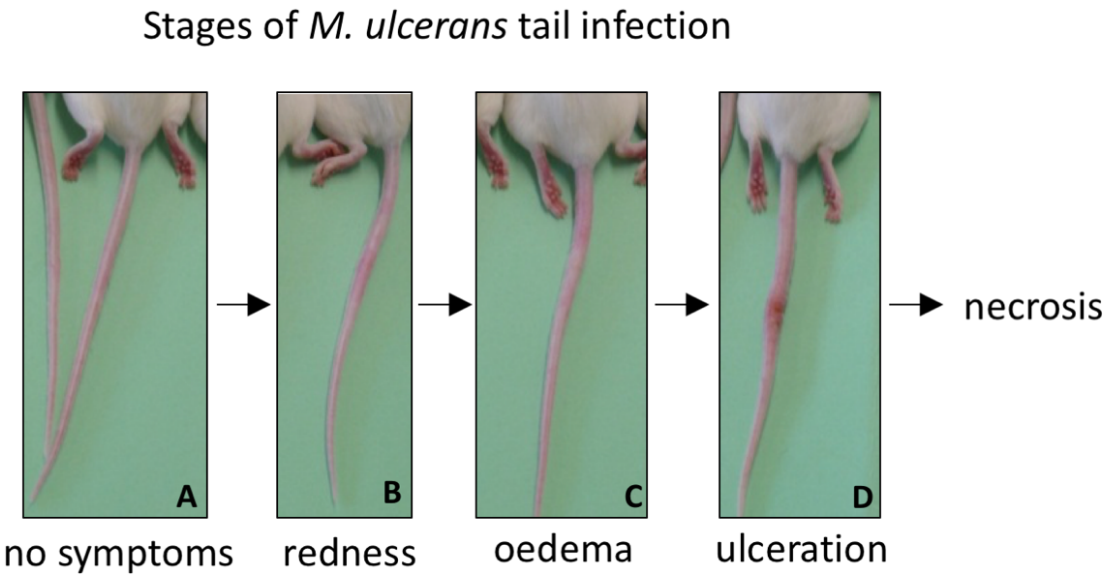

Figure 4. Progression of BU in the murine tail infection model over time.
(A) Healthy mouse tail. (**B)** Appearance of a small sign of redness at the site of tail infection. **(C)** Oedema surrounding the initial site of redness. **(D)** Tail lesion at the point of ulceration. This is typically identified by excessive oedema and redness at the site of imminent ulceration. Mice were sacrificed before ulcerative lesions appeared.

After the scheduled vaccinations, mice were challenged via subcutaneous tail inoculation with 1 x 10^4 CFU of *M. ulcerans* and observed for up to 40 days. In BALB/c and C57BL/6 mice there was no significant difference between the time to ulceration between control mice (mice not vaccinated with recombinant protein, such as R_4Pam_2Cys alone and BCG) and mice vaccinated with either MUL_3720 + R_4Pam_2Cys or Hsp18 + R_4Pam_2Cys (Fig. 5A, B). There was also no significant difference in the time to ulceration between mice that were vaccinated with MUL_3720 + R_4Pam_2Cys or Hsp18 + R_4Pam_2Cys and BCG, the benchmark for mycobacterial vaccine efficacy. Signs of infection in all BALB/c and C57BL/6 mice were visible by day 33 (Table S2 and Table S3) and all mice reached ulceration by day 63, 40 days post-*M. ulcerans* challenge (Fig. 5A, B).

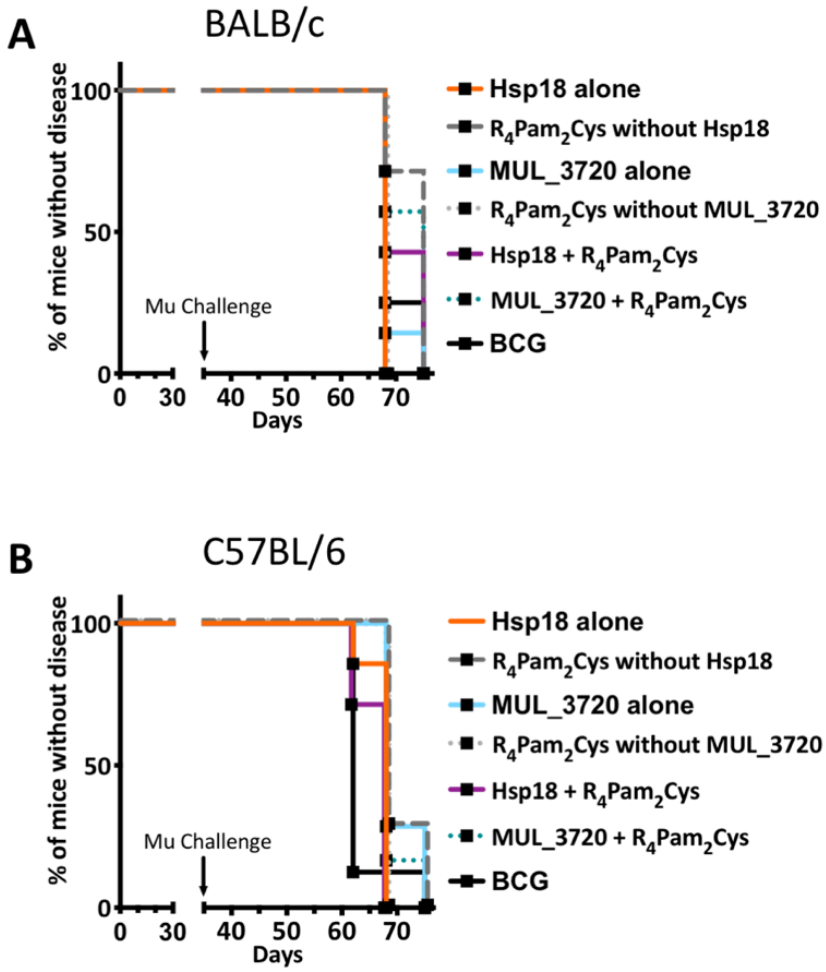

Figure 5. Vaccine performance using murine tail infection model of BU.

Survival analysis showing the time taken (days) for each mouse to reach ulceration for different vaccination groups post *M. ulcerans* (Mu) challenge. **(A)** BALB/c mice (n=7) and (**B)** C57BL/6 mice (n=7). The null hypothesis (no difference in mean antibody responses between treatment groups) was rejected if *$p < 0.05$, **$p < 0.01$, ***$p < 0.001$ or ****$p < 0.0001$.

Antibody titres do not correlate with protection against M. ulcerans

High antibody titres were observed in all mice vaccinated with either recombinant MUL_3720 or Hsp18, particularly in the secondary response after booster vaccination (Fig. 3A-D) prior to *M. ulcerans* challenge. However, mice vaccinated with protein alone or protein plus lipopeptide adjuvant all succumbed to infection by day 75. The sera from mice at the day 63 was used to quantify antibody titres during infection. At day 63 all mice still had detectable protein-specific antibodies against the recombinant protein with which they were vaccinated (Figure 3A-D). In BALB/c mice (Fig. 3A, C) the antibody titres at day 63 were lower than after the secondary response prior to challenge ($p < 0.0001$ for both Hsp18 + R_4Pam_2Cys and MUL_3720 + R_4Pam_2Cys) but remained significantly higher than at

day 0 ($p < 0.0001$ for both Hsp18 + R_4Pam_2Cys and MUL_3720 + R_4Pam_2Cys). In C57BL/6 mice (Fig. 3B, D), antibody titres against MUL_3720 or Hsp18 from mice vaccinated with either protein alone or protein plus lipopeptide adjuvant were also significantly decreased at day 63 compared to the secondary response at day 35 ($p < 0.0001$ and $p = 0.0406$ for MUL_3720 + R_4Pam_2Cys and Hsp18 + R_4Pam_2Cys, respectively). Similar to BALB/c mice, the day 63 respective protein-specific antibodies for MUL_3720 + R_4Pam_2Cys and Hsp18 + R_4Pam_2Cys were significantly higher than at day 0 ($p < 0.0001$ and $p = 0.0004$ for MUL_3720 + R_4Pam_2Cys and Hsp18 + R_4Pam_2Cys, respectively).

Challenge with M. ulcerans did not induce protein-specific antibody levels comparable to vaccination with MUL_3720 or Hsp18.

MUL_3720 and Hsp18 recombinant proteins are immunogenic and capable of inducing protein-specific antibody responses after vaccination. However, only minor detectable antibody responses against either recombinant MUL_3720 or Hsp18 at day 63 (Fig. 3A-D) were found in mice vaccinated with R_4Pam_2Cys alone or BCG then challenged with *M. ulcerans*. These mice had antibody titres of less than 2, with no significant increase above baseline antibody titres (day 0). These responses are much lower than the protein-specific antibody responses generated from MUL_3720 or Hsp18 vaccinated mice, particularly in C57/BL6 mice ($p < 0.0001$) (Supp. Fig. S1). Animals from both mouse strains that were vaccinated with R_4Pam_2Cys alone or BCG showed no increase in protein-specific antibody responses against either recombinant MUL_3720 and Hsp18 on day 63 post-*M. ulcerans* challenge (Fig. 3A-D), even though these two proteins are both expressed in *M. ulcerans*.

Discussion

This study aimed to develop a vaccine against *M. ulcerans* utilizing two previously described cell-wall associated proteins, Hsp18 and MUL_3720 (40-43). Both the MUL_3720 and Hsp18-based vaccines were capable of inducing high antibody titres, but these responses were not associated with protection (Fig. 5). Since this study was performed, two other studies have also developed putative vaccines utilizing Hsp18 and MUL_3720 (29, 30). These vaccine formulations included the following adjuvants: virus replicon particles (29), TLR-4 agonist EM048, Alum and Sigma adjuvant system (30). These vaccine formulations were capable of generating protein-specific antibodies, but similar to this study, these antibodies were not able to control MU infection. This may indicate that these proteins, while strongly immunogenic, play no major role in pathogenesis, so targeting them with potentially neutralizing antibodies induced by the vaccine has no impact on disease.

Alternatively, antibodies raised by these vaccines may not have had the functional potential to control infection. In addition to antigen binding, antibodies engage via their Fc domains with Fcγ receptors (FcγR) present on innate immune cells (NK cells, monocytes, macrophages and neutrophils) to rapidly recruit the anti-microbial activity of the innate immune system. Antibodies with these functions can promote control of a pathogen through the activation of multiple effector cell functions, including Ab dependent cellular cytotoxicity, cellular phagocytosis and/or cytokine and enzyme secretion (55-57). Recent research has shown that mice lacking antibodies have increased susceptibility to *M. tuberculosis* infection (58) and non-human primates treated to deplete B cells also exhibit increased bacterial burden (59). Despite the findings of this research, it is likely that B cells and antibody responses still play a role in controlling *M. ulcerans* infection in this model**,** albeit with different specificities. Future research could use human BU patient cohorts and mouse infection models to attempt to characterize the targets, functional and structural aspects of antibody responses that differentiate subjects able to control BU from susceptible subjects. It might then be possible to use B cell probe technologies to isolate Ag-specific memory B cells from individuals that control *M. ulcerans* infection and then clone the immunoglobulin gene sequences identified (60). Antigen-specific monoclonal Abs (mAbs) could then be generated and characterized for their *in vitro* anti-microbial activity and used in *in vivo* mouse passive transfer studies to determine potential use as mAb therapeutics against BU.

Another explanation for the ineffectiveness of antibodies in this study may be due to the localized immune suppression induced by the *M. ulcerans* toxin mycolactone at the site of infection. Mycolactone diffuses into tissue surrounding the bacteria (61-63). Mycolactone is a cytotoxin that modulates the function of several immune cells (63, 64). The toxin inhibits the Sec61 translocon, affecting T cell activation, impairing T cell responsiveness and distorting cytokine production (62, 63). The mycolactone-induced depletion of T cell homing to peripheral lymph nodes affects subsequent B-cell

activation and migration from the lymphatics (65). The antibodies induced by the vaccine in this study may be functional but unable to access bacteria within the infection or it may be that multiple effector cell functions have been modulated by mycolactone exposure through interference with receptor expression on key innate immune cells, rendering these cells poorly responsive to antibodies. Suppression of protein-specific antibody production in the presence of mycolactone has been observed (66). Mycolactone administered to a different location than the antigen caused no reduction to systemic antigen-specific IgG titres (66), similar to the observations from our study. Monoclonal antibodies against mycolactone have been shown to neutralize the cytotoxic activity of mycolactone *in vitro* indicating that mycolactone could be a viable vaccine target (67). A recent study incorporating the enoyl reductase (ER) enzymatic domain, from the polyketide synthases that form mycolactone, has shown a correlation between ER-specific antibodies and protection against the onset of Buruli ulcer (68). This suggests that there is a role for antibodies in BU protection, though the most effective antigenic targets may be found in the mycolactone biosynthesis pathway.

In this study, the greatest antibody responses were of the IgG1 subclass. Typical antibody responses against proteins occur via B cell isotype switching from IgM (non-specific antibody isotype) to IgG. There are 4 subclasses of IgG (IgG1, IgG2, IgG3 and IgG4) and isotype switching to predominantly IgG1 suggests refinement of immune responses to respond specifically to either MUL_3720 or Hsp18, as IgG1 is capable of binding to protein antigens (69). IgG1 can also bind all forms of FcγR which is required to elicit and mediate effector immune functions as described above (70). The presence of IgG2 suggest further isotype switching from IgG1 to $IgG2_{a/b}$ as the immune response develops. IgG2 is less effective at inducing phagocytosis and fixing complement and is more commonly associated with polysaccharide antigens. Though tests on the recombinant proteins had undetectable levels of lipopolysaccharide (LPS), there could be trace amounts from the *E. coli* expression vector boosting IgG2 responses. Studies analysing antibodies generated during leprosy and TB infection show a switch from IgG1 to IgG2 antibodies for leprosy and a persistence of IgG1 and IgG3 antibodies for TB (71). As isotype switching of antibodies requires help by T helper cells, future work could therefore also incorporate studies on the effect of vaccination and subsequent *M. ulcerans*-infection on T cells as well as antibody responses.

In this study, all mice succumbed to infection in a relatively short period (40 days) compared to previous mouse tail infection models (72) and human BU, where the incubation period is estimated at 4.8 months before the onset of ulceration (73). All BALB/c and C57BL/6 mice succumbed to infection by 40 days after MU infection, even mice that were vaccinated by *M. bovis* BCG. *M. bovis* BCG has been previously shown to delay the onset of disease on average by at least 6 weeks (21, 22, 31). In this study however, there was no significant difference between mice vaccinated with either MUL_3720 or Hsp18 protein alone or with both proteins plus R_4Pam_2Cys. This suggests that *M. bovis* BCG is ineffective at

protecting mice in this model of *M. ulcerans* vaccination. This failure to observe any protective impact of *M. bovis* BCG might be a reflection of the challenge strain of *M. ulcerans* used (strain Mu_1G897) and/or the high challenge dose used (10^4 bacteria). High concentrations ($>10^4$ bacteria) have not been reported in environmental sources of *M. ulcerans* (9, 74-77), consistent with the hypothesis that a relatively small bacterial inoculum is required to establish BU (9). At the time this study was conducted the minimum infectious dose (ID_{50}) for BU had not been determined, however the ID_{50} has since been identified as approximately 3 CFU (48). Future studies should therefore use a murine model that is more representative of a natural *M. ulcerans* infection, reflected both in the mode of *M. ulcerans* entry into the subcutaneous tissue and in the dose of bacteria used for challenge.

Conclusions

Vaccination with either MUL_3720 or Hsp18 proteins induced high antibody titres. These responses were augmented when either protein was linked with the lipopeptide adjuvant R_4Pam_2Cys. However, robust antibody responses did not correlate with protection against challenge with *M. ulcerans*. Future work could test different *M. ulcerans* antigens in vaccine formulations against Buruli ulcer. As mycolactone is a key virulence factor, neutralising this toxin early in infection by targeting the PKS enzymes required for its biosynthesis could be a focus for future vaccination developments. Using a lower *M. ulcerans* inoculum as a more realistic vaccine challenge dose is also warranted.

Acknowledgements

We thank Roy Robins-Browne for providing the pET-30b MOD plasmid used for the expression of recombinant Hsp18.

References

1. Guarner J, Bartlett J, Whitney EA, Raghunathan PL, Stienstra Y, Asamoa K, Etuaful S, Klutse E, Quarshie E, van der Werf TS, van der Graaf WT, King CH, Ashford DA. 2003. Histopathologic features of *Mycobacterium ulcerans* infection. Emerg Inf Dis 9: 651-656.
2. Vincent QB, Ardant MF, Adeye A, Goundote A, Saint-Andre JP, Cottin J, Kempf M, Agossadou D, Johnson C, Abel L, Marsollier L, Chauty A, Alcais A. 2014. Clinical epidemiology of laboratory-confirmed Buruli ulcer in Benin: a cohort study. Lancet Glob Health 2: e422-430.
3. Hayman J, McQueen A. 1985. The pathology of *Mycobacterium ulcerans* infection. Pathology 17: 594-600.
4. Oliveira MS, Fraga AG, Torrado E, Castro AG, Pereira JP, Filho AL, Milanezi F, Schmitt FC, Meyers WM, F. Portaels, Silva MT, Pedrosa J. Infection with *Mycobacterium ulcerans* induces persistent inflammatory responses in mice. Infect Immun 73: 6299-6310
5. Woodring JH, Vandiviere HM, Fried AM, Dillon ML, Williams TD, Melvin IG. 1986. Update: the radiographic features of pulmonary tuberculosis. Am J Roentgenol 146: 497-506.
6. van der Werf TS, van der Graaf WT, Tappero JW, Asiedu K. 1999. *Mycobacterium ulcerans* infection. Lancet 354: 1013-1018.
7. Marsollier L, Robert R, Aubry J, Saint Andre JP, Kouakou H, Legras P, Manceau AL, Mahaza C, Carbonnelle B. 2002. Aquatic insects as a vector for *Mycobacterium ulcerans*. Appl Environ Microbiol 68: 4623-4628.
8. Meyers WM, Shelly WM, Connor DH, Meyers EK. 1974. Human *Mycobacterium ulcerans* infections developing at sites of trauma to skin. Am J Trop Med Hyg 23: 919-923.
9. Stinear T, Davies JK, Jenkin GA, Hayman JA, Oppedisano F, Johnson PD. 2000. Identification of *Mycobacterium ulcerans* in the environment from regions in Southeast Australia in which it is endemic with sequence capture-PCR. Appl Environ Microbiol 66: 3206-3213.
10. Michael JL, Ee Laine T, Maria G, Caroline JL, Simon RC, Paul DRJ, Janet AMF. 2018. Epidemiology of Buruli Ulcer Infections, Victoria, Australia, 2011–2016. Emerg Infect Dis 24: 1988.
11. World Health Organization. 2019. Buruli ulcer - number of new reported cases. *In* Global Health Observatory data repository: http://apps.who.int/gho/data/node.main.A1631. Accessed 19 January 2020.
12. Simpson H, Deribe K, Tabah EN, Peters A, Maman I, Frimpong M, Ampadu E, Phillips R, Saunderson P, Pullan RL, Cano J. 2019. Mapping the global distribution of Buruli ulcer: a systematic review with evidence consensus. Lancet Glob Health 7: e912-e922.

13. Omansen TF, Erbowor-Becksen A, Yotsu R, van der Werf TS, Tiendrebeogo A, Grout L, Asiedu K. 2019. Global Epidemiology of Buruli Ulcer, 2010–2017, and Analysis of 2014 WHO Programmatic Targets. Emerg Inf Dis 25: 2183-2190.
14. Yerramilli A, Tay EL, Stewardson AJ, Kelley PG, Bishop E, Jenkin GA, Starr M, Trevillyan J, Hughes A, Friedman ND, O'Brien DP, Johnson PDR. 2017. The location of Australian Buruli ulcer lesions—Implications for unravelling disease transmission. PLoS Negl Trop Dis 11: e0005800.
15. Sarfo FS, Phillips R, Asiedu K, Ampadu E, Bobi N, Adentwe E, Lartey A, Tetteh I, Wansbrough-Jones M. 2010. Clinical efficacy of combination of rifampin and streptomycin for treatment of *Mycobacterium ulcerans* disease. Antimicrob Agents Chemother 54: 3678-3685.
16. van der Werf TS, Stienstra Y, Johnson RC, Phillips R, Adjei O, Fleischer B, Wansbrough-Jones MH, Johnson PD, Portaels F, van der Graaf WT, Asiedu K. 2005. *Mycobacterium ulcerans* disease. Bulletin of the World Health Organization 83: 785-791.
17. Guarner J. 2018. Buruli Ulcer: Review of a Neglected Skin Mycobacterial Disease. J Clin Micro 56: e01507-01517.
18. Herbinger KH, Brieske D, Nitschke J, Siegmund V, Thompson W, Klutse E, Awua-Boateng NY, Bruhl E, Kunaa L, Schunk M, Adjei O, Loscher T, Bretzel G. 2008. Excision of Pre-Ulcerative Forms of Buruli Ulcer Disease: A Curative Treatment? Infection 37: 20-25
19. Boyd SC, Athan E, Friedman ND, Hughes A, Walton A, Callan P, McDonald A, O'Brien DP. 2012. Epidemiology, clinical features and diagnosis of *Mycobacterium ulcerans* in an Australian population. Med J Aust 196: 341-344.
20. Amofah G, Bonsu F, Tetteh C, Okrah J, Asamoa K, Asiedu K, Addy J. 2002. Buruli ulcer in Ghana: results of a national case search. Emerg Inf Dis 8: 167-170.
21. Tanghe A, Content J, Van Vooren JP, Portaels F, Huygen K. 2001. Protective Efficacy of a DNA Vaccine Encoding Antigen 85A from *Mycobacterium bovis* BCG against Buruli Ulcer. Infect Immun 69: 5403-5411.
22. Tanghe A, Adnet PY, Gartner T, Huygen K. 2007. A booster vaccination with *Mycobacterium bovis* BCG does not increase the protective effect of the vaccine against experimental *Mycobacterium ulcerans* infection in mice. Infect Immun 75: 2642-2644.
23. Phillips RO, Phanzu DM, Beissner M, Badziklou K, Luzolo EK, Sarfo FS, Halatoko WA, Amoako Y, Frimpong M, Kabiru AM, Piten E, Maman I, Bidjada B, Koba A, Awoussi KS, Kobara B, Nitschke J, Wiedemann FX, Kere AB, Adjei O, Loscher T, Fleischer B, Bretzel G, Herbinger KH. 2015. Effectiveness of routine BCG vaccination on buruli ulcer disease: a case-control study in the Democratic Republic of Congo, Ghana and Togo. PLoS Negl Trop Dis 9: e3457.
24. The Uganda Buruli Group. 1969. BCG vaccination against *mycobacterium ulcerans* infection (Buruli ulcer). First results of a trial in Uganda. Lancet 293: 111-115.

25. Smith PG, Revill WD, Lukwago E, Rykushin YP. 1976. The protective effect of BCG against *Mycobacterium ulcerans* disease: a controlled trial in an endemic area of Uganda. Trans R Soc Trop Med Hyg 70: 449-457.
26. Tanghe A, Dangy JP, Pluschke G, Huygen K. 2008. Improved protective efficacy of a species-specific DNA vaccine encoding mycolyl-transferase Ag85A from *Mycobacterium ulcerans* by homologous protein boosting. PLoS Negl Trop Dis 2: e199.
27. Coutanceau E, Legras P, Marsollier L, Reysset G, Cole ST, Demangel C. 2006. Immunogenicity of *Mycobacterium ulcerans* Hsp65 and protective efficacy of a *Mycobacterium leprae* Hsp65-based DNA vaccine against Buruli ulcer. Microb Infect 8: 2075-2081.
28. Roupie V, Pidot SJ, Einarsdottir T, Van Den Poel C, Jurion F, Stinear TP, Huygen K. 2014. Analysis of the vaccine potential of plasmid DNA encoding nine mycolactone polyketide synthase domains in *Mycobacterium ulcerans* infected mice. PLoS Negl Trop Dis 8: e2604.
29. Bolz M, Kerber S, Zimmer G, Pluschke G. 2015. Use of Recombinant Virus Replicon Particles for Vaccination against *Mycobacterium ulcerans* Disease. PLoS Negl Trop Dis 9: e0004011.
30. Bolz M, Benard A, Dreyer AM, Kerber S, Vettiger A, Oehlmann W, Singh M, Duthie MS, Pluschke G. 2016. Vaccination with the Surface Proteins MUL_2232 and MUL_3720 of *Mycobacterium ulcerans* Induces Antibodies but Fails to Provide Protection against Buruli Ulcer. PLoS Negl Trop Dis 10: e0004431.
31. Fraga AG, Martins TG, Torrado E, Huygen K, Portaels F, Silva MT, Castro AG, Pedrosa J. 2012. Cellular immunity confers transient protection in experimental Buruli ulcer following BCG or mycolactone-negative *Mycobacterium ulcerans* vaccination. PloS One 7: e33406.
32. Watanabe M, Nakamura H, Nabekura R, Shinoda N, Suzuki E, Saito H. 2015. Protective effect of a dewaxed whole-cell vaccine against *Mycobacterium ulcerans* infection in mice. Vaccine 33: 2232-2239.
33. Hart BE, Hale LP, Lee S. 2016. Immunogenicity and protection conferred by a recombinant *Mycobacterium marinum* vaccine against Buruli ulcer. Trials Vaccinol 5: 88-91.
34. Converse PJ, Almeida DV, Nuermberger EL, Grosset JH. 2011. BCG-mediated protection against *Mycobacterium ulcerans* infection in the mouse. PLoS Negl Trop Dis 5: e985.
35. Hart BE, Hale LP, Lee S. 2015. Recombinant BCG Expressing *Mycobacterium ulcerans* Ag85A Imparts Enhanced Protection against Experimental Buruli ulcer. PLoS Negl Trop Dis 9: e0004046.
36. Hart BE, Lee S. 2016. Overexpression of a *Mycobacterium ulcerans* Ag85B-EsxH Fusion Protein in Recombinant BCG Improves Experimental Buruli Ulcer Vaccine Efficacy. PLoS Negl Trop Dis 10: e0005229.

37. Trigo G, Martins TG, Fraga AG, Longatto-Filho A, Castro AG, Azeredo J, Pedrosa J. 2013. Phage therapy is effective against infection by *Mycobacterium ulcerans* in a murine footpad model. PLoS Negl Trop Dis 7: e2183.
38. Siegrist C-A. 2018. 2 - Vaccine Immunology, p 16-34. *In* Plotkin SA, Orenstein WA, Offit PA, Edwards KM (ed), Plotkin's Vaccines (Seventh Edition). Elsevier Philadelphia, PA.
39. Plotkin SA. 1999. Vaccination against the major infectious diseases. C R Acad Sci III 322: 943-951.
40. Pidot SJ, Porter JL, Marsollier L, Chauty A, Migot-Nabias F, Badaut C, Benard A, Ruf MT, Seemann T, Johnson PD, Davies JK, Jenkin GA, Pluschke G, Stinear TP. 2010. Serological evaluation of *Mycobacterium ulcerans* antigens identified by comparative genomics. PLoS Negl Trop Dis 4: e872.
41. Pidot SJ, Porter JL, Tobias NJ, Anderson J, Catmull D, Seemann T, Kidd S, Davies JK, Reynolds E, Dashper S, Stinear TP. 2010. Regulation of the 18 kDa heat shock protein in *Mycobacterium ulcerans*: an alpha-crystallin orthologue that promotes biofilm formation. Mol Microbiol 78: 1216-1231.
42. Vettiger A SN, Ruf M-T, Röltgen K, Pluschke G. 2014. Localization of Mycobacterial Antigens by Immunofluorescence Staining of Agarose Embedded Cells. J Mycobact Dis. 4: 150.
43. Dreyer A, Röltgen K, Dangy JP, Ruf MT, Scherr N, Bolz M, Tobias NJ, Moes C, Vettiger A, Stinear TP, Pluschke G. 2015. Identification of the *Mycobacterium ulcerans* protein MUL_3720 as a promising target for the development of a diagnostic test for Buruli ulcer. PLoS Negl Trop Dis 9: e0003477-e0003477.
44. Chua BY, Olson MR, Bedoui S, Sekiya T, Wong CY, Turner SJ, Jackson DC. 2014. The use of a TLR2 agonist-based adjuvant for enhancing effector and memory CD8 T-cell responses. Immunol Cell Biol 92: 377-383.
45. Chua BY, Pejoski D, Turner SJ, Zeng W, Jackson DC. 2011. Soluble proteins induce strong $CD8^+$ T cell and antibody responses through electrostatic association with simple cationic or anionic lipopeptides that target TLR2. J Immunol 187: 1692-1701.
46. Chua BY, Johnson D, Tan A, Earnest-Silveira L, Sekiya T, Chin R, Torresi J, Jackson DC. 2012. Hepatitis C VLPs Delivered to Dendritic Cells by a TLR2 Targeting Lipopeptide Results in Enhanced Antibody and Cell-Mediated Responses. PloS One 7: e47492.
47. Christiansen D, Earnest-Silveira L, Chua B, Boo I, Drummer HE, Grubor-Bauk B, Gowans EJ, Jackson DC, Torresi J. 2018. Antibody Responses to a Quadrivalent Hepatitis C Viral-Like Particle Vaccine Adjuvanted with Toll-Like Receptor 2 Agonists. Viral Immunology 31: 338-343.
48. Wallace JR, Mangas KM, Porter JL, Marcsisin R, Pidot SJ, Howden B, Omansen TF, Zeng W, Axford JK, Johnson PDR, Stinear TP. 2017. *Mycobacterium ulcerans* low infectious dose and

mechanical transmission support insect bites and puncturing injuries in the spread of Buruli ulcer. PLoS Negl Trop Dis 11: e0005553.

49. Laemmli UK. 1970. Cleavage of structural proteins during the assembly of the head of bacteriophage T4. Nature 227: 680-685.
50. Sekiya T, Yamagishi J, Gray JHV, Whitney PG, Martinelli A, Zeng W, Wong CY, Sugimoto C, Jackson DC, Chua BY. 2017. PEGylation of a TLR2-agonist-based vaccine delivery system improves antigen trafficking and the magnitude of ensuing antibody and $CD8^+$ T cell responses. Biomaterials 137: 61-72.
51. Wijayadikusumah AR, Sullivan LC, Jackson DC, Chua BY. 2017. Structure-function relationships of protein-lipopeptide complexes and influence on immunogenicity. Amino acids 49: 1691-1704.
52. Wijayadikusumah AR. 2017. PhD thesis: An evaluation of charged Pam2Cys-based lipopeptides as novel adjuvants for subunit-based vaccines, p 92-120. Minerva Access, University of Melbourne http://hdl.handle.net/11343/198086. Accessed 18 December 2019.
53. Tan AC, Mifsud EJ, Zeng W, Edenborough K, McVernon J, Brown LE, Jackson DC. 2012. Intranasal Administration of the TLR2 Agonist Pam2Cys Provides Rapid Protection against Influenza in Mice. Mol Pharm 9: 2710-2718.
54. Mifsud EJ, Tan AC, Short KR, Brown LE, Chua BY, Jackson DC. 2016. Reducing the impact of influenza-associated secondary pneumococcal infections. Immunol Cell Biol 94: 101-108.
55. Lu LL, Chung AW, Rosebrock TR, Ghebremichael M, Yu WH, Grace PS, Schoen MK, Tafesse F, Martin C, Leung V, Mahan AE, Sips M, Kumar MP, Tedesco J, Robinson H, Tkachenko E, Draghi M, Freedberg KJ, Streeck H, Suscovich TJ, Lauffenburger DA, Restrepo BI, Day C, Fortune SM, Alter G. 2016. A Functional Role for Antibodies in Tuberculosis. Cell 167: 433-443 e414.
56. Damelang T, Rogerson SJ, Kent SJ, Chung AW. 2019. Role of IgG3 in Infectious Diseases. Trends Immunol 40: 197-211.
57. Chung AW, Kumar MP, Arnold KB, Yu WH, Schoen MK, Dunphy LJ, Suscovich TJ, Frahm N, Linde C, Mahan AE, Hoffner M, Streeck H, Ackerman ME, McElrath MJ, Schuitemaker H, Pau MG, Baden LR, Kim JH, Michael NL, Barouch DH, Lauffenburger DA, Alter G. 2015. Dissecting Polyclonal Vaccine-Induced Humoral Immunity against HIV Using Systems Serology. Cell 163: 988-998.
58. Maglione PJ, Xu J, Chan J. 2007. B cells moderate inflammatory progression and enhance bacterial containment upon pulmonary challenge with *Mycobacterium tuberculosis*. J Immunol 178: 7222-7234.
59. Phuah J, Wong EA, Gideon HP, Maiello P, Coleman MT, Hendricks MR, Ruden R, Cirrincione LR, Chan J, Lin PL, Flynn JL. 2016. Effects of B Cell Depletion on Early *Mycobacterium tuberculosis* Infection in Cynomolgus Macaques. Infect Immun 84: 1301-1311.

60. McLean MR, Madhavi V, Wines BD, Hogarth PM, Chung AW, Kent SJ. 2017. Dimeric Fcgamma Receptor Enzyme-Linked Immunosorbent Assay To Study HIV-Specific Antibodies: A New Look into Breadth of Fcgamma Receptor Antibodies Induced by the RV144 Vaccine Trial. J Immunol: 816-826.
61. George KM, Chatterjee D, Gunawardana G, Welty D, Hayman J, Lee R, Small PL. 1999. Mycolactone: a polyketide toxin from *Mycobacterium ulcerans* required for virulence. Science 283: 854-857.
62. Boulkroun S, Guenin-Macé L, Thoulouze MI, Monot M, Merckx A, Langsley G, Bismuth G, Di Bartolo V, Demangel C. 2010. Mycolactone suppresses T cell responsiveness by altering both early signaling and posttranslational events. J Immunol 184: 1436-1444.
63. Baron L, Paatero AO, Morel JD, Impens F, Guenin-Macé L, Saint-Auret S, Blanchard N, Dillmann R, Niang F, Pellegrini S, Taunton J, Paavilainen VO, Demangel C. 2016. Mycolactone subverts immunity by selectively blocking the Sec61 translocon. J Exp Med 213: 2885-2896.
64. Ogbechi J, Hall BS, Sbarrato T, Taunton J, Willis AE, Wek RC, Simmonds RE. 2018. Inhibition of Sec61-dependent translocation by mycolactone uncouples the integrated stress response from ER stress, driving cytotoxicity via translational activation of ATF4. Cell Death Dis 9: 397.
65. Guenin-Macé L, Carrette F, Asperti-Boursin F, Le Bon A, Caleechurn L, Di Bartolo V, Fontanet A, Bismuth G, Demangel C. 2011. Mycolactone impairs T cell homing by suppressing microRNA control of L-selectin expression. Proc Natl Acad Sci USA 108: 12833-12838.
66. Shinoda N, Nakamura H, Watanabe M. 2017. Suppressive effect of mycolactone-containing fraction from *Mycobacterium ulcerans* on antibody production against co-administered antigens. Biomed Res Clin Prac 2: 1-6.
67. Dangy, JP, Scherr N, Gersbach P, Hug MN, Bieri R, Bomio C, Li J, Huber S, Altmann KH, Pluschke G. 2016. Antibody-Mediated Neutralization of the Exotoxin Mycolactone, the Main Virulence Factor Produced by *Mycobacterium ulcerans*. PLoS neglected tropical diseases 10: e0004808.
68. Mangas KM, Buultjens AH, Porter JL, Baines SL, Marion E, Marsollier L, Tobias NJ, Pidot SJ, Quinn KM, Price DJ, Kedzierska K, Zeng W, Jackson DC, Chua BY, Stinear TP. 2020. Vaccine-specific immune responses against *Mycobacterium ulcerans* infection in a low-dose murine challenge model. Infect Immun 88:e00753-19.
69. Schroeder HW, Jr., Cavacini L. 2010. Structure and function of immunoglobulins. J Allergy Clin Immunol 125: S41-S52.
70. Sibéril S, Dutertre CA, Fridman WH, Teillaud JL. 2007. FcγR: The key to optimize therapeutic antibodies? Crit Rev Oncol Haematol 62: 26-33.

71. Sousa AO, Henry S, Marója FM, Lee FK, Brum L, Singh M, Lagrange PH, Aucouturier P. 1998. IgG subclass distribution of antibody responses to protein and polysaccharide mycobacterial antigens in leprosy and tuberculosis patients. Clin Exp Immunol 111: 48-55.

72. Omansen TF, Marcsisin RA, Chua BY, Zeng W, Jackson DC, Porter JL, Stienstra Y, van der Werf TS, Stinear TP. 2019. In Vivo Imaging of Bioluminescent *Mycobacterium ulcerans*: A Tool to Refine the Murine Buruli Ulcer Tail Model. Am J Trop Med Hyg 101: 1312-1321.

73. Loftus MJ, Trubiano JA, Tay EL, Lavender CJ, Globan M, Fyfe JAM, Johnson PDR. 2018. The incubation period of Buruli ulcer (*Mycobacterium ulcerans* infection) in Victoria, Australia - Remains similar despite changing geographic distribution of disease. PLoS Negl Trop Dis 12: e0006323.

74. Fyfe JA, Lavender CJ, Handasyde KA, Legione AR, O'Brien CR, Stinear TP, Pidot SJ, Seemann T, Benbow ME, Wallace JR, McCowan C, Johnson PD. 2010. A major role for mammals in the ecology of *Mycobacterium ulcerans*. PLoS Negl Trop Dis 4: e791.

75. Williamson HR, Benbow ME, Campbell LP, Johnson CR, Sopoh G, Barogui Y, Merritt RW, Small PLC. 2012. Detection of *Mycobacterium ulcerans* in the Environment Predicts Prevalence of Buruli Ulcer in Benin. PLoS Negl Trop Dis 6: e1506.

76. Marion E, Eyangoh S, Yeramian E, Doannio J, Landier J, Aubry J, Fontanet A, Rogier C, Cassisa V, Cottin J, Marot A, Eveillard M, Kamdem Y, Legras P, Deshayes C, Saint-André J-P, Marsollier L. 2010. Seasonal and regional dynamics of *M. ulcerans* transmission in environmental context: deciphering the role of water bugs as hosts and vectors. PLoS Negl Trop Dis 4: e731-e731.

77. Johnson PD, Azuolas J, Lavender CJ, Wishart E, Stinear TP, Hayman JA, Brown L, Jenkin GA, Fyfe JA. 2007. *Mycobacterium ulcerans* in mosquitoes captured during outbreak of Buruli ulcer, southeastern Australia. Emerg Inf Dis 13: 1653-1660.

3.4 Supplementary Material

3.4.1 Supplementary Tables

Table S1. Summary of protein antigen and assay characteristics.

Protein	Size	Function	Expression Vector	Presence of histidine tag (HIS-tag)	Endotoxin concentration	Putative charge[a]	Preferentially bound lipopeptide adjuvant
MUL_3720	22kDa	Putative cell wall associated protein	pDest17	N-terminal 6x histidine tag	Below detectable limit	-13.7	R_4Pam_2Cys at 1:5 protein to lipopeptide ratio
Hsp18	18kDa	Heat shock protein	pET-30b MOD[b]	N-terminal 6x histidine tag	Below detectable limit	-5.8	R_4Pam_2Cys at 1:5 protein to lipopeptide ratio

[a] As calculated by https://pepcalc.com/protein-calculator.php (Innovagen) using translated amino acid sequence from DNA sequence.

[b] Commercial Novagen pET-30b vector was modified to exclude DNA sequence from the end of the *Nde*I restriction site and three bases from the beginning of the *Eco*RV restriction site.

Table S2. *M. ulcerans* challenge outcomes in vaccinated BALB/C mice.

Vaccination group	# mice with ulcers at day 63 (n=7)	# mice with ulcers at day 68 (n=7)	# mice with ulcers at day 75 (n=7)
MUL_3720 + R_4Pam_2Cys	0	3	7
Hsp18 + R_4Pam_2Cys	0	4	7
Mul_3720 alone	0	6	7
R_4Pam_2Cys alone (without MUL_3720)	0	7	-
Hsp18 alone	0	7	-
R_4Pam_2Cys alone (without Hsp18)	0	2	7
BCG	0	5	7

Table S3. *M. ulcerans* challenge outcomes in vaccinated C57BL/6 mice.

Vaccination group	# mice with ulcers at day 63 (n=7)	# mice with ulcers at day 68 (n=7)	# mice with ulcers at day 75 (n=7)
MUL_3720 + R_4Pam_2Cys	0	6	7
Hsp18 + R_4Pam_2Cys	2	7	-
Mul_3720 alone	0	5	7
R_4Pam_2Cys alone (without MUL_3720)	0	7	-
Hsp18 alone	1	7	-
R_4Pam_2Cys alone (without Hsp18)	0	5	7
BCG	6	6	7

3.4.2 Supplementary Figures

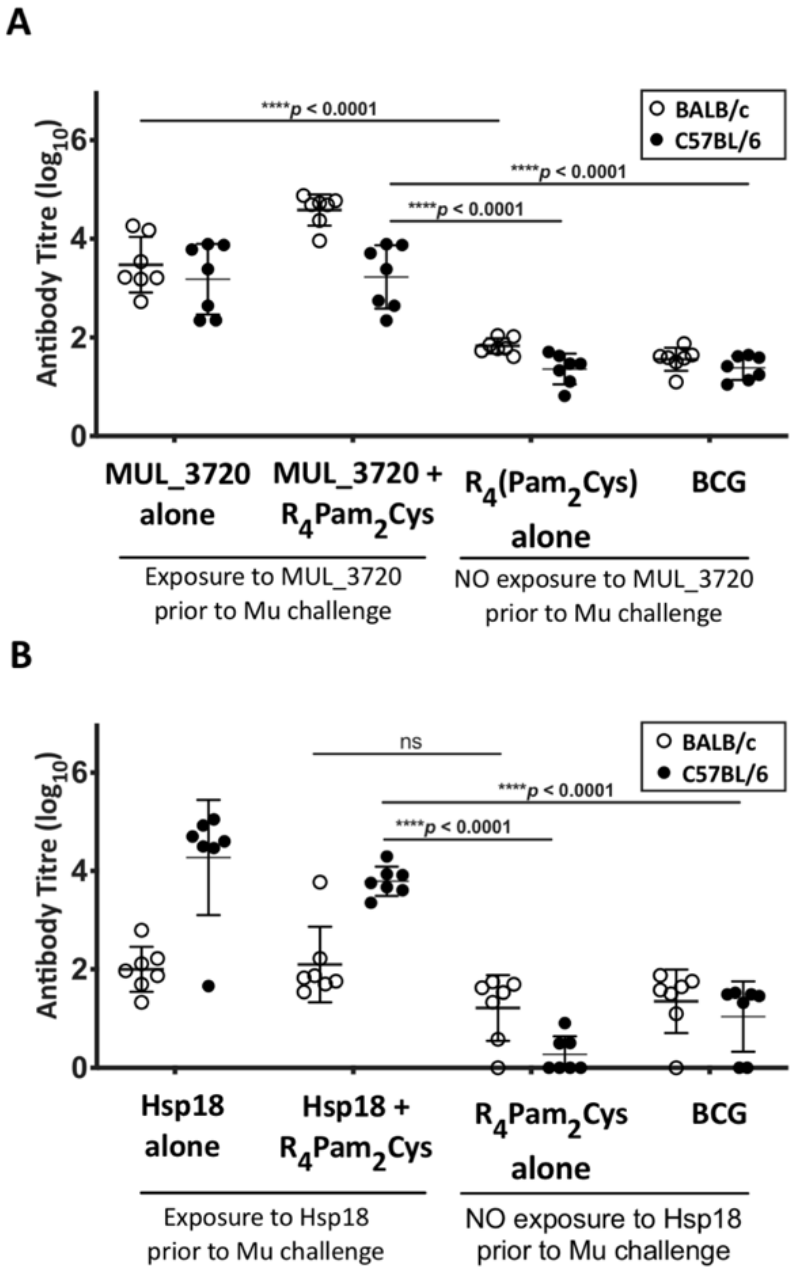

Figure S1. Antibody responses to recombinant MUL_3720 and Hsp18 in mice not vaccinated with protein.

(A) MUL_3720-specific antibody titres and **(B)** Hsp18-specific antibody titres from BALB/c mice (clear circles) and C57BL/6 mice (black circles) at day 63 (post-Mu exposure). The null hypothesis (no difference in mean antibody responses between treatment groups) was rejected if *$p < 0.05$, **$p < 0.01$, ***$p < 0.001$ or ****$p < 0.0001$. The error bars represent standard deviation (n=7).

3.5 Summary

This chapter identified that mice vaccinated with MUL_3720 and Hsp18 produced high protein-specific antibody titres, particularly after a booster vaccination. The protein-specific antibody titre increased significantly in mice vaccinated with MUL_3720+R_4Pam_2Cys and Hsp18+R_4Pam_2Cys. This highlighted the adjuvanting effect of Pam_2Cys in humoral responses. The protein-specific antibody responses primarily comprised of IgG1 antibodies. These antibodies are capable of binding to protein antigens (414). IgG1 can also bind all forms of Fcγ receptors which is required to elicit effector immune functions (414).

Vaccination with either MUL_3720 or Hsp18 proteins could induce strong antibody responses. However, these strong antibody responses did not correlate with protection against challenge with *M. ulcerans* in a murine animal challenge model. This suggests that antibody responses alone are not sufficient to protect against *M. ulcerans* infection or that these are not the ideal vaccine antigens for protection. Another major reason for the ineffectiveness of the vaccines is the presence of *M. ulcerans* toxin, mycolactone (138). Mycolactone has been shown to disrupt normal cell function and prevent immune responses that following antibody binding, such as antibody-dependent cytotoxicity and phagocytosis (132, 149, 153, 155). Future work could test different *M. ulcerans*-specific antigens in a putative vaccine against Buruli ulcer. As mycolactone a key virulence factor and neutralising this toxin early in infection, targeting toxin production should be the focus for future vaccination developments.

All BALB/c and C57BL/6 mice succumbed to infection by 40 days after *M. ulcerans* infection, even mice vaccinated with *M. bovis* BCG. *M. bovis* BCG has been previously shown to delay the onset of disease by an average of six weeks (275, 279, 333). In this chapter there was no significant difference between mice vaccinated with MUL_3720+R_4Pam_2Cys, Hsp18+R_4Pam_2Cys or *M. bovis* BCG. This suggests a comparable protection level to *M. bovis* BCG or, more likely, that *M. bovis* BCG is ineffective at protecting mice in this model of *M. ulcerans* challenge.

In this chapter all BALB/c and C57BL/6 mice succumbed to infection in a relatively short infection period (40 days) compared to human disease (~4.8 months before the onset of ulceration) (415). This study challenged mice with 10^4 CFU, which may be too high a bacterial load for mice to control infection and allow the study of protection. Concentrations of 10^4 bacteria have not been reported in environmental material in any BU endemic areas. Given BU epidemiology suggests environment-to-person spread, then the low environmental burden suggests disease is spread via a low infectious dose (217). At the time this study was conducted the minimum infectious dose was not determined, however the ID_{50} has since been identified as approximately three CFU (101). Future vaccine studies should therefore use a murine model with a more realistic *M. ulcerans* challenge dose.

Chapter 4

Vaccine-specific immune responses against *Mycobacterium ulcerans* infection in a low-dose murine challenge model

4.1 Introduction

This fourth and final results chapter focusses on the development of a vaccine against Buruli ulcer targeting the mycolactone biosynthesis pathway, in a low-dose murine challenge model. As previously shown in Chapters 2 and 3, the protein-adjuvant formulation using *M. tuberculosis* or *M. ulcerans* proteins generated strong protein-specific antibody titres. In this chapter one putative *M. ulcerans* subunit vaccine was formulated. The vaccine comprised an immunogenic protein, enoyl reductase (ER), present in the mycolactone biosynthesis pathway. To complete the vaccine, the protein was associated with the same Pam_2Cys adjuvant, utilised in Chapters 2 and 3.

Buruli ulcer (BU) is primarily a disease of the subcutaneous tissue caused by *Mycobacterium ulcerans* infection. BU is likely caused when *M. ulcerans* is introduced beneath the skin. This might occur if an area of contaminated skin surface is punctured or by insertion of an object contaminated with the bacteria into subcutaneous tissue (e.g. via an insect bite) (90, 99, 101). As discussed in Chapter 3, previous research has shown that as few as three colony forming units (CFU) of bacteria can initiate infection (101). Most animal models challenge with $>10^4$ CFU (275, 332-335, 337, 339-343) and a challenge dose of 10^4 was also used in Chapter 3. This dose is likely to be much greater than a natural infectious dose in humans and other animals (101). Such a high dose may overpower immune responses and underestimate the true efficacy of potential *M. ulcerans* vaccines. For these reasons, a low-dose of *M. ulcerans* in a challenge model was used to evaluate an experimental prime-boost subunit vaccine against BU in this chapter.

The only licensed vaccine against mycobacterial infections for human use is the *Mycobacterium bovis*-derived bacille Calmette-Guérin (BCG) vaccine for prevention of tuberculosis. This vaccine is cross-protective against *M. ulcerans*, but only delays the onset of disease (274, 275, 279). Some studies have enhanced the BCG's efficacy against BU by creating recombinant BCG vaccines (340, 341). Whilst improving the immunogenicity of BCG may be a promising route, there are some weaknesses. The exposure to environmental mycobacteria is believed to decrease the efficacy of the BCG vaccine and administration BCG-exposed populations may be ineffective (416).

M. ulcerans causes disease primarily through the production of a lipid toxin called mycolactone (138). Mycolactone modulates cell function, particularly in immune cells, which enables *M. ulcerans* to escape host immune defences (131-133, 153, 154, 156, 157). The toxin is formed by three polyketide synthases (PKS) encoded by genes on the plasmid pMUM001 (39, 40). Within each PKS are enzymatic domains that form the mycolactone molecule. One of these domains, enoyl reductase (ER), has previously been shown to significantly reduce *M. ulcerans* bacterial load in the footpad of a murine prime-boost vaccination study (335).

This chapter focusses on the development of a subunit vaccine against *M. ulcerans*, targeting the mycolactone biosynthesis pathway. The ER protein found within this pathway was identified as potential antigen. The lipopeptide adjuvant R_4Pam_2Cys, used in Chapters 2 and 3, was again utilised as the adjuvant for the subunit formulations in this study.

4.2 Research Objectives

The main aim of this study was to develop a preventative subunit vaccine against Buruli ulcer, comprising an immunogenic protein domain (found in the mycolactone biosynthesis pathway) bound to a Pam_2Cys-based lipopeptide adjuvant.

- To develop a vaccine formulation comprising ER alongside the lipopeptide adjuvant Pam_2Cys.
- To assess the efficacy of these vaccines at preventing the onset of Buruli ulcer in a physiologically relevant low-dose murine challenge model.
- To explore immune correlates of protection against BU, if any, that are induced by vaccination.

4.3 Results and Discussion

The methods and results for this study have been reported in a manuscript published in *Infection and Immunity.*

Manuscript "Vaccine-specific immune responses against *Mycobacterium ulcerans* infection in a low-dose murine challenge model"

Kirstie M. Mangas, Andrew H. Buultjens, Jessica L. Porter, Sarah L. Baines, Estelle Marion, Laurent Marsollier, Nicholas J. Tobias, Sacha J. Pidot, Kylie M. Quinn, David Price, Sue Finch, Katherine Kedzierska, Weiguang Zeng, David C. Jackson, Brendon Y. Chua and Timothy P. Stinear. **Vaccine-specific immune responses against *Mycobacterium ulcerans* infection in a low-dose murine challenge model.** *Infection and Immunity*; DOI: 10.1128/IAI.00753-19.

The following is the journal-accepted version of the manuscript, formatted to include the figures within the text.

Vaccine-specific immune responses against *Mycobacterium ulcerans* infection in a low-dose murine challenge model.

Kirstie M. Mangas[1], Andrew H. Buultjens[1], Jessica L. Porter[1], Sarah L. Baines[1], Estelle Marion[2], Laurent Marsollier[2], Nicholas J. Tobias[3,4], Sacha J. Pidot[1], Kylie M. Quinn[5], David J. Price[6,7], Katherine Kedzierska[1], Weiguang Zeng[1], David C. Jackson[1], Brendon Y. Chua[1,*] and Timothy P. Stinear[1,*].

1. Department of Microbiology and Immunology, Doherty Institute, University of Melbourne
2. CRCINA, INSERM, Université de Nantes, Université d'Angers, Angers, France
3. Molekulare Biotechnologie, Fachbereich Biowissenschaften, Goethe-Universität Frankfurt, Frankfurt am Main, Germany
4. LOEWE Centre for Translational Biodiversity in Genomics (TBG), Germany
5. Monash Biomedicine Discovery Institute and Department of Biochemistry and Molecular Biology, Monash University, Clayton, VIC 3800, Australia.
6. Victorian Infectious Diseases Reference Laboratory Epidemiology Unit at The Peter Doherty Institute for Infection & Immunity, The University of Melbourne and Royal Melbourne Hospital, VIC 3000, Australia
7. Centre for Epidemiology & Biostatistics, Melbourne School of Population & Global Health, The University of Melbourne, VIC 3010, Australia

* Joint senior authors

Running title: Immune responses against Buruli ulcer

Abstract

The neglected tropical disease Buruli ulcer (BU) is an infection of subcutaneous tissue with *Mycobacterium ulcerans*. There is no effective vaccine. Here, we assessed an experimental prime-boost vaccine in a low-dose murine tail infection model. We used the enoyl reductase (ER) domain of the *M. ulcerans* mycolactone polyketide synthases electrostatically coupled with a previously described TLR-2 agonist-based lipopeptide adjuvant, R_4Pam_2Cys. Mice were vaccinated and then challenged via tail inoculation with 14-20 colony forming units (CFU) of a bioluminescent strain of *M. ulcerans*. Mice receiving either the experimental ER vaccine or *Mycobacterium bovis* bacille Calmette-Guérin (BCG) were both protected, with both groups faring significantly better than non-vaccinated animals ($p<0.05$). To explore potential correlates of protection, a suite of 28 immune parameters were assessed in the mice at the end of the experimental period. Multivariate statistical approaches were used to interrogate the immune response data to develop disease-prognostic models. High levels of IL-2 and low IFN-γ produced in the spleen best predicted control of infection across all vaccine groups. Univariate logistic regression revealed vaccine-specific profiles of protection. High titres of ER-specific IgG serum antibodies together with IL-2 and IL-4 in the draining lymph node (DLN) were associated with protection induced by the ER vaccine. In contrast, high titres of IL-6, TNF-α, IFN-γ and IL-10 in the DLN and low IFN-γ titres in the spleen were associated with protection following BCG vaccination. This study suggests an effective BU vaccine must induce localized, tissue-specific immune profiles with controlled inflammatory responses at the site of infection.

Introduction

Buruli ulcer (BU) is a disease primarily of the subcutaneous tissue caused by infection with *Mycobacterium ulcerans*. BU initially presents as redness of the skin that is often accompanied with oedema and swelling. As the disease progresses, oedema may increase or an open ulcer develop (1, 2), the latter is typically characterised by deep undermined edges with a necrotic core comprised of bacteria, dead skin cells and immune cells (3, 4). Ulcers are predominately found on the extremities of the body such as the upper (27% of cases) and lower limbs (70% of cases) (5). Note that these percentages are for cases from south eastern Australia. The disease is rarely fatal, but if left untreated extensive destruction of subcutaneous tissue can leave victims with significant deformities and lifelong disabilities (3, 6-9).

BU is likely caused when *M. ulcerans* is introduced beneath the skin. This can occur if a region of contaminated skin surface is punctured or by insertion of an object contaminated with the bacteria into subcutaneous tissue (e.g. via an insect bite) (10-12). BU-endemic areas include certain regions of West and Sub-Saharan Africa and south eastern Australia (13, 14).

M. ulcerans is a slow-growing bacterium, with a doubling time greater than 48 hours (15, 16) making it difficult for early disease diagnosis as symptoms can take between 4-5 months to appear after primary infection (17, 18). If diagnosed early, however, BU can be treated effectively by combination antibiotic therapy (19-21). Unfortunately, in many cases the disease can initially be misdiagnosed as other, more common skin infections. Additionally, a large proportion of BU cases in African countries occur in rural villages and poorer areas with limited or no access to health care, with patients facing disfigurement and permanent disability. Given that diagnoses are delayed and usually occur after a lesion has become relatively advanced and ulceration extensive (22), development of an effective BU vaccine to protect those in highly endemic areas is of paramount importance.

Currently, the only licensed vaccine against mycobacterial infections approved for human use is the *M. bovis*-derived bacille Calmette-Guérin (BCG) vaccine for prevention of tuberculosis. This vaccine is cross-protective against *M. ulcerans*, but only delays the onset of disease (23-25). Several experimental vaccines have been tested against *M. ulcerans* infection, as summarised in Table 1. Although different animal models have been utilised to study *M. ulcerans* infections including guinea pig, primate, pig and armadillo (10, 23, 26-31), most studies assessing vaccine efficacy have used mice. Vaccines tested in these murine challenge models have included DNA-based, viral-based, protein subunit and whole cell vaccines (25, 32-35) (Table 1). Among the various vaccines, BCG expressing *M. ulcerans* antigens appears to offer the best protective effect against challenge. Hart et al. (36, 37) showed enhanced protection against BU using a recombinant BCG vaccine that expressed *M. ulcerans* Ag85A or

recombinant Ag85B-EsxH fusion protein in a mouse footpad challenge model. Whilst improving the immunogenicity of BCG may be a promising route, there are also some drawbacks; exposure to environmental mycobacteria is believed to decrease the efficacy of the BCG vaccine and administration in areas where people have been BCG-exposed may be problematic (38).

M. ulcerans causes disease primarily through the production of a lipid toxin called mycolactone (39). Mycolactone modulates cell function, in particular secretion of critical cytokines by specifically inhibiting the Sec61 translocon, enabling *M. ulcerans* to escape host immune defences (40-46). The toxin is formed from simple acetate and propionate precursors by three polyketide synthases (PKS) encoded by genes on the plasmid pMUM001 (47, 48). Within each PKS are enzymatic domains that form the mycolactone molecule. Some of these domains have been found to be immunogenic and in particular immune responses against the enoyl reductase (ER) domain have previously been shown to significantly reduce *M. ulcerans* bacterial load in the footpad of a murine prime-boost vaccination study (49). Based on the immunogenic and protective qualities of ER, we have utilised it as a target antigen for a BU subunit vaccine.

Protein antigens generally require an adjuvant to boost immunogenicity and shape immune responses. A known TLR-2 ligand, R_4Pam_2Cys, has been previously shown to induce robust antibody responses as well as augmented $CD4^+$ and $CD8^+$ T cell responses, possibly through promoting dendritic cell antigen uptake and trafficking to lymph nodes (50, 51). Given BU is a disease where the bacteria can be both extracellular and intracellular, the ability of R_4Pam_2Cys to robustly engage multiple arms of the adaptive immune system may be beneficial for a BU subunit vaccine.

Previous research has shown that as few as three colony forming units (CFU) of bacteria are required to initiate infection (10), however most animal models challenge with $>10^4$ CFU (see Table 1) (25, 32-37, 49, 52-54). This dose is likely to be far higher than the dose of bacteria that leads to natural infection in humans and other animals (10). Such an unrealistic high dose may overwhelm immune responses and underestimate the true efficacy of potential *M. ulcerans* vaccines. For these reasons, we have used a low-dose of *M. ulcerans* in a tail infection challenge model to evaluate an experimental prime-boost subunit vaccine against BU. The experimental subunit vaccine developed here comprised of the *M. ulcerans* mycolactone ER domain protein formulated with the adjuvant, R_4Pam_2Cys. Our murine challenge model with physiologically relevant dosing enabled us to more accurately measure vaccine-induced protection and to explore immune correlates of protection against BU.

Table 1. Summary of putative M. ulcerans vaccines tested in murine model of BU infection (continued next page).

Vaccine type	Description of components	*M. ulcerans* challenge dose	Test for mycolactone production[a]	Challenge model	Efficacy compared to BCG	Ref
DNA-based	pCDNA3 vector encoding Hsp65	10^4 AFB (strain 1615 ATCC35840)	Not mentioned	Tail	Less protective	(52)
DNA-based	V1Jns.tPA vector encoding Ag85A	3 x 10^4 AFB (strain 5150) or 10^5 AFB (strain 04-855)	Not mentioned	Footpad	Less protective	(32, 33)
DNA-based	Primary vaccination with V1Jns.tPA plasmid encoding mycolactone polyketide domains and boosted with recombinant domain proteins emulsified in Gerbu adjuvant.	10^5 AFB (strain 1615)	Not mentioned	Footpad	Less protective	(49)
Viral	Vesicular stomatitis virus (VSV) replicon particles expressing *M. ulcerans* codon optimised antigens MUL_2232 and MUL_3720	30µl of 2.8 x 10^5 CFU/ml stock (8.4 x 10^3 CFU/dose) (strain S1013)	Not mentioned	Footpad	Less protective	(113)
Subunit	MUL2232 and MUL3720 adjuvanted with GLA-SE (EM408)	1.5 x 10^6 or 1.5 x 10^5 CFU (strain S1013)	Not mentioned	Footpad	Less protective	(34)
Live Cell	*M. ulcerans*	$10^{6.3}$ or $10^{4.3}$ viable bacteria	Not mentioned	Footpad	Less protective	(114)
Live cell	*M. marinum*	10^5 bacteria (strain 1615)	Not mentioned	Footpad	More protective[b]	(35)
Live cell recombinant	*M. marinum* expressing Ag85A (on vector)	10^5 bacteria (strain 1615)	Not mentioned	Footpad	More protective[b]	(35)
Live cell recombinant	*M. bovis* BCG expressing Ag85A (on vector pMV261)	10^5 bacteria (strain 1615)	Not mentioned	Footpad	More protective	(36)

Table 1. Summary of putative *M. ulcerans* vaccines tested in murine model of BU infection (continued).

Live cell recombinant	*M. bovis* BCG expressing Ag85B-EsxH fusion protein Ag85A (on vector pMV261)	10^5 bacteria (strain 1615)	Not mentioned	Footpad	More protective	(37)
Inactivated whole cell	Mycolactone-negative *M. ulcerans* (strain 5114)	4 $\log_{10}$ or 3 $\log_{10}$ CFU (strain 98-912)	Not mentioned	Footpad	Less protective	(25)
Inactivated whole cell	Mycolactone-deficient attenuated *M. ulcerans* (strain ATCC19423)	10^6 bacteria (strain TMC1615)	Not mentioned	Footpad	Not compared	(54)
Inactivated whole cell	Formalin-treated *M. ulcerans* (strain TMC1615)	10^6 bacteria (strain TMC1615)	Not mentioned	Footpad	Not compared	(54)
Inactivated whole cell	Dewaxed *M. ulcerans* (strain TMC1615)	10^6 bacteria (strain TMC1615)	Not mentioned	Footpad	Not compared	(54)
Phage	Mycobacteriophage D29 (therapeutic vaccine)	5.5 $\log_{10}$ AFB (strain 1615)	Not mentioned	Footpad	Not comparable	(53)

[a] Identifying whether the bacterial culture used for challenge was assessed for mycolactone production before infection.

[b] Vaccine was more protective than the BCG vaccine, however all mice eventually developed footpad swelling.

Methods

Strains and culture conditions.

Escherichia coli ClearColi© BL21 (DE3) containing the plasmid, pJexpress-ER (strain TPS847) was grown at 37°C in Luria-Bertani (LB) broth (Difco, Becton Dickinson, MD, USA) supplemented with 100 µg/ml ampicillin (Sigma-Aldrich, USA) to express the enoyl reductase (ER) protein (57). Log-phase bioluminescent *Mycobacterium ulcerans* (strain JKD8049 containing integrated plasmid pMV306 *hsp:lux*G13) (10, 60) was grown at 30°C in 7H9 broth or 7H10 agar (Middlebrook, Becton Dickinson, MD, USA) supplemented with oleic acid, albumin, dextrose and catalase growth supplement (OADC) (Middlebrook, Becton Dickinson, MD, USA), 0.5% glycerol (v/v) and 25 µg/ml kanamycin (Sigma-Aldrich, USA). *M. bovis* BCG (strain 'Danish 1331') used for vaccinations was grown at 37°C in 7H9 broth or 7H10 agar supplemented with OADC. Mycobacterial colony counts from cultures or tissue specimens were performed using spot plating as previously described, with plates reads at 10 weeks and then rechecked at 18 weeks (10). All culture extracts were screened by LC-MS for the presence of mycolactones as previously described to ensure bacteria used in challenge experiments remained fully virulent (101).

Recombinant protein expression

Overnight culture of *E. coli* TPS847 was diluted to OD_{600} = 0.05 in LB broth. The culture was incubated at 37°C with shaking at 200 rpm until OD_{600} = 0.6-0.7, followed by the addition of 1 mM IPTG (Isopropyl b-D-1-thiogalactopyr-anoside) to induce protein expression for a further four hours. Cells were then resuspended in wash buffer (8 M urea, 150 mM sodium chloride, 10% glycerol) and sonicated at amplitude 60 (QSonica Ultrasonic Liquid Processor S-4000, Misonix) until the solution turned clear. The lysate was filtered with a 0.22 µM filter (Millipore) to remove cellular debris and protein was column-purified using anti-histidine resin (ClonTech). The resin was washed with wash buffer which was gradually replaced with tris buffer (20 mM Tris-HCl, 150 mM sodium chloride, 10% glycerol) over ten washes followed by two washes with tris buffer containing 20 mM imidazole. Protein was eluted in tris buffer containing 200 mM imidazole and dialysed in phosphate buffered saline (PBS) before concentration using a microcon column (Millipore). Proteins were tested for endotoxin contamination using Pierce™ limulus amoebocyte lysate assay (Thermo Scientific™) and relative size was confirmed by sodium dodecyl sulphate polyacrylamide gel electrophoresis.

Sodium dodecyl sulphate polyacrylamide gel electrophoresis (SDS-PAGE)

Samples were denatured in an equal volume of 2 x sample loading buffer (40% (v/v) 0.5M Tris-HCL pH6.8, 10% glycerol, 1.7% (w/v) SDS, 10% 2-B-mercaptoethanol, 0.13% (w/v) bromophenol blue in distilled water) at 100°C for 5 minutes. Ten microlitres of each sample and SeeBlue® Plus2 pre-stained protein standard (Invitrogen) was loaded onto a 0.5mm 12% polyacrylamide gel under reducing

conditions, as previously described (102). The gel was run in buffer containing 0.3% (w/v) Tris, 1.44% (w/v) glycine and 0.1% (w/v) SDS in distilled water for 1 hour at 150 volts (Mini-protean vertical electrophoresis cell, Bio-Rad), stained in Coomassie stain (45% methanol, 10% acetic acid 0.25% (w/v) Coomassie brilliant blue in distilled water) for 1 hour and destained in Coomassie destain (33% Methanol, 10% acetic acid, 60% distilled water) until protein bands were visualised.

Western Blotting

Protein separated on a 12% polyacrylamide gel was transferred to a nitrocellulose membrane in a tris-glycine transfer buffer (1.5 mM Tris, 12mM glycine, 15 % methanol (v/v) in distilled water) for 1 hour at 100 volts (Mini Trans-Blot Cell, Bio-Rad) and incubated in blocking buffer (5% (w/v) skim milk powder and 0.1% Tween-20 in PBS) overnight at 4°C. The membrane was then incubated with anti6xHIS-HRP antibody (Roche Applied Science, USA) at 1:500 dilution for 2 hours and washed in PBS containing 0.1% Tween-20 prior to exposure to developing solution (Western Lighting Chemiluminescence kit, Perkin Elmer, USA) according to the manufacturer's guidelines. Chemiluminescence was detected using an MF ChemiBIS gel imaging system (DNR Bio-Imaging Systems, Israel).

Particle size analysis of protein antigen and lipopeptide formulations by dynamic light scattering (DLS)

The association between protein and R_4Pam_2Cys was measured using dynamic light scattering (DLS) by mixing 5 µg of protein with increasing amounts of lipopeptide in 50 µl PBS. The size distribution of particles in solution (presented as hydrodynamic radius) were measured in 4µl of cyclin olefin co-polymer cuvettes using a DynaPro NanoStar DLS instrument (Wyatt Technology, CA, USA) equipped with 658nm laser with a scattering angle of 90°. Measurements were acquired in triplicate with each measurement consisting of 30 readings at 5 second intervals at 25°C. Data was analysed using Dynamics software (v7.1.7.16).

Vaccination of animals

The synthesis and purification of the branched cationic lipopeptide, R_4Pam_2Cys, was performed as previously described (103, 104). Each vaccine dose contained 25 µg protein formulated in PBS with R_4Pam_2Cys at a 1:5 molar ratio of protein to lipopeptide in a final volume of 100 µl. Live-attenuated *M. bovis* BCG strain 'Danish 1331' was grown to log phase and stored at -80°C in 20% glycerol until used. Bacteria were washed with PBS and resuspended in 200ul, before administration at 4.7×10^5 bacteria per dose. All vaccines and control formulations were sonicated for 5 minutes in a waterbath sonicator before being administered.

Female 6-week old BALB/c mice were sourced from ARC (Canning Vale, Australia) and housed in individual ventilated cages. Food and water were given *ad libitum*. Experiments were approved by The

University of Melbourne Animal Ethics Committee (Approval identification number: 1613870). For vaccination using R_4Pam_2Cys, animals were inoculated subcutaneously at the base of tail (100µl per dose at 50 µl per flank) and boosted 21 days later with the same formulations. Mice vaccinated with *M. bovis* BCG were given one dose subcutaneously in a similar manner (200 µl per dose at 100µl per flank). There were 10 mice in each vaccination group.

M. ulcerans challenge

Mice were challenged with bioluminescent *M. ulcerans* on day 35 as described previously (10). Briefly, tails of isoflurane anaesthetised mice were dipped in 7H9 culture containing log-phase bioluminescent *M. ulcerans* bacteria (concentration 1.27 x 10^6 CFU/mL (range: 1.07x10^6 – 1.46 x10^6 CFU). Contaminated tails were then pierced once subcutaneously with a sterile 25-G needle. The infectious dose was calculated to be 17 CFU (range: 14-20) using methods previously described (10). Mice were allowed to recover and monitored for up to 24 weeks after infection and sacrificed when tail ulceration was observed wherein spleens, lymph nodes and sera were harvested for immunological analysis.

IVIS imaging

Infected mice were imaged weekly from 6-weeks post-infection to detect the emission of bioluminescence. Images were captured using the Lumina XRS Series III In Vitro Imaging System (IVIS®) (Perkin Elmer, MA, USA) and Living Image Software v3.2 with the following settings: Field of View 24, relative aperture f'1.2, medium binning, 60s exposure. Bioluminescence was calculated using Living Image Software v3.2.

Serum antibody titre measurements

Serum antibody titres were measured by enzyme linked immunosorbent assay (ELISA) (105) using plates (Nunc, Thermo Scientific) that were previously coated with antigen overnight, either purified recombinant ER protein or heat-killed whole cell *M. ulcerans* lysate. The presence of bound antibodies were detected by incubating serum-exposed wells with horse radish peroxidase conjugated rabbit anti-mouse IgG (Dako, Glostrup, Denmark) for 2 hours followed by the addition of the enzyme substrate (0.2mM ABTS in 50mM citric acid containing 0.004% hydrogen peroxide and left to develop for 10-15 minutes before the addition of 50nM sodium fluoride to stop the reaction. Plates were read at dual wavelengths of 505 and 595 nm on plate reader (LabSystems Multiskan Multisoft microplate reader) and antibody titres expressed as the reciprocal of the highest dilution of serum required to achieve an optical density of 0.2.

Intracellular cytokine staining

Single cell suspensions were derived from the spleen and draining lymph nodes and resuspended in RP10 media (RPMI 1640 (Sigma) supplemented with 10% foetal bovine serum (Gibco, ThermoFisher

Scientific, Waltham, MA USA), 2mM L-glutamine, 1mM sodium pyruvate, 55 µM 2-mercaptoethanol, 12 µg gentamycin, 100 U/ml penicillin and 100 µg/ml streptomycin). Spleen and lymph node-derived cells were cultured in 96-well plates (CoStar, Corning, USA) at 1 $x10^7$ cells/per well and 1 $x10^5$ cells/well, respectively 200 µl of RP10 containing 10 U/ml IL-2 (Roche, Mannheim, Germany), 1µg/ml plate-bound anti-CD28 (BD Pharmingen, Becton Dickinson, Clone 37.51) and 20 µg/ml ER protein for 12 hours at 37°C in 5% CO_2. Golgiplug (1µg/ml) (Becton Dickinson) was added for the last 4 hours of incubation. Cells were then stained with 7AAD-Live/Dead stain dye (Biolegend, CA, USA), BV510-anti-B220 (BD Horizon, Becton Dickinson, Clone RA3-6B2), BV605-antiCD4 (Biolegend, Clone RM4-5), APC-Cy7-anti-TCRb (BD Pharmingen, Clone H57-597) and PE-Cy7-anti-CD8 (BD Pharmingen, Clone 53-6.7) anti-mouse monoclonal antibodies at 4°C in the dark. Intracellular staining was performed by fixing cells with Cytofix/Cytoperm solution (Becton Dickinson, USA) followed by permeabilisation and intracellular staining with Perm/Wash buffer (Becton Dickinson) and BV786-IFN-γ (BD Horizon, Clone XM G1.2), AF647-IL-17A (BD Pharmingen, Becton Dickinson, Clone TCII-18H10) and PE-TNF-α (BD Biosciences, Clone MP6-XT22) antibodies for 30 minutes at 4°C before analysis on an LSR Fortessa flow cytometer (BD Biosciences, US). Data analyses were performed using FlowJo (Tree Star, OR, USA).

Cytokine Bead Array

Spleen and lymph node-derived cells were incubated in 500 µl RP10 supplemented with 25 µg/ml ER protein for 72 hours at 37°C in 5% CO_2. Supernatant was collected and a cytokine bead array was performed using a mouse flex set (BD Biosciences, USA) to detect IL-2, IL-4, IL-6, IL-10, IL-17, IFN-γ, TNF, MCP-1, MIP1α, MIP1β as per the manufacturer's instructions. Samples were acquired using a FACSCanto II flow cytometer (BD Biosciences) and cytokine quantities calculated using FCAP Array™ Software v3.0.

Histology and microscopy

Tail tissues from the site of infection were fixed in PBS containing 10% non-buffered formalin then embedded in paraffin and sliced into 10 µM thick segments. The sliced segments were Ziehl Neelsen- or H&E-stained prior to microscope imaging. Images of tail segments were captured using a light microscope (Olympus BX53 Light microscope, Olympus-Life Science).

Statistical analysis

GraphPad Prism software (GraphPad Software v7, CA, USA) was used to perform statistical analyses on the antibody titre, time to luminescence, T cell numbers and cytokine titre data. Antibody titres were analysed using one-way ANOVA with Tukey's correction for multiple comparisons. The time to bioluminescence data was displayed as a Kaplan-Meier plot and differences determined using a Log-

Rank (Mantel-Cox) test. Mann-Whitney tests were performed to compare cytokine titres between protected and diseased mice and for comparisons between vaccination groups. All tests were conducted at the 5% significance level.

Statistical modelling

Twenty-eight data features (*i.e.* the immune parameters measured in each mouse, refer to Table S1) were transformed using the R package *bestNormalize* (106). Transformed features were then normalised (between 0 and 1 for each feature) using the *MinMaxScaler* function of *Scikit-learn* (107). As many of the vaccination outcome observations (time-to-bioluminescence) were right-censored, we employed the Cox proportional hazards regression analysis using the *Scikit-survival* module of *Scikit-learn* in Python (108). Here, univariate analyses were run for each of the 28 features using the continuous response variable of time-to-bioluminescence. The standard metric for assessing the predictive performance of a survival model is the concordance index (CI) (62, 109, 110). A CI >0.7 was used to identify the top six features of this model. Unsupervised learning and data dimensionality reduction is an ideal way to identify structure in continuous data without the influence of labels. The method of *t-Distributed Stochastic Neighbor Embedding* (t-SNE) is a dimensionality reduction technique that retains both the global structure and local layout of the high-dimensional data through exchanging the Euclidean distances between all pair of data points into heavy-tailed conditional probabilities (111). This method is advantageous over conventional principal component analysis (PCA), as it does not rely on a linear assumption and can capture nonlinear relationships (111). We explored the data, independent of labels, by reducing the top six features obtained from the Cox proportional hazards regression analysis to a two-dimensional space using the t-SNE package in *Scikit-learn* (107) . The two clusters detected through visual inspection were objectively defined, with observations assigned to two groups using K-means clustering, as implemented in *Scikit-learn* (107). A multivariate logistic regression classifier was then built using the top six features, with the two clusters identified by *t-SNE* as the response variables. To reduce the possibility of over-fitting, the model was validated through 1,000 random train-test splits, in which 90% of the observations made up each training set. These models were built using the logistic regression classifier as implemented in *Scikit-learn* (107) and Receiver-Operator-Characteristic curves were used to evaluate model performance (112). In order to assess the immune features that were associated with different vaccination groups, a univariate logistic regression analysis was then conducted for each group using *R* (112). The estimated model coefficients were used to assess the direction and strength of the association, and the corresponding p-value used to determine statistical significance at the 5% significance level.

Results

Formulation of the ER-R_4Pam_2Cys subunit vaccine candidate

Mycolactone is the key virulence factor produced by *M. ulcerans* and an attractive vaccine target, but the molecule is poorly immunogenic (55). However, the PKS enzymes used by the bacterium to synthesize mycolactones – are highly conserved and immunogenic (49, 56-58). Therefore, we hypothesized that targeting the conserved enzymatic domains of the mycolactone PKS could be an effective vaccine strategy. One domain in particular, the enoyl reductase (ER) protein domain, elicits serum antibodies in BU patients and healthy controls in BU endemic regions (57). The ER protein expressed as an antigen in a DNA-protein prime-boost vaccine has also been shown to reduce bacterial burden in a mouse footpad *M. ulcerans* challenge model (49). Here, we utilised the ER protein to create a novel BU vaccine candidate by electrostatically associating it with the TLR-2 agonist-based lipopeptide R_4Pam_2Cys. To formulate this vaccine, recombinant 6xHis-tagged ER protein (37 kDa) was first produced and confirmed by SDS-PAGE (Fig. 1A) and western blotting (Fig. 1B). This protein antigen was formulated with R_4Pam_2Cys at various ratios to firstly optimise the formation of protein-lipopeptide complexes. A ratio of 1:1 was sufficient to produce complexes that were larger in size than each constituent on its own (Fig. 1C). While the majority of these complexes were ~300nm in radius (peak 5), the presence of smaller sized particles of ~100nm (peak 4) suggests that not all antigen was incorporated within a complex as this size range corresponds to the size of ER protein (peak 3) or R_4Pam_2Cys alone (peak 2). Although a 1:3 ratio appears to be more effective for the association of these constituents, the size distribution of form complexes was not monodispersed and appeared as two distinct populations (peak 6 and 7). A 1:5 ratio, however, produced a uniform population of complexes that were ~500 nm in radius (peak 8) and this formulation was subsequently used to vaccinate animals.

Evaluation of ER-specific antibody responses in vaccinated mice

To evaluate the ability of the vaccine to induce ER-specific antibody responses, mice were vaccinated, and sera obtained after priming and boosting with the subunit vaccine. Our results showed that primary vaccination with ER + R_4Pam_2Cys resulted in significantly higher levels of ER-specific antibody compared to vaccination with unadjuvanted ER antigen ($p<0.0001$) (Fig. 1D). In fact, there was no significant difference in responses between unvaccinated mice and those vaccinated with a single dose of ER alone, R_4Pam_2Cys only or BCG. Although a second dose of ER alone was able to increase these responses, the titres were still ~100-fold less than levels achieved by boosting mice with ER + R_4Pam_2Cys ($p<0.0001$). These results not only indicate that ER-specific antibodies can be generated in mice and that the use of R_4Pam_2Cys can significantly enhance these responses, but that BCG does not induce cross-reactive antibodies to the ER protein.

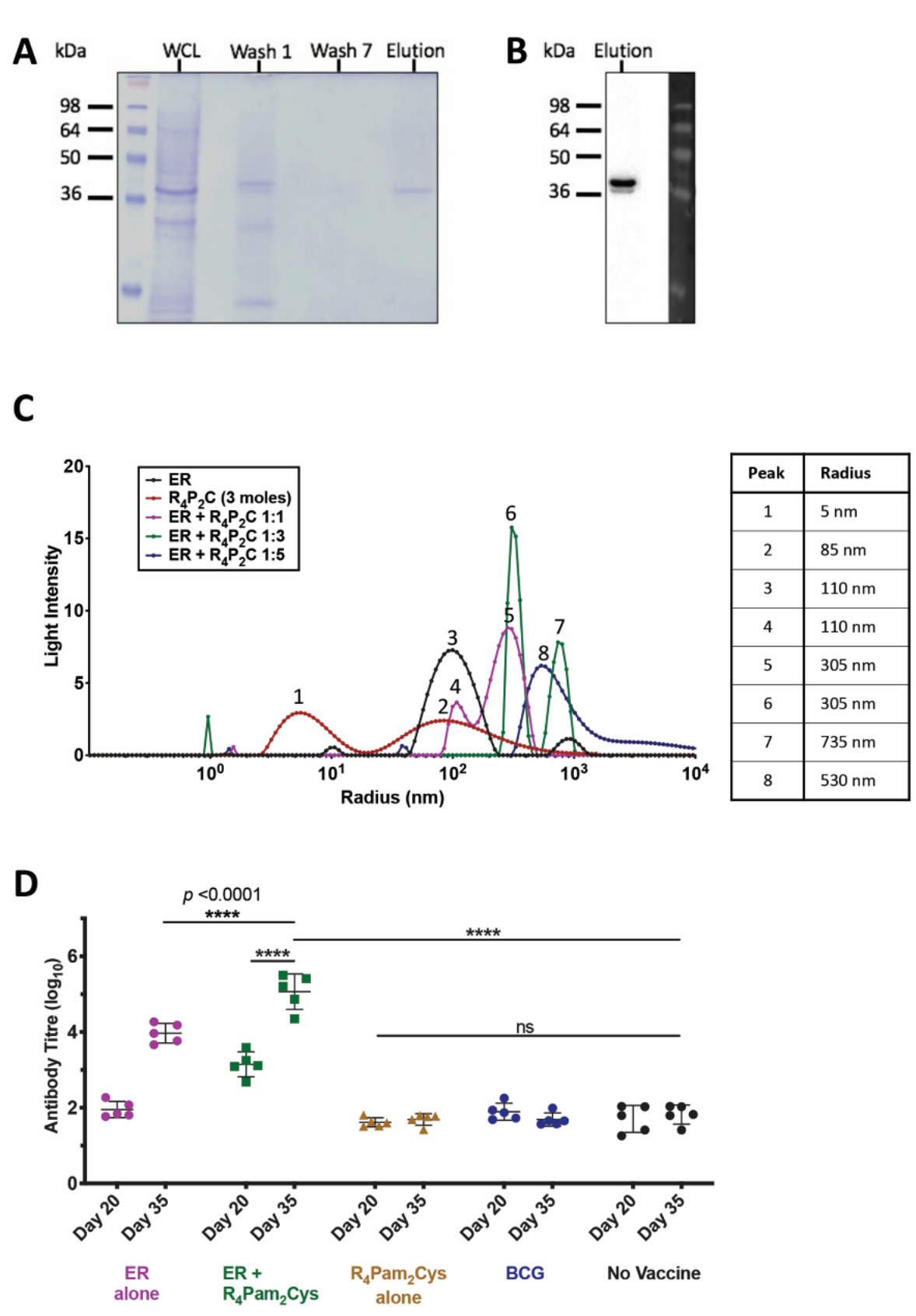

Peak	Radius
1	5 nm
2	85 nm
3	110 nm
4	110 nm
5	305 nm
6	305 nm
7	735 nm
8	530 nm

Figure 1. Analysis of purified recombinant ER protein antigen characteristics and formulation with R_4Pam_2Cys (continued next page).

Figure 1. Analysis of purified recombinant ER protein antigen characteristics and formulation with R_4Pam_2Cys (continued).

(A) The presence of recombinant ER protein (~37 kDa) was monitored by SDS-PAGE at each stage of the purification process; Lane: 1 - Whole cell lysate (WCL), Lane 2 - Wash 1, Lane 3 - Wash 7 and Lane 4 – ER protein elution (containing 10 µg protein). (**B)** Western Blot using an anti-6xHIS-tag antibody to detect the presence of a single band corresponding to the correct molecular weight of the ER protein in the final eluate. **(C)** To analyse the formation of antigen-lipopeptide complexes, a constant amount of antigen was mixed with lipopeptide at different protein:lipopeptide molecular ratios in 50µl of PBS. The size distribution of particles was then analysed by DLS with each profile depicting the hydrodynamic radius (nm) of complexes in each solution. The average radius of each formulation is highlighted in the accompanying table. **(D)** BALB/c mice (n=5/group) were vaccinated on day 0 and day 21 with R_4Pam_2Cys alone, ER antigen alone or antigen formulated with R_4Pam_2Cys or vaccinated with BCG on day 0 only. Total serum (IgG) antibody against recombinant ER protein were measured by ELISA after the primary dose (day 20) and two weeks after the secondary dose (day 35). Statistical tests were conducted at the 5% significance level. The null hypothesis was rejected if there was a significant difference in mean antibody responses between treatment groups. Note: $*p < 0.05$, $**p < 0.01$, $***p < 0.001$ or $****p < 0.0001$. The error bars represent standard deviation (n=5).

Characterisation of a low-dose M. ulcerans murine tail infection model

We have previously described the use of a low-dose tail infection model for studying insect-mediated transmission of *M. ulcerans* (10). We reasoned that because BU patients were likely to be initially infected with a low bacterial inoculum (10, 11, 59) we could use this model to test the protective efficacy of responses induced by the ER + R_4Pam_2Cys vaccine. This model features the use of a bioluminescent strain of *M. ulcerans* (10, 60) and its infectious characteristics are summarised in Fig. 2. Compared to an uninfected tail (Fig 2A and C), sub-cutaneous infection of a tail results in the appearance of a visible ulcer (Fig 2B) exhibiting the highest levels of bioluminescence concentrated around the centre of the lesion (Fig 2D), i.e. where swelling appears to be the greatest, and beginning to diminish around the periphery reflecting a positive correlation between bacterial burden and light emission (61). Histological cross-sections revealed that while tissue integrity of an uninfected tail appears defined and intact (Fig. 2E & F), dramatic differences are observed in the infected tail, typified by loss of muscle, vasculature and epidermis structure and disruptions to surrounding connective tissue (Fig. 2G & H). Further examination of this tissue showed the presence of acid-fast bacilli as well as an infiltration of polymorphonuclear cells (PMNs) (Fig. 2I). Despite evidence of bacteria engulfment by these cells (Fig. 2J), it would appear that this response was insufficient for controlling the infection and preventing disease progression.

Monitoring vaccine efficacy using bioluminescent M. ulcerans and in vivo imaging system (IVIS)

We have previously established a correlation between *M. ulcerans* bioluminescence and bacterial burden (61). Here, we set a threshold of ≥ $5x10^5$ photons/second (equivalent to $2.8x10^5$ CFU) as a measure of ineffective disease control, *i.e.* appearance of disease. Mice were vaccinated subcutaneously and then challenged with an estimated 17 CFU (range 14-20 CFU) of bioluminescent *M. ulcerans* via intradermal tail inoculation. Animals were monitored weekly for changes in bioluminescence using IVIS for up to 24 weeks. Fig. 3A shows an example of the progression of bioluminescence (and therefore disease) in an unvaccinated mouse, up to week 16 whereupon the clinical endpoint of the experiment was reached. Bioluminescence for all mice was recorded across the experimental period. Plots for the different treatment groups show the progression in bioluminescence over time (Fig3B-F). Mice from the ER alone, R_4Pam_2Cys alone and unvaccinated treatment groups displayed the first detectable bioluminescence at week 7. There also appeared to be threshold in bioluminescence, whereby animals expressing ≥$5x10^5$ photons/second from tail lesions became less able to control the infection and progressed to the clinical endpoint (Fig. 3B). The immune response data for all mice is provided (Supplementary Table S1). Using these data, failure-to-protect was defined as tail bioluminescence equal to or greater than $5x10^5$ photons/second at or before week 24 (end of experiment). Therefore, mice were defined as 'protected' if bioluminescence was less than $5x10^5$ photons/second at week 24.

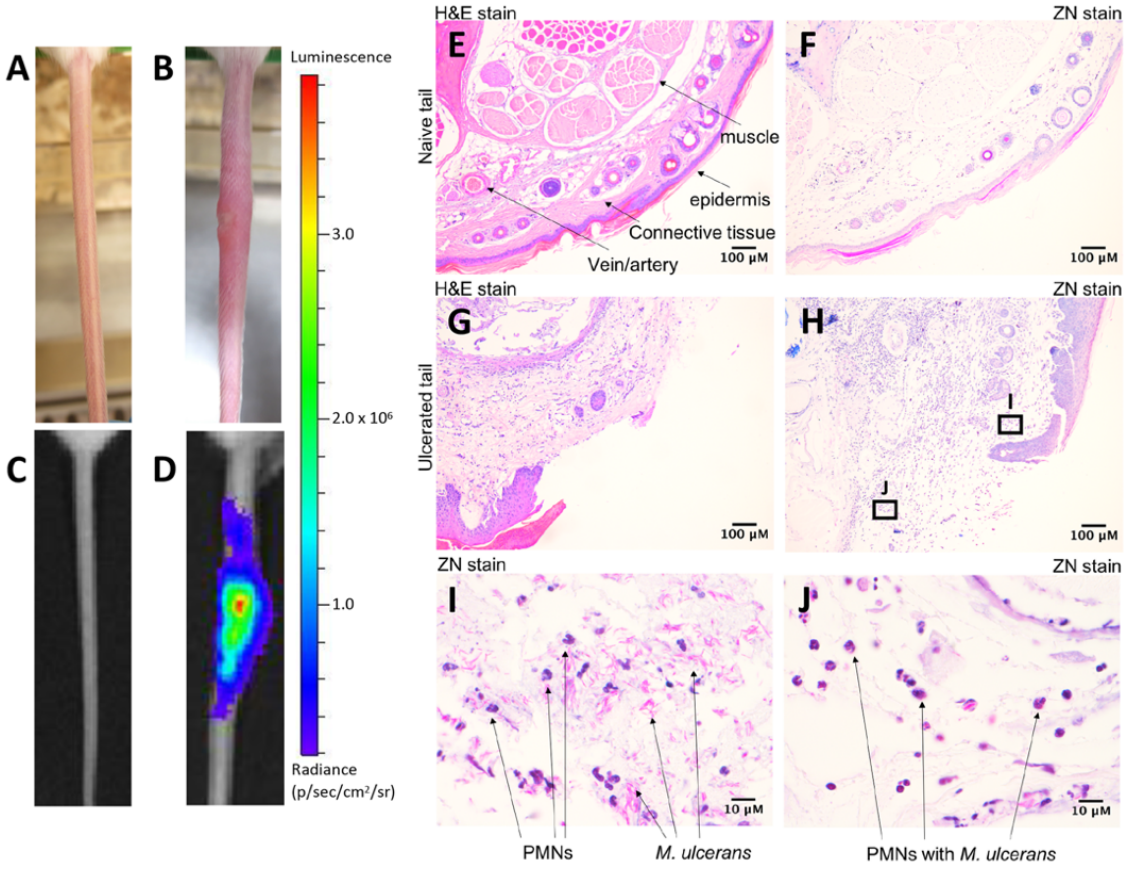

Figure 2. Characterisation of infection using a low-dose bioluminescent *M. ulcerans* strain (continued next page).

Figure 2. Characterisation of infection using a low-dose bioluminescent *M. ulcerans* strain (continued).

Representative light camera images of tails from **(A)** an uninfected BALB/c mouse or **(B)** at the point of ulceration (16 weeks) following intradermal inoculation with 20 CFU of bioluminescent *M. ulcerans*. **(C, D)** The same tails were visualised under an IVIS camera to detect and quantify bioluminescence intensity (as photons/sec). Histological cross section of an **(E, F)** uninfected or **(G, H)** infected tail tissue following haematoxylin & eosin (H&E) and Ziehl-Neelsen (ZN) staining. Zoomed images of the regions indicated within the denoted boxes of **(H)** and depicts the presence of polymorphonuclear cells (PMNs) and acid-fast bacilli (ZN staining) within tissue **(I, J)**.

Vaccination with ER + R_4Pam_2Cys offers similar protection to M. bovis BCG vaccine

Survival analysis was conducted to assess vaccine efficacy by measuring the time from infection until tail bioluminescence at the threshold of $5x10^5$ photons/second was reached. Mice that reached this threshold were defined as 'not protected'. Significantly less ER + R_4Pam_2Cys vaccinated mice (4/10 animals) developed disease compared to unvaccinated mice (9/10 animals), indicating ER + R_4Pam_2Cys provided some level of protection against disease progression compared to no vaccination (Fig. 3B, E & G) ($p<0.01$). Mice vaccinated with BCG were best protected with only 1 animal exceeding the bioluminescence threshold (Fig. 3F & G). Although this number of mice was reduced compared to the ER + R_4Pam_2Cys vaccinated animals, the difference was not significant (Fig. 3G). However, the bacterial burden (as indicated by mean photon counts/sec at the clinical endpoint) in BCG vaccinated mice was lower than animals that received the ER + R_4Pam_2Cys vaccine (means: $6x10^5$ [n=2, range 3.5 – $8.6x10^5$] versus $3.3x10^7$ [n=3, range 2.4 - $4.1x10^7$] photons/sec respectively) consistent with protective superiority of BCG. There was also no significant difference between the protective efficacy of vaccination with ER alone compared with ER + R_4Pam_2Cys, although mice vaccinated with the latter exhibited delayed disease progression (onset at weeks 16- 24) compared to ER vaccinated mice (onset at weeks 8- 16) indicating that formulation of the antigen with the R_4Pam_2Cys adjuvant improved immunity (Fig. 3D, E).

Measuring immune parameters following vaccination and challenge

At the experimental end-point, sera, spleens and draining lymph nodes (DLN) from all animals were collected and several parameters were further analysed; ER-specific antibodies, $CD4^+$ and $CD8^+$ T cells and a panel of 10 murine Th1, Th2 and Th17 cytokines. After *M. ulcerans* challenge, mice vaccinated with ER alone or ER + R_4Pam_2Cys were found to exhibit significantly more ER-specific antibodies than the other treatment groups (Fig 4A) despite not being fully protected. This indicates that, even though the ER protein is highly immunogenic, anti-ER antibodies do not appear to play a major role in controlling infection.

We next investigated if there were any differences in the ability of T cells harvested from the spleens of vaccinated mice to produce cytokines following stimulation with recombinant ER protein (Supplementary Table S1). Our results showed that the numbers of IFN-γ producing $CD4^+$ T cells across all vaccine groups did not differ, and in some cases, were higher in unvaccinated mice compared to those vaccinated with ER + R_4Pam_2Cys vaccine group (Fig 4B), indicating that there was no clear correlation between the frequencies of these cells and protection. Similarly, there also did not appear to be any correlation between TNF-α^+ $CD4^+$ T cells, IFN-γ^+ $CD8^+$ T cells or TNF-α^+ $CD8^+$ T cells and protection (Supplementary Table S1).

Comparing levels of cytokine production between vaccine groups also did not clearly identify any cytokines that correlated with protection (see Supplementary Table S1). For example, higher levels of TNF-α were present in the spleens of unvaccinated mice than BCG vaccinated mice (Fig 4C) and even though BCG vaccination resulted in significantly more IFN-γ in draining lymph nodes compared to unvaccinated mice, this was not observed for ER + R_4Pam_2Cys vaccinated mice (Fig 4D).

We therefore based our analysis on comparisons between diseased or protected mice irrespective of the vaccines they received (Fig. 4E, F). Herein, we identified significant increases of IL-2, IL-6, IL-10 IL-17A, IFN-γ, MIP-1b, TNF-α in the lymph nodes of protected mice (Fig. 4F) and significant increases of IFN-γ, IL-6, and TNF-α in the spleens of diseased mice (Fig. 4E). While these data implicate these cytokines as correlates of protection and disease, it did not rank the importance of each cytokine towards either outcome.

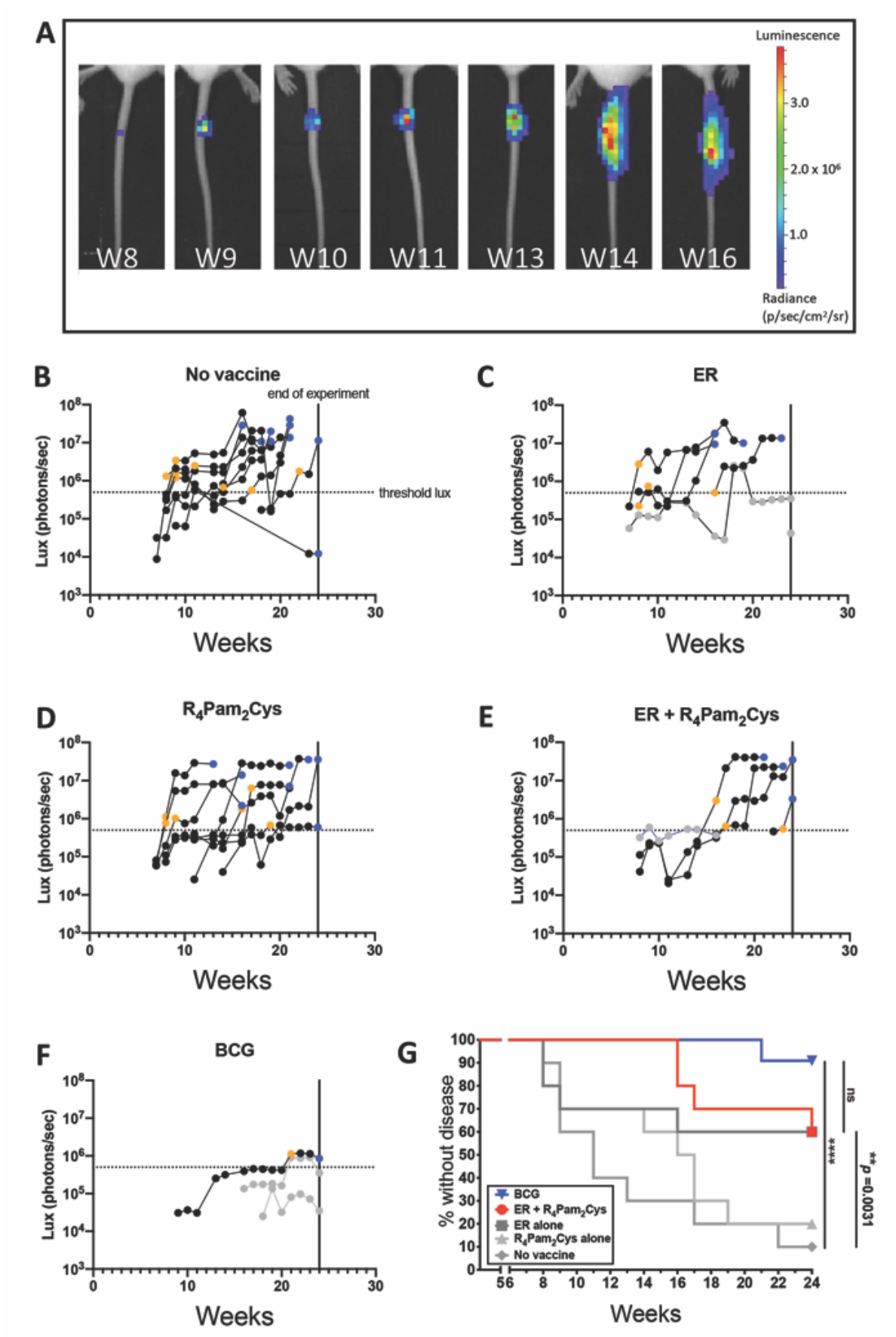

Figure 3. Development of BU over time after vaccination (continued next page).

Figure 3. Development of BU over time after vaccination (continued).

(A) Tails of mice were intradermally infected with 20 CFU of bioluminescent *M. ulcerans* and imaged weekly by IVIS. Representative panels depict the weekly progression of bioluminescent *M. ulcerans* burden in the tail of an unvaccinated mouse over the course of 16 weeks expressed as photons/second. BALB/c mice (n=10/group) were left **(B)** unvaccinated, or vaccinated on day 0 and day 21 with **(C)** ER antigen alone, **(D)** R_4Pam_2Cys alone, , **(E)** ER antigen formulated with R_4Pam_2Cys or **(F)** on day 0 with BCG followed by challenge on week 5 with bioluminescent *M. ulcerans*. Threshold bioluminescence (threshold lux) for disease was defined as $\geq 5 \times 10^5$ photons/second (p/s) as mice that reached this level typically progressed to the clinical (ethical) end point. Mice were classified as diseased if they reached this end point within the 24-weeks following challenge or if their bioluminescence value at week 24 was $\geq 5 \times 10^5$ p/s. Mice were classified as protected if they did not reach this clinical end point and their bioluminescence value was $< 5 \times 10^5$ photons/second. The data point depicting when an infected mouse first exhibited bioluminescence at $\geq 5 \times 10^5$ p/s is represented with a yellow symbol. The data point denoting when a mouse reached clinical endpoint is represented with a blue symbol. Protected mice with detectable bioluminescence are depicted as grey symbols. **G.** Time to bioluminescence measured by IVIS. A survival curve was utilised to analyse the time (weeks) taken for each BU diseased mouse to first reach threshold bioluminescence $\geq 5 \times 10^5$ photons/second. BCG group (upside down triangle) is labelled in blue, ER + R_4Pam_2Cys (circle) is red, and ER alone (square), R_4Pam_2Cys alone (upright triangle) and no vaccine (diamond) groups are depicted in grey. Statistical tests were conducted at the 5% significance level. The null hypothesis was rejected if there was a significant difference in survival between groups. Note: $*p < 0.05$, $**p < 0.01$, $***p < 0.001$ or $****p < 0.0001$.

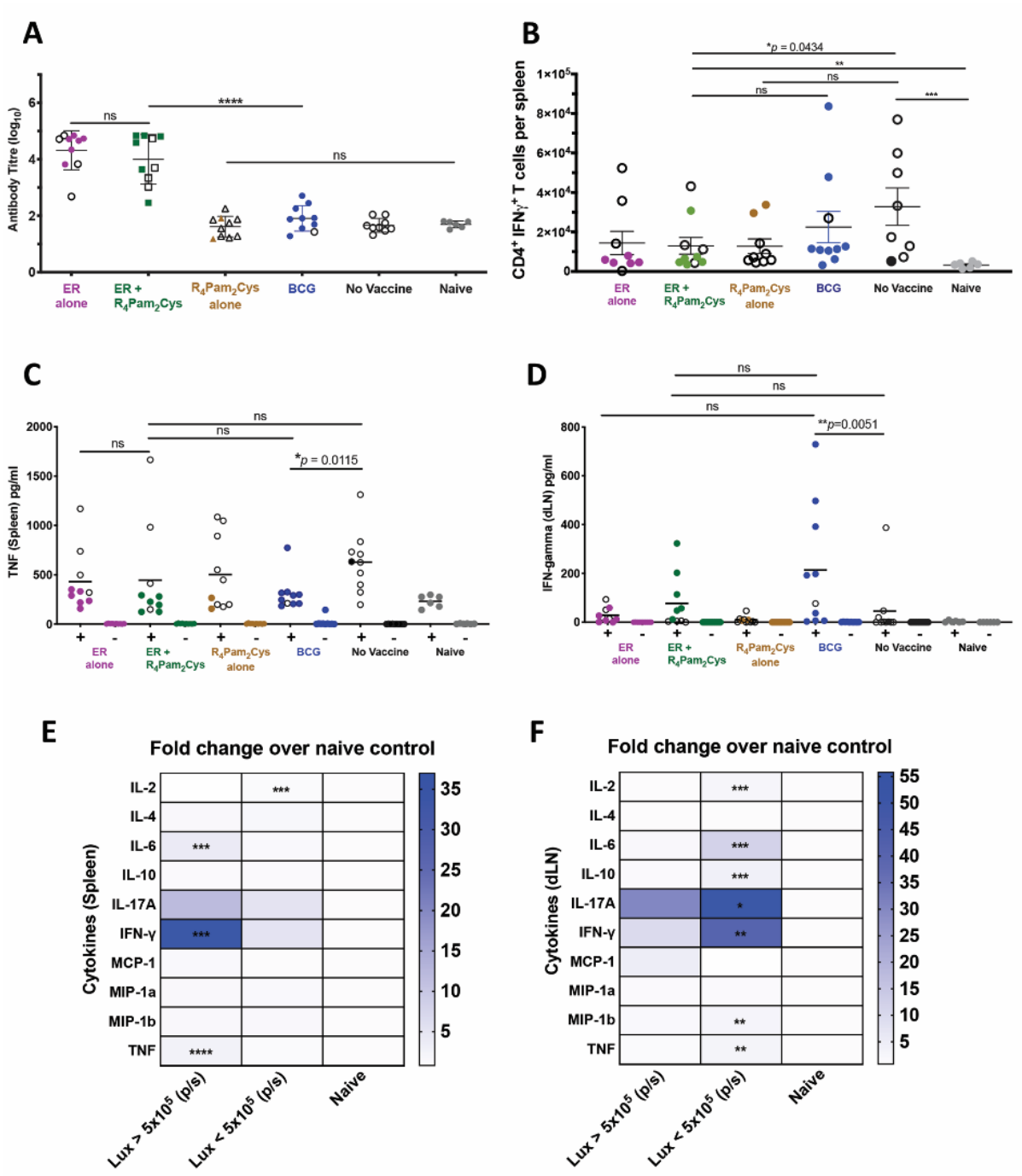

Figure 4. Immune responses after *M. ulcerans* infection (continued next page).

BALB/c mice (n=10/group) were left unvaccinated or vaccinated on day 0 and day 21 with ER antigen alone, ER antigen formulated with R_4Pam_2Cys, R_4Pam_2Cys alone, or on day 0 with BCG followed by challenge on day 36 with bioluminescent *M. ulcerans*. **(A)** Total serum (IgG) antibody against recombinant ER protein were measured by ELISA after the experimental end point. All data points for diseased mice (bioluminescence ≥5 x 10^5 p/s) are depicted with white symbols. Statistical tests were conducted at the 5% significance level. The null hypothesis was rejected if there was a significant difference in mean antibody responses between treatment groups. The error bars represent standard deviation.

Figure 4. Immune responses after *M. ulcerans* infection (continued).

(B) After experimental end point was reached, CD4+ IFN-γ+ T cells were enumerated from the spleen of mice in response to ER protein. The null hypothesis was rejected if there was a significant difference in mean CD4+ IFN-γ+ T cells between treatment groups. Once experimental end point was reached, cytokines from draining lymph nodes and spleens of *M. ulcerans* challenged mice were also measured in response to *in vitro* cell stimulation with recombinant ER protein (Supplementary Table S1). Shown here are cytokine titres **(C)** IFN-γ produced from immune cells in the draining lymph nodes and **(D)** TNF produced from immune cells in the spleen. The null hypothesis was rejected if there was no difference in mean cytokine titres between treatment groups. The black bars represent the mean. Fold change of mean cytokine titres from protected mice (bioluminescence $<5 \times 10^5$ p/s) and diseased mice (bioluminescence $\geq 5 \times 10^5$ p/s) over naïve mice were compared in the **(E)** spleen and **(F)** draining lymph nodes. The null hypothesis was rejected if there was a significant difference in mean cytokine titres between treatment groups. All statistical tests were conducted at the 5% significance level. Note: $*p < 0.05$, $**p < 0.01$, $***p < 0.001$ or $****p < 0.0001$.

Identifying immune responses associated with vaccination outcome

To identify the immune parameters (features) that associate with the response variable 'vaccine protection' (here measured as time to reach our bioluminescence detection threshold) independent of the vaccine used, we conducted univariate survival analyses via the Cox proportional hazards model. We used this model as it accounts for the fact that a subset of mice (observations) were right-censored, as vaccination outcomes were not measured after 24 weeks post challenge. For each of the 28 immunological features, their association with the response variable (time-to-bioluminescence measured in weeks) was ranked using concordance index (CI) scores. The CI is analogous to the area under the ROC curve, with a CI value of 0.5 indicating a random correlation and 1 indicating a perfect, positive correlation (62). The CI for each univariate regression analysis was used to rank the strength of association for each of the 28 features against the response variable. Using a CI cut-off of 0.70, the top six features were identified as well as the direction of their association with prevention of development of bioluminescence (Table 2). Low levels of IFN-γ and high levels of IL-2 produced in mouse splenocytes were the top two immune parameter features influencing this model, reflected in the individual correlation between their respective titres and time-to-bioluminescence (Fig. 5A, B).

Table 2. High-scoring immune features associated with delayed bioluminescence.

Feature number	Feature	Tissue site	Association with delayed bioluminescence	Concordance index
1.	IFN-γ	spleen	negative	0.786
2.	IL-2	spleen	positive	0.769
3.	IL-6	spleen	negative	0.759
4.	TNF-α	spleen	negative	0.745
5.	IL-2	lymph node	positive	0.715
6.	IFN-γ $CD4^+$ T-cell	spleen	negative	0.707

Next, using these top six features, we performed unsupervised machine learning to reveal any structure without the influence of labels, such as arbitrarily imposed bioluminescence thresholds. Here, the data separated into two main clusters. K-means clustering was then applied to assign mice (observations) to the two cluster groups. Inspection of the resulting cluster membership with respect to time to bioluminescence showed a separation of the mice either side of 17 weeks post *M. ulcerans* challenge (Fig. 5C).

Given that the clusters identified through unsupervised learning closely resembled a temporal breakpoint at 17 weeks, we further investigated this binary divide in the data. We used multivariate logistic regression and developed a low-error classifier that could generalize to unseen data, using the underlying structure apparent in the immunological data. We then tested the classifier through extensive cross-validation. Observations (mice) with bioluminescence above threshold between weeks 8-17 were assigned a '0' and '1' for those with bioluminescence detected in weeks 18-24 or no detection throughout the experiment period. The model included the top six features (Table 2) and was validated through 1,000 random train test splits, with 90% of observations comprising the training groups at each split. The resulting classifier probabilities were used to calculate the area under the ROC curve, AUC = 0.91 (True negatives = 1774, True positives = 2662, False negatives = 120, False positives = 444). The low error and generalizable nature of this classifier demonstrates the existence of a robust structure in the data, in the form of two clusters separated around week 17 (Fig. 5D) and highlights the strong association of the six identified immune parameters with outcome. Most notably here it appears that tissue specific immune responses are important, with a correlation between the appearance of a tail ulcer and evidence of a systemic (spleen) responses and protection correlating with both local (draining lymph nodes) and systemic (spleen) response (Table 2). This association of BU and the production of inflammatory cytokines (IL-6, IFN-γ and TNF) as possible markers of infection, indicated that we could also identify correlates of immune protection against BU.

Assessment of vaccine-specific immune responses

To dissect the immune responses associated with ER + R_4Pam_2Cys vaccination versus BCG and the different controls we noted the differences in the percentage of observations (mice) belonging to specific treatment groups between the two clusters observed above (Fig. 5C) separated by week 17. This summary was reflective of the survival analysis and showed that unvaccinated mice and those that received the adjuvant or ER alone were predominantly in the weeks 8-17 cluster, while ER + R_4Pam_2Cys and BCG-vaccinated mice were predominantly in the weeks 18-24 cluster (Fig. 5E). In order to obtain the individual immune profile of the different treatment groups, group-specific univariate logistic regression analyses were undertaken. Here, the response variable was coded as a '1' for membership in a particular group and '0' for membership in all other groups. Analyses were conducted for each of the five treatment groups and the model coefficient weights were used to determine both the strength and direction of association of each feature with that of each treatment group. The resulting *p*-values from the model coefficients were used to assess significance of the associations (Fig. 5F, Supplementary Table S2). The combination of the ER antigen and R_4Pam_2Cys together were important for inducing protective responses that associated with local production of IL-4, IL-2, IL-17A in the DLN, in addition to ER-specific antibody responses. Neither ER antigen or R_4Pam_2Cys alone induced this profile and protection using the former was only linked to ER- but not *M. ulcerans*-specific antibody responses (post-challenge timepoints). In comparison, BCG vaccination-mediated protection was associated with a greater breadth of localised cytokines responses than ER + R_4Pam_2Cys, with higher IL-6, TNF-α and MIP-1β in the DLN. Of note, evidence of systemic inflammation, such as IL-17A and IFN-γ in the spleen was associated with poorer BCG performance.

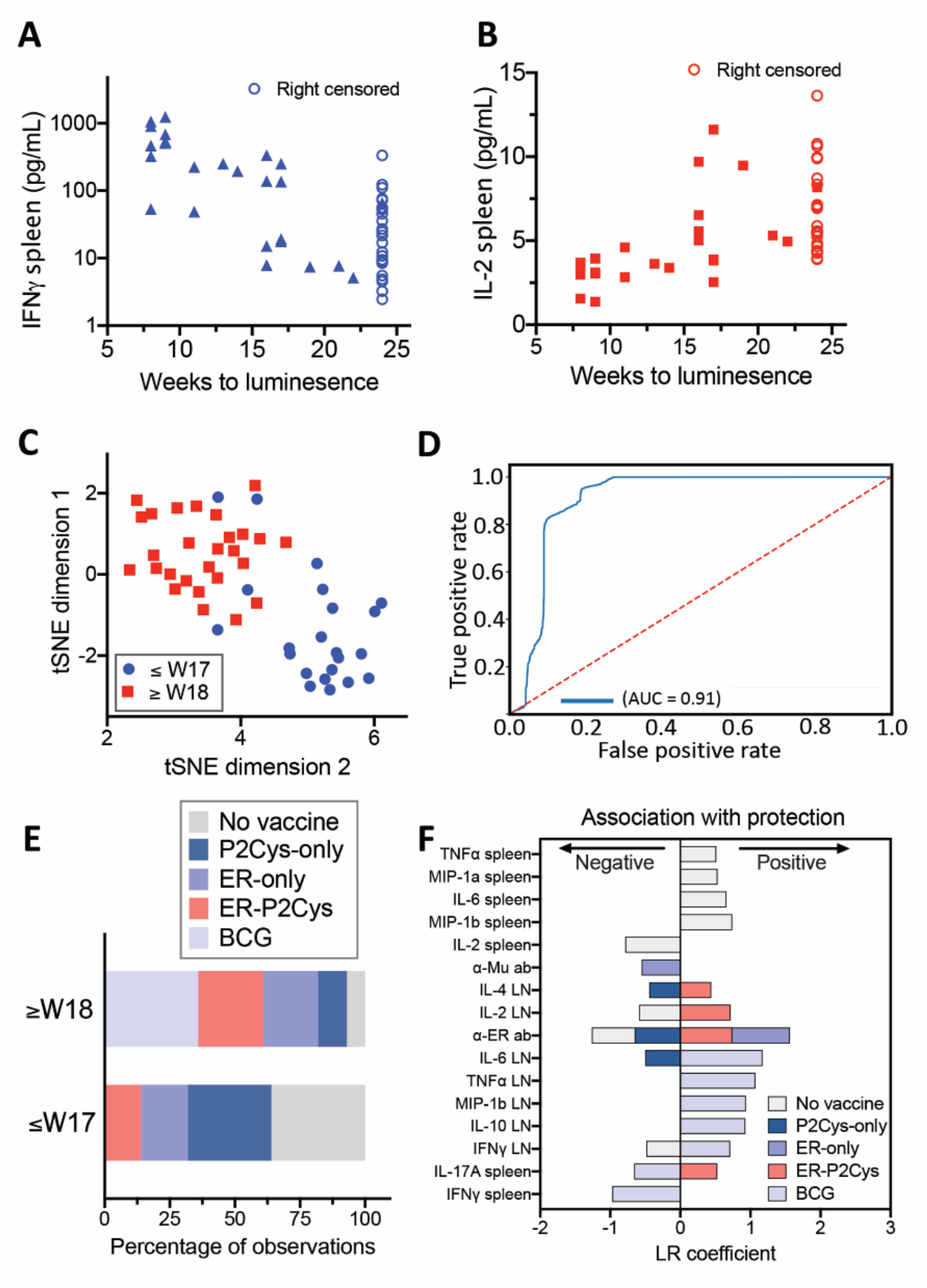

Figure 5. Statistical modelling to identify immune parameters (features) associated with vaccine protection (continued next page).

Figure 5. Statistical modelling to identify immune parameters (features) associated with vaccine protection (continued).

Univariate Cox Proportional hazards models were specified for each of the 28 immunological features to test their association with the response variable (time-to-bioluminescence measured in weeks). The resulting concordance index (CI) scores were obtained and the six features with a CI >0.7 were retained. The inverse associations of the top two features **(A)** IFN-γ and **(B)** IL-2 produced in murine splenocytes at the experimental end-point. **(C)** Plot depicting a two-dimensional representation of the top six features that associate with time-to-bioluminescence from the unsupervised t-SNE. The shapes/colours indicate the two groups identified through K-means clustering, of bioluminescence by 8-17 weeks or at 18 weeks and beyond (up to 24 weeks). **(D)** Receiver operator curve (and corresponding area under curve), displaying the trade-off between sensitivity and specificity across all thresholds for 1,000 random train-test splits of a logistic regression classifier (90% of observations used for training). The red dotted line depicts the expectation of a random classifier and the blue line depicts the model performance. **(E)** Proportion of observations (mice) across treatment groups for each of the classes both 8-17 weeks and 18-24 weeks and those with no detection. **(F)** Group-specific univariate logistic regression analyses for each of the five treatment groups. Model coefficients were used to determine both the strength and direction of association of each feature with that of each treatment group. Depicted are those features with a corresponding p-value<0.05 (Table S2).

Discussion

In this study, we investigated various immune parameters induced by the use of BCG and an experimental subunit vaccine against BU and sought to identify immune correlates associated with protection in a mouse tail infection model. Studies have shown that the tail is a suitable location for infection as BU predominantly affects extremities (11, 52, 63) and in combination with the use of bioluminescent *M. ulcerans,* offers several advantages over footpad, hock or ear infections used in most BU vaccine studies (as shown in Table 1 and (64)). Tail infections are less likely to affect mouse mobility, or cause rapid tissue loss and may also prevent added trauma, inflammation or secondary infections at the challenge site (65). A key feature of this model also allows the use of a significantly lower bacterial challenge dose compared to other studies (approximately 14-20 CFU compared to 10^4-10^6 CFU) (25, 32-37, 49, 52-54) (Table 1) and enables measuring bacterial growth in the same animal over time. This lower dose is likely to be more physiologically relevant, in terms of reflecting the bacterial inoculum that occurs during *M. ulcerans* transmission to humans (10, 11, 59). Sporadic healing of BU disease was also seen in this model, an observation that has been noted in humans and other animals (29, 66-68).

Vaccination with the ER+R_4Pam_2Cys formulation resulted in protection of 60% of mice from BU challenge. The fact that ER+R_4Pam_2Cys was significantly more protective than vaccination with R_4Pam_2Cys alone indicates any non-antigen specific triggering of innate immune responses by this adjuvant (69, 70), (71) was not sufficient for conferring long-lasting protection and the inclusion of the ER protein was necessary to achieve any protective effects. This was further evidenced by vaccinating with ER alone. Despite not seeing any clear significant differences in the clinical outcomes at the end of the trial when compared to ER + R_4Pam_2Cys vaccination, the inclusion of R_4Pam_2Cys delayed disease onset by ~8 weeks and correlated with the induction of significantly more ER-specific antibodies after a primary and booster vaccination (Fig. 3).

ER-specific antibodies were nonetheless insufficient to provide total protection against *M. ulcerans* challenge. This is perhaps not unexpected given that other studies have also reported little correlation between strong BU antibodies and protection, in mice (34) or sera of BU patients (57, 72). To identify other immune correlates associated with the protective effects observed in our study, a Cox proportional hazards regression model was utilized. Here, the univariate analyses allowed us to identify the top six features that most strongly associated with differences in time to detection of bioluminescence. These models assume normalized data, and although we cannot infer how much an increase or decrease in units could affect the clinical outcome, we are able to rank each factor based on its contribution to either disease or protection. This model also considers the effect of each factor in delaying the onset of disease rather than just modelling through a binary ‘protected’ or ‘diseased’ outcome. Similar regression

modelling has been described to predict outcomes for tuberculosis patients after treatment, effect of hospital-acquired *Clostridium difficile* on hospital stay and survival of *Staphylococcus aureus* in milk (73-75). The model assumes that eventually all mice will succumb to disease and due to the constraints in our data, it cannot determine threshold levels of cytokines that will predict disease outcomes.

The cytokines most associated with protection in BCG mice were different to those identified in mice vaccinated with ER+R_4Pam_2Cys, which is not surprising given that BCG is a multi-antigen live-attenuated vaccine and thus likely to utilise both common and distinct protective responses and mechanisms to those induced by our vaccine candidate. Through multivariate logistic regression modelling we identified the presence of IL-2 in the spleen and lymph nodes as markers that were most strongly associated with protection. Although there are no studies that directly link IL-2 with protection against *M. ulcerans*, it plays a key role in the differentiation, proliferation and maintenance of T cell responses (76). Therefore, it is perhaps not surprising that its role in this murine model is likely to be important for the induction of protective adaptive immunity against *M. ulcerans.*

M. ulcerans-specific $CD4^+$ T cells migrate to the site of infection from draining lymph nodes early in infection but are depleted as the infection persists (77), an effect attributed to the ability of the *M. ulcerans* exotoxin mycolactone to impair T cell and macrophage function (41, 44, 78). However, we observed no correlation between levels of cytokine producing $CD4^+$ and $CD8^+$ T cells and protection in vaccinated groups.

We did identify systemic IL-6, TNF-α and IFN-γ (in the spleen) strongly associated with disease. IL-6 is a pro-inflammatory cytokine produced by many cell types in response to pathogens and is linked to the production of TNF-α, both of which can be detected in BU lesions and serum of BU patients (78, 79) (80). TNF-α in particular, plays a key role in inflammatory cell recruitment and in conjunction with IFN-γ, increases the phagocytic ability of macrophages to enhance killing of mycobacteria (81, 82). However many studies have shown that mycolactone suppresses TNF-α production by T cells and especially macrophages (83, 84), decreasing their ability to control BU infection (85).

IFN-γ is important for controlling *M. ulcerans* infection (86) and is also detected at high levels in patients with both developed ulcers and early lesions (87) and healed ulcers (88), where it is believed to mediate macrophage function (89) and drive iNOS expression to facilitate bacterial killing (90). The fact that these cytokines are elevated at a systemic level in the diseased animals in our study but not in lymph nodes draining from the tail suggests that their activity is being dampened at the site of infection. These effects do not appear to be present in protected animals where increased levels of cytokines are

detected in the draining lymph node and not the spleen. Localised, but not systemic presence, of these and other cytokines including IL17A, MIP1b and IL10 are strongly associated with protection.

Although most of the immunosuppression during BU infection can be attributed to mycolactone, chronic inflammation can also be key driver as noted by the increased splenic cytokine levels. Many cell types have been implicated as the cause of immunosuppression in cancers, chronic viral infections (such as HCV, HIV, HBV) and even *M. tuberculosis* infection. These include myeloid-derived suppressor cells (MDSCs) (91) regulatory T cells (T_{reg}) (92) and T helper 17 (T_h17) (93), which can suppress effector T cell function and inhibit NK and dendritic cell activity through direct cell-to-cell interactions or the production of immunosuppressive cytokines. MDSCs in particular can be recruited by IFN-γ (94) and IL-6 (95), both of which are found in higher levels in our unprotected mice. On the other hand, while T_h17 cells are crucial for the control of infection, especially extracellular bacterial and fungal infections, elevated frequencies can lead to tissue inflammation alongside matrix destruction, autoimmunity and vascular activation (96). The observation that higher systemic IL-17A correlates with the lack of protection suggests that these cells play a role in determining BU disease outcomes.

Tissue changes due to chronic infection could also play a compounding effect on the severity of BU disease outcomes. Our histological analysis of BU-infected tail tissue showed a loss of muscle and epidermis, changes in connective tissue and loss of vasculature which may explain why lymphocytes and other immune cells are unable to access the sites of greatest infection and tissue damage. BU tissue necrosis can also extend some distance from the site of bacterial colonisation, an observation that led to the identification of mycolactone as the cause of coagulative necrosis (39, 97, 98). Mycolactone has been well described as causing cell death to skin-resident cells such as fibroblasts, adipocytes, keratinocytes and endothelial cells (39, 99, 100). Primary human dermal microvascular endothelial cells are especially sensitive to mycolactone and after exposure lose their ability to activate a key anticoagulant protein (protein C) after exposure, causing a reduction in intravascular fluidity and preventing immune cell infiltration to the infection site (99). Thus, the combination of immunosuppressive immune host responses and tissue destruction, in conjunction with mycolactone at the site of infection, may increase the risk for poorer disease outcomes for those chronically infected with BU.

Although we have identified several factors associated with disease and protection, our results provide impetus to further expand these profiles and establish their importance. For example, changes in cytokines levels before challenge and throughout the infection phase could be monitored and integrated into models, as well as analysing frequencies of various other innate- and adaptive-immune cell populations and identifying those that produce cytokines of interest. In evaluating and demonstrating

that a subunit vaccine can protect against BU in our mouse challenge model, albeit not as efficacious as BCG, our results showed that protection can be mediated through different immune mechanisms. Disease progression was also commonly linked to the presence of pro-inflammatory cytokines in the spleen and not the lymph node. These profiles suggest that localised and not systemic responses are more important for conferring protection and also provide a template that could guide the design and development of novel vaccination strategies against BU.

Finally, we conclude that the mycolactone biosynthesis pathway constitutes a viable vaccine target to protect against *M. ulcerans*. As *M. ulcerans* is slow-growing and requires its highly conserved mycolactone PKS for virulence, the development of resistance is unlikely. As such, approaches based on the use of multiple PKS enzymatic domains may prove even more efficacious. Moreover, studies that have introduced *M. ulcerans* and *M. marinum*-specific proteins into BCG have been shown to increase its protective effect, while BCG alone has no long-term efficacy (24, 32, 36, 37). Collectively, this demonstrates the additive power of using a broader suite of antigens and the potential for a viable vaccine against BU.

Acknowledgments

We thank Laura Leone for expert assistance with histology. This research was supported by the National Health and Medical Research Council, Australia (GNT1008549). The funders had no role in study design, data collection and interpretation, or the decision to submit the work for publication.

References

1. Guarner J, Bartlett J, Whitney EA, Raghunathan PL, Stienstra Y, Asamoa K, Etuaful S, Klutse E, Quarshie E, van der Werf TS, van der Graaf WT, King CH, Ashford DA. 2003. Histopathologic features of *Mycobacterium ulcerans* infection. Emerg Infect Dis 9:651-656.
2. Vincent QB, Ardant MF, Adeye A, Goundote A, Saint-Andre JP, Cottin J, Kempf M, Agossadou D, Johnson C, Abel L, Marsollier L, Chauty A, Alcais A. 2014. Clinical epidemiology of laboratory-confirmed Buruli ulcer in Benin: a cohort study. Lancet Glob Health 2:e422-30.
3. Hayman J, McQueen A. 1985. The pathology of *Mycobacterium ulcerans* infection. Pathology 17:594-600.
4. Oliveira MS, Fraga AG, Torrado E, Castro AG, Pereira JP, Filho AL, Milanezi F, Schmitt FC, Meyers WM, Portaels F, Silva MT, Pedrosa J. 2005. Infection with *Mycobacterium ulcerans* induces persistent inflammatory responses in mice. Infect Immun 73:6299-310.
5. Yerramilli A, Tay EL, Stewardson AJ, Kelley PG, Bishop E, Jenkin GA, Starr M, Trevillyan J, Hughes A, Friedman ND, O'Brien DP, Johnson PDR. 2017. The location of Australian Buruli ulcer lesions-Implications for unravelling disease transmission. PLoS Negl Trop Dis 11:e0005800.
6. van der Werf TS, van der Graaf WT, Tappero JW, Asiedu K. 1999. *Mycobacterium ulcerans* infection. Lancet 354:1013-8.
7. Pszolla N, Sarkar MR, Strecker W, Kern P, Kinzl L, Meyers WM, Portaels F. 2003. Buruli ulcer: a systemic disease. Clin Infect Dis 37:e78-82.
8. Loftus MJ, Tay EL, Globan M, Lavender CJ, Crouch SR, Johnson PDR, Fyfe JAM. 2018. Epidemiology of Buruli Ulcer Infections, Victoria, Australia, 2011-2016. Emerg Infect Dis 24:1988-97.
9. Toll A, Gallardo F, Ferran M, Gilaberte M, Iglesias M, Gimeno JL, Rondini S, Pujol RM. 2005. Aggressive multifocal Buruli ulcer with associated osteomyelitis in an HIV-positive patient. Clin Exp Dermatol 30:649-51.
10. Wallace JR, Mangas KM, Porter JL, Marcsisin R, Pidot SJ, Howden B, Omansen TF, Zeng W, Axford JK, Johnson PDR, Stinear TP. 2017. *Mycobacterium ulcerans* low infectious dose and mechanical transmission support insect bites and puncturing injuries in the spread of Buruli ulcer. PLoS Negl Trop Dis 11:e0005553.
11. Marsollier L, Robert R, Aubry J, Saint Andre JP, Kouakou H, Legras P, Manceau AL, Mahaza C, Carbonnelle B. 2002. Aquatic insects as a vector for *Mycobacterium ulce*rans. Appl Environ Microbiol 68:4623-8.
12. Meyers WM, Shelly WM, Connor DH, Meyers EK. 1974. Human *Mycobacterium ulcerans* infections developing at sites of trauma to skin. Am J Trop Med Hyg 23:919-23.

13. Buultjens AH, Vandelannoote K, Meehan CJ, Eddyani M, de Jong BC, Fyfe JAM, Globan M, Tobias NJ, Porter JL, Tomita T, Tay EL, Seemann T, Howden BP, Johnson PDR, Stinear TP. 2018. Comparative Genomics Shows That *Mycobacterium ulcerans* Migration and Expansion Preceded the Rise of Buruli Ulcer in Southeastern Australia. Appl Environ Microbiol 84.
14. Simpson H, Deribe K, Tabah EN, Peters A, Maman I, Frimpong M, Ampadu E, Phillips R, Saunderson P, Pullan RL, Cano J. 2019. Mapping the global distribution of Buruli ulcer: a systematic review with evidence consensus. Lancet Glob Health 7:e912-e922.
15. Stinear TP, Seemann T, Pidot S, Frigui W, Reysset G, Garnier T, Meurice G, Simon D, Bouchier C, Ma L, Tichit M, Porter JL, Ryan J, Johnson PD, Davies JK, Jenkin GA, Small PL, Jones LM, Tekaia F, Laval F, Daffe M, Parkhill J, Cole ST. 2007. Reductive evolution and niche adaptation inferred from the genome of *Mycobacterium ulcerans*, the causative agent of Buruli ulcer. Genome Res 17:192-200.
16. Marsollier L, Stinear T, Aubry J, Saint Andre JP, Robert R, Legras P, Manceau AL, Audrain C, Bourdon S, Kouakou H, Carbonnelle B. 2004. Aquatic plants stimulate the growth of and biofilm formation by *Mycobacterium ulcerans* in axenic culture and harbor these bacteria in the environment. Appl Environ Microbiol 70:1097-103.
17. Loftus MJ, Trubiano JA, Tay EL, Lavender CJ, Globan M, Fyfe JAM, Johnson PDR. 2018. The incubation period of Buruli ulcer (*Mycobacterium ulcerans* infection) in Victoria, Australia - Remains similar despite changing geographic distribution of disease. PLoS Negl Trop Dis 12:e0006323.
18. Trubiano JA, Lavender CJ, Fyfe JA, Bittmann S, Johnson PD. 2013. The incubation period of Buruli ulcer (*Mycobacterium ulcerans* infection). PLoS Negl Trop Dis 7:e2463.
19. Sarfo FS, Phillips R, Asiedu K, Ampadu E, Bobi N, Adentwe E, Lartey A, Tetteh I, Wansbrough-Jones M. 2010. Clinical efficacy of combination of rifampin and streptomycin for treatment of *Mycobacterium ulcerans* disease. Antimicrob Agents Chemother 54:3678-85.
20. Nienhuis WA, Stienstra Y, Thompson WA, Awuah PC, Abass KM, Tuah W, Awua-Boateng NY, Ampadu EO, Siegmund V, Schouten JP, Adjei O, Bretzel G, van der Werf TS. 2010. Antimicrobial treatment for early, limited *Mycobacterium ulcerans* infection: a randomised controlled trial. Lancet 375:664-72.
21. Wadagni AC, Barogui YT, Johnson RC, Sopoh GE, Affolabi D, van der Werf TS, de Zeeuw J, Kleinnijenhuis J, Stienstra Y. 2018. Delayed versus standard assessment for excision surgery in patients with Buruli ulcer in Benin: a randomised controlled trial. Lancet Infect Dis 18:650-656.
22. Zingue D, Bouam A, Tian RBD, Drancourt M. 2018. Buruli Ulcer, a Prototype for Ecosystem-Related Infection, Caused by *Mycobacterium ulcerans*. Clin Microbiol Rev 31.

23. Tanghe A, Adnet PY, Gartner T, Huygen K. 2007. A booster vaccination with *Mycobacterium bovis* BCG does not increase the protective effect of the vaccine against experimental *Mycobacterium ulcerans* infection in mice. Infect Immun 75:2642-4.
24. Converse PJ, Almeida DV, Nuermberger EL, Grosset JH. 2011. BCG-mediated protection against *Mycobacterium ulcerans* infection in the mouse. PLoS Negl Trop Dis 5:e985.
25. Fraga AG, Martins TG, Torrado E, Huygen K, Portaels F, Silva MT, Castro AG, Pedrosa J. 2012. Cellular immunity confers transient protection in experimental Buruli ulcer following BCG or mycolactone-negative *Mycobacterium ulcerans* vaccination. PLoS One 7:e33406.
26. Walsh DS, Dela Cruz EC, Abalos RM, Tan EV, Walsh GP, Portaels F, Meyers WM. 2007. Clinical and histologic features of skin lesions in a cynomolgus monkey experimentally infected with *Mycobacterium ulcerans* (Buruli ulcer) by intradermal inoculation. Am J Trop Med Hyg 76:132-4.
27. Ortiz RH, Leon DA, Estevez HO, Martin A, Herrera JL, Romo LF, Portaels F, Pando RH. 2009. Differences in virulence and immune response induced in a murine model by isolates of *Mycobacterium ulcerans* from different geographic areas. Clin Exp Immunol 157:271-81.
28. Bolz M, Ruggli N, Ruf MT, Ricklin ME, Zimmer G, Pluschke G. Experimental infection of the pig with *Mycobacterium ulcerans:* a novel model for studying the pathogenesis of Buruli ulcer disease. Plos Negl Trop Dis: e0004678.
29. Marion E, Jarry U, Cano C, Savary C, Beauvillain C, Robbe-Saule M, Preisser L, Altare F, Delneste Y, Jeannin P, Marsollier L. 2016. FVB/N Mice Spontaneously Heal Ulcerative Lesions Induced by *Mycobacterium ulcerans* and Switch *M. ulcerans* into a Low Mycolactone Producer. J Immunol 196:2690-2698.
30. Bénard A, Sala C, Pluschke G. *Mycobacterium ulcerans* Mouse Model Refinement for Pre-Clinical Profiling of Vaccine Candidates. PloS One 11: e0167059.
31. Walsh DS, Meyers, WM, Krieg RE, Walsh GP. 1999. Transmission of *Mycobacterium ulcerans* to the nine-banded armadillo. Am J Trop Med Hyg 61: 694-7.
32. Tanghe A, Content J, Van Vooren JP, Portaels F, Huygen K. 2001. Protective efficacy of a DNA vaccine encoding antigen 85A from *Mycobacterium bovis* BCG against Buruli ulcer. Infect Immun 69:5403-11.
33. Tanghe A, Dangy JP, Pluschke G, Huygen K. 2008. Improved protective efficacy of a species-specific DNA vaccine encoding mycolyl-transferase Ag85A from *Mycobacterium ulcerans* by homologous protein boosting. PLoS Negl Trop Dis 2:e199.
34. Bolz M, Benard A, Dreyer AM, Kerber S, Vettiger A, Oehlmann W, Singh M, Duthie MS, Pluschke G. 2016. Vaccination with the Surface Proteins MUL_2232 and MUL_3720 of *Mycobacterium ulcerans* Induces Antibodies but Fails to Provide Protection against Buruli Ulcer. PLoS Negl Trop Dis 10:e0004431.

35. Hart BE, Hale LP, Lee S. 2016. Immunogenicity and protection conferred by a recombinant *Mycobacterium marinum* vaccine against Buruli ulcer. Trials Vaccinol 5:88-91.
36. Hart BE, Hale LP, Lee S. 2015. Recombinant BCG Expressing *Mycobacterium ulcerans* Ag85A Imparts Enhanced Protection against Experimental Buruli ulcer. PLoS Negl Trop Dis 9:e0004046.
37. Hart BE, Lee S. 2016. Overexpression of a *Mycobacterium ulcerans* Ag85B-EsxH Fusion Protein in Recombinant BCG Improves Experimental Buruli Ulcer Vaccine Efficacy. PLoS Negl Trop Dis 10:e0005229.
38. Gowthaman U, Mushtaq K, Tan AC, Rai PK, Jackson DC, Agrewala JN. 2015. Challenges and solutions for a rational vaccine design for TB-endemic regions. Crit Rev Microbiol 41:389-98.
39. George KM, Chatterjee D, Gunawardana G, Welty D, Hayman J, Lee R, Small PL. 1999. Mycolactone: a polyketide toxin from *Mycobacterium ulcerans* required for virulence. Science 283:854-7.
40. Ogbechi J, Hall BS, Sbarrato T, Taunton J, Willis AE, Wek RC, Simmonds RE. 2018. Inhibition of Sec61-dependent translocation by mycolactone uncouples the integrated stress response from ER stress, driving cytotoxicity via translational activation of ATF4. Cell Death Dis 9:397.
41. Baron L, Paatero AO, Morel JD, Impens F, Guenin-Macé L, Saint-Auret S, Blanchard N, Dillmann R, Niang F, Pellegrini S, Taunton J, Paavilainen VO, Demangel C. 2016. Mycolactone subverts immunity by selectively blocking the Sec61 translocon. J Exp Med 213:2885-2896.
42. Coutanceau E, Decalf J, Martino A, Babon A, Winter N, Cole ST, Albert ML, Demangel C. 2007. Selective suppression of dendritic cell functions by *Mycobacterium ulcerans* toxin mycolactone. J Exp Med 204:1395-403.
43. Meier JL, Burkart MD. 2011. Proteomic analysis of polyketide and nonribosomal peptide biosynthesis. Curr Opin Chem Biol 15:48-56.
44. Boulkroun S, Guenin-Macé L, Thoulouze MI, Monot M, Merckx A, Langsley G, Bismuth G, Di Bartolo V, Demangel C. 2010. Mycolactone suppresses T cell responsiveness by altering both early signaling and posttranslational events. J Immunol 184:1436-44.
45. Pahlevan AA, Wright DJ, Andrews C, George KM, Small PL, Foxwell BM. 1999. The inhibitory action of *Mycobacterium ulcerans* soluble factor on monocyte/T cell cytokine production and NF-kappa B function. J Immunol 163:3928-35.
46. Torrado E, Fraga AG, Logarinho E, Martins TG, Carmona JA, Gama JB, Carvalho MA, Proença F, Castro AG, Pedrosa J. 2010. IFN-γ–Dependent Activation of Macrophages during Experimental Infections by *Mycobacterium ulcerans* Is Impaired by the Toxin Mycolactone. J Immunol 184:947.

47. Stinear TP, Mve-Obiang A, Small PL, Frigui W, Pryor MJ, Brosch R, Jenkin GA, Johnson PD, Davies JK, Lee RE, Adusumilli S, Garnier T, Haydock SF, Leadlay PF, Cole ST. 2004. Giant plasmid-encoded polyketide synthases produce the macrolide toxin of *Mycobacterium ulcerans*. Proc Natl Acad Sci USA 101:1345-9.
48. Stinear TP, Pryor MJ, Porter JL, Cole ST. 2005. Functional analysis and annotation of the virulence plasmid pMUM001 from *Mycobacterium ulcerans*. Microbiology 151:683-92.
49. Roupie V, Pidot SJ, Einarsdottir T, Van Den Poel C, Jurion F, Stinear TP, Huygen K. 2014. Analysis of the vaccine potential of plasmid DNA encoding nine mycolactone polyketide synthase domains in *Mycobacterium ulcerans* infected mice. PLoS Negl Trop Dis 8:e2604.
50. Chua BY, Zeng W, Jackson DC. 2008. Synthesis of toll-like receptor-2 targeting lipopeptides as self-adjuvanting vaccines. Methods Mol Biol 494:247-61.
51. Wang Z, Kedzierski L, Nuessing S, Chua BY, Quinones-Parra SM, Huber VC, Jackson DC, Thomas PG, Kedzierska K. 2016. Establishment of memory $CD8^+$ T cells with live attenuated influenza virus across different vaccination doses. J Gen Virol 97:3205-3214.
52. Coutanceau E, Legras P, Marsollier L, Reysset G, Cole ST, Demangel C. 2006. Immunogenicity of *Mycobacterium ulcerans* Hsp65 and protective efficacy of a *Mycobacterium leprae* Hsp65-based DNA vaccine against Buruli ulcer. Microbes Infect 8:2075-81.
53. Trigo G, Martins TG, Fraga AG, Longatto-Filho A, Castro AG, Azeredo J, Pedrosa J. 2013. Phage therapy is effective against infection by *Mycobacterium ulcerans* in a murine footpad model. PLoS Negl Trop Dis 7:e2183.
54. Watanabe M, Nakamura H, Nabekura R, Shinoda N, Suzuki E, Saito H. 2015. Protective effect of a dewaxed whole-cell vaccine against *Mycobacterium ulcerans* infection in mice. Vaccine 33:2232-9.
55. Dangy JP, Scherr N, Gersbach P, Hug MN, Bieri R, Bomio C, Li J, Huber S, Altmann KH, Pluschke G. 2016. Antibody-Mediated Neutralization of the Exotoxin Mycolactone, the Main Virulence Factor Produced by *Mycobacterium ulcerans*. PLoS Negl Trop Dis 10:e0004808.
56. Porter JL, Tobias NJ, Pidot SJ, Falgner S, Tuck KL, Vettiger A, Hong H, Leadlay PF, Stinear TP. 2013. The cell wall-associated mycolactone polyketide synthases are necessary but not sufficient for mycolactone biosynthesis. PLoS One 8:e70520.
57. Pidot SJ, Porter JL, Marsollier L, Chauty A, Migot-Nabias F, Badaut C, Benard A, Ruf MT, Seemann T, Johnson PD, Davies JK, Jenkin GA, Pluschke G, Stinear TP. 2010. Serological evaluation of *Mycobacterium ulcerans* antigens identified by comparative genomics. PLoS Negl Trop Dis 4:e872.
58. Pidot SJ, Hong H, Seemann T, Porter JL, Yip MJ, Men A, Johnson M, Wilson P, Davies JK, Leadlay PF, Stinear TP. 2008. Deciphering the genetic basis for polyketide variation among mycobacteria producing mycolactones. BMC Genomics 9:462.

59. Meyers WM, Shelly WM, Connor DH, Meyers EK. 1974. Human Mycobacterium ulcerans infections developing at sites of trauma to skin. Am J Trop Med Hyg 23: 919-23.
60. Omansen TF, Porter JL, Johnson PDR, van der Werf TS, Stienstra Y, Stinear TP. 2015. In-vitro Activity of Avermectins against *Mycobacterium ulcerans.* PLoS Negl Trop Dis 9:e0003549.
61. Omansen TF, Marcsisin RA, Chua BY, Zeng W, Jackson DC, Porter JL, Stienstra Y, van der Werf TS, Stinear TP. 2019. In Vivo Imaging of Bioluminescent *Mycobacterium ulcerans*: A Tool to Refine the Murine Buruli Ulcer Tail Model. Am J Trop Med Hyg In Press.
62. Van Belle V, Pelckmans K, Van Huffel S, Suykens JA. 2011. Support vector methods for survival analysis: a comparison between ranking and regression approaches. Artif Intell Med 53:107-18.
63. Marion E, Jarry U, Cano C, Savary C, Beauvillain C, Robbe-Saule M, Preisser L, Altare F, Delneste Y, Jeannin P, Marsollier L. 2016. FVB/N Mice Spontaneously Heal Ulcerative Lesions Induced by *Mycobacterium ulcerans* and Switch *M. ulcerans* into a Low Mycolactone Producer. J Immunol 196:2690-2698.
64. Bénard A, Sala C, Pluschke G. 2016. *Mycobacterium ulcerans* Mouse Model Refinement for Pre-Clinical Profiling of Vaccine Candidates. PLoS One 11:e0167059.
65. Kamala T. Hock immunization: a humane alternative to mouse footpad injections.
66. O'Brien DP, Murrie A, Meggyesy P, Priestley J, Rajcoomar A, Athan E. 2019. Spontaneous healing of *Mycobacterium ulcerans* disease in Australian patients. PLoS Negl Trop Dis 13:e0007178.
67. Marion E, Chauty A, Kempf M, Le Corre Y, Delneste Y, Croue A, Marsollier L. 2016. Clinical Features of Spontaneous Partial Healing During *Mycobacterium ulcerans* Infection. Open Forum Infect Dis 3:ofw013.
68. Silva-Gomes R, Marcq E, Trigo G, Gonçalves CM, Longatto-Filho A, Castro AG, Pedrosa J, Fraga AG. 2015. Spontaneous Healing of *Mycobacterium ulcerans* Lesions in the Guinea Pig Model. PLoS Negl Trop Dis 9:e0004265.
69. Tan AC, Mifsud EJ, Zeng W, Edenborough K, McVernon J, Brown LE, Jackson DC. 2012. Intranasal administration of the TLR2 agonist Pam2Cys provides rapid protection against influenza in mice. Mol Pharm 9: 2710-18.
70. Mifsud EJ, Tan AC, Reading PC, Jackson DC. 2016. Mapping the pulmonary environment of animals protected from virulent H1N1 influenza infection using the TLR-2 agonist Pam2Cys. Immunol Cell Biol 94: 169-176.
71. Mifsud EJ, Tan AC, Short KR, Brown LE, Chua BY, Jackson DC**.** 2016. Reducing the impact of influenza-associated secondary pneumococcal infections. Immunol Cell Biol 94: 101-8
72. Gooding TM, Johnson PD, Campbell DE, Hayman JA, Hartland EL, Kemp AS, Robins-Browne RM. 2001. Immune response to infection with *Mycobacterium ulcerans*. Infect Immun 69:1704-7.

73. Tolosie K, Sharma MK. 2014. Application of Cox Proportional Hazards Model in Case of Tuberculosis Patients in Selected Addis Ababa Health Centres, Ethiopia. Tuberc Res Treat https://doi.org/10.1155/2014/536976.
74. Cole SR, Hudgens MG. 2010. Survival analysis in infectious disease research: Describing events in time. AIDS 24: 2423-31.
75. Forster AJ, Taljaard M, Oake N, Wilson K, Roth V, van Walraven C. 2012. The effect of hospital-acquired infection with *Clostridium difficile* on length of stay in hospital. Can Med Assoc J 184:37-42.
76. Kalia V, Sarkar S. 2018. Regulation of Effector and Memory CD8 T Cell Differentiation by IL-2-A Balancing Act. Front Immunol 9:2987.
77. Fraga AG, Martins TG, Torrado E, Saraiva M, Pereira DR, Meyers WM, Portaels F, Silva MT, Castro AG, Pedrosa J. 2011. *Mycobacterium ulcerans* triggers T-cell immunity followed by local and regional but not systemic immunosuppression. Infect Immun 79: 421-30.
78. Phillips R, Sarfo FS, Guenin-Macé L, Decalf J, Wansbrough-Jones M, Albert ML, Demangel C. 2009. Immunosuppressive signature of cutaneous *Mycobacterium ulcerans* infection in the peripheral blood of patients with buruli ulcer disease. J Infect Dis 200:1675-84.
79. Kiszewski AE, Becerril E, Aguilar LD, Kader IT, Myers W, Portaels F, Hernandez Pando R. 2006. The local immune response in ulcerative lesions of Buruli disease. Clin Exp Immunol 143:445-51.
80. Peduzzi E, Groeper C, Schutte D, Zajac P, Rondini S, Mensah-Quainoo E, Spagnoli GC, Pluschke G, Daubenberger CA. 2007. Local activation of the innate immune system in Buruli ulcer lesions. J Invest Dermatol 127: 638-45.
81. Ray JCJ, Wang J, Chan J, Kirschner DE. 2008. The timing of TNF and IFN-gamma signaling affects macrophage activation strategies during *Mycobacterium tuberculosis* infection. J Theor Biol 252:24-38.
82. Cavalcanti YV, Brelaz MC, Neves JK, Ferraz JC, Pereira VR. 2012. Role of TNF-Alpha, IFN-Gamma, and IL-10 in the Development of Pulmonary Tuberculosis. Pulm Med 2012:745483.
83. Hall BS, Hill K, McKenna M, Ogbechi J, High S, Willis AE, Simmonds RE. 2014. The Pathogenic Mechanism of the *Mycobacterium ulcerans* Virulence Factor, Mycolactone, Depends on Blockade of Protein Translocation into the ER. PLoS Pathog 10:e1004061.
84. Pahlevan AA, Wright DJM, Andrews C, George KM, Small PLC, Foxwell BM. 1999. The Inhibitory Action of *Mycobacterium ulcerans* Soluble Factor on Monocyte/T Cell Cytokine Production and NF-κB Function. J Immunol 163:3928.
85. Torrado E, Adusumilli S, Fraga AG, Small PLC, Castro AG, Pedrosa J. 2007. Mycolactone-Mediated Inhibition of Tumor Necrosis Factor Production by Macrophages Infected with *Mycobacterium ulcerans* Has Implications for the Control of Infection. Infect Immun 75:3979.

86. Bieri R, Bolz M, Ruf M-T, Pluschke G. 2016. Interferon-γ Is a Crucial Activator of Early Host Immune Defense against *Mycobacterium ulcerans* Infection in Mice. PLoS Negl Trop Dis 10:e0004450.
87. Phillips R, Horsfield C, Mangan J, Laing K, Etuaful S, Awuah P, Nyarko K, Osei-Sarpong F, Butcher P, Lucas S, Wansbrough-Jones M. 2006. Cytokine mRNA expression in *Mycobacterium ulcerans*-infected human skin and correlation with local inflammatory response. Infect Immun 74:2917-24.
88. Westenbrink BD, Stienstra Y, Huitema MG, Thompson WA, Klutse EO, Ampadu EO, Boezen HM, Limburg PC, van der Werf TS. 2005. Cytokine responses to stimulation of whole blood from patients with Buruli ulcer disease in Ghana. Clin Diagn Lab Immunol 12:125-9.
89. Torrado E, Fraga AG, Logarinho E, Martins TG, Carmona JA, Gama JB, Carvalho MA, Proenca F, Castro AG, Pedrosa J. 2010. IFN-gamma-dependent activation of macrophages during experimental infections by *Mycobacterium ulcerans* is impaired by the toxin mycolactone. J Immunol 184:947-55.
90. Flynn JL, Chan J. 2001. Immunology of tuberculosis. Annu Rev Immunol 19:93-129.
91. Magcwebeba T, Dorhoi A, du Plessis N. 2019. The Emerging Role of Myeloid-Derived Suppressor Cells in Tuberculosis. Front Immunol 10:917.
92. Boer MC, Joosten SA, Ottenhoff TH. 2015. Regulatory T-Cells at the Interface between Human Host and Pathogens in Infectious Diseases and Vaccination. Front Immunol 6:217.
93. Isailovic N, Daigo K, Mantovani A, Selmi C. 2015. Interleukin-17 and innate immunity in infections and chronic inflammation. J Autoimmun 60:1-11.
94. Greifenberg V, Ribechini E, Rossner S, Lutz MB. 2009. Myeloid-derived suppressor cell activation by combined LPS and IFN-gamma treatment impairs DC development. Eur J Immunol 39:2865-76.
95. Jiang M, Chen J, Zhang W, Zhang R, Ye Y, Liu P, Yu W, Wei F, Ren X, Yu J. 2017. Interleukin-6 Trans-Signaling Pathway Promotes Immunosuppressive Myeloid-Derived Suppressor Cells via Suppression of Suppressor of Cytokine Signaling 3 in Breast Cancer. Front Immunol 8:1840.
96. Miossec P, Kolls JK. 2012. Targeting IL-17 and TH17 cells in chronic inflammation. Nat Rev Drug Discov 11:763-76.
97. Forbes BR, Wannan JS, Kirkland WB. 1954. Indolent cutaneous ulceration due to infection with *Mycobacterium ulcerans*. Med J Aust 41:475-9.
98. Adusumilli S, Mve-Obiang A, Sparer T, Meyers W, Hayman J, Small PL. 2005. *Mycobacterium ulcerans* toxic macrolide, mycolactone modulates the host immune response and cellular location of M. ulcerans in vitro and in vivo. Cell Microbiol 7:1295-304.
99. Ogbechi J, Ruf MT, Hall BS, Bodman-Smith K, Vogel M, Wu HL, Stainer A, Esmon CT, Ahnstrom J, Pluschke G, Simmonds RE. 2015. Mycolactone-Dependent Depletion of

Endothelial Cell Thrombomodulin Is Strongly Associated with Fibrin Deposition in Buruli Ulcer Lesions. *PLoS Pathog* 11:e1005011.

100. George KM, Pascopella L, Welty DM, Small PL. 2000. A *Mycobacterium ulcerans* toxin, mycolactone, causes apoptosis in guinea pig ulcers and tissue culture cells. Infect Immun 68:877-83.
101. Hong H, Gates PJ, Staunton J, Stinear T, Cole ST, Leadlay PF, Spencer JB. 2003. Identification using LC-MSn of co-metabolites in the biosynthesis of the polyketide toxin mycolactone by a clinical isolate of *Mycobacterium ulcerans*. Chem Commun: 2822-2823.
102. Laemmli UK. 1970. Cleavage of structural proteins during the assembly of the head of bacteriophage T4. Nature 227:680-685.
103. Sekiya T, Yamagishi J, Gray JHV, Whitney PG, Martinelli A, Zeng W, Wong CY, Sugimoto C, Jackson DC, Chua BY. 2017. PEGylation of a TLR2-agonist-based vaccine delivery system improves antigen trafficking and the magnitude of ensuing antibody and $CD8^+$ T cell responses. Biomaterials 137:61-72.
104. Wijayadikusumah AR, Zeng W, McQuilten HA, Wong CY, Jackson DC, Chua BY. 2019. Geometry of a TLR2-Agonist-Based Adjuvant Can Affect the Resulting Antigen-Specific Immune Response. Mol Pharm 16:2037-2047.
105. Chua BY, Pejoski D, Turner SJ, Zeng W, Jackson DC. 2011. Soluble proteins induce strong $CD8^+$ T cell and antibody responses through electrostatic association with simple cationic or anionic lipopeptides that target TLR2. J Immunol 187:1692-701.
106. Beasley TM, Erickson S, Allison DB. 2009. Rank-based inverse normal transformations are increasingly used, but are they merited? Behav Genet 39:580-95.
107. Pedregosa F, Varoquaux G, Gramfort A, Michel V, Thirion B, Grisel O, Blondel M, Prettenhofer P, Weiss R, Dubourg V, Vanderplas J, Passos A, Cournapeau D, Brucher M, Perrot M, Duchesnay E. 2011. Scikit-learn: Machine Learning in Python. J Mach Learn Res 12:2825-2830.
108. Polsterl S, Gupta P, Wang L, Conjeti S, Katouzian A, Navab N. 2016. Heterogeneous ensembles for predicting survival of metastatic, castrate-resistant prostate cancer patients. F1000Res 5:2676.
109. Evers L, Messow CM. 2008. Sparse kernel methods for high-dimensional survival data. Bioinformatics 24:1632-8.
110. Shivaswamy PK, Chu W, Jansche M. 2007. A support vector approach to censored targets. Icdm 2007: Proceedings of the Seventh IEEE International Conference on Data Mining doi:10.1109/Icdm.2007.93:655-660.
111. van der Maaten L, Hinton G. 2008. Visualizing Data using t-SNE. J Mach Learn Res 9:2579-2605.

112. Team RC. 2014. R: A Language and Environment for Statistical Computing, R Foundation for Statistical Computing, Vienna, Austria. Website: http://www.R-project.org/ [Accessed June 2019].

113. Bolz M, Kerber S, Zimmer G, Pluschke G. 2015. Use of Recombinant Virus Replicon Particles for Vaccination against *Mycobacterium ulcerans* Disease. PLoS Negl Trop Dis 9:e0004011.

114. Fenner F. 1957. Homologous and heterologous immunity in infections of mice with *Mycobacterium ulcerans* and *Mycobacterium balnei*. Am Rev Tuberc 76:76-89.

4.4 Supplementary Material

4.4.1 Supplementary Tables

Table S1. Vaccination Data (continued next five pages).

Vaccine Group	Mouse ID	Disease Yes (Y)/ No (blank)	CFU/ml	*IS2404* qPCR	ER Ab	MU-WCL Ab
BCG	G12M1				2.256	0.7392
BCG	G12M2				1.954	1.201
BCG	G12M3				1.898	3.749
BCG	G12M4				1.576	2.499
BCG	G12M5				1.237	0.951
BCG	G5M1				1.922	0.1634
BCG	G5M2	Y	1.33×10^4	35.48	1.429	3.67
BCG	G5M3				1.694	1.891
BCG	G5M4		2.7×10^4	37.77	2.448	3.675
BCG	G5M5		1.7×10^4	38.78	2.709	1.288
ER + R_4Pam_2Cys	G2M1			no ct	2.464	3.062
ER + R_4Pam_2Cys	G2M2				4.839	3.696
ER + R_4Pam_2Cys	G2M3	Y	3.06×10^4	31.24	4.733	0.8907
ER + R_4Pam_2Cys	G2M4	Y	2.66×10^5	35.53	3.02	1.176
ER + R_4Pam_2Cys	G2M5				3.639	1.512
ER + R_4Pam_2Cys	G9M1	Y	2.7×10^4	31.24	3.697	2.312
ER + R_4Pam_2Cys	G9M2				4.809	0.908
ER + R_4Pam_2Cys	G9M3	Y	2.9×10^4	33.94	3.339	1.926
ER + R_4Pam_2Cys	G9M4				4.588	0.5648
ER + R_4Pam_2Cys	G9M5				4.839	0
ER alone	G1M1	Y	2.26×10^4	31.06	4.839	1.377
ER alone	G1M2	Y	1.73×10^5	36.2	2.681	0
ER alone	G1M3	Y	2.88×10^5	35.63	3.829	0.3014
ER alone	G1M4				4.339	0.9413
ER alone	G1M5	Y	3.54×10^5	35.76	4.715	0
ER alone	G8M1				4.839	0
ER alone	G8M2				4.733	0.632
ER alone	G8M3		8.3×10^3	37.56	4.659	2.029
ER alone	G8M4				3.818	0.8006
ER alone	G8M5		4.3×10^3	37.23	4.715	2.584
R_4Pam_2Cys	G10M1	Y	3.6×10^4	30.27	2.256	0.8197
R_4Pam_2Cys	G10M2				1.912	1.041
R_4Pam_2Cys	G10M3	Y	2.5×10^5	27.27	1.878	1.311
R_4Pam_2Cys	G10M4	Y	4.5×10^4	28.73	1.556	1.66
R_4Pam_2Cys	G10M5	Y	4.2×10^4	32.59	1.282	0
R_4Pam_2Cys	G3M1	Y	1.33×10^3	32.51	1.859	3.773
R_4Pam_2Cys	G3M2				1.186	1.696
R_4Pam_2Cys	G3M3	Y	1.06×10^4	31.83	1.748	2.719
R_4Pam_2Cys	G3M4	Y	6.66×10^3	34.05	1.224	0.8924
R_4Pam_2Cys	G3M5	Y	2.79×10^5	30.86	1.282	1.119
No Vaccination	G13M1	Y	2.8×10^4	31.8	1.586	3.262
No Vaccination	G13M2	Y	9.342×10^3	29.6	1.576	3.914
No Vaccination	G13M3	Y	2.9×10^4	36.23	1.649	1.499
No Vaccination	G13M4	Y	2.5×10^5	27.95	2.044	1.657
No Vaccination	G13M5	Y	3.7×10^4	34.88	1.743	0.2277
No Vaccination	G6M1				0	0.347
No Vaccination	G6M2	Y	2.8×10^4	35.55	1.468	3.459
No Vaccination	G6M3	Y	2.9×10^4	37.45	1.545	1.088
No Vaccination	G6M4	Y	2.2×10^4	35.56	2.044	3.292
No Vaccination	G6M5	Y	2.5×10^4	33.94	1.319	1.523
Naïve	G14M1				1.598	1.806
Naïve	G14M2				1.806	1.511
Naïve	G14M3				1.511	1.522
Naïve	G7M1				1.687	1.637
Naïve	G7M2				1.778	1.521
Naïve	G7M3				1.791	1.598

Table S1. Vaccination Data (continued 1).

Vaccine Group	Time to LUX (weeks)	Time to LUX threshold first reached (weeks)	Time to ulceration (weeks)	Severity score at endpoint or end of experiment (EOE) (between 0-3)	Healed Yes (Y)/ No (blank)
BCG	NA	NA			
BCG	NA	NA			
BCG	NA	NA			
BCG	NA	NA			
BCG	NA	NA			
BCG	NA	NA			
BCG	9	21	Not reached by EOE	2.5-3	
BCG	NA	NA			
BCG	18	NA	Not reached by EOE	0.5-1	
BCG	16	NA	Not reached by EOE	1	
ER + R_4Pam_2Cys	8	NA	Not reached by EOE	0	Y
ER + R_4Pam_2Cys	NA	NA			
ER + R_4Pam_2Cys	22	24	Not reached by EOE	2	
ER + R_4Pam_2Cys	8	17	24	3	
ER + R_4Pam_2Cys	NA	NA			
ER + R_4Pam_2Cys	16	16	Not reached by EOE	3	
ER + R_4Pam_2Cys	NA	NA			
ER + R_4Pam_2Cys	8	16	21	3	
ER + R_4Pam_2Cys	NA	NA			
ER + R_4Pam_2Cys	NA	NA			
ER alone	16	16	24	3	
ER alone	7	8	16	3	
ER alone	8	9	16	3	
ER alone	NA	NA			
ER alone	8	8	19	3	
ER alone	NA	NA			
ER alone	NA	NA			
ER alone	7	NA	EOE	1.5	
ER alone	NA	NA			
ER alone	24	NA	Not reached by EOE	0.5	
R_4Pam_2Cys	7	8	13	3	
R_4Pam_2Cys	NA	NA			
R_4Pam_2Cys	7	8	16	3	
R_4Pam_2Cys	14	17	24	3	
R_4Pam_2Cys	8	14	21	3	
R_4Pam_2Cys	11	17	Not reached by EOE	2	
R_4Pam_2Cys	NA	NA			
R_4Pam_2Cys	7	9	16	3	
R_4Pam_2Cys	8	19	24	2.5-3	
R_4Pam_2Cys	10	16	21	3	
No Vaccination	8	8	24	1	
No Vaccination	7	13	21	3	
No Vaccination	8	9	16	3	
No Vaccination	8	9	19	3	
No Vaccination	7	9	22	3	
No Vaccination	NA	NA			
No Vaccination	18	22	Not reached by EOE	3	
No Vaccination	9	11	19	3	
No Vaccination	13	17	21	3	
No Vaccination	8	11	22	3	
Naïve					
Naïve					
Naïve					
Naïve					
Naïve					
Naïve					

Table S1. Vaccination Data (continued 2).

Vaccine Group	Luminescence (photons/second) by week															
	7	8	9	10	11	13	14	16	17	18	19	20	21	22	23	24
BCG																
BCG																
BCG																
BCG																
BCG																
BCG																
BCG			30900	36700	30800	252000	315000	393000	453000	444000	425000	419000	1130000	1170000	1140000	856000
BCG																
BCG										25100	135000	32100	80900	97100	71900	35000
BCG								135000	176000	176000	184000	163000	908000	871000	909000	354000
ER + R_4Pam_2Cys		325000	596000	263000	361000	540000	527000	369000	*	*	*	*	*	*	*	*
ER + R_4Pam_2Cys																
ER + R_4Pam_2Cys														467000	544000	3310000
ER + R_4Pam_2Cys		114000	201000	231000	25500	33500	197000	318000	634000	682000	646000	2.1E+07	2.2E+07	2.3E+07	2.4E+07	
ER + R_4Pam_2Cys																
ER + R_4Pam_2Cys								393000	636000	2950000	3320000	2940000	3560000	1.3E+07	1.2E+07	3.5E+07
ER + R_4Pam_2Cys																
ER + R_4Pam_2Cys		41400	231000	245000	20800	135000	256000	2970000	2.1E+07	4.2E+07	4E+07	4.1E+07	4.1E+07			
ER + R_4Pam_2Cys																
ER + R_4Pam_2Cys																
ER alone								503000	2480000	2250000	2570000	3670000	1.3E+07	1.4E+07	1.4E+07	
ER alone	221000	2860000	6070000	1960000	5740000	6790000	5960000	9510000								
ER alone		228000	743000	231000	222000	6640000	7860000	1.8E+07								
ER alone																
ER alone		541000	514000	619000	302000	308000	1040000	1.8E+07	3.5E+07	1.2E+07	1E+07					
ER alone																
ER alone																
ER alone	58500	132000	120000	113000	282000	273000	132000	36300	29300	2570000	2200000	294000	289000	330000	342000	352000
ER alone																
ER alone																43500
R_4Pam_2Cys	63000	1120000	1.6E+07	1.4E+07	2.9E+07	2.7E+07										
R_4Pam_2Cys																
R_4Pam_2Cys	81600	763000	5410000	5370000	8080000	8030000	8720000	2200000								
R_4Pam_2Cys							40000	232000	6350000	7790000	7610000	7790000	6350000	3.7E+07	3.6E+07	
R_4Pam_2Cys		110000	339000	369000	284000	293000	928000	2.9E+07	2.6E+07	2.4E+07	2.8E+07	2.4E+07	2.6E+07			
R_4Pam_2Cys					25600	329000	371000	369000	579000	61800	290000	671000	593000	593000	630000	601000
R_4Pam_2Cys																
R_4Pam_2Cys	58500	195000	1020000	750000	943000	8030000	8210000	1.4E+07								
R_4Pam_2Cys		73200	280000	315000	401000	196000	235000	257000	384000	371000	679000	330000	1700000	2170000	2060000	3.6E+07
R_4Pam_2Cys				320000	303000	381000	164000	1830000	2620000	3870000	4060000	1180000	7080000			
No Vaccination		1320000	2100000	2000000	553000	*	*	*	*	*	*	*	*	*	12200	12200
No Vaccination	31800	32000	364000	216000	212000	731000	505000	2290000	6170000	6360000	7790000	1.4E+07	1.4E+07			
No Vaccination		312000	1200000	1130000	802000	244000	828000	2.9E+07								
No Vaccination		343000	1610000	1610000	1820000	1670000	1660000	1.4E+07	1.1E+07	6360000	1.1E+07					
No Vaccination	8770	442000	3440000	3350000	5300000	4880000	5430000	6.1E+07	1.2E+07	1.1E+07						
No Vaccination																
No Vaccination										172000	188000	455000	452000	1770000	1490000	1.1E+07
No Vaccination			65600	63600	583000	406000	679000	1090000	3430000	3610000	2E+07					
No Vaccination						177000	285000	304000	568000	1300000	1390000	3000000	2.9E+07			
No Vaccination		168000	415000	425000	2470000	2370000	2320000	5460000	2.1E+07	2.1E+07	158000	4630000	4.2E+07			
Naïve																
Naïve																
Naïve																
Naïve																
Naïve																
Naïve																

Table S1. Vaccination Data (continued 3).

Vaccine Group	Spleen CD4+ T cells			Spleen CD8+ T cells		
	$CD4^+$ T cells	$CD4^+$ IFN-γ^+ cells	CD4+ TNF-α+ T cells	$CD8^+$ T cells	$CD8^+$ IFN-γ^+ T cells	$CD8^+$ TNF-α T cells
BCG	1733000	10918	9012	645576	2324	2776
BCG	3664264	3188	5130	1417721	2552	4111
BCG	1419346	10503	1845	695040	4865	904
BCG	2955501	11526	10049	1059197	2436	3601
BCG	7271703	83625	53811	2534235	7096	11657
BCG	1769083	11322	7430	1018738	2343	4381
BCG	3748574	26990	19493	1411101	5362	8043
BCG	4054932	47848	9326	1755120	10882	5792
BCG	3520861	12675	7746	1835520	2203	3487
BCG	4155386	6233	3449	1535300	1305	3531
ER + R_4Pam_2Cys	2350100	30786	13161	1167613	4320	4904
ER + R_4Pam_2Cys	2852859	6562	11126	1325614	3844	3977
ER + R_4Pam_2Cys	1745692	4364	2968	768104	1690	3380
ER + R_4Pam_2Cys	1837007	11206	2756	490860	2307	1669
ER + R_4Pam_2Cys	2738593	4656	4656	1373589	1304	5357
ER + R_4Pam_2Cys	3430134	13378	12005	1612060	4997	5642
ER + R_4Pam_2Cys	3714119	4828	2154	1701843	1872	4595
ER + R_4Pam_2Cys	5017868	43154	7527	2305299	10143	3227
ER + R_4Pam_2Cys	2688199	3495	3226	1146379	2178	2637
ER + R_4Pam_2Cys	3098113	7435	3408	1329721	2792	3324
ER alone	80458	274	153	24081	79	51
ER alone	7173145	52364	27258	2986683	15829	11051
ER alone	4207771	35766	20197	1803331	12623	5590
ER alone	1773807	4612	1951	879876	2200	4575
ER alone	3622914	14129	3043	1298590	5064	390
ER alone	0	0	0	0	0	0
ER alone	2463510	4434	2710	965526	927	3283
ER alone	2848212	7975	4557	787006	1574	2361
ER alone	1893759	4166	2462	778638	934	2336
ER alone	3514622	5975	4218	1343975	2285	2688
R_4Pam_2Cys	4062107	8937	6499	1768765	8313	3714
R_4Pam_2Cys	2455970	14245	7122	1161143	3019	10218
R_4Pam_2Cys	4691140	33776	15481	1756433	14227	6148
R_4Pam_2Cys	1732540	5717	1559	305057	1190	397
R_4Pam_2Cys	3467088	4507	3363	1529905	3825	1683
R_4Pam_2Cys	4236970	5084	7203	1782020	2317	6415
R_4Pam_2Cys	14084908	29578	30987	6292808	9439	25801
R_4Pam_2Cys	2991369	7179	52050	1611171	8056	12889
R_4Pam_2Cys	3073699	5840	3688	1429082	3716	4001
R_4Pam_2Cys	0	0	0	0	0	0
No Vaccination	7193546	76971	10071	2866601	33539	1777
No Vaccination	5121907	17414	9219	2517694	8308	5287
No Vaccination	3655275	33263	13525	1636230	13090	6054
No Vaccination	0	0	0	0	0	0
No Vaccination	6401868	49935	16005	3678164	27586	12874
No Vaccination	3735004	5229	3399	1648935	1566	3133
No Vaccination	4162893	12905	7493	2101083	5253	6303
No Vaccination	3646443	7293	5105	2314962	5556	3472
No Vaccination	0	0	0	0	0	0
No Vaccination	6175745	59905	8028	2508054	21820	6019
Naïve	2576978	4123	9535	1349458	2969	3104
Naïve	1000435	1901	3802	428547	1029	3043
Naïve	1817382	3635	4725	809219	1618	2266
Naïve	2706659	5143	4601	864373	2074	3198
Naïve	2424267	3394	4364	1013336	1216	3851
Naïve	777761	1400	933	372332	410	968

Table S1. Vaccination Data (continued 4).

Vaccine Group	Spleen cytokines										
	IL-2	IL-4	IL-6	IL-10	IL-12	IL-17A	IFN-γ	MCP-1	MIP-1α	MIP-1β	TNF
BCG	4.27	1.72	252.19	709.2	0	83.98	3.24	735.92	1023.79	1612.53	205.65
BCG	5.26	0	290.43	343.1	0	16.01	8.45	326.91	1267.67	2533.21	184.27
BCG	4.67	3.25	241.14	382.69	0	94.51	21.6	696.05	959.98	1951.99	773.74
BCG	5.49	0	262.31	413.93	0	53.17	4.52	226.46	1064.65	1948.68	208.02
BCG	3.9	0.04	1342.28	348.43	0	8.07	9.47	300.37	1047.64	1944.55	316.46
BCG	5.88	0	458.1	414.54	0	31.78	2.45	1002.61	928.32	1650	298.85
BCG	5.31	0.04	341.03	340.73	0	36.22	7.68	486.72	876.27	1687.003437	211.11
BCG	6.94	0.9	350.29	289.31	0	10.37	8.72	475.11	890.65	1446.796657	291.26
BCG	5.5	1.5	467.5	326.55	0	12.33	5.5	831.18	791.97	1383.642194	324.45
BCG	10.62	2.15	380.22	434.8	0	106.32	35.59	613.51	981.47	1716.966771	245.58
ER + R_4Pam_2Cys	8.71	2.67	300.5	404.59	0	131.39	16.87	463.25	628.08	1070.93	292.52
ER + R_4Pam_2Cys	8.35	2.36	392.95	703.71	0	697.2	110.78	387.79	966.46	1915.89	226.43
ER + R_4Pam_2Cys	8.17	0	192.07	660.98	0	199.86	65.79	147.53	667.96	1200.72	124.18
ER + R_4Pam_2Cys	3.82	0	1337.84	426.27	0	582.42	136.5	1822.99	1143.54	2437.54	981.83
ER + R_4Pam_2Cys	5.46	3.25	458.01	883.26	0	552.04	333.45	519.7	891.33	1694.09	280.2
ER + R_4Pam_2Cys	6.52	1.61	490.37	488.53	0	34.78	15.13	925.12	764.99	1579.92	412.2
ER + R_4Pam_2Cys	4.83	1.72	251.85	279.7	0	165.32	52.88	98.76	756.35	1182.19	124.63
ER + R_4Pam_2Cys	5.01	0	1150.41	292.98	0	737.08	336.48	969.57	936.12	1755.6	1665.85
ER + R_4Pam_2Cys	10.77	0.04	176.73	255.64	0	139.98	24.48	305.74	756.75	1491.22	194.8
ER + R_4Pam_2Cys	4.37	0.21	361.65	612.32	0	430.29	73.07	334.16	753.76	1387.07	148.64
ER alone	5.56	0	776.25	373.89	0	284.22	138.93	466.44	981.1	1687.92	738.7
ER alone	3.67	1.83	2581.14	818.7	0	886.7	907.08	1853.82	860.31	1655.53	1168.65
ER alone	3.94	3.35	1129.72	1100.04	0	578.57	1243.95	386.28	1240.81	2331.12	497.91
ER alone	9.97	0.9	269.65	499.91	0	41.92	12.32	717.6	578.11	868.08	331.96
ER alone	3.69	1.72	487.15	309.2	0	56.6	325.27	324.63	876.5	1584.54	320.32
ER alone	3.95	1.94	424.33	650.76	0	540.26	76.38	362.26	911.86	1918.33	157.28
ER alone	9.9	0	183.37	291.65	0	38.27	26.94	318	779.42	1440.23	218.75
ER alone	13.63	1.83	173.71	488.83	0	37.9	123.01	321.43	612.13	1079.7	235.61
ER alone	7.05	0	377.03	305.98	0	50.32	56.15	929	584.91	1001.3	289.74
ER alone	7.13	2.05	239.03	476.87	0	127.38	45.43	542.26	880.75	1807.34	350.77
R_4Pam_2Cys	1.55	1.39	697.9	405.49	0	9.62	53.46	970.4	712.31	1170.16	448.74
R_4Pam_2Cys	5.57	0.77	356.29	443.91	0	25.49	9.21	430.94	1049.95	2157.06	266
R_4Pam_2Cys	2.98	1.61	1153.04	632.61	0	478.87	1060.21	562.51	831.18	1147.42	550.63
R_4Pam_2Cys	3.88	0	560.6	223.37	0	38.65	19.13	394.63	960.67	1710.82	1085.19
R_4Pam_2Cys	3.39	0	564.46	364.55	0	146.01	194.26	421.87	1327.28	3049.33	1047.61
R_4Pam_2Cys	11.61	3.53	169.82	309.79	0	47.91	17.67	250.93	866.49	1342.62	175.21
R_4Pam_2Cys	4.4	0	218.78	270.11	0	21.28	4.86	346.96	888.39	1681.36	156.6
R_4Pam_2Cys	3.11	0.77	1996.82	721.17	0	970.52	509.16	1664.57	782.7	1457.02	891.94
R_4Pam_2Cys	9.48	0	196.69	402.49	0	12.33	7.44	264.87	753.36	1228.09	198.33
R_4Pam_2Cys	9.7	0.9	200.03	451.82	0	12.09	7.86	278.99	695.98	1151.18	198.56
No Vaccination	3.55	2.46	2440.05	388.08	0	822.04	464.45	1517.71	903.61	1903.75	633.08
No Vaccination	3.62	0	1137.17	546.66	0	396.72	250.82	954.93	1348.07	3107.64	1312.51
No Vaccination	3.04	1.15	1768.28	436.32	0	237.92	523.67	1068.7	985.61	1895.71	835.12
No Vaccination	3.95	4.27	2827.19	428.44	0	949.33	538.11	1590.15	904.75	2011.84	708.29
No Vaccination	1.37	0.64	1001.25	538.3	0	177.07	681.74	231.71	744.02	1244.82	399.66
No Vaccination	5.52	0	204.85	416.95	0	34.24	10.82	315.93	1204.37	2051.69	196.44
No Vaccination	4.96	0	572.54	426.92	0	6.19	5.12	925.55	1081.09	2573.47	323.16
No Vaccination	4.6	0	192.25	347.16	0	30.84	49.01	207.43	1241.87	2606.27	518.52
No Vaccination	2.53	0	1441.21	245.83	0	235.98	251.58	591.9	907.96	1771.92	731.73
No Vaccination	2.83	0.5	1238.52	238.35	0	188.79	224.66	596.59	876.05	1790.67	625.32
Naïve	4.66	0	188.84	332.16	0	23.67	13.12	254.94	875.16	1611.18	144.12
Naïve	2.7	0	384.17	397.68	0	43.41	1.71	689.49	759.56	1733.62	297.07
Naïve	5.36	0.36	190.13	358.23	0	14.23	2.58	401.58	725.8	1146.01	274.95
Naïve	6.1	0	163.51	291.06	0	22.27	13.74	447.77	377.16	502.5	215.16
Naïve	9.16	0	203.29	236.33	0	14.14	4.79	476.77	429.67	548.64	178.92
Naïve	6.14	2.96	317.38	376.71	0	32.29	14.22	849.49	472.76	711.35	276.2

Table S1. Vaccination Data (continued 5).

Vaccine Group	Draining lymph node cytokines										
	IL-2	IL-4	IL-6	IL-10	IL-12	IL-17A	IFN-γ	MCP-1	MIP-1α	MIP-1β	TNF
BCG	5.21	0	883.07	60.54	0	20.13	729.32	12.35	1794.69	2251.9	126.85
BCG	2.87	0	792.66	46.53	0	6.5	392.33	0	2070.52	2092.42	110.48
BCG	2.35	0	79.04	46.79	0	166.91	497.55	9.73	1007.29	2300.06	155.69
BCG	4.04	0	61.59	31.48	0	3.1	6.81	18.66	1145.53	1253.02	22.04
BCG	8.52	0	728.43	26.63	0	2.36	3.41	0	2093.43	1754.87	39.53
BCG	5.26	0	124.64	48.63	0	15.39	37.28	0	1362.07	2459.089885	40.77
BCG	6.96	0.36	231.62	52.05	0	1.61	76.87	0	1378.24	2768.707247	46.77
BCG	5.23	0	401.69	56.82	0	33.94	192.9	9.73	1457.41	2898.270809	51.56
BCG	8.21	0	406.55	34.56	0	5.88	198.09	0	1319.71	3479.423883	70.51
BCG	5.5	2.15	48.55	10.02	0	1.78	6.33	9.73	1575.12	1507.399166	25.86
ER + R_4Pam_2Cys	17.91	3.25	24.78	19.34	0	21.96	48.13	0	1847.62	1277.96	17.66
ER + R_4Pam_2Cys	25.03	0	26.55	33.27	0	57.25	114.23	0	1207.23	1344.28	16.47
ER + R_4Pam_2Cys	13.96	0.64	3.28	4.41	0	11.96	3.38	12.35	1574.06	491.68	6.26
ER + R_4Pam_2Cys	9.66	0	9.32	0.75	0	10.06	4.36	92.17	1540	714.29	22.65
ER + R_4Pam_2Cys	15.05	2.05	20.67	16.37	0	11.92	11.95	11.1	1791.53	1293.81	10.43
ER + R_4Pam_2Cys	0	0.64	0	0	0	0	0	0	24.81	13.61	0
ER + R_4Pam_2Cys	33.06	0.04	60.22	29.94	0	17.34	202.59	0	905.67	1882.91	33.78
ER + R_4Pam_2Cys	2.48	0	5.8	0.96	0	1.06	6.05	0	853.07	312.44	15
ER + R_4Pam_2Cys	31.05	2.15	71.09	51.26	0	60.11	323.12	0	932.05	1457.02	47.18
ER + R_4Pam_2Cys	37.33	0	36.12	24.35	0	40.27	57.19	17.71	1009.78	1674.34	24.05
ER alone	14.44	0	3.74	0	0	1.38	19.57	713.97	1419.89	2246.92	4.49
ER alone	9.81	5.56	37.82	38.7	0	17.96	93.49	0	1329.89	1591.15	31.74
ER alone	5.11	1.61	79.61	26.63	0	89.28	14.64	0	1621.87	1333.25	14.31
ER alone	5.04	0	12.69	3.64	0	0.59	7.57	11.1	1189.3	385.29	11.78
ER alone	0.81	0	3.38	3.9	0	2.36	51.01	12.35	537.55	276.42	5.7
ER alone	39.49	0.04	37.82	32.25	0	43.06	59.32	8.18	900.87	1566.16	27.68
ER alone	10.91	0	30.63	10.02	0	3.57	12.02	0	809.5	739.46	15.68
ER alone	0.58	0	0	0	0	0	0	0	157.03	52.61	1.87
ER alone	12.47	0	28.33	12.69	0	2.4	26.87	8.18	1416.56	1208.12	26.06
ER alone	3.29	0.04	8.3	0	0	0.98	0.93	0	614.71	142.4	8.9
R_4Pam_2Cys	2.15	0	6.52	4.16	0	1.99	13.97	0	989.04	453.5	9.09
R_4Pam_2Cys	8.64	0	51.64	32.25	0	1.22	7.54	0	1575.84	3216.22	23.04
R_4Pam_2Cys	0.94	0	2.87	0	0	1.09	1.26	0	1113.75	381.14	9.09
R_4Pam_2Cys	8.54	0	48.03	8.63	0	0	3.4	0	1821.86	1525.96	52.4
R_4Pam_2Cys	1.79	0	8.79	2.16	0	2.76	11.31	0	1516.25	547.41	14.25
R_4Pam_2Cys	4.18	0	5.81	5.16	0	0	0.7	12.35	1616.79	487.17	5.52
R_4Pam_2Cys	10.53	0	13.16	12.93	0	1.07	9.26	9.73	1864.33	1051.03	5.52
R_4Pam_2Cys	1.72	0	15.61	10.26	0	22.61	46.91	0	1626.61	707.59	16.08
R_4Pam_2Cys	0.78	0	1.05	0	0	0.1	0.06	3.57	524.02	138.69	0.97
R_4Pam_2Cys	0.73	0	0.34	5.4	0	0.49	0.1	0	551.32	140.33	1.33
No Vaccination	3.92	0	9.67	1.98	0	0.31	0.25	6.33	1120.48	354.65	10.82
No Vaccination	0	0	4.99	0	0	0	1.61	0	447.53	146.16	0
No Vaccination	1.64	0.9	33.78	10.74	0	5.72	47.46	0	1312.35	332.33	12.17
No Vaccination	4.25	0	9.72	1.29	0	0.66	0.22	14.64	1275.43	1667.34	10.24
No Vaccination	1.42	2.15	128.64	18.35	0	113.51	19.77	19.59	1500.25	1332.16	21.04
No Vaccination	5.03	1.39	10.93	8.56	0	0.02	1.85	0	1863.92	504.6	7.01
No Vaccination	2.05	0	3.02	2.85	0	0	0	0	684.74	183.21	6.82
No Vaccination	7.19	0	63.61	49.58	0	24.79	387.42	0	2412.08	5375.12	62.61
No Vaccination	0.94	0	8.7	8.08	0	0	0	20.5	1537.14	441.37	4.78
No Vaccination	1.28	0	7.68	7.11	0	0	0.32	22.24	1357.03	404.71	1.87
Naïve	4.37	0	19.38	9.53	0	0	2.1	9.73	937.68	496.86	10.62
Naïve	0	0	3.79	1.29	0	0	0.14	0	367.42	82.71	8.71
Naïve	1.02	0	3.23	3.38	0	0	0	16.72	172.17	59.42	5.33
Naïve	7.55	2.15	11.93	4.41	0	0.41	4.68	12.35	1202.08	574.43	14.9
Naïve	5.44	0.64	17	8.32	0	0.51	0.93	0	1091.36	1050.6	12.95
Naïve	7.98	0	22.97	10.5	0	1.4	9.93	0	1060.25	723.35	13.72

Table S2. Summary of group-specific univariate logistic regression coefficients.

	BCG		ER-P2Cys		ER-only		P2Cys-only		No vaccine	
Immune feature	LR Coeff	LR *p* value	LR Coeff	LR *p* value	LR Coeff	LR *p* value	LR Coeff	LR *p* value	LR Coeff	LR *p* value
IFNγ spleen	-0.970334	5.18107E-05								
IL-17A spleen	-0.6581086	0.008910258	0.527210872	0.038671909						
IFNγ LN	0.71026919	0.002068383							-0.485159411	0.040614066
IL-10 LN	0.92850964	9.35692E-06								
MIP-1b LN	0.93515547	0.000107064								
TNFα LN	1.07063887	2.14102E-06								
IL-6 LN	1.1727529	8.90177E-08					-0.500637492	0.043264091		
α-ER Ab			0.742637202	0.000579998	0.820818242	0.000112331	-0.650347172	0.003006284	-0.61238649	0.005461893
IL-2 LN			0.717051905	0.00301907					-0.58712933	0.016836051
IL-4 LN			0.441270194	0.031378683			-0.442894015	0.030729409		
α-Mu Ab					-0.55016423	0.017325056				
IL-2 spleen									-0.785568828	0.001501458
MIP-1b spleen									0.739183217	0.002999798
IL-6 spleen									0.658389303	0.008871559
MIP-1a spleen									0.531277708	0.03710721
TNFα spleen									0.514612636	0.043773074

4.5 Summary

In this chapter, vaccination with the ER+R_4Pam_2Cys formulation resulted in protection of 60% of mice from BU challenge. Although more of these vaccinated mice reached our defined disease outcome after 24 weeks compared to BCG-vaccinated mice, the difference was not statistically significant.

ER+R_4Pam_2Cys was significantly more protective than vaccination with R_4Pam_2Cys alone indicating that the inclusion of the ER protein was necessary to achieve any protective effects. This was further shown by vaccinating with ER alone. Though there were no significant differences in clinical outcomes when compared to ER+R_4Pam_2Cys vaccination, the inclusion of R_4Pam_2Cys delayed disease onset by ~8 weeks. This correlated with the induction of significantly more ER-specific antibodies after a primary and booster vaccination, compared to ER alone vaccination. Although the presence of ER-specific antibodies correlated to protection in this murine model of BU, the antibodies proved inadequate at providing complete protection against *M. ulcerans* challenge. This supports the results found in Chapter 3, alongside previous studies with mice (337) or sera of BU patients (128, 180), which suggest that strong BU antibodies alone cannot prevent BU disease.

The murine challenge model in this chapter, challenged mice with a significantly lower bacterial dose compared to other studies (14-20 CFU compared to 10^4-10^6 CFU) (275, 332-335, 337, 339-343) and enabled the measurement of bacterial growth in the same animal over time. Mice in this study also took longer to succumb to infection (seven weeks or more), particularly in comparison to Chapter 3. This longer infectious period enabled the exploration of the potential vaccine-induced correlates of BU infection. By utilising a Cox proportional hazards regression model, this chapter identified that the cytokines most associated with protection in BCG mice were different to those identified in ER+R_4Pam_2Cys vaccine mice. As BCG is a multi-antigen live-attenuated vaccine it is likely to utilise both common and distinct protective responses and mechanisms to those induced by the ER+R_4Pam_2Cys vaccine candidate. The immune correlates most associated with protection were the presence of IL-2 in the spleen and lymph nodes. The presence of systemic IL-6, TNF-α and IFN-γ (in the spleen) are more strongly associated with disease. Additionally, the localised but not systemic presence of these and other cytokines including IL17A, MIP-1β and IL-10 are strongly associated with protection. Although many factors associated with disease and protection have been identified, future studies should further explore these associations and determine their importance with respect to protection against infection. To confirm the correlates of protection induced by this vaccine, future experiments could utilise transgenic or knock-out mice, particularly mice lacking TLR-2 to confirm the vaccine's mode of action. Cytokines IL-2, IL17A, MIP-1β or IL-10 could also be depleted during *M. ulcerans* infection to measure the impact their absence has on bacterial control. As cytokines IL-6, TNF-

α and IFN-γ produced systemically were more greatly linked to disease, the effect of depleting these cytokines during *M. ulcerans* infection on the time to ulceration could also be measured.

In evaluating the efficacy of ER+R_4Pam_2Cys compared to BCG against BU in this study, results showed that protection can be mediated through different immune mechanisms. The mycolactone biosynthesis pathway forms a promising vaccine target to protect against BU. As *M. ulcerans* is slow-growing and requires its highly conserved cell wall-associated PKS for virulence (40, 41, 183, 417), the PKS domains could be an appealing target for antibodies. As such, future vaccine could incorporate a wider suite of PKS enzymatic domains to target the biosynthesis pathway.

Chapter 5

Conclusion

5.1 Introduction

This thesis explored vaccines against mycobacterial diseases TB and BU. There are numerous challenges in the pursuit of a successful mycobacterial vaccine. One of the major challenges is that the correlates of protection are not well defined, making it difficult to choose the most appropriate vaccine targets. BCG still remains the most effective vaccine against TB, however it provides variable protection against pulmonary tuberculosis in adults (268, 269) and does not provide long-lived protection against BU (274, 279, 418). This thesis explored experimental vaccines compared to the current BCG vaccine, attempting to assess immune correlates of protection against TB and BU.

5.2 Key findings and Implications

The main approach explored throughout this thesis was protein-subunit vaccination in conjunction with the lipopeptide adjuvant Pam_2Cys. Some of the findings mirror immune responses seen in previous vaccination studies for both mycobacterial diseases using murine infection models, which will be described further below. However, there were also new findings that broaden our understanding of correlates of protection, particularly against BU that will help shape future vaccine designs.

The TLR-agonist Pam_2Cys, can enhance protein-specific responses against MTB and MU

The vaccines tested in all three chapters induced significant protein-specific responses to ESAT-6 and Ag85B (Chapter 2), Hsp18 and MUL_3720 (Chapter 3), and the mycolactone PKS ER protein (Chapter 4) associated with Pam_2Cys. As identified in Chapters 3 and 4, protein-specific antibody responses were significantly higher with the addition of Pam_2Cys compared to vaccination with protein alone. However, *M. ulcerans* or MTB protein + Pam_2Cys produced only minor amounts of $CD4^+$ or $CD8^+$ protein-specific T cells. This suggested that Pam_2Cys is having an adjuvant-enhanced effect, however was not effective at increasing protein-specific $CD4^+$ and $CD8^+$ T cells.

Rather than significantly increasing total immune cell numbers, the adjuvant may instead be influencing the type of immune responses. This was seen by the differences in cytokine production between ESAT and Ag85B (Chapter 2), and ER (Chapter 4) vaccination with and without R_4Pam_2Cys. It was also evidenced by the increase in antibody responses to protein + Pam_2Cys with all vaccines trialled. Antibody production can be influenced by $CD4^+$ T-helper cells, as B cells often require two activation signals to induce antibody production (419); the first signal from the antigen binding to the B cell receptor and the second signal is usually provided by an activated helper T cell (420). T_h1, T_h2, T_h17 and follicular helper T cells have been implicated in aiding antibody production (421-423). There was no significant increase in Ag85B-specific (Chapter 2) or ER-specific (Chapter 4) $CD4^+$ T cells compared to protein alone vaccination. However, there was an overall increase in protein-specific

antibody titres for groups vaccinated with protein + Pam_2Cys compared to groups vaccinated with protein alone. This further implies that although T cell numbers did not significantly increase, the adjuvant might be influencing $CD4^+$ T cell responses to aid B cell activation and antibody production in this thesis. The antibody responses to MUL_3720 and Hsp18 vaccination (Chapter 3) were predominately subtype IgG1 with some $IgG2_a$ also present. This indicates refinement of the immune response due to protein exposure, as IgG1 subtypes are capable of binding proteins (414). This isotype switching would have been influenced by $CD4^+$ T-helper cells (419). Significantly higher protein-specific antibody titres were induced against ESAT-6 and Ag85B (Chapter 2), Hsp18 and MUL_3720 (Chapter 3), and ER (Chapter 4) proteins when given with the R_4Pam_2Cys adjuvant, compared to protein alone. This thesis supported previous findings, identifying these four proteins as being capable of generating strong antibody responses in mice (180, 335, 337, 362, 424, 425).

Vaccination with ER+R_4Pam_2Cys was found to generate significant amounts of IL-2 and IL-4 in the draining lymph nodes (DLN), and IL-17A in the spleen, and also induce protection compared to unvaccinated mice (Chapter 4), however there was no significant increase in $CD4^+$ or $CD8^+$ T cell numbers compared to protein alone vaccination. In this study, although there was no significant difference between the number of BU diseased mice between ER alone and ER+R_4Pam_2Cys vaccinated groups, the addition of R_4Pam_2Cys delayed the time it took mice to reach the luminescence threshold of BU (16 weeks or longer for ER+R_4Pam_2Cys, compared to between 7-13 weeks for ER alone groups) (Chapter 4). This suggests that the adjuvant was helping to shape the immune response to ER protein.

It's been previously shown in the context of viral infections that the TLR-2 agonist Pam_2Cys increases antibody responses, $CD8^+$ T cell responses, DC activation and antigen trafficking to lymph nodes (LN) (379, 386). The vaccines described in all three results chapters showed increases in antibody responses above protein-alone, and ESAT-6+R_4Pam_2Cys vaccination increased $CD8^+$ T cells but not $CD4^+$ T cells (Chapter 2). ER-specific responses were identified in the DLN of *M. ulcerans* infected mice, though ER-trafficking to LN was not specifically examined (Chapter 4). This thesis included the first evaluation of Pam_2Cys as an adjuvant to enhance protection against mycobacterial diseases. The results from this thesis show that although Pam_2Cys increased protein-specific responses to mycobacterial antigens, this lipopeptide adjuvant may be better suited for use in vaccines against viral infections rather than mycobacterial infections. Pam_2Cys has previously been shown to increase protection against viral infections such as influenza (379, 386) and hepatitis C (390, 391), and can protect against the secondary infection with *Streptococcus pneumoniae* in influenza-infected mice (392). Pam_2Cys is even capable of protecting against influenza when administered in the absence of pathogen-specific antigens (388, 389). However, from the results presented in this thesis (in particular Chapter 4) it appears that while Pam_2Cys enhances mycobacterial protein immunogenicity, it is not wholly protective (Chapter 4).

High protein-specific antibody titres were identified in all three results chapters. These antibody responses did not correlate with protection against MUL_3720 and Hsp18 in Chapter 3, however they did correlate to protection with ER+R_4Pam_2Cys vaccination (Chapter 4). This difference in results may be due to antigen selection or due to the low-dose BU challenge model, both discussed further below. Previous research has shown MTB-specific antibodies can play a role in protection during latent infection (174, 409), but there is limited data to suggest that antibodies against *M. ulcerans* play a role in controlling infection (104, 128, 337). Antibodies against mycolactone can be used to control *M. ulcerans* infection in mice (208). T_h1 responses do not completely protect against TB or BU (129, 275, 426, 427), so there may be a supporting role for antibodies against these diseases. MTB antibodies may be effective during the pathogen's extracellular phase(s). Antibodies against the mycolactone PKS enzymes may promote early opsonisation of *M. ulcerans*, disabling mycolactone biosynthesis, permitting the host to clear the infection early.

Significance of the animal model used to assess vaccine efficacy

This thesis employed two mouse models of *M. ulcerans* infection. In Chapter 3, vaccine efficacy was tested against a high-dose model (infectious dose of $1x10^4$ CFU) compared to Chapter 4, whereby vaccine efficacy was tested in a low-dose model (infectious dose of 14-20 CFU).

In Chapter 3, upon challenge with *M. ulcerans* all C57BL/6 and BALB/c mice developed ulcers by day 40 post-infection. No significant difference was observed in the proportion of time-to-onset of ulceration between groups vaccinated with BCG compared to protein and adjuvant vaccination. Previously the BCG vaccine has been found to be capable of preventing the onset of BU by between 6-8 weeks compared to naïve mice (279), which is approximately equal to the delay of BU onset in Chapter 3. Though there was no association between vaccine-induced antibody responses and protection, the true efficacy of the antibody response in this study was difficult to measure in the animal model utilised in Chapter 3. All mice in the study succumbed to infection in a very short amount of time (40 days) whereas in humans, it takes significantly longer (around 4.8 months) for ulcers to develop (415). This aggressive model of BU infection makes it difficult to assess the impact of vaccines and reinforces the need to utilise animal models that best emulate the natural history of the disease in the target host of the vaccine.

Subsequent to the research described in Chapter 4, a new murine model of BU was developed (101). As discussed in Chapter 4, previous models used much higher bacterial challenge doses (generally between 10^4-10^6 CFU) (331), which did not reflect bacterial loads identified in environmental samples and the newly identified ID_{50} of 3 CFU (101). The challenge model utilized in Chapter 4 was the first vaccination study to utilise a low-dose challenge in a murine model of BU. In this model, the BCG vaccine was capable of delaying BU, however was not fully capable of preventing the onset of BU in

three out of ten mice. This provides validity to the model, as BCG doesn't provide complete protection against BU in in other mouse models and humans (274-279). In this model, BU infection was only monitored for 24 weeks, therefore it cannot be deduced whether the remaining BCG vaccinated mice were protected or whether the onset of disease was just delayed. In this low-dose BU challenge model almost 90% of unvaccinated mice succumbed to BU in the 24-week monitoring period.

The role of antigen selection in vaccine immunogenicity.

The choice of vaccination antigen is a major consideration for subunit vaccine design. Unlike whole-cell vaccines, subunit vaccines focus on a specific pathogen-associated molecule and induce a restricted range of immune responses (428). As subunit vaccines are more specific, one potential benefit of this approach is that they induce less side-effects compared to whole cell vaccination (428). This thesis chose known immunogenic proteins, ESAT-6, Ag85B, Hsp18, MUL_3720 and ER as they have been proven to be immunogenic in humans (180, 295, 370, 376, 424, 429, 430). These antigens may require an effective adjuvant to shape the immune response, as vaccination with these proteins alone does not control MTB or *M. ulcerans*.

In Chapter 2, the addition of Pam_2Cys adjuvant did not significantly increase $CD4^+$ or $CD8^+$ T cells against Ag85B and only slightly increased $CD8^+$ T cells against ESAT-6 antigen. These two proteins are well described MTB immunogens in animal models (362, 363, 371, 374, 375) and humans (295, 370, 424, 429, 430), therefore it was unsurprising that they generated strong cell-mediated responses on their own. MUL_3720 and Hsp18 have been previously used in vaccinations and shown to induce strong antibody responses in mice with alternative adjuvants (GLA-SE and viral replicon particles). Similar to the results in Chapter 3, these previous studies found that antibodies against MUL_3720 and Hsp18 did not control disease. ER+R_4Pam_2Cys vaccination in Chapter 4 could significantly protect against BU, and there was no significant difference between the addition of the adjuvant and ER alone vaccination. This suggests that ER may be a better vaccine target than Hsp18 and MUL_3720, though all three proteins are cell wall-associated (356, 376, 417). The reasons for the enhanced suitability of ER as an *M. ulcerans*-vaccine antigen will be discussed further below. Recent vaccines against TB have combined antigens and shown increased immunogenicity to these protein combinations (287, 290, 292-295, 297, 299, 341, 365, 375, 431, 432). Future mycobacterial vaccines could incorporate more than one antigen, as it is unlikely that just one antigen will produce a broad enough immune response to control TB or BU.

The mycolactone biosynthesis pathway is a promising vaccine target.

Both recombinant MUL_3720 or Hsp18-based vaccine candidates were capable of eliciting strong antibody production, however the two vaccines were unsuccessful at preventing or delaying the onset of BU. Two previous BU vaccine studies have incorporated MUL_3720 and Hsp18 into putative

vaccines (336, 337). These studies identified strong protein-specific antibody responses to both proteins, which also did not correlate with protection against *M. ulcerans* challenge (336, 337). This suggests that these two proteins may not be ideal antigens for a *M. ulcerans* vaccine, though they are recognised by the murine immune system. This highlights a key challenge of *M. ulcerans* vaccine development, as the immune responses essential for protection are unclear and it is unknown whether antibody responses are even required. Another challenge for BU vaccine development is overcoming the immunosuppressive and cytotoxic effects of the mycolactone toxin. Neutralising antibodies against mycolactone have shown potential as a therapeutic treatment for BU (208). Additionally, non-mycolactone producing strains of *M. ulcerans* do not cause BU (183), therefore targeting or obstructing the mycolactone production pathway could be key to protecting against BU. As previously mentioned, the mycolactone-producing PKS are cell wall-associated (417) and highly conserved enzyme complexes in *M. ulcerans* (40, 41). Consequently, the PKS make an attractive target for specific antibodies as the PKS are required by all virulent *M. ulcerans* and are accessible for opsonising or neutralising antibodies. If opsonising antibodies to *M. ulcerans* can be generated early in infection (433, 434), they may be capable of targeting *M. ulcerans* for destruction and simultaneously inactivating toxin synthesis.

Chapter 4 assessed an experimental *M. ulcerans* prime-boost vaccine in a low-dose murine tail model of BU infection and the ER+R_4Pam_2Cys vaccine displayed promising results. Survival analysis showed mice receiving ER+R_4Pam_2Cys or the BCG vaccine were equally well protected, with both groups faring significantly better than unvaccinated animals. This research highlights the power of vaccines as tools to investigate potential correlates of protection.

Machine learning approaches to develop statistical disease-prognostic models identified higher levels of IL-2 and low IFN-γ produced in the spleen best predicted control of infection. High levels of IL-2 have not previously been linked to protection, though this is perhaps not a surprising finding, as IL-2 is the main T-cell signalling cytokine for differentiation and expansion (435). Cox proportional hazards regression modelling revealed vaccine-specific profiles of protection. High titres of ER-specific IgG serum antibodies, IL-2 and IL-4 in the DLN were associated with protection induced by the experimental ER vaccine. Similar to TB, previous studies have linked IFN-γ with healing in *M. ulcerans* (129, 175, 176), however from this study a high level of splenic IFN-γ appeared to be a marker of disease and IFN-γ in the DLN was linked with protection. This study also found that high levels of splenic inflammatory cytokines were associated with disease progression, suggesting the need for effective vaccines to induce controlled inflammatory responses at the site of infection.

Immune correlates of protection differ between vaccine formulations.

Vaccination with ER+R_4Pam_2Cys and the BCG vaccine in a low-dose murine tail model of BU infection (Chapter 4), showed that mice vaccinated with both vaccines were equally well protected, with both treatment groups faring significantly better than unvaccinated animals. This enabled the vaccines to be used tools to investigate potential correlates of protection.

ER+R_4Pam_2Cys-induced protection was linked to IL-2, IL-4, ER-specific antibodies in the DLN and IL-17A in the spleen. BCG-induced protection was associated with IL-6, TNF-α, IFN-γ and IL-10 and low IL-17A and IFN-γ in the spleen. As both the ER+R_4Pam_2Cys and BCG vaccines provided protection with different immune responses, this study indicates there is likely to be more than one path for protection against BU. An effective BU vaccine might induce varied, tissue-specific immune profiles. Attempts to define correlates of protection will need to consider that responses are vaccine-specific. The impact of host genetic variations also needs to be considered, as human responses to TB and BU can vary by genetics (179, 436-438). Vaccines that induce a broad range of immune responses might be the most effective (221).

Mycobacterial vaccines using the TLR-2 agonist, Pam_2Cys, can induce IL-17 responses.

As shown in Chapter 2 and Chapter 4, ESAT-6, Ag85B and ER conjugated to R_4Pam_2Cys are all capable of inducing IL-17A compared to protein alone vaccination. ESAT-6 and Ag85B have been previously shown to induce IL-17 responses (431, 439, 440). The role of IL-17 in mycobacterial infections is somewhat complex. The lack of IL-17 increases susceptibility to TB in murine models (170, 441, 442), however T_h17 cells have been shown to increase TB pathogenesis (443, 444). In the low-dose BU challenge model (Chapter 4), although IL-17 was increased by ER-vaccination, it was not found to be significantly linked to protection by univariate logistic regression. The production of IL-17 may be finely tuned in mycobacterial diseases, whereby too much causes enhanced disease progression (443, 444). The role of IL-17 requires more study, as it is clear that T_h1 responses alone do not protect against TB or BU (129, 275, 426, 427). The vaccines from this study could be used to further elucidate the role of IL-17 in control of mycobacterial diseases.

Vaccination route induced different immune responses to the same vaccine formulation.

As depicted in Chapter 2, the administration of ESAT-6+R_4Pam_2Cys intranasally compared to subcutaneously generated different immune responses in mice lungs and spleens. Though both routes induced low numbers of $CD4^+$ and $CD8^+$ T cells in the lungs, subcutaneous vaccination could induce higher $CD8^+$ T cells in the spleen compared to intranasal vaccination. When measuring vaccine-induced cytokine it appeared that intranasal vaccination was the most effective at inducing cytokine responses. Cytokine production was much higher in the lungs than the spleen. ESAT-6+R_4Pam_2Cys could only induce very minor splenic responses via intranasal or subcutaneous vaccination. Other studies have

identified an improvement to BCG vaccination when administering the vaccine through alternative routes, such as intranasally and intravenously (270, 445, 446). A recent study measuring the efficacy of intravenous BCG, found that it could protect against virulent MTB challenge in nine out of ten non-human primates (270). In addition to the findings from this study, these results suggest that not only is vaccine formulation a key factor for vaccine-induced protection, but the route of administration plays an important role in generating vaccine immunity.

For TB, where the majority of primary infection occurs in the lungs, intranasal or intravenous vaccination may be the most effective route for protection. The vaccine should be capable of priming the lungs and cells associated with the respiratory system, as the efficacy and tolerability of dermal and subcutaneous vaccination can be impacted by many factors (e.g. depth and location of vaccination) (447). There are some barriers to the implementation of intranasal and intravenous vaccination. Although intranasal vaccine is much less invasive compared to dermal or intravenous vaccination, it's less favoured for use as it is difficult to deduce whether the full dose has been administered due the anatomical and physiological differences in nasal environment (448). Intravenous injection allows the vaccine to travel through the immune system much more easily, however it is more difficult to administer (449). This method is more expensive and labour intensive, as well as potentially distressing to some patients (449, 450), thus could be problematic in more rural communities and for children.

5.3 Limitations and Strengths

Animal models

Animals models are an essential tool to understand the development of infectious diseases and immune responses, but they may not fully emulate human infection with a particular pathogen. In the case of TB, laboratory mice do not naturally generate a latent MTB infection (451, 452). In the case of BU, animal ethics constrained experiments from continuing once the point of ulceration had been reached. Therefore, healing from BU could not be studied in the scope of this PhD. Mice and humans can also recognise different antigenic epitopes and therefore mount slightly different immune responses to the same antigens (453, 454). This difference may not be identified until pre-clinical trials of a vaccine successful in animal models begin in humans. Fortunately, mice are highly fecund, which enables the rapid generation of statistically significant numbers for studies. There are numerous genetically modified mouse models that can incorporate human-specific responses (455, 456), such as the HHD mouse model used in results Chapter 2.

One strength of this thesis is the utilisation of the novel low-dose challenge model for *M. ulcerans* infection. This thesis includes the first vaccine study to utilise this model, which reflects the likely natural bacterial load for infection and route of infection. This model has an incubation period similar

to humans (415) and therefore helps close the gap between animal model of infection and human infection. The use of this model also enhanced the study of immune correlates as there was a clearer divide between BU-protected and diseased mice. This provided more robust support for the association of immune responses with either clinical outcome.

Statistical modelling

The use of univariate logistic regression permitted simultaneous exploration of many experimental variables and modelling of immune responses that associated with BU vaccine protection or failure. Such models are limited by the input variables measured and here, the models were built retrospectively as a way to explore patterns in the immune response data. Future research could experimentally test vaccines based on specific model predictions of protection and then iterate the experiment with optimised vaccine formulations. This approach would have the dual benefit of improving vaccine efficacy and implicating specific immune responses in protection.

Availability of technology

The findings in this thesis were partially controlled by the available technology and assays. However, experimental design was refined as resources became available. A few examples are the availability of the IVIS to measure bacterial load and the use of dynamic light scattering (DLS) to measure the particle-size to extrapolate binding between protein and adjuvant complexes. For instance, the DLS improved sensitivity, requiring less protein and adjuvant for analysis and improved the method of identifying protein-adjuvant binding between Chapter 3 and Chapter 4. This may have future implications for identifying correlates of protection. As more complex and sensitive assays are developed and data analysis tools become more sophisticated, this may enable researchers to more sharply define protective immune responses.

5.4 Future Directions

Mycobacterial vaccine formulation

One suggestion arising from this thesis is that future BU vaccine approaches should focus on targeting the mycolactone biosynthesis pathway. As previously described, mycolactone is a major virulence determinant for *M. ulcerans* and the PKS responsible for its biosynthesis are highly conserved (40, 41) and recognised by the immune system (180). Similarly, for TB, future vaccines could target more conserved proteins or proteins more highly expressed during latency to remove the bacteria when they are least active. Some putative TB vaccine studies are already moving in this direction (297, 457, 458). New combinations of adjuvants should also be studied. Although Pam_2Cys is capable of generating protein-specific responses against bacterial pathogens, its protective capabilities appear to be better suited against viral infections (388-391).

Understanding immune correlates of protection

One of the difficulties in identifying the protective immune response is the comparison of large data sets quantifying the different levels of immune cells, chemokines and cytokines present during vaccination and infection. As the immune system works together to protect its host during infection, small changes and different immunological parameters (and combinations of parameters) can make it difficult to identify the specific responses which promote protection. Future studies could focus on a wider suite of immune parameters, including innate immune responses, to produce a more complete picture of the host responses induced by vaccination or infection. This thesis incorporated the use of machine learning approaches to help clarify those immune responses most associated with protection or disease. In future, as this approach becomes more refined, it could be a useful tool to refine rational vaccine design.

4.5 Conclusions

This thesis highlights some of the challenges of designing protein subunit vaccines against two mycobacterial pathogens. Without knowing possible correlates of protection, the choice of immunogenic targets and adjuvants remains based on empiric testing. The vaccines built and tested in Chapters 2, 3 and 4 induced different immune responses however none showed better protection than BCG (Chapter 3 and 4, specifically). Targeting the mycolactone biosynthesis pathway has been discovered as a viable focus for vaccination. Also, as shown in all chapters, the addition of Pam_2Cys induced strong protein-specific antibody responses, with the caveat that strong antibody responses alone did not correlate with protection against BU. This thesis suggests that it is possible to build a vaccine that will induce protection against BU. Future studies will hopefully expand on the findings from this thesis to produce successful mycobacterial vaccines against TB and BU.

Bibliography

1. Ventura M, Canchaya C, Tauch A, Chandra G, Fitzgerald GF, Chater KF, van Sinderen D. 2007. Genomics of Actinobacteria: tracing the evolutionary history of an ancient phylum. Microbiol Mol Biol Rev 71:495-548.
2. Gupta RS, Lo B, Son J. 2018. Phylogenomics and Comparative Genomic Studies Robustly Support Division of the Genus *Mycobacterium* into an Emended Genus *Mycobacterium* and Four Novel Genera. Front Microbiol 9:67-67.
3. Tortoli E, Meehan CJ, Grottola A, Fregni Serpini G, Fabio A, Trovato A, Pecorari M, Cirillo DM. 2019. Genome-based taxonomic revision detects a number of synonymous taxa in the genus *Mycobacterium*. Infect Genet Evol 75:103983.
4. Barka EA, Vatsa P, Sanchez L, Gaveau-Vaillant N, Jacquard C, Meier-Kolthoff JP, Klenk HP, Clement C, Ouhdouch Y, van Wezel GP. 2016. Taxonomy, Physiology, and Natural Products of Actinobacteria. Microbiol Mol Biol Rev 80:1-43.
5. van der Meij A, Worsley SF, Hutchings MI, van Wezel GP. 2017. Chemical ecology of antibiotic production by actinomycetes. FEMS Microbiol Rev 41:392-416.
6. Berdy J. 2005. Bioactive microbial metabolites. J Antibiot 58:1-26.
7. Genilloud O. 2017. Actinomycetes: still a source of novel antibiotics. Nat Prod Rep 34:1203-1232.
8. Procopio RE, Silva IR, Martins MK, Azevedo JL, Araujo JM. 2012. Antibiotics produced by *Streptomyces*. Braz J Infect Dis 16:466-71.
9. Prasanna AN, Mehra S. 2013. Comparative phylogenomics of pathogenic and non-pathogenic mycobacterium. PLoS One 8:e71248.
10. Cosma CL, Sherman DR, Ramakrishnan L. 2003. The secret lives of the pathogenic mycobacteria. Annu Rev Microbiol 57:641-76.
11. Tortoli E, Fedrizzi T, Meehan CJ, Trovato A, Grottola A, Giacobazzi E, Serpini GF, Tagliazucchi S, Fabio A, Bettua C, Bertorelli R, Frascaro F, De Sanctis V, Pecorari M, Jousson O, Segata N, Cirillo DM. 2017. The new phylogeny of the genus *Mycobacterium*: The old and the news. Infect Genet Evol 56:19-25.
12. Stinear TP, Jenkin GA, Johnson PD, Davies JK. 2000. Comparative genetic analysis of *Mycobacterium ulcerans* and *Mycobacterium marinum* reveals evidence of recent divergence. J Bacteriol 182:6322-30.
13. Brown-Elliott BA, Simmer PJ, Trovato A, Hyle EP, Droz S, Buckwalter SP, Borroni E, Branda JA, Iana E, Mariottini A, Nelson J, Matteelli A, Toney NC, Scarparo C, de Man TJB, Vasireddy R, Gandhi RT, Wengenack NL, Cirillo DM, Wallace RJ, Tortoli E. 2018. *Mycobacterium decipiens* sp. nov., a new species closely related to the *Mycobacterium tuberculosis* complex. Int J Syst Evol Microbiol 68:3557-3562.

14. Sapriel G, Brosch R. 2019. Shared Pathogenomic Patterns Characterize a New Phylotype, Revealing Transition toward Host-Adaptation Long before Speciation of *Mycobacterium tuberculosis*. Genome Biol Evol 11:2420-2438.
15. Stinear TP, Seemann T, Harrison PF, Jenkin GA, Davies JK, Johnson PDR, Abdellah Z, Arrowsmith C, Chillingworth T, Churcher C, Clarke K, Cronin A, Davis P, Goodhead I, Holroyd N, Jagels K, Lord A, Moule S, Mungall K, Norbertczak H, Quail MA, Rabbinowitsch E, Walker D, White B, Whitehead S, Small PLC, Brosch R, Ramakrishnan L, Fischbach MA, Parkhill J, Cole ST. 2008. Insights from the complete genome sequence of *Mycobacterium marinum* on the evolution of *Mycobacterium tuberculosis*. Genome Res 18:729-741.
16. Gey van Pittius NC, Sampson SL, Lee H, Kim Y, van Helden PD, Warren RM. 2006. Evolution and expansion of the *Mycobacterium tuberculosis* PE and PPE multigene families and their association with the duplication of the ESAT-6 (esx) gene cluster regions. BMC Evol Biol 6:95.
17. World Health Organization. 2006. The Stop TB Strategy. https://www.who.int/tb/publications/2006/en/. Accessed 16 Jun 2019.
18. Zumla A, Mullan Z. 2006. Turning the tide against tuberculosis. Lancet 367:877-878.
19. World Health Organization. 2014. Global strategy and targets for tuberculosis prevention, care and control after 2015. *In* Resolution develop by the Exeutive Board, 134th Session, 67th World Health Assembly https://www.who.int/tb/post2015_strategy/en/. Accessed 28 December 2019.
20. World Health Organization. 2015. End TB Strategy. *In* WHO report on the proposed post-2015 TB Strategy and targets https://www.who.int/tb/post2015_strategy/en/. Accessed 28 December 2019.
21. Koch R. 1882. Die Atiologic der Tuberkulose. Berliner Klinische Wochenschrift 15:221-30.
22. Frothingham R, Hills HG, Wilson KH. 1994. Extensive DNA sequence conservation throughout the *Mycobacterium tuberculosis* complex. J Clin Microbiol 32:1639-43.
23. Brosch R, Gordon SV, Marmiesse M, Brodin P, Buchrieser C, Eiglmeier K, Garnier T, Gutierrez C, Hewinson G, Kremer K, Parsons LM, Pym AS, Samper S, van Soolingen D, Cole ST. 2002. A new evolutionary scenario for the *Mycobacterium tuberculosis* complex. Proc Natl Acad Sci USA 99:3684.
24. Proano-Perez F, Rigouts L, Brandt J, Dorny P, Ron J, Chavez MA, Rodriguez R, Fissette K, Van Aerde A, Portaels F, Benitez-Ortiz W. 2006. Preliminary observations on *Mycobacterium* spp. in dairy cattle in Ecuador. Am J Trop Med Hyg 75:318-23.
25. Clarke C, Van Helden P, Miller M, Parsons S. 2016. Animal-adapted members of the *Mycobacterium tuberculosis* complex endemic to the southern African subregion. J S Afr Vet Assoc 87:1322-1322.
26. Brites D, Loiseau C, Menardo F, Borrell S, Boniotti MB, Warren R, Dippenaar A, Parsons SDC, Beisel C, Behr MA, Fyfe JA, Coscolla M, Gagneux S. 2018. A New Phylogenetic

Framework for the Animal-Adapted *Mycobacterium tuberculosis* Complex. Front Microbiol 9:2820.

27. Durnez L, Eddyani M, Mgode GF, Katakweba A, Katholi CR, Machang'u RR, Kazwala RR, Portaels F, Leirs H. 2008. First detection of mycobacteria in African rodents and insectivores, using stratified pool screening. Appl Environ Microbiol 74:768-73.
28. Malone KM, Gordon SV. 2017. *Mycobacterium tuberculosis* Complex Members Adapted to Wild and Domestic Animals. Adv Exp Med Biol 1019:135-154.
29. Brodin P, Eiglmeier K, Marmiesse M, Billault A, Garnier T, Niemann S, Cole ST, Brosch R. 2002. Bacterial artificial chromosome-based comparative genomic analysis identifies *Mycobacterium microti* as a natural ESAT-6 deletion mutant. Infect Immun 70:5568-5578.
30. Delahay RJ, Cheeseman CL, Clifton-Hadley RS. 2001. Wildlife disease reservoirs: the epidemiology of *Mycobacterium bovis* infection in the European badger (Meles meles) and other British mammals. Tuberculosis 81:43-9.
31. Corner LA, O'Meara D, Costello E, Lesellier S, Gormley E. 2012. The distribution of *Mycobacterium bovis* infection in naturally infected badgers. Vet J 194:166-72.
32. Palmer MV, Thacker TC, Waters WR, Gortázar C, Corner LAL. 2012. *Mycobacterium bovis*: A Model Pathogen at the Interface of Livestock, Wildlife, and Humans. Vet Med Int 2012:236205-236205.
33. Cole ST, Brosch R, Parkhill J, Garnier T, Churcher C, Harris D, Gordon SV, Eiglmeier K, Gas S, Barry CE, 3rd, Tekaia F, Badcock K, Basham D, Brown D, Chillingworth T, Connor R, Davies R, Devlin K, Feltwell T, Gentles S, Hamlin N, Holroyd S, Hornsby T, Jagels K, Krogh A, McLean J, Moule S, Murphy L, Oliver K, Osborne J, Quail MA, Rajandream MA, Rogers J, Rutter S, Seeger K, Skelton J, Squares R, Squares S, Sulston JE, Taylor K, Whitehead S, Barrell BG. 1998. Deciphering the biology of *Mycobacterium tuberculosis* from the complete genome sequence. Nature 393:537-44.
34. Tønjum T, Welty DB, Jantzen E, Small PL. 1998. Differentiation of *Mycobacterium ulcerans*, *M. marinum*, and *M. haemophilum*: mapping of their relationships to *M. tuberculosis* by fatty acid profile analysis, DNA-DNA hybridization, and 16S rRNA gene sequence analysis. J Clin Microbiol 36:918-25.
35. Eddyani M, Portaels F. 2007. Survival of *Mycobacterium ulcerans* at 37°C. Clin Microbiol Infect 13:1033-1035.
36. Stinear TP, Seemann T, Pidot S, Frigui W, Reysset G, Garnier T, Meurice G, Simon D, Bouchier C, Ma L, Tichit M, Porter JL, Ryan J, Johnson PD, Davies JK, Jenkin GA, Small PL, Jones LM, Tekaia F, Laval F, Daffe M, Parkhill J, Cole ST. 2007. Reductive evolution and niche adaptation inferred from the genome of *Mycobacterium ulcerans*, the causative agent of Buruli ulcer. Genome Res 17:192-200.

37. Doig KD, Holt KE, Fyfe JA, Lavender CJ, Eddyani M, Portaels F, Yeboah-Manu D, Pluschke G, Seemann T, Stinear TP. 2012. On the origin of *Mycobacterium ulcerans*, the causative agent of Buruli ulcer. BMC Genomics 13:258.

38. Stinear TP, Hong H, Frigui W, Pryor MJ, Brosch R, Garnier T, Leadlay PF, Cole ST. 2005. Common evolutionary origin for the unstable virulence plasmid pMUM found in geographically diverse strains of *Mycobacterium ulcerans*. J Bacteriol 187:1668-76.

39. Stinear TP, Pryor MJ, Porter JL, Cole ST. 2005. Functional analysis and annotation of the virulence plasmid pMUM001 from *Mycobacterium ulcerans*. Microbiology 151:683-92.

40. Stinear TP, Mve-Obiang A, Small PL, Frigui W, Pryor MJ, Brosch R, Jenkin GA, Johnson PD, Davies JK, Lee RE, Adusumilli S, Garnier T, Haydock SF, Leadlay PF, Cole ST. 2004. Giant plasmid-encoded polyketide synthases produce the macrolide toxin of *Mycobacterium ulcerans*. Proc Natl Acad Sci USA 101:1345-9.

41. Yip MJ, Porter JL, Fyfe JA, Lavender CJ, Portaels F, Rhodes M, Kator H, Colorni A, Jenkin GA, Stinear T. 2007. Evolution of Mycobacterium ulcerans and other mycolactone-producing mycobacteria from a common *Mycobacterium marinum* progenitor. J Bacteriol 189:2021-9.

42. Kaser M, Hauser J, Small P, Pluschke G. 2009. Large sequence polymorphisms unveil the phylogenetic relationship of environmental and pathogenic mycobacteria related to *Mycobacterium ulcerans*. Appl Environ Microbiol 75:5667-75.

43. Rondini S, Kaser M, Stinear T, Tessier M, Mangold C, Dernick G, Naegeli M, Portaels F, Certa U, Pluschke G. 2007. Ongoing genome reduction in *Mycobacterium ulcerans*. Emerg Infect Dis 13:1008-15.

44. Mac CP, Tolhurst JC, et al. 1948. A new mycobacterial infection in man. J Pathol Bacteriol 60:93-122.

45. Alsop DG. 1972. The bairnsdale ulcer. Aust N Z J Surg 41:317-9.

46. Cook A. 1970. Mengo Hospital Notes, 1897, Makerere Medical School Library. Br Med J 2:378-79.

47. Clancey JK, Dodge OG, Lunn HF, Oduori ML. 1961. Mycobacterial skin ulcers in Uganda. Lancet 2:951-4.

48. Lunn HF, Connor DH, Wilks NE, Barnley GR, Kamunvi F, Clancey JK, Bee JD. 1965. Buruli (Mycobacterial) Ulceration in Uganda. (a New Focus of Buruli Ulcer in Madi District, Uganda): Report of a Field Study. East Afr Med J 42:275-88.

49. World Health Organization. 2004. Resolution WHA57.1 Surveillance and control of Mycobacterium ulcerans disease (Buruli ulcer), p 1-2. *In* 57th World Health Assembly, 17-22 May 2004. Resolutions and Decisions. Geneva, World Health Organization.

50. Woodring JH, Vandiviere HM, Fried AM, Dillon ML, Williams TD, Melvin IG. 1986. Update: the radiographic features of pulmonary tuberculosis. Am J Roentgen146:497-506.

51. Guarner J, Bartlett J, Whitney EA, Raghunathan PL, Stienstra Y, Asamoa K, Etuaful S, Klutse E, Quarshie E, van der Werf TS, van der Graaf WT, King CH, Ashford DA. 2003. Histopathologic features of *Mycobacterium ulcerans* infection. Emerg Infect Dis 9:651-656.
52. van der Werf TS, van der Graaf WT, Tappero JW, Asiedu K. 1999. *Mycobacterium ulcerans* infection. Lancet 354:1013-8.
53. O'Garra A, Redford PS, McNab FW, Bloom CI, Wilkinson RJ, Berry MP. 2013. The immune response in tuberculosis. Annu Rev Immunol 31:475-527.
54. Harisinghani MG, McLoud TC, Shepard JA, Ko JP, Shroff MM, Mueller PR. 2000. Tuberculosis from head to toe. Radiographics 20:449-70.
55. Perez-Velez CM, Marais BJ. 2012. Tuberculosis in Children. New Engl J of Med 367:348-361.
56. Leonard JM. 2017. Central Nervous System Tuberculosis. Microbiol Spectr 5 doi:10.1128/microbiolspec.TNMI7-0044-2017.
57. Kumar A, Farhana A, Guidry L, Saini V, Hondalus M, Steyn AJC. 2011. Redox homeostasis in mycobacteria: the key to tuberculosis control? Expert Rev Mol Med 13:e39.
58. World Health Organization. 2019. Global tuberculosis report 2019. World Health Organization, Geneva. Licence: CCBY-NC-S3.0IGO. Accessed 20 December 2019.
59. Vincent QB, Ardant MF, Adeye A, Goundote A, Saint-Andre JP, Cottin J, Kempf M, Agossadou D, Johnson C, Abel L, Marsollier L, Chauty A, Alcais A. 2014. Clinical epidemiology of laboratory-confirmed Buruli ulcer in Benin: a cohort study. Lancet Glob Health 2:e422-30.
60. Hayman J, McQueen A. 1985. The pathology of *Mycobacterium ulcerans* infection. Pathology 17:594-600.
61. Pszolla N, Sarkar MR, Strecker W, Kern P, Kinzl L, Meyers WM, Portaels F. 2003. Buruli ulcer: a systemic disease. Clin Infect Dis 37:e78-82.
62. Loftus MJ, Kettleton-Butler N, Wade D, Whitby RM, Johnson PD. 2018. A severe case of *Mycobacterium ulcerans* (Buruli ulcer) osteomyelitis requiring a below-knee amputation. Med J Aust 208:290-291.
63. Toll A, Gallardo F, Ferran M, Gilaberte M, Iglesias M, Gimeno JL, Rondini S, Pujol RM. 2005. Aggressive multifocal Buruli ulcer with associated osteomyelitis in an HIV-positive patient. Clin Exp Dermatol 30:649-51.
64. Yerramilli A, Tay EL, Stewardson AJ, Kelley PG, Bishop E, Jenkin GA, Starr M, Trevillyan J, Hughes A, Friedman ND, O'Brien DP, Johnson PDR. 2017. The location of Australian Buruli ulcer lesions—Implications for unravelling disease transmission. PLOS Negl Trop Dis 11:e0005800.
65. Vincent QB, Ardant MF, Marsollier L, Chauty A, Alcais A, Franco-Beninese Buruli Research G. 2014. HIV infection and Buruli ulcer in Africa. Lancet Infect Dis 14:796-7.

66. Wanda F, Nkemenang P, Ehounou G, Tchaton M, Comte E, Toutous Trellu L, Masouye I, Christinet V, O'Brien DP. 2014. Clinical features and management of a severe paradoxical reaction associated with combined treatment of Buruli ulcer and HIV co-infection. BMC Infect Dis 14:423.

67. Komenan K, Elidje EJ, Ildevert GP, Yao KI, Kanga K, Kouame KA, Abdoulaye S, Hamdam KS, Yao YP, Jean-Marie K. 2013. Multifocal Buruli Ulcer Associated with Secondary Infection in HIV Positive Patient. Case Rep Med 2013:348628.

68. Kibadi K, Colebunders R, Muyembe-Tamfum JJ, Meyers WM, Portaels F. 2010. Buruli ulcer lesions in HIV-positive patient. Emerg Infect Dis 16:738-9.

69. Johnson PD, Stinear T, Small PL, Pluschke G, Merritt RW, Portaels F, Huygen K, Hayman JA, Asiedu K. 2005. Buruli ulcer (*M. ulcerans* infection): new insights, new hope for disease control. PLoS Med 2:e108.

70. World Health Organization. 2018. Estimated TB incidence rates, 2017. *In* Global tuberculosis report 2018. Accessed 19 Jun 2019.

71. World Health Organization. 2019. World Health Organisation Map Production: Control of Neglected Tropical Diseases (NTD) http://gamapserver.who.int/mapLibrary/. Accessed 20 January 2020.

72. Oxlade O, Murray M. 2012. Tuberculosis and poverty: why are the poor at greater risk in India? PloS One 7:e47533-e47533.

73. Kwan CK, Ernst JD. 2011. HIV and Tuberculosis: a Deadly Human Syndemic. Clin Microbiol Rev 24:351.

74. Narasimhan P, Wood J, Macintyre CR, Mathai D. 2013. Risk factors for tuberculosis. Pulm Med 2013:828939-828939.

75. World Health Organization. 2015. Tuberculosis Fact Sheet No. 104, *on* World Health Organization http://www.who.int/mediacentre/factsheets/fs104/en/. Accessed 4 April 2019.

76. Manoff SB, Farzadegan H, Munoz A, Astemborski JA, Vlahov D, Rizzo RT, Solomon L, Graham NM. 1996. The effect of latent Mycobacterium tuberculosis infection on human immunodeficiency virus (HIV) disease progression and HIV RNA load among injecting drug users. J Infect Dis 174:299-308.

77. Bruchfeld J, Correia-Neves M, Källenius G. 2015. Tuberculosis and HIV Coinfection. Cold Spring Harbor perspectives in medicine 5:a017871-a017871.

78. O'Brien CR, McMillan E, Harris O, O'Brien DP, Lavender CJ, Globan M, Legione AR, Fyfe JA. 2011. Localised *Mycobacterium ulcerans* infection in four dogs. Aust Vet J 89:506-10.

79. Sakaguchi K, Iima H, Hirayama K, Okamoto M, Matsuda K, Miyasho T, Kasamatsu M, Hasegawa K, Taniyama H. 2011. *Mycobacterium ulcerans* infection in an Indian flap-shelled turtle (Lissemys punctata punctata). J Vet Med Sci 73:1217-20.

80. van Zyl A, Daniel J, Wayne J, McCowan C, Malik R, Jelfs P, Lavender CJ, Fyfe JA. 2010. *Mycobacterium ulcerans* infections in two horses in south-eastern Australia. Aust Vet J 88:101-6.

81. Elsner L, Wayne J, O'Brien CR, McCowan C, Malik R, Hayman JA, Globan M, Lavender CJ, Fyfe JA. 2008. Localised *Mycobacterium ulcerans* infection in a cat in Australia. J Feline Med Surg 10:407-12.

82. Fyfe JA, Lavender CJ, Handasyde KA, Legione AR, O'Brien CR, Stinear TP, Pidot SJ, Seemann T, Benbow ME, Wallace JR, McCowan C, Johnson PD. 2010. A major role for mammals in the ecology of *Mycobacterium ulcerans*. PLoS Negl Trop Dis 4:e791.

83. Mve-Obiang A, Lee RE, Umstot ES, Trott KA, Grammer TC, Parker JM, Ranger BS, Grainger R, Mahrous EA, Small PL. 2005. A newly discovered mycobacterial pathogen isolated from laboratory colonies of Xenopus species with lethal infections produces a novel form of mycolactone, the *Mycobacterium ulcerans* macrolide toxin. Infect Immun 73:3307-12.

84. Stragier P, Hermans K, Stinear T, Portaels F. 2008. First report of a mycolactone-producing *Mycobacterium infection* in fish agriculture in Belgium. FEMS Microbiol Lett 286:93-5.

85. Omansen TF, Erbowor-Becksen A, Yotsu R, van der Werf TS, Tiendrebeogo A, Grout L, Asiedu K. 2019. Global Epidemiology of Buruli Ulcer, 2010–2017, and Analysis of 2014 WHO Programmatic Targets. Emerg Infect Dis 25:2183-2190.

86. World Health Organization. 2019. Buruli ulcer - number of new reported cases. http://apps.who.int/gho/data/node.main.A1631. Accessed 29 January.

87. Johnson PDR. 2019. Buruli Ulcer in Australia, p 61-76. *In* Pluschke G, Röltgen K (ed), Buruli Ulcer: *Mycobacterium ulcerans* Disease doi:10.1007/978-3-030-11114-4_3. Springer International Publishing.

88. Department of Health and Human Services SGoV, Australia. 2020. Local Government areas surveillance report, *on* State Government of Victoria, Australia. https://www2.health.vic.gov.au/public-health/infectious-diseases/infectious-diseases-surveillance/interactive-infectious-disease-reports/local-government-areas-surveillance-report. Accessed January 20.

89. Ottenhoff TH, Kaufmann SH. 2012. Vaccines against tuberculosis: where are we and where do we need to go? PLoS Pathog 8:e1002607.

90. Meyers WM, Shelly WM, Connor DH, Meyers EK. 1974. Human *Mycobacterium ulcerans* infections developing at sites of trauma to skin. Am J Trop Med Hyg 23:919-23.

91. Merritt RW, Walker ED, Small PLC, Wallace JR, Johnson PDR, Benbow ME, Boakye DA. 2010. Ecology and Transmission of Buruli Ulcer Disease: A Systematic Review. PLoS Negl Trop Dis 4:e911.

92. Sakamoto K. 2012. The Pathology of *Mycobacterium tuberculosis* Infection. Vet Pathol 49:423-439.

93. Turner RD, Chiu C, Churchyard GJ, Esmail H, Lewinsohn DM, Gandhi NR, Fennelly KP. 2017. Tuberculosis Infectiousness and Host Susceptibility. J of Inf Dis 216:S636-S643.

94. O'Brien DP, Wynne JW, Buultjens AH, Michalski WP, Stinear TP, Friedman ND, Hughes A, Athan E. 2017. Exposure Risk for Infection and Lack of Human-to-Human Transmission of *Mycobacterium ulcerans* Disease, Australia. Emerg Infect Dis 23:837-840.

95. Stinear T, Ross BC, Davies JK, Marino L, Robins-Browne RM, Oppedisano F, Sievers A, Johnson PD. 1999. Identification and characterization of IS2404 and IS2606: two distinct repeated sequences for detection of *Mycobacterium ulcerans* by PCR. J Clin Microbiol 37:1018-23.

96. Marsollier L, Severin T, Aubry J, Merritt RW, Saint Andre JP, Legras P, Manceau AL, Chauty A, Carbonnelle B, Cole ST. 2004. Aquatic snails, passive hosts of *Mycobacterium ulcerans*. Appl Environ Microbiol 70:6296-8.

97. Marsollier L, Stinear T, Aubry J, Saint Andre JP, Robert R, Legras P, Manceau AL, Audrain C, Bourdon S, Kouakou H, Carbonnelle B. 2004. Aquatic plants stimulate the growth of and biofilm formation by *Mycobacterium ulcerans* in axenic culture and harbor these bacteria in the environment. Appl Environ Microbiol 70:1097-103.

98. Johnson PD, Azuolas J, Lavender CJ, Wishart E, Stinear TP, Hayman JA, Brown L, Jenkin GA, Fyfe JA. 2007. *Mycobacterium ulcerans* in mosquitoes captured during outbreak of Buruli ulcer, southeastern Australia. Emerg Infect Dis 13:1653-60.

99. Marsollier L, Robert R, Aubry J, Saint Andre JP, Kouakou H, Legras P, Manceau AL, Mahaza C, Carbonnelle B. 2002. Aquatic insects as a vector for *Mycobacterium ulcerans*. Appl Environ Microbiol 68:4623-8.

100. Eddyani M, Ofori-Adjei D, Teugels G, De Weirdt D, Boakye D, Meyers WM, Portaels F. 2004. Potential role for fish in transmission of *Mycobacterium ulcerans* disease (Buruli ulcer): an environmental study. Appl Environ Microbiol 70:5679-81.

101. Wallace JR, Mangas KM, Porter JL, Marcsisin R, Pidot SJ, Howden B, Omansen TF, Zeng W, Axford JK, Johnson PDR, Stinear TP. 2017. *Mycobacterium ulcerans* low infectious dose and mechanical transmission support insect bites and puncturing injuries in the spread of Buruli ulcer. PLoS Negl Trop Dis 11:e0005553.

102. Fraga AG, Barbosa AM, Ferreira CM, Fevereiro J, Pedrosa J, Torrado E. 2018. Immune-evasion Strategies of Mycobacteria and Their Implications for the Protective Immune Response. Curr Issues Mol Biol 25:169-198.

103. Cooper AM. 2009. Cell-mediated immune responses in tuberculosis. Annu Rev Immunol 27:393-422.

104. Fevereiro J, Fraga AG, Pedrosa J. 2019. The Immunology of Buruli Ulcer, p 135-158. *In* Pluschke G, Röltgen K (ed), Buruli Ulcer: *Mycobacterium ulcerans* Disease doi:10.1007/978-3-030-11114-4_8. Springer International Publishing.

105. Frankel A, Penrose C, Emer J. 2009. Cutaneous tuberculosis: a practical case report and review for the dermatologist. J Clin Aesthet Dermatol 2:19-27.

106. Verrall AJ, Netea MG, Alisjahbana B, Hill PC, van Crevel R. 2014. Early clearance of *Mycobacterium tuberculosis*: a new frontier in prevention. Immunology 141:506-513.

107. Acuña-Villaorduña C, Jones-López EC, Fregona G, Marques-Rodrigues P, Gaeddert M, Geadas C, Hadad DJ, White LF, Pereira Dutra Molina L, Vinhas S, Ribeiro-Rodrigues R, Salgame P, Palaci M, Alland D, Ellner JJ, Dietze R. 2018. Intensity of exposure to pulmonary tuberculosis determines risk of tuberculosis infection and disease. Eur Resp J 51:1701578.

108. Jones-López EC, Acuña-Villaorduña C, Fregona G, Marques-Rodrigues P, White LF, Hadad DJ, Dutra-Molina LP, Vinhas S, McIntosh AI, Gaeddert M, Ribeiro-Rodrigues R, Salgame P, Palaci M, Alland D, Ellner JJ, Dietze R. 2017. Incident *Mycobacterium tuberculosis* infection in household contacts of infectious tuberculosis patients in Brazil. BMC Infect Dis 17:576-576.

109. Reichler MR, Khan A, Sterling TR, Zhao H, Moran J, McAuley J, Bessler P, Mangura B, Tuberculosis Epidemiologic Studies Consortium Task Order T. 2018. Risk and Timing of Tuberculosis Among Close Contacts of Persons with Infectious Tuberculosis. J Infect Dis 218:1000-1008.

110. Sloot R, Schim van der Loeff MF, Kouw PM, Borgdorff MW. 2014. Risk of Tuberculosis after Recent Exposure. A 10-Year Follow-up Study of Contacts in Amsterdam. Am J Resp Crit Care Med 190:1044-1052.

111. Whalen CC, Zalwango S, Chiunda A, Malone L, Eisenach K, Joloba M, Boom WH, Mugerwa R. 2011. Secondary attack rate of tuberculosis in urban households in Kampala, Uganda. PloS one 6:e16137-e16137.

112. Ai J-W, Ruan Q-L, Liu Q-H, Zhang W-H. 2016. Updates on the risk factors for latent tuberculosis reactivation and their managements. Emerg Microbes Infect 5:e10-e10.

113. Erkens CGM, Slump E, Verhagen M, Schimmel H, Cobelens F, van den Hof S. 2016. Risk of developing tuberculosis disease among persons diagnosed with latent tuberculosis infection in the Netherlands. Eur Resp J 48:1420.

114. Cooper AM, Khader SA. 2008. The role of cytokines in the initiation, expansion, and control of cellular immunity to tuberculosis. Immunol Rev 226:191-204.

115. Cavalcanti YV, Brelaz MC, Neves JK, Ferraz JC, Pereira VR. 2012. Role of TNF-Alpha, IFN-Gamma, and IL-10 in the Development of Pulmonary Tuberculosis. Pulm Med 2012:745483.

116. Flynn JL, Chan J. 2003. Immune evasion by *Mycobacterium tuberculosis*: living with the enemy. Curr Opin Immunol 15:450-455.

117. Zhai W, Wu F, Zhang Y, Fu Y, Liu Z. 2019. The Immune Escape Mechanisms of *Mycobacterium tuberculosis*. Int J Mol Sci 20:340.

118. Pieters J. 2008. *Mycobacterium tuberculosis* and the Macrophage: Maintaining a Balance. Cell Host Microbe 3:399-407.

119. Jayachandran R, Sundaramurthy V, Combaluzier B, Mueller P, Korf H, Huygen K, Miyazaki T, Albrecht I, Massner J, Pieters J. 2007. Survival of Mycobacteria in Macrophages Is Mediated by Coronin 1-Dependent Activation of Calcineurin. Cell 130:37-50.

120. Pai M, Behr MA, Dowdy D, Dheda K, Divangahi M, Boehme CC, Ginsberg A, Swaminathan S, Spigelman M, Getahun H, Menzies D, Raviglione M. 2016. Tuberculosis. Nature Rev Dis Primers 2:16076.

121. Ramakrishnan L. 2012. Revisiting the role of the granuloma in tuberculosis. Nature Rev Immunol 12:352.

122. Phillips R, Horsfield C, Mangan J, Laing K, Etuaful S, Awuah P, Nyarko K, Osei-Sarpong F, Butcher P, Lucas S, Wansbrough-Jones M. 2006. Cytokine mRNA expression in *Mycobacterium ulcerans*-infected human skin and correlation with local inflammatory response. Infect Immun 74:2917-24.

123. Phillips R, Sarfo FS, Guenin-Macé L, Decalf J, Wansbrough-Jones M, Albert ML, Demangel C. 2009. Immunosuppressive signature of cutaneous *Mycobacterium ulcerans* infection in the peripheral blood of patients with buruli ulcer disease. J Infect Dis 200:1675-84.

124. Kiszewski AE, Becerril E, Aguilar LD, Kader IT, Myers W, Portaels F, Hernandez Pando R. 2006. The local immune response in ulcerative lesions of Buruli disease. Clin Exp Immunol 143:445-51.

125. Ortiz RH, Leon DA, Estevez HO, Martin A, Herrera JL, Romo LF, Portaels F, Pando RH. 2009. Differences in virulence and immune response induced in a murine model by isolates of *Mycobacterium ulcerans* from different geographic areas. Clin Exp Immunol 157:271-81.

126. Westenbrink BD, Stienstra Y, Huitema MG, Thompson WA, Klutse EO, Ampadu EO, Boezen HM, Limburg PC, van der Werf TS. 2005. Cytokine responses to stimulation of whole blood from patients with Buruli ulcer disease in Ghana. Clin Diagn Lab Immunol 12:125-9.

127. Fraga AG, Martins TG, Torrado E, Saraiva M, Pereira DR, Meyers WM, Portaels F, Silva MT, Castro AG, Pedrosa J, Pedrosa J. 2011. *Mycobacterium ulcerans* triggers T-cell immunity followed by local and regional but not systemic immunosuppression. Infect Immun 79:421-30.

128. Gooding TM, Johnson PD, Campbell DE, Hayman JA, Hartland EL, Kemp AS, Robins-Browne RM. 2001. Immune response to infection with *Mycobacterium ulcerans*. Infect Immun 69:1704-7.

129. Gooding TM, Johnson PD, Smith M, Kemp AS, Robins-Browne RM. 2002. Cytokine profiles of patients infected with *Mycobacterium ulcerans* and unaffected household contacts. Infect Immun 70:5562-7.

130. Gooding TM, Kemp AS, Robins-Browne RM, Smith M, Johnson PD. 2003. Acquired T-helper 1 lymphocyte anergy following infection with *Mycobacterium ulcerans*. Clin Infect Dis 36:1076-7.

131. Ogbechi J, Hall BS, Sbarrato T, Taunton J, Willis AE, Wek RC, Simmonds RE. 2018. Inhibition of Sec61-dependent translocation by mycolactone uncouples the integrated stress response from ER stress, driving cytotoxicity via translational activation of ATF4. Cell Death Dis 9:397.

132. Baron L, Paatero AO, Morel JD, Impens F, Guenin-Macé L, Saint-Auret S, Blanchard N, Dillmann R, Niang F, Pellegrini S, Taunton J, Paavilainen VO, Demangel C. 2016. Mycolactone subverts immunity by selectively blocking the Sec61 translocon. J Exp Med 213:2885-2896.

133. Boulkroun S, Guenin-Macé L, Thoulouze MI, Monot M, Merckx A, Langsley G, Bismuth G, Di Bartolo V, Demangel C. 2010. Mycolactone suppresses T cell responsiveness by altering both early signaling and posttranslational events. J Immunol 184:1436-44.

134. Connor DH, Lunn HF. 1965. *Mycobacterium ulcerans* infection (with comments on pathogenesis). Int J Lepr 33:Suppl:698-709.

135. Krieg RE, Hockmeyer WT, Connor DH. 1974. Toxin of *Mycobacterium ulcerans*: Production and Effects in Guinea Pig Skin. Arch Dermatol 110:783-788.

136. Read JK, Heggie CM, Meyers WM, Connor DH. 1974. Cytotoxic activity of *Mycobacterium ulcerans*. Infect Immun 9:1114-22.

137. Hockmeyer WT, Krieg RE, Reich M, Johnson RD. 1978. Further characterization of *Mycobacterium ulcerans* toxin. Infect Immun 21:124-128.

138. George KM, Chatterjee D, Gunawardana G, Welty D, Hayman J, Lee R, Small PL. 1999. Mycolactone: a polyketide toxin from *Mycobacterium ulcerans* required for virulence. Science 283:854-7.

139. Judd TC, Bischoff A, Kishi Y, Adusumilli S, Small PL. 2004. Structure determination of mycolactone C via total synthesis. Org Lett 6:4901-4.

140. Hong H, Spencer JB, Porter JL, Leadlay PF, Stinear T. 2005. A novel mycolactone from a clinical isolate of *Mycobacterium ulcerans* provides evidence for additional toxin heterogeneity as a result of specific changes in the modular polyketide synthase. Chembiochem 6:643-8.

141. Hong H, Stinear T, Porter J, Demangel C, Leadlay PF. 2007. A novel mycolactone toxin obtained by biosynthetic engineering. Chembiochem 8:2043-7.

142. Rohr J. 2000. A New Role for Polyketides. Angew Chem Int Ed Engl 39:2847-2849.

143. Keatinge-Clay AT. 2012. The structures of type I polyketide synthases. Nat Prod Rep 29:1050-1073.

144. Hong H, Stinear T, Skelton P, Spencer JB, Leadlay PF. 2005. Structure elucidation of a novel family of mycolactone toxins from the frog pathogen *Mycobacterium* sp. MU128FXT by mass spectrometry. Chem Commun doi:10.1039/b506835e:4306-8.

145. Spangenberg T, Kishi Y. 2010. Highly sensitive, operationally simple, cost/time effective detection of the mycolactones from the human pathogen *Mycobacterium ulcerans*. Chem Commun 46:1410-2.

146. Mve-Obiang A, Lee RE, Portaels F, Small PL. 2003. Heterogeneity of mycolactones produced by clinical isolates of Mycobacterium ulcerans: implications for virulence. Infect Immun 71:774-83.

147. Scherr N, Gersbach P, Dangy J-P, Bomio C, Li J, Altmann K-H, Pluschke G. 2013. Structure-activity relationship studies on the macrolide exotoxin mycolactone of *Mycobacterium ulcerans*. PLoS Negl Trop Dis 7:e2143-e2143.

148. Coutanceau E, Marsollier L, Brosch R, Perret E, Goossens P, Tanguy M, Cole ST, Small PL, Demangel C. 2005. Modulation of the host immune response by a transient intracellular stage of *Mycobacterium ulcerans*: the contribution of endogenous mycolactone toxin. Cell Microbiol 7:1187-96.

149. George KM, Pascopella L, Welty DM, Small PL. 2000. A *Mycobacterium ulcerans* toxin, mycolactone, causes apoptosis in guinea pig ulcers and tissue culture cells. Infect Immun 68:877-83.

150. Dobos KM, Small PL, Deslauriers M, Quinn FD, King CH. 2001. *Mycobacterium ulcerans* cytotoxicity in an adipose cell model. Infect Immun 69:7182-6.

151. Bozzo C, Tiberio R, Graziola F, Pertusi G, Valente G, Colombo E, Small PL, Leigheb G. 2010. A *Mycobacterium* ulcerans toxin, mycolactone, induces apoptosis in primary human keratinocytes and in HaCaT cells. Microbes Infect 12:1258-63.

152. George KM, Barker LP, Welty DM, Small PL. 1998. Partial purification and characterization of biological effects of a lipid toxin produced by *Mycobacterium ulcerans*. Infect Immun 66:587-93.

153. Coutanceau E, Decalf J, Martino A, Babon A, Winter N, Cole ST, Albert ML, Demangel C. 2007. Selective suppression of dendritic cell functions by *Mycobacterium ulcerans* toxin mycolactone. J Exp Med 204:1395-403.

154. Meier JL, Burkart MD. 2011. Proteomic analysis of polyketide and nonribosomal peptide biosynthesis. Curr Opin Chem Biol 15:48-56.

155. Guenin-Macé L, Carrette F, Asperti-Boursin F, Le Bon A, Caleechurn L, Di Bartolo V, Fontanet A, Bismuth G, Demangel C. 2011. Mycolactone impairs T cell homing by suppressing microRNA control of L-selectin expression. Proc Natl Acad Sci USA 108:12833-8.

156. Pahlevan AA, Wright DJ, Andrews C, George KM, Small PL, Foxwell BM. 1999. The inhibitory action of *Mycobacterium ulcerans* soluble factor on monocyte/T cell cytokine production and NF-kappa B function. J Immunol 163:3928-35.

157. Torrado E, Fraga AG, Logarinho E, Martins TG, Carmona JA, Gama JB, Carvalho MA, Proença F, Castro AG, Pedrosa J. 2010. IFN-γ–Dependent Activation of Macrophages during

Experimental Infections by *Mycobacterium ulcerans* Is Impaired by the Toxin Mycolactone. J Immunol 184:947.

158. Rook GA. 2007. Th2 cytokines in susceptibility to tuberculosis. Curr Mol Med 7:327-37.
159. Caccamo N, Guggino G, Joosten SA, Gelsomino G, Di Carlo P, Titone L, Galati D, Bocchino M, Matarese A, Salerno A, Sanduzzi A, Franken WPJ, Ottenhoff THM, Dieli F. 2010. Multifunctional $CD4^+$ T cells correlate with active *Mycobacterium tuberculosis* infection. Eur J Immunol 40:2211-2220.
160. Cooper AM, Dalton DK, Stewart TA, Griffin JP, Russell DG, Orme IM. 1993. Disseminated tuberculosis in interferon gamma gene-disrupted mice. J Exp Med 178:2243-7.
161. Flynn JL, Chan J, Triebold KJ, Dalton DK, Stewart TA, Bloom BR. 1993. An essential role for interferon gamma in resistance to *Mycobacterium tuberculosis* infection. J Exp Med 178:2249-54.
162. Krensky AM, Clayberger C. 2009. Biology and clinical relevance of granulysin. Tissue Antigens 73:193-198.
163. Rozot V, Vigano S, Mazza-Stalder J, Idrizi E, Day CL, Perreau M, Lazor-Blanchet C, Petruccioli E, Hanekom W, Goletti D, Bart P-A, Nicod L, Pantaleo G, Harari A. 2013. *Mycobacterium tuberculosis*-specific $CD8^+$ T cells are functionally and phenotypically different between latent infection and active disease. Eur J Immunol 43:1568-1577.
164. Gehring AJ, Dobos KM, Belisle JT, Harding CV, Boom WH. 2004. *Mycobacterium tuberculosis* LprG (Rv1411c): a novel TLR-2 ligand that inhibits human macrophage class II MHC antigen processing. J Immunol 173:2660-8.
165. Noss EH, Pai RK, Sellati TJ, Radolf JD, Belisle J, Golenbock DT, Boom WH, Harding CV. 2001. Toll-Like Receptor 2-Dependent Inhibition of Macrophage Class II MHC Expression and Antigen Processing by 19-kDa Lipoprotein of *Mycobacterium tuberculosis*. J Immunol 167:910.
166. Pecora ND, Gehring AJ, Canaday DH, Boom WH, Harding CV. 2006. *Mycobacterium tuberculosis* LprA is a lipoprotein agonist of TLR2 that regulates innate immunity and APC function. J Immunol 177:422-9.
167. Baena A, Porcelli SA. 2009. Evasion and subversion of antigen presentation by *Mycobacterium tuberculosis*. Tissue Antigens 74:189-204.
168. Harding CV, Boom WH. 2010. Regulation of antigen presentation by *Mycobacterium tuberculosis*: a role for Toll-like receptors. Nature Rev Microbiol 8:296-307.
169. Bhatt K, Verma S, Ellner JJ, Salgame P. 2015. Quest for Correlates of Protection against Tuberculosis. Clin Vaccine Immunol 22:258-266.
170. Freches D, Korf H, Denis O, Havaux X, Huygen K, Romano M. 2013. Mice genetically inactivated in interleukin-17A receptor are defective in long-term control of *Mycobacterium tuberculosis* infection. Immunology 140:220-31.

171. Maglione PJ, Xu J, Chan J. 2007. B cells moderate inflammatory progression and enhance bacterial containment upon pulmonary challenge with *Mycobacterium tuberculosis*. J Immunol 178:7222-34.

172. Vordermeier HM, Venkataprasad N, Harris DP, Ivanyi J. 1996. Increase of tuberculous infection in the organs of B cell-deficient mice. Clin Exp Immunol 106:312-316.

173. Johnson CM, Cooper AM, Frank AA, Bonorino CBC, Wysoki LJ, Orme IM. 1997. *Mycobacterium tuberculosis* aerogenic rechallenge infections in B cell-deficient mice. Tuber Lung Dis 78:257-261.

174. Lu LL, Chung AW, Rosebrock TR, Ghebremichael M, Yu WH, Grace PS, Schoen MK, Tafesse F, Martin C, Leung V, Mahan AE, Sips M, Kumar MP, Tedesco J, Robinson H, Tkachenko E, Draghi M, Freedberg KJ, Streeck H, Suscovich TJ, Lauffenburger DA, Restrepo BI, Day C, Fortune SM, Alter G. 2016. A Functional Role for Antibodies in Tuberculosis. Cell 167:433-443.e14.

175. Nausch N, Antwi-Berko D, Mubarik Y, Abass KM, Owusu W, Owusu-Dabo E, Debrah LB, Debrah AY, Jacobsen M, Phillips RO. 2017. Analysis of *Mycobacterium ulcerans*-specific T-cell cytokines for diagnosis of Buruli ulcer disease and as potential indicator for disease progression. PLoS Negl Trop Dis 11:e0005415-e0005415.

176. O'Brien DP, Murrie A, Meggyesy P, Priestley J, Rajcoomar A, Athan E. 2019. Spontaneous healing of *Mycobacterium ulcerans* disease in Australian patients. PLoS Negl Trop Dis 13:e0007178-e0007178.

177. Bieri R, Bolz M, Ruf M-T, Pluschke G. 2016. Interferon-γ Is a Crucial Activator of Early Host Immune Defense against *Mycobacterium ulcerans* Infection in Mice. PLoS Negl Trop Dis 10:e0004450.

178. Torrado E, Fraga AG, Logarinho E, Martins TG, Carmona JA, Gama JB, Carvalho MA, Proenca F, Castro AG, Pedrosa J. 2010. IFN-gamma-dependent activation of macrophages during experimental infections by *Mycobacterium ulcerans* is impaired by the toxin mycolactone. J Immunol 184:947-55.

179. Bibert S, Bratschi MW, Aboagye SY, Collinet E, Scherr N, Yeboah-Manu D, Beuret C, Pluschke G, Bochud P-Y. 2017. Susceptibility to *Mycobacterium ulcerans* Disease (Buruli ulcer) Is Associated with IFNG and iNOS Gene Polymorphisms. Front Microbiol 8:1903.

180. Pidot SJ, Porter JL, Marsollier L, Chauty A, Migot-Nabias F, Badaut C, Benard A, Ruf MT, Seemann T, Johnson PD, Davies JK, Jenkin GA, Pluschke G, Stinear TP. 2010. Serological evaluation of *Mycobacterium ulcerans* antigens identified by comparative genomics. PLoS Negl Trop Dis 4:e872.

181. Marion E, Jarry U, Cano C, Savary C, Beauvillain C, Robbe-Saule M, Preisser L, Altare F, Delneste Y, Jeannin P, Marsollier L. 2016. FVB/N Mice Spontaneously Heal Ulcerative

Lesions Induced by *Mycobacterium ulcerans* and Switch M. ulcerans into a Low Mycolactone Producer. J Immunol 196:2690-2698.

182. Bolz M, Ruggli N, Borel N, Pluschke G, Ruf MT. 2016. Local Cellular Immune Responses and Pathogenesis of Buruli Ulcer Lesions in the Experimental *Mycobacterium ulcerans* Pig Infection Model. PLoS Negl Trop Dis 10:e0004678.
183. Oliveira MS, Fraga AG, Torrado E, Castro AG, Pereira JP, Filho AL, Milanezi F, Schmitt FC, Meyers WM, Portaels F, Silva MT, Pedrosa J. 2005. Infection with *Mycobacterium ulcerans* induces persistent inflammatory responses in mice. Infect Immun 73:6299-310.
184. Silva-Gomes R, Marcq E, Trigo G, Gonçalves CM, Longatto-Filho A, Castro AG, Pedrosa J, Fraga AG. 2015. Spontaneous Healing of *Mycobacterium ulcerans* Lesions in the Guinea Pig Model. PLoS Negl Trop Dis 9:e0004265.
185. Centre for Disease Control. December 19, 2014 2014. Testing For Tuberculosis (TB), *on* Centre for Disease Control. http://www.cdc.gov/tb/publications/factsheets/testing/tb_factsheet.pdf. Accessed 19 January 2020.
186. Cudahy P, Shenoi SV. 2016. Diagnostics for pulmonary tuberculosis. Postgrad Med J 92:187-193.
187. Horne DJ, Kohli M, Zifodya JS, Schiller I, Dendukuri N, Tollefson D, Schumacher SG, Ochodo EA, Pai M, Steingart KR. 2019. Xpert MTB/RIF and Xpert MTB/RIF Ultra for pulmonary tuberculosis and rifampicin resistance in adults. Cochrane Database Syst Rev doi:10.1002/14651858.CD009593.pub4.
188. Broger T, Sossen B, du Toit E, Kerkhoff AD, Schutz C, Ivanova Reipold E, Ward A, Barr DA, Macé A, Trollip A, Burton R, Ongarello S, Pinter A, Lowary TL, Boehme C, Nicol MP, Meintjes G, Denkinger CM. 2019. Novel lipoarabinomannan point-of-care tuberculosis test for people with HIV: a diagnostic accuracy study. Lancet Infect Dis 19:852-861.
189. van der Werf TS, Stienstra Y, Johnson RC, Phillips R, Adjei O, Fleischer B, Wansbrough-Jones MH, Johnson PD, Portaels F, van der Graaf WT, Asiedu K. 2005. *Mycobacterium ulcerans* disease. Bulletin World Health Organisation 83:785-91.
190. Fyfe JA, Lavender CJ, Johnson PD, Globan M, Sievers A, Azuolas J, Stinear TP. 2007. Development and application of two multiplex real-time PCR assays for the detection of *Mycobacterium ulcerans* in clinical and environmental samples. Appl Environ Microbiol 73:4733-40.
191. Guarner J. 2018. Buruli ulcer: Review of a Neglected Skin Mycobacterial Disease. J Clin Microbiol 56:e01507-17.
192. Sarfo FS, Phillips R, Asiedu K, Ampadu E, Bobi N, Adentwe E, Lartey A, Tetteh I, Wansbrough-Jones M. 2010. Clinical efficacy of combination of rifampin and streptomycin for treatment of *Mycobacterium ulcerans* disease. Antimicrob Agents Chemother 54:3678-85.

193. World Health Organization. 2010. *Treatment of tuberculosis: guidelines (fourth edition)*. Accessed 20 December 2019.

194. Sylvia S, Xue H, Zhou C, Shi Y, Yi H, Zhou H, Rozelle S, Pai M, Das J. 2017. Tuberculosis detection and the challenges of integrated care in rural China: A cross-sectional standardized patient study. PLoS Med 14:e1002405-e1002405.

195. Cambanis A, Yassin MA, Ramsay A, Bertel Squire S, Arbide I, Cuevas LE. 2005. Rural poverty and delayed presentation to tuberculosis services in Ethiopia. Trop Med Int Health 10:330-335.

196. Röltgen K, Pluschke G. 2019. Buruli Ulcer: History and Disease Burden, p 1-41. *In* Pluschke G, Röltgen K (ed), Buruli Ulcer: *Mycobacterium ulcerans* Disease doi:10.1007/978-3-030-11114-4_1. Springer International Publishing.

197. Agbenorku P, Donwi IK, Kuadzi P, Saunderson P. 2012. Buruli ulcer: treatment challenges at three centres in Ghana. J Trop Med 2012:371915.

198. Centers for Disease Control and Prevention. 2003. Treatment of Tuberculosis, American Thoracic Society, CDC and Infectous Diseases Society of America. Morbidity and Mortality Weekly Report 52: 19-74

199. World Health Organization. 2018. Global tuberculosis report 2018. Licence: CCBY-NC-SA3.0IGO. Accessed 17 September 2019.

200. Department of Control of Neglected Tropical Diseases. 2012. Treatment of *Mycobacterium ulcerans* disease (Buruli ulcer): Guidance for health workers. World Health Organization, Geneva. Accessed 15 Dec 2019.

201. Herbinger KH, Brieske D, Nitschke J, Siegmund V, Thompson W, Klutse E, Awua-Boateng NY, Bruhl E, Kunaa L, Schunk M, Adjei O, Loscher T, Bretzel G. 2008. Excision of Pre-Ulcerative Forms of Buruli Ulcer Disease: A Curative Treatment? Infection doi:10.1007/s15010-008-8073-4.

202. Nienhuis WA, Stienstra Y, Thompson WA, Awuah PC, Abass KM, Tuah W, Awua-Boateng NY, Ampadu EO, Siegmund V, Schouten JP, Adjei O, Bretzel G, van der Werf TS. 2010. Antimicrobial treatment for early, limited *Mycobacterium ulcerans* infection: a randomised controlled trial. Lancet 375:664-72.

203. Phillips RO, Sarfo FS, Abass MK, Abotsi J, Wilson T, Forson M, Amoako YA, Thompson W, Asiedu K, Wansbrough-Jones M. 2014. Clinical and bacteriological efficacy of rifampin-streptomycin combination for two weeks followed by rifampin and clarithromycin for six weeks for treatment of *Mycobacterium ulcerans* disease. Antimicrob Agents Chemother 58:1161-6.

204. Marsollier L, Honore N, Legras P, Manceau AL, Kouakou H, Carbonnelle B, Cole ST. 2003. Isolation of three *Mycobacterium ulcerans* strains resistant to rifampin after experimental chemotherapy of mice. Antimicrob Agents Chemother 47:1228-32.

205. Klis S, Stienstra Y, Phillips RO, Abass KM, Tuah W, van der Werf TS. 2014. Long term streptomycin toxicity in the treatment of Buruli Ulcer: follow-up of participants in the BURULICO drug trial. PLoS Negl Trop Dis 8:e2739-e2739.

206. Omansen TF, Porter JL, Johnson PDR, van der Werf TS, Stienstra Y, Stinear TP. 2015. In-vitro Activity of Avermectins against *Mycobacterium ulcerans*. PLoS Negl Trop Dis 9:e0003549.

207. Scherr N, Pluschke G, Thompson CJ, Ramón-García S. 2015. Selamectin Is the Avermectin with the Best Potential for Buruli Ulcer Treatment. PLoS Negl Trop Dis 9:e0003996.

208. Dangy J-P, Scherr N, Gersbach P, Hug MN, Bieri R, Bomio C, Li J, Huber S, Altmann K-H, Pluschke G. 2016. Antibody-Mediated Neutralization of the Exotoxin Mycolactone, the Main Virulence Factor Produced by *Mycobacterium ulcerans*. PLoS Negl Trop Dis 10:e0004808.

209. Schütte D, Pluschke G. 2009. Immunosuppression and treatment-associated inflammatory response in patients with *Mycobacterium ulcerans* infection (Buruli ulcer). Expert Opin Biol Th 9:187-200.

210. Institute of Medicine (US) Committee on Regulating Occupational Exposure to Tuberculosis. 2001. F, Respiratory Protection and Control of Tuberculosis in Health Care and Other Facilities. *In* Field MJ (ed), Tuberculosis in the Workplace doi:10.17226/10045, Washington (DC).

211. Dharmadhikari AS, Mphahlele M, Stoltz A, Venter K, Mathebula R, Masotla T, Lubbe W, Pagano M, First M, Jensen PA, van der Walt M, Nardell EA. 2012. Surgical face masks worn by patients with multidrug-resistant tuberculosis: impact on infectivity of air on a hospital ward. Am J Resp Crit Care Med 185:1104-1109.

212. Marston BJ, Diallo MO, Horsburgh CR, Jr., Diomande I, Saki MZ, Kanga JM, Patrice G, Lipman HB, Ostroff SM, Good RC. 1995. Emergence of Buruli ulcer disease in the Daloa region of Cote d'Ivoire. Am J Trop Med Hyg 52:219-24.

213. Pouillot R, Matias G, Wondje CM, Portaels F, Valin N, Ngos F, Njikap A, Marsollier L, Fontanet A, Eyangoh S. 2007. Risk Factors for Buruli Ulcer: A Case Control Study in Cameroon. PLoS Negl Trop Dis 1:e101.

214. Tricia YJQ, Eugene A, Margaret JH, Julie AP, Jane R-H, Andrew H, Paul DRJ. 2007. Risk Factors for *Mycobacterium ulcerans* Infection, Southeastern Australia. Emerg Infect Dis 13:1661.

215. Raghunathan PL, Whitney EAS, Asamoa K, Stienstra Y, Taylor JTH, Amofah GK, Ofori-Adjei D, Dobos K, Guarner J, Martin S, Pathak S, Klutse E, Etuaful S, van der Graaf WTA, van der Werf TS, King CH, Tappero JW, Ashford DA. 2005. Risk Factors for Buruli Ulcer Disease (Mycobacterium ulcerans Infection): Results from a Case-Control Study in Ghana. Clin Infect Dis 40:1445-1453.

216. Johnson F, Makoutode M, Sopoh GE, Elsen P, Gbovi J, Pouteau LH, Meyers WM, Boko M, Portaels F. 2005. Buruli ulcer distribution in Benin. Emerg Infect Dis 11: 500-501.

217. Stinear T, Davies JK, Jenkin GA, Hayman JA, Oppedisano F, Johnson PD. 2000. Identification of *Mycobacterium ulcerans* in the environment from regions in Southeast Australia in which it is endemic with sequence capture-PCR. Appl Environ Microbiol 66:3206-13.
218. Vandelannoote K, Durnez L, Amissah D, Gryseels S, Dodoo A, Yeboah S, Addo P, Eddyani M, Leirs H, Ablordey A, Portaels F. 2010. Application of real-time PCR in Ghana, a Buruli ulcer-endemic country, confirms the presence of *Mycobacterium ulcerans* in the environment. FEMS Microbiol Lett 304:191-4.
219. Beverley PCL. 2002. Immunology of vaccination. Br Med Bull 62:15-28.
220. Clem AS. 2011. Fundamentals of vaccine immunology. Glob Inf Dis 3:73-78.
221. Pulendran B, Ahmed R. 2011. Immunological mechanisms of vaccination. Nature Immunol 12:509-517.
222. Siegrist C-A. 2018. 2 - Vaccine Immunology, p 16-34.e7. *In* Plotkin SA, Orenstein WA, Offit PA, Edwards KM (ed), Plotkin's Vaccines (Seventh Edition). Elsevier Philadelphia, PA.
223. Tosi MF. 2005. Innate immune responses to infection. J Allergy Clin Imunol 116:241-249.
224. Palucka K, Banchereau J. 1999. Dendritic Cells: A Link Between Innate and Adaptive Immunity. J Clin Immunol 19:12-25.
225. Steinman RM, Hemmi H. 2006. Dendritic Cells: Translating Innate to Adaptive Immunity, p 17-58. *In* Pulendran B, Ahmed R (ed), From Innate Immunity to Immunological Memory doi:10.1007/3-540-32636-7_2. Springer Berlin Heidelberg, Berlin, Heidelberg.
226. Netea MG, Joosten LAB, Latz E, Mills KHG, Natoli G, Stunnenberg HG, O'Neill LAJ, Xavier RJ. 2016. Trained immunity: A program of innate immune memory in health and disease. Science 352:aaf1098.
227. Ratajczak W, Niedźwiedzka-Rystwej P, Tokarz-Deptuła B, Deptuła W. 2018. Immunological memory cells. Cent Eur J Immunol 43:194-203.
228. Hoffman W, Lakkis FG, Chalasani G. 2016. B Cells, Antibodies, and More. Clin J Am Soc Nephrol 11:137-154.
229. Kang S-M, Compans RW. 2009. Host responses from innate to adaptive immunity after vaccination: molecular and cellular events. Mol Cells 27:5-14.
230. Koretzky GA. 2010. Multiple Roles of CD4 and CD8 in T Cell Activation. J Immunol 185:2643.
231. Jaigirdar SA, MacLeod MKL. 2015. Development and Function of Protective and Pathologic Memory CD4 T Cells. Front Immunol 6:456.
232. Corthay A. 2009. How do regulatory T cells work? Scand J Immunol 70:326-336.
233. Zhang N, Bevan MJ. 2011. $CD8^+$ T cells: foot soldiers of the immune system. Immunity 35:161-168.
234. Amanna IJ, Slifka MK. 2011. Contributions of humoral and cellular immunity to vaccine-induced protection in humans. Virology 411:206-215.

235. Awate S, Babiuk LA, Mutwiri G. 2013. Mechanisms of action of adjuvants. Front Immunol 4:114-114.

236. Coffman RL, Sher A, Seder RA. 2010. Vaccine adjuvants: putting innate immunity to work. Immunity 33:492-503.

237. Plotkin SA. 1999. Vaccination against the major infectious diseases. Plotkin SA. 1999. Vaccination against the major infectious diseases. C R Acad Sci III 322: 943-951.

238. Pichichero ME. 2013. Protein carriers of conjugate vaccines: characteristics, development, and clinical trials. Human Vaccin Immunother 9:2505-2523.

239. Jacobs BL, Langland JO, Kibler KV, Denzler KL, White SD, Holechek SA, Wong S, Huynh T, Baskin CR. 2009. *Vaccinia* virus vaccines: past, present and future. Antiviral Res 84:1-13.

240. Griffin DE. 2018. Measles Vaccine. Viral immunol 31:86-95.

241. Averhoff FM, Khudyakov Y, Nelson NP. 2018. 24 - Hepatitis A Vaccines, p 319-341.e15. *In* Plotkin SA, Orenstein WA, Offit PA, Edwards KM (ed), Plotkin's Vaccines (Seventh Edition). Elsevier Philadelphia, PA.

242. Sagliocca L, Amoroso P, Stroffolini T, Adamo B, Tosti ME, Lettieri G, Esposito C, Buonocore S, Pierri P, Mele A. 1999. Efficacy of hepatitis A vaccine in prevention of secondary hepatitis A infection: a randomised trial. Lancet 353:1136-1139.

243. Van Damme P, Ward JW, Shouval D, Zanetti A. 2018. 25 - Hepatitis B Vaccines, p 342-374.e17. *In* Plotkin SA, Orenstein WA, Offit PA, Edwards KM (ed), Plotkin's Vaccines (Seventh Edition) Elsevier Philadelphia, PA.

244. Van Damme P. 2016. Long-term Protection After Hepatitis B Vaccine. J Inf Dis 214:1-3.

245. Kash N, Lee MA, Kollipara R, Downing C, Guidry J, Tyring SK. 2015. Safety and Efficacy Data on Vaccines and Immunization to Human Papillomavirus. J Clin Med 4:614-633.

246. Schiller JT, Castellsagué X, Garland SM. 2012. A review of clinical trials of human papillomavirus prophylactic vaccines. Vaccine 30 Suppl 5:F123-F138.

247. Redding L, Weiner DB. 2009. DNA vaccines in veterinary use. Expert review of vaccines 8:1251-1276.

248. Rupprecht CE, Hanlon CA, Slate D. 2004. Oral vaccination of wildlife against rabies: opportunities and challenges in prevention and control. Dev Biol 119:173-84.

249. Hanlon L, Argyle D, Bain D, Nicolson L, Dunham S, Golder MC, McDonald M, McGillivray C, Jarrett O, Neil JC, Onions DE. 2001. Feline leukemia virus DNA vaccine efficacy is enhanced by coadministration with interleukin-12 (IL-12) and IL-18 expression vectors. J Virol 75:8424-8433.

250. Fine PE. 1995. Variation in protection by BCG: implications of and for heterologous immunity. Lancet 346:1339-45.

251. Mangtani P, Abubakar I, Ariti C, Beynon R, Pimpin L, Fine PEM, Rodrigues LC, Smith PG, Lipman M, Whiting PF, Sterne JA. 2013. Protection by BCG Vaccine Against Tuberculosis: A Systematic Review of Randomized Controlled Trials. Clin Infect Dis 58:470-480.

252. Luca S, Mihaescu T. 2013. History of BCG Vaccine. Maedica (Buchar) 8:53-58.

253. Lewis KN, Liao R, Guinn KM, Hickey MJ, Smith S, Behr MA, Sherman DR. 2003. Deletion of RD1 from *Mycobacterium tuberculosis* mimics bacille Calmette-Guerin attenuation. J Infect Dis 187:117-23.

254. Majlessi L, Brodin P, Brosch R, Rojas MJ, Khun H, Huerre M, Cole ST, Leclerc C. 2005. Influence of ESAT-6 secretion system 1 (RD1) of *Mycobacterium tuberculosis* on the interaction between mycobacteria and the host immune system. J Immunol 174:3570-9.

255. Pym AS, Brodin P, Brosch R, Huerre M, Cole ST. 2002. Loss of RD1 contributed to the attenuation of the live tuberculosis vaccines *Mycobacterium bovis* BCG and *Mycobacterium microti*. Mol Microbiol 46:709-17.

256. Brodin P, Majlessi L, Marsollier L, de Jonge MI, Bottai D, Demangel C, Hinds J, Neyrolles O, Butcher PD, Leclerc C, Cole ST, Brosch R. 2006. Dissection of ESAT-6 system 1 of *Mycobacterium tuberculosis* and impact on immunogenicity and virulence. Infect Immun 74:88-98.

257. Gao LY, Guo S, McLaughlin B, Morisaki H, Engel JN, Brown EJ. 2004. A mycobacterial virulence gene cluster extending RD1 is required for cytolysis, bacterial spreading and ESAT-6 secretion. Mol Microbiol 53:1677-93.

258. Abdallah AM, Bestebroer J, Savage NDL, de Punder K, van Zon M, Wilson L, Korbee CJ, van der Sar AM, Ottenhoff THM, van der Wel NN, Bitter W, Peters PJ. 2011. Mycobacterial Secretion Systems ESX-1 and ESX-5 Play Distinct Roles in Host Cell Death and Inflammasome Activation. J Immunol 187:4744.

259. Conrad WH, Osman MM, Shanahan JK, Chu F, Takaki KK, Cameron J, Hopkinson-Woolley D, Brosch R, Ramakrishnan L. 2017. Mycobacterial ESX-1 secretion system mediates host cell lysis through bacterium contact-dependent gross membrane disruptions. Proc Natl Acad Sci USA 114:1371.

260. Brodin P, Rosenkrands I, Andersen P, Cole ST, Brosch R. 2004. ESAT-6 proteins: protective antigens and virulence factors? Trends Microbiol 12:500-8.

261. de Jonge MI, Pehau-Arnaudet G, Fretz MM, Romain F, Bottai D, Brodin P, Honore N, Marchal G, Jiskoot W, England P, Cole ST, Brosch R. 2007. ESAT-6 from *Mycobacterium tuberculosis* dissociates from its putative chaperone CFP-10 under acidic conditions and exhibits membrane-lysing activity. J Bacteriol 189:6028-34.

262. Ganguly N, Giang PH, Gupta C, Basu SK, Siddiqui I, Salunke DM, Sharma P. 2008. *Mycobacterium tuberculosis* secretory proteins CFP-10, ESAT-6 and the CFP10:ESAT6

complex inhibit lipopolysaccharide-induced NF-kappaB transactivation by downregulation of reactive oxidative species (ROS) production. Immunol Cell Biol 86:98-106.

263. Guinn KM, Hickey MJ, Mathur SK, Zakel KL, Grotzke JE, Lewinsohn DM, Smith S, Sherman DR. 2004. Individual RD1-region genes are required for export of ESAT-6/CFP-10 and for virulence of *Mycobacterium tuberculosis*. Mol Microbiol 51:359-70.
264. Harboe M, Oettinger T, Wiker HG, Rosenkrands I, Andersen P. 1996. Evidence for occurrence of the ESAT-6 protein in *Mycobacterium tuberculosis* and virulent *Mycobacterium bovis* and for its absence in *Mycobacterium bovis* BCG. Infect Immun 64:16-22.
265. Fortune SM, Jaeger A, Sarracino DA, Chase MR, Sassetti CM, Sherman DR, Bloom BR, Rubin EJ. 2005. Mutually dependent secretion of proteins required for mycobacterial virulence. Proc Natl Acad Sci USA 102:10676-10681.
266. McLaughlin B, Chon JS, MacGurn JA, Carlsson F, Cheng TL, Cox JS, Brown EJ. 2007. A mycobacterium ESX-1-secreted virulence factor with unique requirements for export. PLoS Pathog 3:e105-e105.
267. Trunz BB, Fine PEM, Dye C. 2006. Effect of BCG vaccination on childhood tuberculous meningitis and miliary tuberculosis worldwide: a meta-analysis and assessment of cost-effectiveness. Lancet 367:1173-1180.
268. Sterne JA, Rodrigues LC, Guedes IN. 1998. Does the efficacy of BCG decline with time since vaccination? Int J Tuberc Lung Dis 2:200-7.
269. Andersen P, Doherty TM. 2005. The success and failure of BCG - implications for a novel tuberculosis vaccine. Nat Rev Microbiol 3:656-62.
270. Darrah PA, Zeppa JJ, Maiello P, Hackney JA, Wadsworth MH, Hughes TK, Pokkali S, Swanson PA, Grant NL, Rodgers MA, Kamath M, Causgrove CM, Laddy DJ, Bonavia A, Casimiro D, Lin PL, Klein E, White AG, Scanga CA, Shalek AK, Roederer M, Flynn JL, Seder RA. 2020. Prevention of tuberculosis in macaques after intravenous BCG immunization. Nature 577:95-102.
271. Hesseling AC, Marais BJ, Gie RP, Schaaf HS, Fine PE, Godfrey-Faussett P, Beyers N. 2007. The risk of disseminated Bacille Calmette-Guerin (BCG) disease in HIV-infected children. Vaccine 25:14-8.
272. World Health Organization. 2007. Meeting of the Global Advisory Committee on Vaccine Safety, 29-30 November 2006. In *Weekly Epidemiological Record*, Geneva. 82: 18-24. Accessed 20 December 2019.
273. The Uganda Buruli Group. 1969. BCG vaccination against *mycobacterium ulcerans* infection (Buruli ulcer). First results of a trial in Uganda. Lancet 293:111-5.
274. Converse PJ, Almeida DV, Nuermberger EL, Grosset JH. 2011. BCG-mediated protection against *Mycobacterium ulcerans* infection in the mouse. PLoS Negl Trop Dis 5:e985.

275. Fraga AG, Martins TG, Torrado E, Huygen K, Portaels F, Silva MT, Castro AG, Pedrosa J. 2012. Cellular immunity confers transient protection in experimental Buruli ulcer following BCG or mycolactone-negative *Mycobacterium ulcerans* vaccination. PLoS One 7:e33406.

276. Portaels F, Aguiar J, Debacker M, Guedenon A, Steunou C, Zinsou C, Meyers WM. 2004. *Mycobacterium bovis* BCG vaccination as prophylaxis against *Mycobacterium ulcerans* osteomyelitis in Buruli ulcer disease. Infect Immun 72:62-5.

277. Smith PG, Revill WD, Lukwago E, Rykushin YP. 1976. The protective effect of BCG against *Mycobacterium ulcerans* disease: a controlled trial in an endemic area of Uganda. Trans R Soc Trop Med Hyg 70:449-57.

278. Nackers F, Dramaix M, Johnson RC, Zinsou C, Robert A, E DEBB, Glynn JR, Portaels F, Tonglet R. 2006. BCG vaccine effectiveness against Buruli ulcer: a case-control study in Benin. Am J Trop Med Hyg 75:768-74.

279. Tanghe A, Adnet PY, Gartner T, Huygen K. 2007. A booster vaccination with *Mycobacterium bovis* BCG does not increase the protective effect of the vaccine against experimental *Mycobacterium ulcerans* infection in mice. Infect Immun 75:2642-4.

280. Tang J, Yam W-C, Chen Z. 2016. *Mycobacterium tuberculosis* infection and vaccine development. Tuberculosis 98:30-41.

281. Kaufmann SHE, Weiner J, von Reyn CF. 2017. Novel approaches to tuberculosis vaccine development. Int J Infect Dis 56:263-267.

282. Lietman T, Blower SM. 2000. Potential impact of tuberculosis vaccines as epidemic control agents. Clin Infect Dis 30 Suppl 3:S316-22.

283. da Costa C, Walker B, Bonavia A. 2015. Tuberculosis Vaccines - state of the art, and novel approaches to vaccine development. Int J Infect Dis 32:5-12.

284. Kaufmann SH, Lange C, Rao M, Balaji KN, Lotze M, Schito M, Zumla AI, Maeurer M. 2014. Progress in tuberculosis vaccine development and host-directed therapies-a state of the art review. Lancet Respir Med 2:301-320.

285. Montagnani C, Chiappini E, Galli L, de Martino M. 2014. Vaccine against tuberculosis: what's new? BMC Infect Dis 14 Suppl 1:S2.

286. Tameris MD, Hatherill M, Landry BS, Scriba TJ, Snowden MA, Lockhart S, Shea JE, McClain JB, Hussey GD, Hanekom WA, Mahomed H, McShane H. 2013. Safety and efficacy of MVA85A, a new tuberculosis vaccine, in infants previously vaccinated with BCG: a randomised, placebo-controlled phase 2b trial. Lancet 381:1021-8.

287. Abel B, Tameris M, Mansoor N, Gelderbloem S, Hughes J, Abrahams D, Makhethe L, Erasmus M, Kock Md, van der Merwe L, Hawkridge A, Veldsman A, Hatherill M, Schirru G, Pau MG, Hendriks J, Weverling GJ, Goudsmit J, Sizemore D, McClain JB, Goetz M, Gearhart J, Mahomed H, Hussey GD, Sadoff JC, Hanekom WA. 2010. The Novel Tuberculosis Vaccine,

AERAS-402, Induces Robust and Polyfunctional CD4+ and CD8+ T Cells in Adults. Am J Resp Crit Care Med 181:1407-1417.

288. Smaill F, Jeyanathan M, Smieja M, Medina MF, Thanthrige-Don N, Zganiacz A, Yin C, Heriazon A, Damjanovic D, Puri L, Hamid J, Xie F, Foley R, Bramson J, Gauldie J, Xing Z. 2013. A Human Type 5 Adenovirus–Based Tuberculosis Vaccine Induces Robust T Cell Responses in Humans Despite Preexisting Anti-Adenovirus Immunity. Sci Trans Med 5:205ra134.
289. Radošević K, Wieland CW, Rodriguez A, Weverling GJ, Mintardjo R, Gillissen G, Vogels R, Skeiky YAW, Hone DM, Sadoff JC, van der Poll T, Havenga M, Goudsmit J. 2007. Protective Immune Responses to a Recombinant Adenovirus Type 35 Tuberculosis Vaccine in Two Mouse Strains: CD4 and CD8 T-Cell Epitope Mapping and Role of Gamma Interferon. Infect Immun 75:4105.
290. Ahsan MJ. 2015. Recent advances in the development of vaccines for tuberculosis. Ther Adv Vaccines 3:66-75.
291. Lahey T, Laddy D, Hill K, Schaeffer J, Hogg A, Keeble J, Dagg B, Ho MM, Arbeit RD, von Reyn CF. 2016. Immunogenicity and Protective Efficacy of the DAR-901 Booster Vaccine in a Murine Model of Tuberculosis. PloS One 11:e0168521-e0168521.
292. Lu J-b, Chen B-w, Wang G-z, Fu L-l, Shen X-b, Su C, Du W-x, Yang L, Xu M. 2015. Recombinant tuberculosis vaccine AEC/BC02 induces antigen-specific cellular responses in mice and protects guinea pigs in a model of latent infection. J Microbiol Immunol Infect 48:597-603.
293. Montoya J, Solon JA, Cunanan SR, Acosta L, Bollaerts A, Moris P, Janssens M, Jongert E, Demoitie MA, Mettens P, Gatchalian S, Vinals C, Cohen J, Ofori-Anyinam O. 2013. A randomized, controlled dose-finding phase II study of the M72/AS01 candidate tuberculosis vaccine in healthy PPD-positive adults. J Clin Immunol 33:1360-75.
294. Day CL, Tameris M, Mansoor N, van Rooyen M, de Kock M, Geldenhuys H, Erasmus M, Makhethe L, Hughes EJ, Gelderbloem S, Bollaerts A, Bourguignon P, Cohen J, Demoitie MA, Mettens P, Moris P, Sadoff JC, Hawkridge A, Hussey GD, Mahomed H, Ofori-Anyinam O, Hanekom WA. 2013. Induction and regulation of T-cell immunity by the novel tuberculosis vaccine M72/AS01 in South African adults. Am J Respir Crit Care Med 188:492-502.
295. van Dissel JT, Arend SM, Prins C, Bang P, Tingskov PN, Lingnau K, Nouta J, Klein MR, Rosenkrands I, Ottenhoff THM, Kromann I, Doherty TM, Andersen P. 2010. Ag85B–ESAT-6 adjuvanted with IC31® promotes strong and long-lived *Mycobacterium tuberculosis* specific T cell responses in naïve human volunteers. Vaccine 28:3571-3581.
296. Geldenhuys H, Mearns H, Miles DJC, Tameris M, Hokey D, Shi Z, Bennett S, Andersen P, Kromann I, Hoff ST, Hanekom WA, Mahomed H, Hatherill M, Scriba TJ, van Rooyen M, Bruce McClain J, Ryall R, de Bruyn G. 2015. The tuberculosis vaccine H4:IC31 is safe and

induces a persistent polyfunctional CD4 T cell response in South African adults: A randomized controlled trial. Vaccine 33:3592-3599.

297. Luabeya AKK, Kagina BMN, Tameris MD, Geldenhuys H, Hoff ST, Shi Z, Kromann I, Hatherill M, Mahomed H, Hanekom WA, Andersen P, Scriba TJ, Schoeman E, Krohn C, Day CL, Africa H, Makhethe L, Smit E, Brown Y, Suliman S, Hughes EJ, Bang P, Snowden MA, McClain B, Hussey GD. 2015. First-in-human trial of the post-exposure tuberculosis vaccine H56:IC31 in *Mycobacterium tuberculosis* infected and non-infected healthy adults. Vaccine 33:4130-4140.

298. Stylianou E, Griffiths KL, Poyntz HC, Harrington-Kandt R, Dicks MD, Stockdale L, Betts G, McShane H. 2015. Improvement of BCG protective efficacy with a novel chimpanzee adenovirus and a modified vaccinia Ankara virus both expressing Ag85A. Vaccine 33:6800-6808.

299. Baldwin SL, Bertholet S, Reese VA, Ching LK, Reed SG, Coler RN. 2012. The importance of adjuvant formulation in the development of a tuberculosis vaccine. J Immunol 188:2189-2197.

300. Chen Q, Yang X, Li Y, He X, Ma X, Ma L, Guo Z, Li L. 2011. Preventive effects of *Mycobacterium vaccae* on HIV-associated tuberculosis: a systematic review. J Evid Based Med 4:122-9.

301. Yang XY, Chen QF, Li YP, Wu SM. 2011. *Mycobacterium vaccae* as adjuvant therapy to anti-tuberculosis chemotherapy in never-treated tuberculosis patients: a meta-analysis. PLoS One 6:e23826.

302. Sharma SK, Katoch K, Sarin R, Balambal R, Kumar Jain N, Patel N, Murthy KJR, Singla N, Saha PK, Khanna A, Singh U, Kumar S, Sengupta A, Banavaliker JN, Chauhan DS, Sachan S, Wasim M, Tripathi S, Dutt N, Jain N, Joshi N, Penmesta SRR, Gaddam S, Gupta S, Khamar B, Dey B, Mitra DK, Arora SK, Bhaskar S, Rani R. 2017. Efficacy and Safety of *Mycobacterium indicus pranii* as an adjunct therapy in Category II pulmonary tuberculosis in a randomized trial. Sci Rep 7:3354.

303. Cardona P-J. 2006. RUTI: A new chance to shorten the treatment of latent tuberculosis infection. Tuberculosis 86:273-289.

304. Grode L, Ganoza CA, Brohm C, Weiner J, Eisele B, Kaufmann SHE. 2013. Safety and immunogenicity of the recombinant BCG vaccine VPM1002 in a phase 1 open-label randomized clinical trial. Vaccine 31:1340-1348.

305. Arbues A, Aguilo JI, Gonzalo-Asensio J, Marinova D, Uranga S, Puentes E, Fernandez C, Parra A, Cardona PJ, Vilaplana C, Ausina V, Williams A, Clark S, Malaga W, Guilhot C, Gicquel B, Martin C. 2013. Construction, characterization and preclinical evaluation of MTBVAC, the first live-attenuated *M. tuberculosis*-based vaccine to enter clinical trials. Vaccine 31:4867-4873.

306. Tameris M, Geldenhuys H, Luabeya AK, Smit E, Hughes JE, Vermaak S, Hanekom WA, Hatherill M, Mahomed H, McShane H, Scriba TJ. 2014. The Candidate TB Vaccine, MVA85A, Induces Highly Durable Th1 Responses. PLoS One 9:e87340.

307. Graves A, van Zyl-Smit R, Esmail A, Bateman M, Dawson R, Goldin J, van Rikxoort E, Douoguih M, Pau M, Sadoff J, Bennett S, Snowden M, Gearhart J, Ishmukhamedov S, Schrager L, McClain J, Bateman E, Hokey D. 2014. Adenoviral-vectored tuberculosis vaccine AERAS-402 enhances T cell cytokine response in TB+ patients. (VAC12P.1026). J Immunol 192:206.15.

308. Smaill F, Xing Z. 2014. Human type 5 adenovirus-based tuberculosis vaccine: is the respiratory route of delivery the future? Expert Rev Vaccines 13:927-930.

309. Kashangura R, Jullien S, Garner P, Johnson S. 2019. MVA85A vaccine to enhance BCG for preventing tuberculosis. The Cochrane Database Syst Rev 4:CD012915-CD012915.

310. Walker KB, Guo M, Guo Y, Poecheim J, Velmurugan K, Schrager LK. 2016. Novel approaches to preclinical research and TB vaccine development. Tuberculosis 99:S12-S15.

311. Tait DR, Hatherill M, Van Der Meeren O, Ginsberg AM, Van Brakel E, Salaun B, Scriba TJ, Akite EJ, Ayles HM, Bollaerts A, Demoitié M-A, Diacon A, Evans TG, Gillard P, Hellström E, Innes JC, Lempicki M, Malahleha M, Martinson N, Mesia Vela D, Muyoyeta M, Nduba V, Pascal TG, Tameris M, Thienemann F, Wilkinson RJ, Roman F. 2019. Final Analysis of a Trial of M72/AS01E Vaccine to Prevent Tuberculosis. New Engl J Med 381:2429-2439.

312. Coler RN, Bertholet S, Pine SO, Orr MT, Reese V, Windish HP, Davis C, Kahn M, Baldwin SL, Reed SG. 2012. Therapeutic Immunization against *Mycobacterium tuberculosis* Is an Effective Adjunct to Antibiotic Treatment. New Engl J Med 381:2429-2439.

313. Bertholet S, Ireton GC, Ordway DJ, Windish HP, Pine SO, Kahn M, Phan T, Orme IM, Vedvick TS, Baldwin SL, Coler RN, Reed SG. 2010. A defined tuberculosis vaccine candidate boosts BCG and protects against multidrug-resistant *Mycobacterium tuberculosis*. Sci Trans Med 2:53ra74-53ra74.

314. Penn-Nicholson A, Tameris M, Smit E, Day TA, Musvosvi M, Jayashankar L, Vergara J, Mabwe S, Bilek N, Geldenhuys H, Luabeya AK-K, Ellis R, Ginsberg AM, Hanekom WA, Reed SG, Coler RN, Scriba TJ, Hatherill M. 2018. Safety and immunogenicity of the novel tuberculosis vaccine ID93 + GLA-SE in BCG-vaccinated healthy adults in South Africa: a randomised, double-blind, placebo-controlled phase 1 trial. Lancet Resp Med 6:287-298.

315. Masonou T, Hokey DA, Lahey T, Halliday A, Berrocal-Almanza LC, Wieland-Alter WF, Arbeit RD, Lalvani A, von Reyn CF. 2019. $CD4^+$ T cell cytokine responses to the DAR-901 booster vaccine in BCG-primed adults: A randomized, placebo-controlled trial. PloS One 14:e0217091-e0217091.

316. von Reyn CF, Lahey T, Arbeit RD, Landry B, Kailani L, Adams LV, Haynes BC, Mackenzie T, Wieland-Alter W, Connor RI, Tvaroha S, Hokey DA, Ginsberg AM, Waddell R. 2017.

Safety and immunogenicity of an inactivated whole cell tuberculosis vaccine booster in adults primed with BCG: A randomized, controlled trial of DAR-901. PloS One 12:e0175215-e0175215.

317. Abubakar I, Pimpin L, Ariti C, Beynon R, Mangtani P, Sterne JAC, Fine PEM, Smith PG, Lipman M, Elliman D, Watson JM, Drumright LN, Whiting PF, Vynnycky E, Rodrigues LC. 2013. Systematic review and meta-analysis of the current evidence on the duration of protection by bacillus Calmette-Guérin vaccination against tuberculosis. Health Technol Assess 17:1-vi.
318. Weng H, Huang J-Y, Meng X-Y, Li S, Zhang G-Q. 2016. Adjunctive therapy of *Mycobacterium vaccae* vaccine in the treatment of multidrug-resistant tuberculosis: A systematic review and meta-analysis. Biomed Rep 4:595-600.
319. Bourinbaiar AS, Batbold U, Efremenko Y, Sanjagdorj M, Butov D, Damdinpurev N, Grinishina E, Mijiddorj O, Kovolev M, Baasanjav K, Butova T, Prihoda N, Batbold O, Yurchenko L, Tseveendorj A, Arzhanova O, Chunt E, Stepanenko H, Sokolenko N, Makeeva N, Tarakanovskaya M, Borisova V, Reid A, Kalashnikov V, Nyasulu P, Prabowo SA, Jirathitikal V, Bain AI, Stanford C, Stanford J. 2019. Phase III, placebo-controlled, randomized, double-blind trial of tableted, therapeutic TB vaccine (V7) containing heat-killed *M. vaccae* administered daily for one month. J Clin Tuberc Other Mycobact Dis 18:100141-100141.
320. Kamal R, Pathak V, Kumari A, Natrajan M, Katoch K, Kar HK. 2017. Addition of Mycobacterium indicus pranii vaccine as an immunotherapeutic to standard chemotherapy in borderline leprosy: a double-blind study to assess clinical improvement (preliminary report). Br J Dermatol 176:1388-1389.
321. Prabowo SA, Painter H, Zelmer A, Smith SG, Seifert K, Amat M, Cardona P-J, Fletcher HA. 2019. RUTI Vaccination Enhances Inhibition of Mycobacterial Growth ex vivo and Induces a Shift of Monocyte Phenotype in Mice. Front Immunol 10:894.
322. Nell AS, D'Lom E, Bouic P, Sabaté M, Bosser R, Picas J, Amat M, Churchyard G, Cardona P-J. 2014. Safety, tolerability, and immunogenicity of the novel antituberculous vaccine RUTI: randomized, placebo-controlled phase II clinical trial in patients with latent tuberculosis infection. PloS One 9:e89612-e89612.
323. Kaufmann SHE, Cotton MF, Eisele B, Gengenbacher M, Grode L, Hesseling AC, Walzl G. 2014. The BCG replacement vaccine VPM1002: from drawing board to clinical trial. Expert Rev Vaccines 13:619-630.
324. Gengenbacher M, Kaiser P, Schuerer S, Lazar D, Kaufmann SHE. 2016. Post-exposure vaccination with the vaccine candidate Bacillus Calmette–Guérin ΔureC::hly induces superior protection in a mouse model of subclinical tuberculosis. Microbes Infect 18:364-368.
325. Gonzalo-Asensio J, Marinova D, Martin C, Aguilo N. 2017. MTBVAC: Attenuating the Human Pathogen of Tuberculosis (TB) Toward a Promising Vaccine against the TB Epidemic. Front Immunol 8:1803-1803.

326. Tameris M, Mearns H, Penn-Nicholson A, Gregg Y, Bilek N, Mabwe S, Geldenhuys H, Shenje J, Luabeya AKK, Murillo I, Doce J, Aguilo N, Marinova D, Puentes E, Rodríguez E, Gonzalo-Asensio J, Fritzell B, Thole J, Martin C, Scriba TJ, Hatherill M, Africa H, Arendsen D, Botes N, Cloete Y, De Kock M, Erasmus M, Jack L, Kafaar F, Kalepu X, Khomba NG, Kruger S, Leopeng T, Makhethe L, Mouton A, Mulenga H, Musvosvi M, Noble J, Opperman F, Reid T, Rossouw S, Schreuder C, Smit E, Steyn M, Tyambethu P, Van Rooyen E, Veldsman A. 2019. Live-attenuated *Mycobacterium tuberculosis* vaccine MTBVAC versus BCG in adults and neonates: a randomised controlled, double-blind dose-escalation trial. Lancet Resp Med 7:757-770.

327. Walsh DS, Dela Cruz EC, Abalos RM, Tan EV, Walsh GP, Portaels F, Meyers WM. 2007. Clinical and histologic features of skin lesions in a cynomolgus monkey experimentally infected with *Mycobacterium ulcerans* (Buruli ulcer) by intradermal inoculation. Am J Trop Med Hyg 76:132-4.

328. Bolz M, Ruggli N, Ruf MT, Ricklin ME, Zimmer G, Pluschke G. 2014. Experimental infection of the pig with *Mycobacterium ulcerans*: a novel model for studying the pathogenesis of Buruli ulcer disease. PLoS Negl Trop Dis 8:e2968.

329. Benard A, Sala C, Pluschke G. 2016. *Mycobacterium ulcerans* Mouse Model Refinement for Pre-Clinical Profiling of Vaccine Candidates. PLoS One 11:e0167059.

330. Walsh DS, Meyers WM, Krieg RE, Walsh GP. 1999. Transmission of *Mycobacterium ulcerans* to the nine-banded armadillo. Am J Trop Med Hyg 61:694-7.

331. Mangas KM, Buultjens AH, Porter JL, Baines SL, Marion E, Marsollier L, Tobias NJ, Pidot SJ, Quinn KM, Price DJ, Kedzierska K, Zeng W, Jackson DC, Chua BY, Stinear TP. 2019. Vaccine-specific immune responses against *Mycobacterium ulcerans* infection in a low-dose murine challenge model. Infect Immun doi:10.1128/IAI.00753-19.

332. Coutanceau E, Legras P, Marsollier L, Reysset G, Cole ST, Demangel C. 2006. Immunogenicity of *Mycobacterium ulcerans* Hsp65 and protective efficacy of a *Mycobacterium leprae* Hsp65-based DNA vaccine against Buruli ulcer. Microbes Infect 8:2075-81.

333. Tanghe A, Content J, Van Vooren JP, Portaels F, Huygen K. 2001. Protective Efficacy of a DNA Vaccine Encoding Antigen 85A from *Mycobacterium bovis* BCG against Buruli ulcer. Infect Immun 69:5403-5411.

334. Tanghe A, Dangy JP, Pluschke G, Huygen K. 2008. Improved protective efficacy of a species-specific DNA vaccine encoding mycolyl-transferase Ag85A from *Mycobacterium ulcerans* by homologous protein boosting. PLoS Negl Trop Dis 2:e199.

335. Roupie V, Pidot SJ, Einarsdottir T, Van Den Poel C, Jurion F, Stinear TP, Huygen K. 2014. Analysis of the vaccine potential of plasmid DNA encoding nine mycolactone polyketide synthase domains in *Mycobacterium ulcerans* infected mice. PLoS Negl Trop Dis 8:e2604.

336. Bolz M, Kerber S, Zimmer G, Pluschke G. 2015. Use of Recombinant Virus Replicon Particles for Vaccination against *Mycobacterium ulcerans* Disease. PLoS Negl Trop Dis 9:e0004011.

337. Bolz M, Benard A, Dreyer AM, Kerber S, Vettiger A, Oehlmann W, Singh M, Duthie MS, Pluschke G. 2016. Vaccination with the Surface Proteins MUL_2232 and MUL_3720 of *Mycobacterium ulcerans* Induces Antibodies but Fails to Provide Protection against Buruli Ulcer. PLoS Negl Trop Dis 10:e0004431.

338. Fenner F. 1957. Homologous and heterologous immunity in infections of mice with *Mycobacterium ulcerans* and *Mycobacterium balnei*. Am Rev Tuberc 76:76-89.

339. Hart BE, Hale LP, Lee S. 2016. Immunogenicity and protection conferred by a recombinant *Mycobacterium marinum* vaccine against Buruli ulcer. Trials Vaccinol 5:88-91.

340. Hart BE, Hale LP, Lee S. 2015. Recombinant BCG Expressing Mycobacterium ulcerans Ag85A Imparts Enhanced Protection against Experimental Buruli ulcer. PLoS Negl Trop Dis 9:e0004046.

341. Hart BE, Lee S. 2016. Overexpression of a *Mycobacterium ulcerans* Ag85B-EsxH Fusion Protein in Recombinant BCG Improves Experimental Buruli ulcer Vaccine Efficacy. PLoS Negl Trop Dis 10:e0005229.

342. Watanabe M, Nakamura H, Nabekura R, Shinoda N, Suzuki E, Saito H. 2015. Protective effect of a dewaxed whole-cell vaccine against *Mycobacterium ulcerans* infection in mice. Vaccine 33:2232-9.

343. Trigo G, Martins TG, Fraga AG, Longatto-Filho A, Castro AG, Azeredo J, Pedrosa J. 2013. Phage therapy is effective against infection by *Mycobacterium ulcerans* in a murine footpad model. PLoS Negl Trop Dis 7:e2183.

344. Spenney JG, Lamb RN, Cobbs CG. 1971. Recurrent tetanus. South Med J 64:859; 862.

345. Turner TB, Velasco-Joven EA, Prudovsky S. 1958. Studies on the prophylaxis and treatment of tetanus. II. Studies pertaining to treatment. Bulletin of the Johns Hopkins Hospital 102:71-84.

346. Johnson S. 1997. Antibody responses to clostridial infection in humans. Clin Infect Dis 25 Suppl 2:S173-7.

347. Looney JM, Edsall G, Ipsen J, Chasen WH. 1956. Persistence of Antitoxin Levels after Tetanus-Toxoid Inoculation in Adults, and Effect of a Booster Dose after Various Intervals. New Engl J Med 254:6-12.

348. Dharmadhikari AS, Nardell EA. 2008. What animal models teach humans about tuberculosis. Am J Resp Cell Mol Biol 39:503-508.

349. Singh AK, Gupta UD. 2018. Animal models of tuberculosis: Lesson learnt. Indian J Med Res 147:456-463.

350. Zhan L, Tang J, Sun M, Qin C. 2017. Animal Models for Tuberculosis in Translational and Precision Medicine. Frontiers Microbiol 8:717-717.

351. Gupta UD, Katoch VM. 2005. Animal models of tuberculosis. Tuberculosis 85:277-293.

352. Barbaric I, Miller G, Dear TN. 2007. Appearances can be deceiving: phenotypes of knockout mice. Brief Funct Genomics 6:91-103.

353. Zinkernagel RM. 2003. On natural and artificial vaccinations. Annu Rev Immunol 21:515-46.

354. Skjot RL, Oettinger T, Rosenkrands I, Ravn P, Brock I, Jacobsen S, Andersen P. 2000. Comparative evaluation of low-molecular-mass proteins from Mycobacterium tuberculosis identifies members of the ESAT-6 family as immunodominant T-cell antigens. Infect Immun 68:214-20.

355. Andersen P, Askgaard D, Ljungqvist L, Bennedsen J, Heron I. 1991. Proteins released from *Mycobacterium tuberculosis* during growth. Infect Immun 59:1905-1910.

356. Diaz D, Dobeli H, Yeboah-Manu D, Mensah-Quainoo E, Friedlein A, Soder N, Rondini S, Bodmer T, Pluschke G. 2006. Use of the immunodominant 18-kiloDalton small heat shock protein as a serological marker for exposure to *Mycobacterium ulcerans*. Clin Vaccine Immunol 13:1314-21.

357. Pidot SJ, Porter JL, Tobias NJ, Anderson J, Catmull D, Seemann T, Kidd S, Davies JK, Reynolds E, Dashper S, Stinear TP. 2010. Regulation of the 18 kDa heat shock protein in *Mycobacterium ulcerans*: an alpha-crystallin orthologue that promotes biofilm formation. Mol Microbiol 78:1216-31.

358. Pluschke G. 2011. Personal Communication.

359. Guo S, Xue R, Li Y, Wang SM, Ren L, Xu JJ. 2012. The CFP10/ESAT6 complex of Mycobacterium *tuberculosis* may function as a regulator of macrophage cell death at different stages of tuberculosis infection. Med Hypotheses 78:389-92.

360. Tan T, Lee WL, Alexander DC, Grinstein S, Liu J. 2006. The ESAT-6/CFP-10 secretion system of *Mycobacterium marinum* modulates phagosome maturation. Cell Microbiol 8:1417-29.

361. Mustafa AS, Oftung F, Amoudy HA, Madi NM, Abal AT, Shaban F, Rosen Krands I, Andersen P. 2000. Multiple epitopes from the *Mycobacterium tuberculosis* ESAT-6 antigen are recognized by antigen-specific human T cell lines. Clin Infect Dis 30 Suppl 3:S201-5.

362. Brandt L, Elhay M, Rosenkrands I, Lindblad EB, Andersen P. 2000. ESAT-6 subunit vaccination against *Mycobacterium tuberculosis*. Infect Immun 68:791-5.

363. Reiley WW, Calayag MD, Wittmer ST, Huntington JL, Pearl JE, Fountain JJ, Martino CA, Roberts AD, Cooper AM, Winslow GM, Woodland DL. 2008. ESAT-6-specific CD4 T cell responses to aerosol *Mycobacterium tuberculosis* infection are initiated in the mediastinal lymph nodes. Proc Natl Acad Sci USA 105:10961-6.

364. Skjot RL, Brock I, Arend SM, Munk ME, Theisen M, Ottenhoff TH, Andersen P. 2002. Epitope mapping of the immunodominant antigen TB10.4 and the two homologous proteins TB10.3 and TB12.9, which constitute a subfamily of the esat-6 gene family. Infect Immun 70:5446-53.

365. Dietrich J, Aagaard C, Leah R, Olsen AW, Stryhn A, Doherty TM, Andersen P. 2005. Exchanging ESAT6 with TB10.4 in an Ag85B fusion molecule-based tuberculosis subunit vaccine: efficient protection and ESAT6-based sensitive monitoring of vaccine efficacy. J Immunol 174:6332-9.

366. Billeskov R, Vingsbo-Lundberg C, Andersen P, Dietrich J. 2007. Induction of CD8 T cells against a novel epitope in TB10.4: correlation with mycobacterial virulence and the presence of a functional region of difference-1. J Immunol 179:3973-81.

367. Kamath A, Woodworth JS, Behar SM. 2006. Antigen-specific $CD8^+$ T cells and the development of central memory during *Mycobacterium tuberculosis* infection. J Immunol 177:6361-9.

368. Hervas-Stubbs S, Majlessi L, Simsova M, Morova J, Rojas MJ, Nouze C, Brodin P, Sebo P, Leclerc C. 2006. High frequency of CD4+ T cells specific for the TB10.4 protein correlates with protection against *Mycobacterium tuberculosis* infection. Infect Immun 74:3396-407.

369. Belisle JT, Vissa VD, Sievert T, Takayama K, Brennan PJ, Besra GS. 1997. Role of the major antigen of *Mycobacterium tuberculosis* in cell wall biogenesis. Science 276:1420-2.

370. Huygen K. 2014. The Immunodominant T-Cell Epitopes of the Mycolyl-Transferases of the Antigen 85 Complex of *M. tuberculosis*. Front Immunol 5:321.

371. Horwitz MA, Lee BW, Dillon BJ, Harth G. 1995. Protective immunity against tuberculosis induced by vaccination with major extracellular proteins of *Mycobacterium tuberculosis*. Proc Natl Acad Sci U S A 92:1530-4.

372. Tanghe A, Denis O, Lambrecht B, Motte V, van den Berg T, Huygen K. 2000. Tuberculosis DNA vaccine encoding Ag85A is immunogenic and protective when administered by intramuscular needle injection but not by epidermal gene gun bombardment. Infect Immun 68:3854-60.

373. Scriba TJ, Tameris M, Mansoor N, Smit E, van der Merwe L, Isaacs F, Keyser A, Moyo S, Brittain N, Lawrie A, Gelderbloem S, Veldsman A, Hatherill M, Hawkridge A, Hill AV, Hussey GD, Mahomed H, McShane H, Hanekom WA. 2010. Modified vaccinia Ankara-expressing Ag85A, a novel tuberculosis vaccine, is safe in adolescents and children, and induces polyfunctional CD4+ T cells. Eur J Immunol 40:279-90.

374. Takamura S, Matsuo K, Takebe Y, Yasutomi Y. 2005. Ag85B of mycobacteria elicits effective CTL responses through activation of robust Th1 immunity as a novel adjuvant in DNA vaccine. J Immunol 175:2541-7.

375. Weinrich Olsen A, van Pinxteren LA, Meng Okkels L, Birk Rasmussen P, Andersen P. 2001. Protection of mice with a tuberculosis subunit vaccine based on a fusion protein of antigen 85b and esat-6. Infect Immun 69:2773-8.

376. Dreyer A, Röltgen K, Dangy JP, Ruf MT, Scherr N, Bolz M, Tobias NJ, Moes C, Vettiger A, Stinear TP, Pluschke G. 2015. Identification of the *Mycobacterium ulcerans* protein

MUL_3720 as a promising target for the development of a diagnostic test for Buruli ulcer. PLoS NEgl Trop Dis 9:e0003477-e0003477.

377. Porter JL, Tobias NJ, Pidot SJ, Falgner S, Tuck KL, Vettiger A, Hong H, Leadlay PF, Stinear TP. 2013. The cell wall-associated mycolactone polyketide synthases are necessary but not sufficient for mycolactone biosynthesis. PLoS One 8:e70520.
378. Pidot SJ, Hong H, Seemann T, Porter JL, Yip MJ, Men A, Johnson M, Wilson P, Davies JK, Leadlay PF, Stinear TP. 2008. Deciphering the genetic basis for polyketide variation among mycobacteria producing mycolactones. BMC Genomics 9:462.
379. Chua BY, Pejoski D, Turner SJ, Zeng W, Jackson DC. 2011. Soluble proteins induce strong $CD8^+$ T cell and antibody responses through electrostatic association with simple cationic or anionic lipopeptides that target TLR2. J Immunol 187:1692-701.
380. Mifsud EJ, Tan AC, Jackson DC. 2014. TLR Agonists as Modulators of the Innate Immune Response and Their Potential as Agents Against Infectious Disease. Front Immunol 5:79.
381. Takeuchi O, Akira S. 2001. Toll-like receptors; their physiological role and signal transduction system. Int Immunopharmacol 1:625-35.
382. Jackson DC, Lau YF, Le T, Suhrbier A, Deliyannis G, Cheers C, Smith C, Zeng W, Brown LE. 2004. A totally synthetic vaccine of generic structure that targets Toll-like receptor 2 on dendritic cells and promotes antibody or cytotoxic T cell responses. Proc Natl Acad Sci USA 101:15440-5.
383. Schenk M, Belisle JT, Modlin RL. 2009. TLR2 Looks at Lipoproteins. Immunity 31:847-849.
384. Kang JY, Nan X, Jin MS, Youn S-J, Ryu YH, Mah S, Han SH, Lee H, Paik S-G, Lee J-O. 2009. Recognition of Lipopeptide Patterns by Toll-like Receptor 2-Toll-like Receptor 6 Heterodimer. Immunity 31:873-884.
385. Weigt H, Muhlradt PF, Emmendorffer A, Krug N, Braun A. 2003. Synthetic mycoplasma-derived lipopeptide MALP-2 induces maturation and function of dendritic cells. Immunobiology 207:223-33.
386. Chua BY, Olson MR, Bedoui S, Sekiya T, Wong CY, Turner SJ, Jackson DC. 2014. The use of a TLR2 agonist-based adjuvant for enhancing effector and memory CD8 T-cell responses. Immunol Cell Biol 92:377-83.
387. Wijayadikusumah AR, Sullivan LC, Jackson DC, Chua BY. 2017. Structure-function relationships of protein-lipopeptide complexes and influence on immunogenicity. Amino Acids 49:1691-1704.
388. Tan AC, Mifsud EJ, Zeng W, Edenborough K, McVernon J, Brown LE, Jackson DC. 2012. Intranasal Administration of the TLR2 Agonist Pam2Cys Provides Rapid Protection against Influenza in Mice. Mol Pharm doi:10.1021/mp300257x.

389. Mifsud EJ, Tan ACL, Reading PC, Jackson DC. 2016. Mapping the pulmonary environment of animals protected from virulent H1N1 influenza infection using the TLR-2 agonist Pam2Cys. Immunol Cell Biol94:169-176.

390. Chua BY, Johnson D, Tan A, Earnest-Silveira L, Sekiya T, Chin R, Torresi J, Jackson DC. 2012. Hepatitis C VLPs Delivered to Dendritic Cells by a TLR2 Targeting Lipopeptide Results in Enhanced Antibody and Cell-Mediated Responses. PLoS One 7:e47492.

391. Christiansen D, Earnest-Silveira L, Chua B, Boo I, Drummer HE, Grubor-Bauk B, Gowans EJ, Jackson DC, Torresi J. 2018. Antibody Responses to a Quadrivalent Hepatitis C Viral-Like Particle Vaccine Adjuvanted with Toll-Like Receptor 2 Agonists. Viral Immunol 31:338-343.

392. Mifsud EJ, Tan AC, Short KR, Brown LE, Chua BY, Jackson DC. 2016. Reducing the impact of influenza-associated secondary pneumococcal infections. Immunol Cell Biol 94:101-8.

393. World Health Organization 2007. Revised BCG vaccination guidelines for infants at risk for HIV infection. In *Weekly Epidemiological Record*, Geneva 82:193–196.

394. Schutz C, Meintjes G, Almajid F, Wilkinson RJ, Pozniak A. 2010. Clinical management of tuberculosis and HIV-1 co-infection. European Respiratory Journal 36:1460.

395. Wood R, Maartens G, Lombard CJ. 2000. Risk Factors for Developing Tuberculosis in HIV-1-Infected Adults From Communities With a Low or Very High Incidence of Tuberculosis. J Acquir Immune Defic Syndr 23: 75-80

396. Brandt L, Oettinger T, Holm A, Andersen AB, Andersen P. 1996. Key epitopes on the ESAT-6 antigen recognized in mice during the recall of protective immunity to *Mycobacterium tuberculosis*. J Immunol 157:3527-33.

397. Bennekov T, Dietrich J, Rosenkrands I, Stryhn A, Doherty TM, Andersen P. 2006. Alteration of epitope recognition pattern in Ag85B and ESAT-6 has a profound influence on vaccine-induced protection against *Mycobacterium tuberculosis*. Eur J Immunol 36:3346-55.

398. Davila J, McNamara LA, Yang Z. 2012. Comparison of the predicted population coverage of tuberculosis vaccine candidates Ag85B-ESAT-6, Ag85B-TB10.4, and Mtb72f via a bioinformatics approach. PLoS One 7:e40882.

399. Li W, Deng G, Li M, Zeng J, Zhao L, Liu X, Wang Y. 2014. A recombinant adenovirus expressing CFP10, ESAT6, Ag85A and Ag85B of *Mycobacterium tuberculosis* elicits strong antigen-specific immune responses in mice. Mol Immunol 62:86-95.

400. Almeida AS, Lago PM, Boechat N, Huard RC, Lazzarini LC, Santos AR, Nociari M, Zhu H, Perez-Sweeney BM, Bang H, Ni Q, Huang J, Gibson AL, Flores VC, Pecanha LR, Kritski AL, Lapa e Silva JR, Ho JL. 2009. Tuberculosis is associated with a down-modulatory lung immune response that impairs Th1-type immunity. J Immunol 183:718-31.

401. Rueda CM, Marin ND, Garcia LF, Rojas M. 2010. Characterization of CD4 and CD8 T cells producing IFN-gamma in human latent and active tuberculosis. Tuberculosis 90:346-53.

402. Yao S, Huang D, Chen CY, Halliday L, Wang RC, Chen ZW. 2014. $CD4^+$ T cells contain early extrapulmonary tuberculosis (TB) dissemination and rapid TB progression and sustain multieffector functions of $CD8^+$ T and $CD3^-$ lymphocytes: mechanisms of $CD4^+$ T cell immunity. J Immunol 192:2120-32.

403. Cho S, Mehra V, Thoma-Uszynski S, Stenger S, Serbina N, Mazzaccaro RJ, Flynn JL, Barnes PF, Southwood S, Celis E, Bloom BR, Modlin RL, Sette A. 2000. Antimicrobial activity of MHC class I-restricted $CD8^+$ T cells in human tuberculosis. Proc Natl Acad Sci USA 97:12210-5.

404. Silva BD, Trentini MM, da Costa AC, Kipnis A, Junqueira-Kipnis AP. 2014. Different phenotypes of $CD8^+$ T cells associated with bacterial load in active tuberculosis. Immunol Lett 160:23-32.

405. Pascolo S, Bervas N, Ure JM, Smith AG, Lemonnier FA, Pérarnau B. 1997. HLA-A2.1–restricted Education and Cytolytic Activity of $CD8^+$ T Lymphocytes from β2 Microglobulin (β2m) HLA-A2.1 Monochain Transgenic H-2Db β2m Double Knockout Mice. J Exp Med 185:2043-2051.

406. Firat H, Garcia-Pons F, Tourdot S, Pascolo S, Scardino A, Garcia Z, Michel M-L, Jack RW, Jung G, Kosmatopoulos K, Mateo L, Suhrbier A, Lemonnier FA, Langlade-Demoyen P. 1999. H-2 class I knockout, HLA-A2.1-transgenic mice: a versatile animal model for preclinical evaluation of antitumor immunotherapeutic strategies. Eur J Immunol 29:3112-3121.

407. Ellis JM, Henson V, Slack R, Ng J, Hartzman RJ, Katovich Hurley C. 2000. Frequencies of HLA-A2 alleles in five U.S. population groups. Predominance Of A*02011 and identification of HLA-A*0231. Hum Immunol 61:334-40.

408. Fernandez-Viña MA, Falco M, Sun Y, Stastny P. 1992. DNA typing for HLA class I alleles: I. Subsets of HLA-A2 and of -A28. Hum Immunol33:163-173.

409. Zeng G, Zhang G, Chen X. 2018. Th1 cytokines, true functional signatures for protective immunity against TB? Cell Mol Immunol 15:206-215.

410. Kaufmann SHE. 2002. Protection against tuberculosis: cytokines, T cells, and macrophages. Ann Rheum Dis 61:ii54.

411. Boyd SC, Athan E, Friedman ND, Hughes A, Walton A, Callan P, McDonald A, O'Brien DP. 2012. Epidemiology, clinical features and diagnosis of *Mycobacterium ulcerans* in an Australian population. Med J Aust 196:341-4.

412. Amofah G, Bonsu F, Tetteh C, Okrah J, Asamoa K, Asiedu K, Addy J. 2002. Buruli ulcer in Ghana: results of a national case search. Emerg Infect Dis 8:167-70.

413. Vettiger A SN, Ruf M-T, Röltgen K, Pluschke G. 2014. Localization of Mycobacterial Antigens by Immunofluorescence Staining of Agarose Embedded Cells. J Mycobact Dis 4:150.

414. Schroeder HW, Jr., Cavacini L. 2010. Structure and function of immunoglobulins. J Allergy Clin Immunol 125:S41-S52.

415. Loftus MJ, Trubiano JA, Tay EL, Lavender CJ, Globan M, Fyfe JAM, Johnson PDR. 2018. The incubation period of Buruli ulcer (*Mycobacterium ulcerans* infection) in Victoria, Australia - Remains similar despite changing geographic distribution of disease. PLoS Negl Trop Dis 12:e0006323.

416. Gowthaman U, Mushtaq K, Tan AC, Rai PK, Jackson DC, Agrewala JN. 2015. Challenges and solutions for a rational vaccine design for TB-endemic regions. Crit Rev Microbiol 41:389-98.

417. Porter JL, Tobias NJ, Pidot SJ, Falgner S, Tuck KL, Vettiger A, Hong H, Leadlay PF, Stinear TP. 2013. The cell wall-associated mycolactone polyketide synthases are necessary but not sufficient for mycolactone biosynthesis. PloS One 8:e70520-e70520.

418. Phillips RO, Phanzu DM, Beissner M, Badziklou K, Luzolo EK, Sarfo FS, Halatoko WA, Amoako Y, Frimpong M, Kabiru AM, Piten E, Maman I, Bidjada B, Koba A, Awoussi KS, Kobara B, Nitschke J, Wiedemann FX, Kere AB, Adjei O, Loscher T, Fleischer B, Bretzel G, Herbinger KH. 2015. Effectiveness of routine BCG vaccination on buruli ulcer disease: a case-control study in the Democratic Republic of Congo, Ghana and Togo. PLoS Negl Trop Dis 9:e3457.

419. Luckheeram RV, Zhou R, Verma AD, Xia B. 2012. $CD4^+$ T cells: differentiation and functions. Clin Dev Immunol 2012:925135.

420. Parker DC. 1993. T Cell-Dependent B Cell Activation. Annu Rev Immunol 11:331-360.

421. Fazilleau N, Mark L, McHeyzer-Williams LJ, McHeyzer-Williams MG. 2009. Follicular helper T cells: lineage and location. Immunity 30:324-335.

422. Mitsdoerffer M, Lee Y, Jäger A, Kim H-J, Korn T, Kolls JK, Cantor H, Bettelli E, Kuchroo VK. 2010. Proinflammatory T helper type 17 cells are effective B-cell helpers. Proc Natl Acad Sci USA 107:14292.

423. Smith KM, Pottage L, Thomas ER, Leishman AJ, Doig TN, Xu D, Liew FY, Garside P. 2000. Th1 and Th2 CD4+ T cells provide help for B cell clonal expansion and antibody synthesis in a similar manner in vivo. J Immunol 165:3136-44.

424. Macedo GC, Bozzi A, Weinreich HR, Bafica A, Teixeira HC, Oliveira SC. 2011. Human T cell and antibody-mediated responses to the *Mycobacterium tuberculosis* recombinant 85A, 85B, and ESAT-6 antigens. Clin Dev Immunol 2011:351573.

425. Meerak J, Wanichwecharungruang SP, Palaga T. 2013. Enhancement of immune response to a DNA vaccine against *Mycobacterium tuberculosis* Ag85B by incorporation of an autophagy inducing system. Vaccine 31:784-790.

426. Zuñiga J, Torres-García D, Santos-Mendoza T, Rodriguez-Reyna TS, Granados J, Yunis EJ. 2012. Cellular and humoral mechanisms involved in the control of tuberculosis. Clin Deve Immunol 2012:193923-193923.

427. Majlessi L, Simsova M, Jarvis Z, Brodin P, Rojas MJ, Bauche C, Nouze C, Ladant D, Cole ST, Sebo P, Leclerc C. 2006. An increase in antimycobacterial Th1-cell responses by prime-boost

protocols of immunization does not enhance protection against tuberculosis. Infect Immun 74:2128-37.

428. Vartak A, Sucheck SJ. 2016. Recent Advances in Subunit Vaccine Carriers. Vaccines 4:12.

429. Cardoso FL, Antas PR, Milagres AS, Geluk A, Franken KL, Oliveira EB, Teixeira HC, Nogueira SA, Sarno EN, Klatser P, Ottenhoff TH, Sampaio EP. 2002. T-cell responses to the *Mycobacterium tuberculosis*-specific antigen ESAT-6 in Brazilian tuberculosis patients. Infect Immun 70:6707-14.

430. van Pinxteren LAH, Ravn P, Agger EM, Pollock J, Andersen P. 2000. Diagnosis of Tuberculosis Based on the Two Specific Antigens ESAT-6 and CFP10. Clin Diagn Lab Immunol 7:155.

431. Hatano S, Tamura T, Umemura M, Matsuzaki G, Ohara N, Yoshikai Y. 2016. Recombinant *Mycobacterium bovis* bacillus Calmette–Guérin expressing Ag85B-IL-7 fusion protein enhances IL-17A-producing innate γδ T cells. Vaccine 34:2490-2495.

432. Shi C, Yuan S, Zhang H, Zhang T, Wang L, Xu Z. 2009. Cell-mediated immune responses and protective efficacy against infection with *Mycobacterium tuberculosis* induced by Hsp65 and hIL-2 fusion protein in mice. Scand J Immunol 69:140-9.

433. Lu LL, Chung AW, Rosebrock TR, Ghebremichael M, Yu WH, Grace PS, Schoen MK, Tafesse F, Martin C, Leung V, Mahan AE, Sips M, Kumar MP, Tedesco J, Robinson H, Tkachenko E, Draghi M, Freedberg KJ, Streeck H, Suscovich TJ, Lauffenburger DA, Restrepo BI, Day C, Fortune SM, Alter G. 2016. A Functional Role for Antibodies in Tuberculosis. Cell 167:433-443 e14.

434. Damelang T, Rogerson SJ, Kent SJ, Chung AW. 2019. Role of IgG3 in Infectious Diseases. Trends Immunol 40:197-211.

435. Ross SH, Cantrell DA. 2018. Signaling and Function of Interleukin-2 in T Lymphocytes. Annual Rev Immunol 36:411-433.

436. Correa-Macedo W, Cambri G, Schurr E. 2019. The Interplay of Human and *Mycobacterium tuberculosis* Genomic Variability. Front Genetics 10:865.

437. Capela C, Dossou AD, Silva-Gomes R, Sopoh GE, Makoutode M, Menino JF, Fraga AG, Cunha C, Carvalho A, Rodrigues F, Pedrosa J. 2016. Genetic Variation in Autophagy-Related Genes Influences the Risk and Phenotype of Buruli Ulcer. PLoS Negl Trop Dis 10:e0004671.

438. Stienstra Y, van der Werf TS, Oosterom E, Nolte IM, van der Graaf WTA, Etuaful S, Raghunathan PL, Whitney EAS, Ampadu EO, Asamoa K, Klutse EY, te Meerman GJ, Tappero JW, Ashford DA, van der Steege G. 2006. Susceptibility to Buruli ulcer is associated with the SLC11A1 (NRAMP1) D543N polymorphism. Genes Immun 7:185-189.7:185-189.

439. Chatterjee S, Dwivedi VP, Singh Y, Siddiqui I, Sharma P, Van Kaer L, Chattopadhyay D, Das G. 2011. Early secreted antigen ESAT-6 of *Mycobacterium tuberculosis* promotes protective T helper 17 cell responses in a toll-like receptor-2-dependent manner. PLoS Pathog 7:e1002378.

440. Lindenstrøm T, Woodworth J, Dietrich J, Aagaard C, Andersen P, Agger EM. 2012. Vaccine-induced th17 cells are maintained long-term postvaccination as a distinct and phenotypically stable memory subset. Infection and immunity 80:3533-3544.

441. Okamoto Yoshida Y, Umemura M, Yahagi A, O'Brien RL, Ikuta K, Kishihara K, Hara H, Nakae S, Iwakura Y, Matsuzaki G. 2010. Essential role of IL-17A in the formation of a mycobacterial infection-induced granuloma in the lung. J Immunol 184:4414-22.

442. Segueni N, Tritto E, Bourigault M-L, Rose S, Erard F, Le Bert M, Jacobs M, Di Padova F, Stiehl DP, Moulin P, Brees D, Chibout S-D, Ryffel B, Kammüller M, Quesniaux VF. 2016. Controlled *Mycobacterium tuberculosis* infection in mice under treatment with anti-IL-17A or IL-17F antibodies, in contrast to TNFα neutralization. Sci Rep 6:36923-36923.

443. Lyadova IV, Panteleev AV. 2015. Th1 and Th17 Cells in Tuberculosis: Protection, Pathology, and Biomarkers. Mediators Inflamm 2015:854507.

444. Umemura M, Yahagi A, Hamada S, Begum MD, Watanabe H, Kawakami K, Suda T, Sudo K, Nakae S, Iwakura Y, Matsuzaki G. 2007. IL-17-mediated regulation of innate and acquired immune response against pulmonary *Mycobacterium* bovis bacille Calmette-Guerin infection. J Immunol 178:3786-96.

445. Chen L, Wang J, Zganiacz A, Xing Z. 2004. Single Intranasal Mucosal *Mycobacterium bovis* BCG Vaccination Confers Improved Protection Compared to Subcutaneous Vaccination against Pulmonary Tuberculosis. Infect Immun 72:238.

446. Giri PK, Verma I, Khuller GK. 2006. Protective efficacy of intranasal vaccination with *Mycobacterium bovis* BCG against airway *Mycobacterium tuberculosis* challenge in mice. J Infect 53:350-356.

447. Herzog C. 2014. Influence of parenteral administration routes and additional factors on vaccine safety and immunogenicity: a review of recent literature. Expert Rev Vaccines 13:399-415.

448. Riese P, Sakthivel P, Trittel S, Guzmán CA. 2014. Intranasal formulations: promising strategy to deliver vaccines. Expert Opin Drug Delivery 11:1619-1634.

449. Stoner KL, Harder H, Fallowfield LJ, Jenkins VA. 2015. Intravenous versus Subcutaneous Drug Administration. Which Do Patients Prefer? A Systematic Review. Patient 8:145-153.

450. Dychter SS, Gold DA, Haller MF. 2012. Subcutaneous Drug Delivery: A Route to Increased Safety, Patient Satisfaction, and Reduced Costs. J Infus Nursi 35.

451. Pedroza-Roldán C, Flores-Valdez MA. 2017. Recent mouse models and vaccine candidates for preventing chronic/latent tuberculosis infection and its reactivation. Pathog Dis 75.

452. Kramnik I, Beamer G. 2016. Mouse models of human TB pathology: roles in the analysis of necrosis and the development of host-directed therapies. Semin Imunopathol 38:221-237.

453. Mestas J, Hughes CCW. 2004. Of Mice and Not Men: Differences between Mouse and Human Immunology. J Immunol 172:2731.

454. Apt A, Kramnik I. 2009. Man and mouse TB: contradictions and solutions. Tuberculosis 89:195-8.

455. Calderon VE, Valbuena G, Goez Y, Judy BM, Huante MB, Sutjita P, Johnston RK, Estes DM, Hunter RL, Actor JK, Cirillo JD, Endsley JJ. 2013. A Humanized Mouse Model of Tuberculosis. PLoS One 8:e63331.

456. Walsh NC, Kenney LL, Jangalwe S, Aryee K-E, Greiner DL, Brehm MA, Shultz LD. 2017. Humanized Mouse Models of Clinical Disease. Annu Rev Pathol 12:187-215.

457. Su H, Zhu S, Zhu L, Kong C, Huang Q, Zhang Z, Wang H, Xu Y. 2017. Mycobacterium tuberculosis Latent Antigen Rv2029c from the Multistage DNA Vaccine A39 Drives TH1 Responses via TLR-mediated Macrophage Activation. Front Microbiol 8:2266.

458. Singh S, Saraav I, Sharma S. 2014. Immunogenic potential of latency associated antigens against *Mycobacterium tuberculosis*. Vaccine 32:712-6.